DRVNA INDUSTRIJA

Tieghemella heckelii Pierre.

4/18

DRVNA INDUSTRIJA

ZNANSTVENI ČASOPIS ZA PITANJA DRVNE TEHNOLOGIJE
SCIENTIFIC JOURNAL OF WOOD TECHNOLOGY

DRVNA INDUSTRIJA je časopis koji objavljuje znanstvene i stručne radove te ostale priloge iz cjelokupnog područja iskorištavanja šuma, istraživanja svojstava i primjene drva, mehaničke i kemijske prerade drva, svih proizvodnih grana te trgovine drvom i drvnim proizvodima.

Časopis izlazi četiri puta u godini.

DRVNA INDUSTRIJA journal contains research contributions and reviews covering the entire field of forest exploitation, wood properties and application, mechanical and chemical conversion and modification of wood, and all aspects of manufacturing and trade of wood and wood products.

The journal is published quarterly.

Sadržaj
Contents

Petr Čech[1]

Comparison of VOC Emissions from Natural Wood and Heat Treated Wood

Usporedba emisije hlapljivih organskih spojeva iz prirodnog drva i toplinski obrađenog drva

ABSTRACT • *This paper describes the emissions of Volatile Organic Compounds (VOC) emitted by solid Spruce (Picea abies) and Poplar (Populus alba) wood treated at 200 °C and 180 °C. The emissions of VOC from heat treated wood and air-dried (natural) wood were compared with GC-MS analysis. The focus was on the influence of temperature, on the quality and quantity of volatile organic compounds, especially on the amount of emitted phenol and furfural. Furfural and phenol are typical chemicals produced as a result of thermal degradation of wood components. The emission was analyzed as a function of time after heat-treatment. The influence of the finishing with waterborne lacquer on VOC emission was also investigated.*
The results of this research have shown that heat treated wood emitted more VOC-components of furfural and phenol than untreated wood (natural wood). The amount of emitted VOC declines with increasing the time between wood modification and measurement of VOC emissions emitted by tested samples. Heat treated wood finished by waterborne lacquer emitted a very high concentration of Buthoxy-ethanol. The finished surface does not decrease the amount of emissions escaping from heat-treated spruce and poplar wood.

Keywords: VOC emissions, spruce, poplar, heat-treated wood, gas chromatography

SAŽETAK • *U radu su predstavljeni rezultati istraživanja emisije hlapljivih organskih spojeva (VOC) iz cjelovitog drva smreke (Picea abies) i drva topole (Populus alba), toplinski obrađenoga pri 180 i 200 °C. Emisije VOC-a iz toplinski obrađenog drva i iz prosušenoga neobrađenog (prirodnog) drva uspoređene su primjenom GC-MS analize. Naglasak istraživanja bio je na utjecaju temperature na kvalitetu i količinu hlapljivih organskih spojeva, posebice na količinu emitiranog fenola i furfurala. Furfural i fenol tipični su kemijski spojevi koji nastaju toplinskom degradacijom drvnih komponenata. Emisija VOC-a analizirana je u ovisnosti o vremenu nakon toplinske obrade. Istraživan je i utjecaj završne obrade drva premazima na bazi vode na emisiju VOC-a.*
Rezultati istraživanja pokazali su da toplinski obrađeno drvo emitira više VOC komponenata furfurala i fenola nego neobrađeno (prirodno) drvo. Količina emitiranog VOC-a smanjuje se s porastom vremenskog razmaka između toplinske obrade drvnih uzoraka i mjerenja emisije VOC-a. Toplinski obrađeno drvo koje je završno obrađeno

---
[1] Author is research assistant at Faculty of Forestry and Wood Technology, Mendel University in Brno, Czech Republic.
[1] Autor je znanstveni asistent Fakulteta šumarstva i drvne tehnologije, Mendelovo sveučilište u Brnu, Republika Češka.

vodenim lakom emitiralo je vrlo visoku koncentraciju butoksietanola. Završna obrada toplinski obrađenog drva vodenim lakom nije pridonijela smanjenju emisije VOC-a iz toplinski obrađenog drva smreke i topole.

Ključne riječi: *emisije hlapljivih organskih spojeva, smreka, topola, toplinski obrađeno drvo, plinska kromatografija*

1 INTRODUCTION
1. UVOD

Heat-treatment of timber is used to modify the properties of wood to resist dimensional changes in different humidity (Westin *et al.,* 2001), to achieve better heat insulation, improved decay and weather resistance, reduced deformations due to changes of equilibrium moisture content and new shades of colour as an alternative to tropical hardwood.

The heat treatment process involves exposing wood to elevated temperatures from 160 to 260 °C (Militz, 2002). The temperature and duration of heat treatment generally vary from 180 to 280 °C and 15 min. to 24 h depending on the process, wood species, sample size, moisture content of the sample and the desired mechanical properties, resistance to biological attack and dimensional stability of the final product (Militz, 2002; Kamdem *et al.*, 2002; Sanderman and Augistin, 1964).

Heat-treated wood is an eco-friendly alternative to impregnated wood materials, and heat treated wood can be used for garden, kitchen and sauna furniture, cladding on wooden buildings, bathroom cabinets, floor material, musical instruments, ceilings, inner and outer bricks, doors and window joinery and a variety of other outdoor and indoor wood applications (Syrjanen and Oy, 2001).

The main constituents of wood are cellulose, hemicelluloses, and lignin, which are accompanied by minor amounts of extractives and inorganic compounds. The volatile organic compounds (VOCs) emitted from wood during the drying process have been well investigated (Lavery and Milota, 2000; Milota, 2000), also as a function of temperature (Banerjee *et al.*,1998; Su *et al.*, 1999; Wu and Milota, 1999) and humidity (Banerjee *et al.*, 1998; Wu and Milota, 1999). The chemical changes occurring during the actual heat-treatment were also analysed (Kotilainen, 2000). Currently, there are already some reports on VOCs emitted from heat-treated wood. Since heat-treated wood materials and products are used indoors, safety and impact of these new materials on the indoor air quality should be determined. This is especially important, as it has been found that the soluble extracts of heat-treated maritime pine and poplar timber contained potentially toxic polynuclear aromatic hydrocarbon (PAH) derivatives (Kamdem *et al.*, 2000).

Heat treatment affects all the wood components, i.e. cellulose, hemicelluloses, lignin, and extractives. Emissions and degradation products of wood differ according to wood species. Differences can be especially detected between hardwood and softwood, which have different cell types (Sjöström, 1993).

Thermally modified wood is less hygroscopic and more dimensionally stable.

This has been attributed to degradation of hemicelluloses and to condensation reactions that hinder the uptake of moisture by forming new bonds between wood polymers such as lignin (Alén *et al.*, 2002; Sivonen *et al.*, 2002; Windeisen *et al.*, 2007; Tjeerdsma and Militz, 2005). Degradation of hemicelluloses may take place via formation of soluble carbohydrates, and formation of volatile products (Alén *et al.*, 2002; Windeisen and Wegener, 2009). Furans are well known thermal degradation products of polysaccharides; for example furfural (F) and 5-(hydroxymethyl) furfural (HMF) are abundant (Alén *et al.*, 2002; Peters *et al.*, 2008).

Long and Wang (2007) investigated the emissions from four common woods (spruce, poplar, masson pine, and Eucalyptus urophylla) at room temperature using high-performance liquid chromatography and gas chromatography, and the results revealed the principles of release for aldehydes and terpenes. Similarly, Hyttinen *et al*. (2010) compared the VOCs emitted from air-dried and heat-treated Norway spruce, Scots pine, and European poplar woods in an enclosed metal chamber and discovered the effect of different treatment conditions on volatile compounds.

Furfurals have a nutty smell and contribute a lot to the odour of heat-treated wood together with other substances such as maltol or acetic acid (Miller, 1998). Furfural is very volatile and an essential part of VOCs. Furfural can also evaporate from finished products.

The aim of the research was to find differences in the amount of Volatile Organic Compounds emitted by heat-treated samples at different temperatures (180 °C and 200 °C) and untreated wood without finished surface compared to those with finished surface with the waterborne lacquer. The investigation of VOC emissions emitted by heat-treated wood has to be focused on the influence of the finished surfaces of tested samples on the amount of VOC emissions.

It is very important to find correlation between the type of waterborne lacquer used for the surface finishing and VOC emissions and also to identify individual volatile organic compounds from the thermally modified wood without finishing.

2 MATERIALS AND METHODS
2. MATERIJALI I METODE

The tested woods (spruce (*Picea abies* L. Karst.) with the density of 0.41 g/cm³ and poplar (*Populus alba* L.) with the density of 0.39 g/cm³) obtained from KATRES company Ltd., Czech supplier of heat-treated wood, were investigated. The pre-dried wood samples were modified at 180 °C and 200 °C in a heat treatment process.

2.1 Density determination of test samples
2.1. Određivanje gustoće uzoraka drva

Prior to heat treatment, samples were dried in a heating oven at 103 ± 2 °C. The oven-dry weight of the samples was determined. After the heat treatment, the oven-dry weight of the same samples was re-measured. The weight loss (W_L) of the samples, caused by heat treatment, was calculated according to the following formula,

$$WL\ (\%)=100\ (W_{BH} - W_{AH})/W_{BH} \tag{1}$$

where W_{BH} is the initial oven-dry weight of the sample prior to heat treatment (g) and W_{AH} is the oven-dry weight of the samples after heat treatment (g). The equilibrium moisture content (EMC) of the test samples was determined before the tests.

The air-dried density of the samples was determined according to the following formula (ISO 3131 1975),

$$D_{12}= M_{12}/V_{12}\ (g/cm^3) \tag{2}$$

where M is the sample weight (g) and V is the sample volume (cm^3)

Untreated and heat-treated wood samples were prepared from the same tree. Air-dried wood samples were taken from the normal manufacturing process, wrapped in aluminium foils and delivered to the test laboratory.

The samples were cut into pieces with dimensions 740 mm x 40 mm x 2 mm (longitudinal, tangential, axial) and then divided into two halves.

The first half of these samples was put into the test chamber. The samples of heat-treated material were obtained directly from the production of heat-treated wood. These wood samples were also divided into two halves.

One half of these heat-treated samples were put into the chamber (ISO 16000-9, 2007) immediately after the delivery from the plant, where they were treated.

The second halves of untreated as well as heat treated samples were finished by waterborne lacquer (with non-volatile share of 35 %).

Acryl-polyurethane water dispersion is achieved with the addition of special binders and water repellents. This coating system contains about 10 % of 2-buthoxyethanol (CAS: 111-76-2); 0.05 % of Benzisothiazolinon (CAS: 2634-33-5); 0.1 % of Methylisothiazolinon (CAS: 2682-20-4); 0.015 % of reaction mixture 5-chlor-2-methylisothiazol-3(2H)- on and 2-methylisothiazol-3(2H)-on (CAS:55965-84-9).

The finished samples were placed into the chamber three hours after finishing.

2.2 Methodology of research
2.2. Metodologija istraživanja

In step 1, the samples of the air-dried wood (spruce and poplar) with an area of 1 m^2 were prepared for testing. Then, VOC emission emitted by different wood samples was collected into the desorption tubes on the sorbent Tenax TA (ISO 16000 part 1 and 5, 2007).
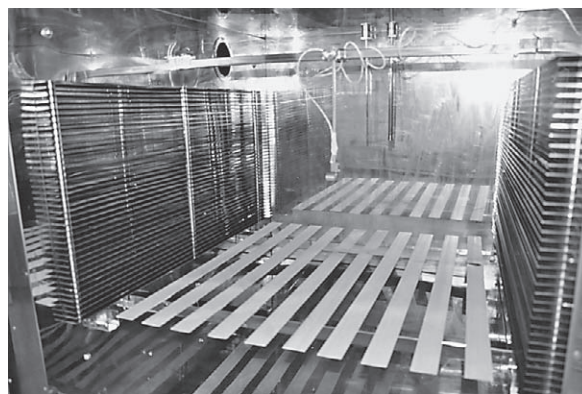
Figure 1 Testing sample in small space chamber
Slika 1. Ispitni uzorci u maloj komori

By using a gas chromatograph with a mass spectrometer and a thermal desorption, the VOC emission structure was determined along with the amount of individual emitted compounds trapped in the steel sampling tube. The conducted analyses provide qualitative and quantitative data on the concentrations of selected VOC and the total volatile organic compounds (TVOC) in $\mu g \cdot m^{-3}$.

In step 2, the pre-dried wood samples were modified at 180 °C and 200 °C in a heat treatment process. Then, VOC emission from heat treated wood was collected using the same methods as in the previous case.

In step 3, the samples of heat treated wood were finished by waterborne lacquer (brush application), whereby deposition of coating films was selected in the amount of 120 $g \cdot m^{-2}$. The curing process of this coating system is carried out using a chemical reaction (crosslinking) and evaporation of the solvent (water). The saturation time of the coating film is 2-3 hours (depending on the method of application of the coating system). Measurement of VOC emissions from test samples started 3 hours after finishing. The thickness of the dry coating film was detected by ultrasonic coating thickness gage (PosiTector 200) in range 60-70 μm.

2.3 Thermal modification process
2.3. Proces toplinske obrade

Thermal modification was carried out using a small-scale laboratory heat treatment chamber (Katres company Ltd., Czech Republic) at 180 or 200 °C. The schedule of the five-stage thermall modification process throughout 50 hours was achieved with a temperature control system. Data of the heat-treatment process was monitored by (wet and dry bulb) thermometer, consisting of two thermometers, one dry and the other kept moist with water on a sock. Values give an indication of atmospheric humidity i.e. psychrometer diference.

The maximum temperatures (180 or 200 °C) were maintained for 3h.

2.4 Air samples
2.4. Uzorci zraka

In the present study, air samples from tested samples were collected onto Tenax TA adsorbent (sampling rate 200 mL·min^{-1}, time 180 min) from small space

chamber (volume of 1 m^3). Air samples were analysed with a gas chromatograph (HP 6890) equipped with a mass selective detector (MSD 5973) after thermal desorption at 250 °C for 3 min (Scientific Instrument Services TD4). The column was HP-5MS (column length 30 m, i.d. 0.25 mm, film thickness 1 μm), and the identification of the compounds was accomplished by retention times, standard compounds, and GC-MS data library (NIS 05).

The total VOC emission was first calculated by combining the peak areas of all identified compounds, after which the relative proportion of individual compounds was calculated from the total emission. The TVOC value is defined to be the integrated detector response value in toluene equivalents of compounds eluting between and including C$_6$ to C$_{16}$ as given in ISO 16000-6.

VOC emissions from test samples were measured as a function of time (time from insertion of test sample into the test chamber).

3 RESULTS
3. REZULTATI

This research deals with VOC emissions emitted by solid Spruce (*Picea abies*) and Poplar (*Populus alba*) wood treated at 200 °C and 180 °C. The emissions of Volatile Organic Compounds from heat treated wood and air-dried (natural) wood were compared with GC-MS analysis.

VOC emissions from test samples were measured as a function of time (time from insertion of test sample into the test chamber). VOC emissions from natural wood, heat treated wood and finished surface of

Table 1 VOCs emitted by tested sample of untreated wood – spruce
Tablica 1. Emisija VOC-a iz uzoraka netretirane smrekovine

No.	Compounds *Kemijski spoj*	After 3 hours[a] *Nakon 3 sata*	After 24 hours[a] *Nakon 24 sata*	After 72 hours[a] *Nakon 72 sata*	After 672 hours[a] Nakon 672 sata
	Natural wood - untreated *Prirodno, netretirano drvo*	Spruce wood / *Drvo smreke*			
No.	Unit / *Jedinica*	μg/m^3	μg/m^3	μg/m^3	μg/m^3
1	Ethyl Acetate	< 0.1	< 0.1	(0.2 ± 0.1)	< 0.1
2	Benzene	< 0.1	(0.2 ± 0.1)	(0.2 ± 0.1)	(0.2 ± 0.1)
3	1-Methoxy-2-Propanol	(0.3 ± 0.1)[b]	(0.1 ± 0.03)	< 0.1	(0.8 ± 0.2)
4	Pentanal	(2 ± 0.6)	(1.3 ± 0.4)	(1.1 ± 0.3)	(0.6 ± 0.2)
5	Trichlorethylene	< 0.1	< 0.1	< 0.1	< 0.1
6	Toluene	(1 ± 0.3)	(1 ± 0.3)	(1.2 ± 0.4)	(2 ± 0.6)
7	Hexanal	(5.4 ± 1.6)	(4.4 ± 1.3)	(3.8 ± 1.1)	(2.1 ± 0.6)
8	Tetrachloretylene	< 0.1	(0.2 ± 0.1)	(0.2 ± 0.1)	(0.2 ± 0.1)
9	n-Butyl acetate	(1.3 ± 0.4)	(0.4 ± 0.1)	(0.9 ± 0.3)	(0.9 ± 0.3)
10	**Furfural**	**(7.8 ± 2.3)**	**(2.5 ± 0.8)**	**(1.8 ± 0.5)**	**(1 ± 0.3)**
11	Ethylbenzene	(0.7 ± 0.2)	(0.2 ± 0.1)	(0.5 ± 0.2)	(0.7 ± 0.2)
12	m,p-Xylene	(1.8 ± 0.5)	(0.8 ± 0.2)	(1.8 ± 0.5)	(2 ± 0.6)
13	Styrene	< 0.1	(0.1 ± 0.03)	< 0.1	< 0.1
14	o-Xylene	(0.4 ± 0.1)	(0.1 ± 0.03)	(0.4 ± 0.1)	(0.4 ± 0.1)
15	Butoxy-Ethanol	(0.3 ± 0.1)	(0.1 ± 0.03)	< 0.1	< 0.1
16	α-Pinene	(0.1 ± 0.03)	(0.1 ± 0.03)	(0.1 ± 0.03)	(0.3 ± 0.1)
17	Camphene	< 0.1	< 0.1	< 0.1	(0.2 ± 0.1)
18	3-Ethyl-Toluene	(0.3 ± 0.1)	(0.3 ± 0.1)	(0.3 ± 0.1)	(0.3 ± 0.1)
19	4-Ethyl-Toluene	(0.3 ± 0.1)	(0.3 ± 0.1)	(0.4 ± 0.1)	(0.3 ± 0.1)
20	1,3,5-Trimethyl-Benzene	< 0.1	< 0.1	< 0.1	< 0.1
21	**Phenol**	**(0.7 ± 0.2)**	**(0.5 ± 0.2)**	**(0.5 ± 0.2)**	**(0.3 ± 0.1)**
22	β-Pinene	(0.4 ± 0.1)	(0.4 ± 0.1)	(0.2 ± 0.1)	(0.2 ± 0.1)
23	2-Ethyl Toluene	(0.1 ± 0.03)	(0.1 ± 0.03)	(0.1 ± 0.03)	(0.1 ± 0.03)
24	Myrcene	< 0.1	< 0.1	< 0.1	< 0.1
25	1,2,4-Trimethyl-Benzene	< 0.1	(0.2 ± 0.1)	(0.2 ± 0.1)	(0.2 ± 0.1)
26	α-Phellandrene	< 0.1	< 0.1	< 0.1	< 0.1
27	3-δ-Carene	(0.6 ± 0.2)	(0.4 ± 0.1)	(0.4 ± 0.1)	(0.4 ± 0.1)
28	1,2,3-Trimethyl-Benzene	(0.1 ± 0.03)	(0.1 ± 0.03)	(0.1 ± 0.03)	(0.1 ± 0.03)
29	Limonene	(1.1 ± 0.3)	(0.4 ± 0.1)	(0.4 ± 0.1)	(0.1 ± 0.03)
30	γ-Terpinene	< 0.1	< 0.1	< 0.1	< 0.1
31	Bornyl Acetate	< 0.1	< 0.1	< 0.1	< 0.1
32	**TVOC$_{MS}$[c]**	**(44 ± 13)**	**(22 ± 7)**	**(19 ± 6)**	**(17 ± 5)**

[a] Time of measurement (time from insertion of test sample into the test chamber) / *vrijeme mjerenja (vrijeme od stavljanja uzorka u komoru do vremena provedbe mjerenja)*; [b] results are shown as average result ± expanded measurement uncertainty / *rezultati su prikazani kao prosječna vrijednost rezultata ± proširena mjerna nesigurnost*; [c] TVOC$_{MS}$ – Total Volatile Organic Compounds determined by Mass Spectrometry / *ukupna emisija hlapljivih organskih spojeva određena masenom spektrometrijom*

Table 2 VOCs emitted by tested sample of untreated wood – poplar
Tablica 2. Emisija VOC-a iz uzoraka netretirane topolovine

	Compounds *Kemijski spoj*	**After 3 hours**[a] *Nakon 3 sata*	**After 24 hours**[a] *Nakon 24 sata*	**After 72 hours**[a] *Nakon 72 sata*	**After 672 hours**[a] *Nakon 672 sata*
	Natural wood – untreated *Prirodno, netretirano drvo*	**Poplar wood** *Drvo topole*			
No.	Unit / *Jedinica*	$\mu g/m^3$	$\mu g/m^3$	$\mu g/m^3$	$\mu g/m^3$
1	Ethyl Acetate	(0.2 ± 0.1)[b]	(0.4 ± 0.1)	< 0.1	< 0.1
2	Benzene	< 0.1	< 0.1	< 0.1	< 0.1
3	1-Methoxy-2-Propanol	(0.1 ± 0.03)	< 0.1	< 0.1	(0.8 ± 0.2)
4	Pentanal	(1.6 ± 0.5)	(0.8 ± 0.2)	(0.3 ± 0.1)	(0.3 ± 0.1)
5	Trichlorethylene	< 0.1	< 0.1	< 0.1	< 0.1
6	Toluene	(0.8 ± 0.2)	(0.7 ± 0.2)	(0.5 ± 0.2)	(0.7 ± 0.2)
7	Hexanal	(10.1 ± 3)	(5.1 ± 1.5)	(0.9 ± 0.3)	(0.8 ± 0.2)
8	Tetrachloretylene	< 0.1	< 0.1	(0.2 ± 0.1)	(0.2 ± 0.1)
9	n-Butyl acetate	(1.4 ± 0.4)	(0.4 ± 0.1)	(0.8 ± 0.2)	(0.8 ± 0.2)
10	**Furfural**	**(1.3 ± 0.4)**	**(1 ± 0.3)**	**(0.3 ± 0.1)**	**(0.3 ± 0.1)**
11	Ethylbenzene	(0.7 ± 0.2)	(0.2 ± 0.1)	(0.2 ± 0.1)	(0.4 ± 0.1)
12	m,p-Xylene	(2.2 ± 0.7)	(0.7 ± 0.2)	(0.8 ± 0.2)	(1.2 ± 0.4)
13	Styrene	< 0.1	(0.1 ± 0.03)	< 0.1	(0.1 ± 0.03)
14	o-Xylene	(0.4 ± 0.1)	(0.1 ± 0.03)	(0.1 ± 0.03)	(0.3 ± 0.1)
15	Butoxy-Ethanol	(0.1 ± 0.03)	< 0.1	< 0.1	< 0.1
16	α-Pinene	< 0.1	< 0.1	(0.1 ± 0.03)	(0.1 ± 0.03)
17	Camphene	< 0.1	< 0.1	< 0.1	< 0.1
18	3-Ethyl-Toluene	(0.1 ± 0.03)	(0.1 ± 0.03)	< 0.1	(0.1 ± 0.03)
19	4-Ethyl-Toluene	(0.3 ± 0.1)	(0.3 ± 0.1)	(0.1 ± 0.03)	(0.1 ± 0.03)
20	1,3,5-Trimethyl-Benzene	< 0.1	< 0.1	< 0.1	< 0.1
21	**Phenol**	**(0.7 ± 0.2)**	**(0.8 ± 0.2)**	**(0.3 ± 0.1)**	**(0.5 ± 0.2)**
22	β-Pinene	(0.1 ± 0.03)	(0.1 ± 0.03)	(0.1 ± 0.03)	(0.1 ± 0.03)
23	2-Ethyl Toluene	(0.1 ± 0.03)	(0.1 ± 0.03)	(0.1 ± 0.03)	(0.1 ± 0.03)
24	Myrcene	< 0.1	< 0.1	< 0.1	< 0.1
25	1,2,4-Trimethyl-Benzene	< 0.1	< 0.1	< 0.1	< 0.1
26	α-Phellandrene	< 0.1	< 0.1	< 0.1	< 0.1
27	3-δ-Carene	(0.1 ± 0.03)	(0.1 ± 0.03)	(0.1 ± 0.03)	(0.2 ± 0.1)
28	1,2,3-Trimethyl-Benzene	(0.1 ± 0.03)	(0.1 ± 0.03)	(0.1 ± 0.03)	(0.1 ± 0.03)
29	Limonene	(0.1 ± 0.03)	(0.1 ± 0.03)	(0.1 ± 0.03)	(0.1 ± 0.03)
30	γ-Terpinene	< 0.1	< 0.1	< 0.1	< 0.1
31	Bornyl Acetate	< 0.1	< 0.1	< 0.1	< 0.1
32	**TVOC$_{MS}$**[c]	**(24 ± 7)**	**(13 ± 4)**	**(10 ± 3)**	**(8 ± 2)**

[a] Time of measurement (time from insertion of test sample into the test chamber) / *vrijeme mjerenja (vrijeme od stavljanja uzoraka u komoru do vremena provedbe mjerenja)*; [b] results are shown as average result ± expanded measurement uncertainty / *rezultati su prikazani kao prosječna vrijednost rezultata ± proširena mjerna nesigurnost*; [c] TVOC$_{MS}$ – Total Volatile Organic Compounds determined by Mass Spectrometry / *ukupna emisija hlapljivih organskih spojeva određena masenom spektrometrijom*

heat treated wood were monitored during one month (i.e. 28 days) according the standard ČSN EN ISO 16000-9.

The results of measurements of emissions emitted by native spruce and poplar in dependence of time after the sample preparation are shown in Tables 1 and 2.

The surface of natural wood samples was treated by grinding before insertion of the test sample into the test chamber. Therefore, the wood structure was disturbed. This fact caused gradual release of chemicals, especially aldehydes (Pentanal, Hexanal). The values of TVOC is decreasing in time.

Based on the obtained results (Tables 1 to 4), it is concluded that heat-treatment of wood increases the quantity of VOC emissions emitted by tested samples. The main difference was found in the amount of emitted furfural and phenol in the gaseous blend evaporated by heat-treated spruce and poplar in normal conditions.

The temperature of heat-treatment has a great influence on the treated wood.

The higher the temperature during spruce heat-treatment, the higher are the furfural emissions. Furfural and phenol are typical chemicals produced as a result of thermal degradation of wood components.

The surface finished by waterborne lacquer does not decrease the amount of emissions escaping from heat-treated spruce and poplar wood. Surprisingly, waterborne lacquers even elevated the amount of VOCs.

Figures 2 and 4 show the influence of wood modification temperature and of the time between the VOC measurement and wood modification. The amount of VOC emission decreases with the decreasing temperature of wood modification. The amount of emitted VOC declines with the increasing time between wood modification and measurement of VOC emissions emitted by tested samples. Heat-treated spruce wood

Table 3 VOCs emitted by tested sample of heat treated spruce wood at temperature of 180 and 200 °C
Tablica 3. Emisija VOC-a iz ispitnog uzorka toplinski obrađene smrekovine pri temperaturi 180 i 200 °C

No.	Compounds *Kemijski spoj*	Unit / *Jedinica*	180 °C				200 °C			
	Wood treatment process *Temperatura obrade drva*		After 3 hours[a] *Nakon 3 sata*	After 24 hours[a] *Nakon 24 sata*	After 72 hours[a] *Nakon 72 sata*	After 672 hours[a] *Nakon 672 sata*	After 3 hours[a] *Nakon 3 sata*	After 24 hours[a] *Nakon 24 sata*	After 72 hours[a] *Nakon 72 sata*	After 672 hours[a] *Nakon 672 sata*
			μg/m³	μg/m³	μg/m³	μg/m³	μg/m³	μg/m³	μg/m³	μg/m³
1	Ethyl Acetate		< 0.1	< 0.1	< 0.1	< 0.1	(0.2 ± 0.1)	(0.2 ± 0.1)	(0.7 ± 0.2)	< 0.1
2	Benzene		< 0.1	< 0.1	(0.2 ± 0.1)	< 0.1	(0.2 ± 0.1)	< 0.1	(0.2 ± 0.1)	< 0.1
3	1-Methoxy-2-Propanol		(0.1 ± 0.03)[b]	< 0.1	< 0.1	< 0.1	(0.1 ± 0.03)	(0.1 ± 0.03)	< 0.1	< 0.1
4	Pentanal		(0.5 ± 0.2)	(0.3 ± 0.1)	(0.3 ± 0.1)	(0.3 ± 0.1)	(0.8 ± 0.2)	(0.3 ± 0.1)	(0.3 ± 0.1)	(0.3 ± 0.1)
5	Trichlorethylene		< 0.1	< 0.1	< 0.1	< 0.1	< 0.1	< 0.1	< 0.1	< 0.1
6	Toluene		(3.5 ± 1.1)	(0.3 ± 0.1)	(0.8 ± 0.2)	(0.8 ± 0.2)	(0.8 ± 0.2)	(0.3 ± 0.1)	(0.8 ± 0.2)	(0.8 ± 0.2)
7	Hexanal		(1.3 ± 0.4)	(0.3 ± 0.1)	(0.3 ± 0.1)	(0.3 ± 0.1)	(1.3 ± 0.4)	(0.1 ± 0.03)	(0.3 ± 0.1)	(0.3 ± 0.1)
8	Tetrachloretylene		(0.2 ± 0.1)	< 0.1	(0.2 ± 0.1)	(0.2 ± 0.1)	(0.2 ± 0.1)	< 0.1	(0.2 ± 0.1)	(0.2 ± 0.1)
9	n-Butyl acetate		(2.1 ± 0.6)	(0.4 ± 0.1)	(0.6 ± 0.2)	(0.4 ± 0.1)	(1.6 ± 0.5)	< 0.1	< 0.1	(0.3 ± 0.1)
10	Furfural		(207.8 ± 62.3)	(144.5 ± 43.4)	(117.2 ± 35.2)	(39.7 ± 11.9)	(227.3 ± 68.2)	(172.8 ± 51.8)	(147.4 ± 44.2)	(49.6 ± 14.9)
11	Ethylbenzene		(1.2 ± 0.4)	(0.2 ± 0.1)	(0.4 ± 0.1)	(0.2 ± 0.1)	(0.7 ± 0.2)	(0.2 ± 0.1)	< 0.1	(0.2 ± 0.1)
12	m,p-Xylene		(4.7 ± 1.4)	(0.5 ± 0.2)	(1 ± 0.3)	(0.7 ± 0.2)	(2 ± 0.6)	(0.5 ± 0.2)	(0.2 ± 0.1)	(0.7 ± 0.2)
13	Styrene		(0.3 ± 0.1)	< 0.1	(0.1 ± 0.03)	< 0.1	< 0.1	< 0.1	< 0.1	< 0.1
14	o-Xylene		(0.8 ± 0.2)	(0.1 ± 0.03)	(0.3 ± 0.1)	(0.1 ± 0.03)	(0.4 ± 0.1)	(0.2 ± 0.1)	(0.1 ± 0.03)	(0.1 ± 0.03)
15	Butoxy-Ethanol		(0.1 ± 0.03)	< 0.1	< 0.1	< 0.1	(0.1 ± 0.03)	(0.1 ± 0.03)	< 0.1	< 0.1
16	α-Pinene		(0.8 ± 0.2)	(0.3 ± 0.1)	(0.5 ± 0.2)	(0.1 ± 0.03)	(0.3 ± 0.1)	(0.3 ± 0.1)	(0.5 ± 0.2)	(0.1 ± 0.03)
17	Camphene		(0.2 ± 0.1)	< 0.1	< 0.1	< 0.1	(0.2 ± 0.1)	(0.3 ± 0.1)	(0.2 ± 0.1)	< 0.1
18	3-Ethyl-Toluene		(0.8 ± 0.2)	(0.1 ± 0.03)	(0.3 ± 0.1)	(0.1 ± 0.03)	(0.4 ± 0.1)	(0.1 ± 0.03)	(0.3 ± 0.1)	(0.1 ± 0.03)
19	4-Ethyl-Toluene		(0.9 ± 0.3)	(0.1 ± 0.03)	(0.3 ± 0.1)	(0.1 ± 0.03)	(0.4 ± 0.1)	(0.1 ± 0.03)	(0.3 ± 0.1)	(0.3 ± 0.1)
20	1,3,5-Trimethyl-Benzene		< 0.1	< 0.1	< 0.1	< 0.1	< 0.1	< 0.1	< 0.1	< 0.1
21	**Phenol**		**(4.7 ± 1.4)**	**(3.3 ± 1)**	**(2.2 ± 0.7)**	**(1.5 ± 0.5)**	**(10.3 ± 3.1)**	**(3.7 ± 1.1)**	**(2.4 ± 0.7)**	**(1.8 ± 0.5)**
22	β-Pinene		(0.1 ± 0.03)	(0.1 ± 0.03)	(0.1 ± 0.03)	(0.1 ± 0.03)	(0.1 ± 0.03)	(0.1 ± 0.03)	(0.2 ± 0.1)	(0.1 ± 0.03)
23	2-Ethyl Toluene		(0.1 ± 0.03)	(0.1 ± 0.03)	(0.1 ± 0.03)	(0.1 ± 0.03)	(0.1 ± 0.03)	(0.1 ± 0.03)	(0.1 ± 0.03)	(0.1 ± 0.03)
24	Myrcene		< 0.1	< 0.1	< 0.1	< 0.1	< 0.1	< 0.1	< 0.1	< 0.1
25	1,2,4-Trimethyl-Benzene		(0.5 ± 0.2)	< 0.1	(0.2 ± 0.1)	< 0.1	(0.2 ± 0.1)	(0.1 ± 0.03)	(0.2 ± 0.1)	< 0.1
26	α-Phellandrene		< 0.1	< 0.1	< 0.1	< 0.1	< 0.1	< 0.1	< 0.1	< 0.1
27	3-δ-Carene		(0.2 ± 0.1)	(0.1 ± 0.03)	(0.1 ± 0.03)	(0.1 ± 0.03)	(0.2 ± 0.1)	(0.1 ± 0.03)	(0.2 ± 0.1)	(0.1 ± 0.03)
28	1,2,3-Trimethyl-Benzene		(0.1 ± 0.03)	(0.1 ± 0.03)	(0.1 ± 0.03)	(0.1 ± 0.03)	(0.1 ± 0.03)	(0.1 ± 0.03)	(0.1 ± 0.03)	(0.1 ± 0.03)
29	Limonene		(0.6 ± 0.2)	(0.2 ± 0.1)	(0.2 ± 0.1)	(0.1 ± 0.03)	(0.7 ± 0.2)	(0.1 ± 0.03)	(0.1 ± 0.03)	(0.1 ± 0.03)
30	γ-Terpinene		< 0.1	< 0.1	< 0.1	< 0.1	< 0.1	< 0.1	< 0.1	< 0.1
31	Bornyl Acetate		< 0.1	< 0.1	< 0.1	< 0.1	< 0.1	< 0.1	< 0.1	< 0.1
32	**TVOC$_{MS}$[c]**		**(98 ± 29)**	**(51 ± 15)**	**(46 ± 14)**	**(22 ± 7)**	**(90 ± 27)**	**(80 ± 24)**	**(54 ± 16)**	**(27 ± 8)**

Table 4 VOCs emitted by tested sample of heat treated poplar wood at temperature 180 and 200 °C
Tablica 4. Emisija VOC-a iz ispitnog uzorka toplinski obrađene topolovine pri temperaturi 180 i 200 °C

No.	Compounds / *Kemijski spoj*	Unit / *Jedinica*	180 °C				200 °C			
	Wood treatment process *Temperatura obrade drva*		After 3 hours[a] *Nakon 3 sata*	After 24 hours[a] *Nakon 24 sata*	After 72 hours[a] *Nakon 72 sata*	After 672 hours[a] *Nakon 672 sata*	After 3 hours[a] *Nakon 3 sata*	After 24 hours[a] *Nakon 24 sata*	After 72 hours[a] *Nakon 72 sata*	After 672 hours[a] *Nakon 672 sata*
			$\mu g/m^3$	$\mu g/m^3$	$\mu g/m^3$	$\mu g/m^3$	$\mu g/m^3$	$\mu g/m^3$	$\mu g/m^3$	$\mu g/m^3$
1	Ethyl Acetate		(0.2 ± 0.1)[b]	(0.2 ± 0.1)	< 0.1	< 0.1	(0.7 ± 0.2)	< 0.1	< 0.1	< 0.1
2	Benzene		< 0.1	< 0.1	< 0.1	< 0.1	< 0.1	(0.2 ± 0.1)	(0.2 ± 0.1)	(0.2 ± 0.1)
3	1-Methoxy-2-Propanol		(0.1 ± 0.03)	< 0.1	< 0.1	< 0.1	(0.1 ± 0.03)	(0.1 ± 0.03)	< 0.1	< 0.1
4	Pentanal		(0.5 ± 0.2)	(0.3 ± 0.1)	(0.3 ± 0.1)	(0.1 ± 0.03)	(0.5 ± 0.2)	(0.3 ± 0.1)	(0.3 ± 0.1)	(0.3 ± 0.1)
5	Trichlorethylene		< 0.1	< 0.1	< 0.1	< 0.1	< 0.1	< 0.1	< 0.1	< 0.1
6	Toluene		(0.7 ± 0.2)	(0.2 ± 0.1)	< 0.1	(0.5 ± 0.2)	(0.5 ± 0.2)	(1 ± 0.3)	(1 ± 0.3)	(1.2 ± 0.4)
7	Hexanal		(1.1 ± 0.3)	(0.3 ± 0.1)	(0.3 ± 0.1)	(0.3 ± 0.1)	(0.6 ± 0.2)	(0.3 ± 0.1)	(0.4 ± 0.1)	(0.3 ± 0.1)
8	Tetrachloretylene		(0.2 ± 0.1)	< 0.1	< 0.1	(0.2 ± 0.1)	< 0.1	(0.2 ± 0.1)	(0.2 ± 0.1)	(0.2 ± 0.1)
9	n-Butyl acetate		(3.6 ± 1.1)	(0.3 ± 0.1)	(0.9 ± 0.3)	(0.4 ± 0.1)	(0.8 ± 0.2)	(0.4 ± 0.1)	(0.1 ± 0.03)	(0.1 ± 0.03)
10	Furfural		(47.7 ± 14.3)	(32.3 ± 9.7)	(26.7 ± 8)	(13.8 ± 4.1)	(76.5 ± 23)	(48.2 ± 14.5)	(34.2 ± 10.3)	(18.7 ± 5.6)
11	Ethylbenzene		(1.7 ± 0.5)	(0.2 ± 0.1)	(0.2 ± 0.1)	(0.2 ± 0.1)	(0.4 ± 0.1)	(0.2 ± 0.1)	(0.2 ± 0.1)	(0.2 ± 0.1)
12	m,p-Xylene		(5 ± 1.5)	(0.3 ± 0.1)	(0.8 ± 0.2)	(0.7 ± 0.2)	(1.2 ± 0.4)	(0.7 ± 0.2)	(0.3 ± 0.1)	(0.5 ± 0.2)
13	Styrene		< 0.1	< 0.1	< 0.1	< 0.1	< 0.1	< 0.1	< 0.1	(0.1 ± 0.03)
14	o-Xylene		(1.1 ± 0.3)	(0.1 ± 0.03)	(0.1 ± 0.03)	(0.1 ± 0.03)	(0.3 ± 0.1)	(0.3 ± 0.1)	(0.1 ± 0.03)	(0.1 ± 0.03)
15	Butoxy-Ethanol		(0.1 ± 0.03)	< 0.1	< 0.1	< 0.1	(0.3 ± 0.1)	(0.1 ± 0.03)	< 0.1	< 0.1
16	α-Pinene		(0.1 ± 0.03)	(0.1 ± 0.03)	(0.1 ± 0.03)	(0.1 ± 0.03)	(0.1 ± 0.03)	(0.1 ± 0.03)	(0.1 ± 0.03)	(0.1 ± 0.03)
17	Camphene		< 0.1	< 0.1	< 0.1	< 0.1	< 0.1	< 0.1	< 0.1	< 0.1
18	3-Ethyl-Toluene		(0.4 ± 0.1)	(0.1 ± 0.03)	< 0.1	(0.1 ± 0.03)	(0.4 ± 0.1)	< 0.1	(0.3 ± 0.1)	(0.3 ± 0.1)
19	4-Ethyl-Toluene		< 0.1	(0.1 ± 0.03)	< 0.1	(0.1 ± 0.03)	(0.4 ± 0.1)	< 0.1	(0.3 ± 0.1)	(0.3 ± 0.1)
20	1,3,5-Trimethyl-Benzene		< 0.1	< 0.1	< 0.1	< 0.1	< 0.1	< 0.1	< 0.1	< 0.1
21	Phenol		(41.6 ± 12.5)	(33.4 ± 10.0)	(25.5 ± 7.7)	(16.3 ± 4.9)	(185.3 ± 55.6)	(93.7 ± 28.1)	(63.5 ± 19.1)	(41.7 ± 12.5)
22	β-Pinene		(0.1 ± 0.03)	(0.1 ± 0.03)	(0.1 ± 0.03)	(0.1 ± 0.03)	(0.1 ± 0.03)	(0.1 ± 0.03)	(0.1 ± 0.03)	(0.1 ± 0.03)
23	2-Ethyl Toluene		(0.1 ± 0.03)	(0.1 ± 0.03)	< 0.1	(0.1 ± 0.03)	(0.1 ± 0.03)	(0.1 ± 0.03)	(0.1 ± 0.03)	(0.1 ± 0.03)
24	Myrcene		< 0.1	< 0.1	< 0.1	< 0.1	< 0.1	< 0.1	< 0.1	< 0.1
25	1,2,4-Trimethyl-Benzene		(0.2 ± 0.1)	< 0.1	< 0.1	< 0.1	(0.2 ± 0.1)	(0.2 ± 0.1)	(0.2 ± 0.1)	(0.2 ± 0.1)
26	α-Phellandrene		< 0.1	< 0.1	< 0.1	< 0.1	< 0.1	< 0.1	< 0.1	< 0.1
27	3-δ-Carene		(0.4 ± 0.1)	(0.1 ± 0.03)	(0.1 ± 0.03)	(0.2 ± 0.1)	(0.1 ± 0.03)	(0.2 ± 0.1)	(0.1 ± 0.03)	(0.1 ± 0.03)
28	1,2,3-Trimethyl-Benzene		(0.1 ± 0.03)	(0.1 ± 0.03)	(0.1 ± 0.03)	(0.1 ± 0.03)	(0.1 ± 0.03)	(0.1 ± 0.03)	(0.1 ± 0.03)	(0.1 ± 0.03)
29	Limonene		(0.1 ± 0.03)	(0.1 ± 0.03)	(0.1 ± 0.03)	(0.1 ± 0.03)	(0.2 ± 0.1)	(0.1 ± 0.03)	(0.1 ± 0.03)	(0.1 ± 0.03)
30	γ-Terpinene		< 0.1	< 0.1	< 0.1	< 0.1	< 0.1	< 0.1	< 0.1	< 0.1
31	Bornyl Acetate		< 0.1	< 0.1	< 0.1	< 0.1	< 0.1	< 0.1	< 0.1	< 0.1
32	TVOC$_{MS}$[c]		(59 ± 18)	(52 ± 17)	(42 ± 12)	(20 ± 6)	(137 ± 41)	(112 ± 34)	(48 ± 14)	(27 ± 8)

Figure 2 Amount of Furfural and Phenol emitted by heat-treated spruce wood after 3, 24, 72 and 672 h
Slika 2. Količina furfurala i fenola koju emitira toplinski obrađena smrekovina nakon 3, 24, 72 i 672 sata

Figure 3 Comparison of TVOC from Norway Spruce – heat treated wood at 180 °C and 200 °C and untreated wood
Slika 3. Usporedba TVOC-a koju emitira smrekovina – toplinski obrađena pri 180 i 200 °C i neobrađeno (prirodno) drvo
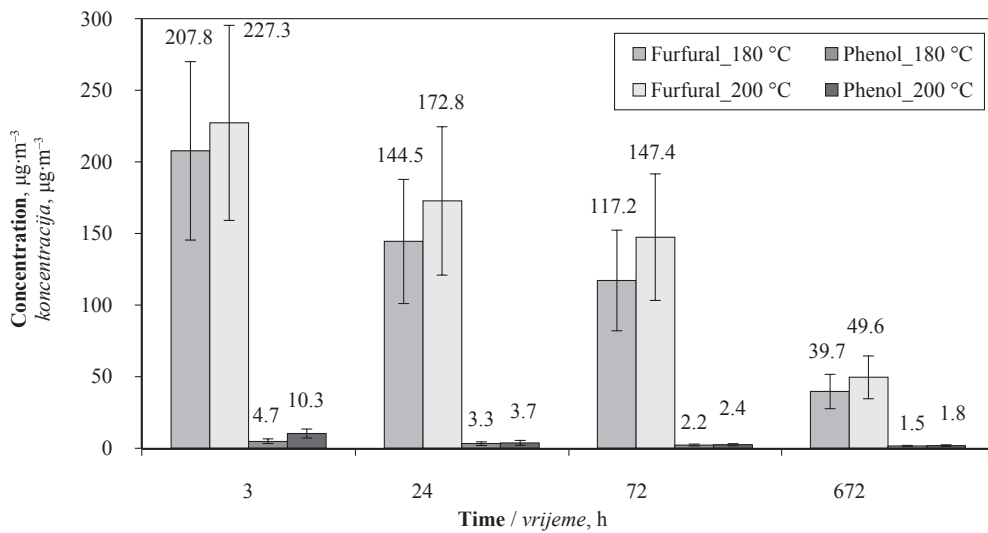

Figure 4 Amount of Furfural and Phenol emitted by heat-treated poplar wood after 3, 24, 72 and 672 h
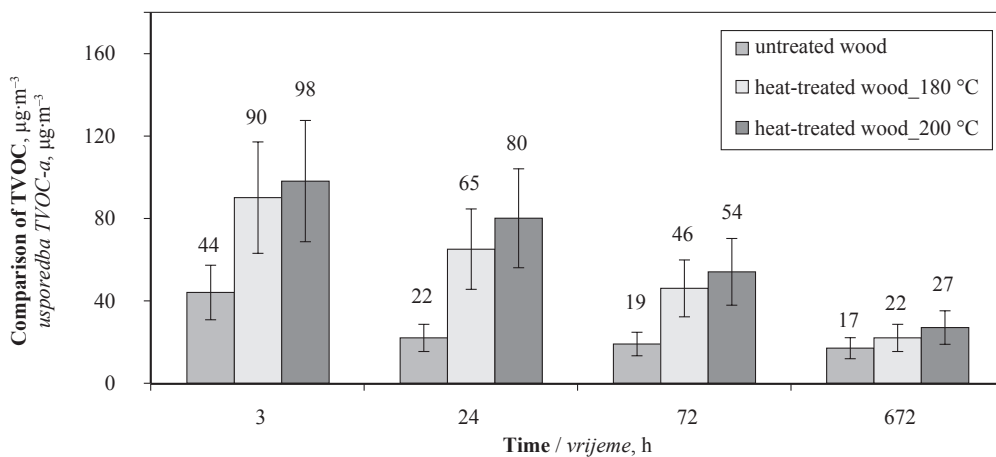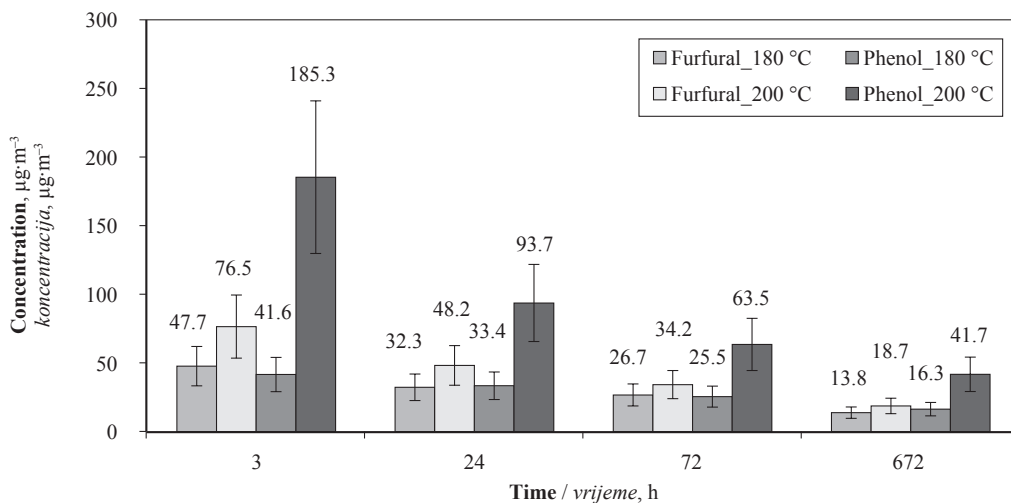**Slika 4.** Količina furfurala i fenola koju emitira toplinski obrađena topolovina nakon 3, 24, 72 i 672 sata
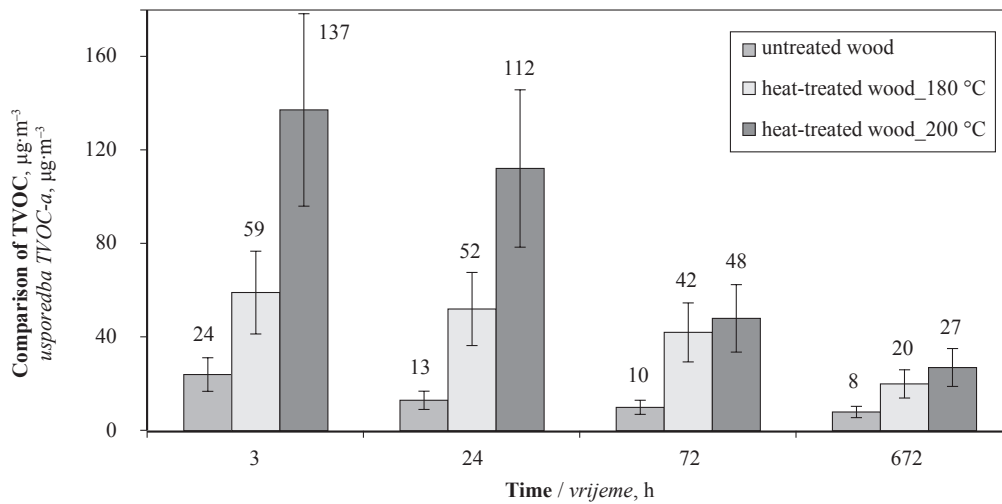
Figure 5 Comparison of TVOC from White Poplar– heat treated wood at 180 °C and 200 °C and untreated wood
Slika 5. Usporedba TVOC-a koji emitira topolovina – toplinski obrađena pri 180 i 200 °C i neobrađeno (prirodno) drvo

emitted more Fufural than Phenol, while the opposite was observed with heat-treated poplar wood.

Figures 3 and 5 show a comparison of TVOC from heat treated wood - spruce (*Picea abies*) and poplar (*Populus alba* L.) at 180 °C and 200 °C and untreated wood in dependence on time. The highest concentration of TVOC was emitted by thermowood at 200 °C. The measured values of TVOC decrease in time.

Figures 6 and 8 show the influence of wood modification temperature and of time between VOC measurement and surface finishing. The amount of VOC emission decreases with the decreasing temperature of wood modification. Heat treated spruce wood emitted a higher amount of furfural 3 hours after finishing (299 $\mu g \cdot m^{-3}$), while heat treated poplar wood emitted higher concentration of phenol (129 $\mu g \cdot m^{-3}$) after finishing.

Figures 7 and 9 present data of TVOC emitted by heat treated spruce and poplar wood before and after finishing. TVOC emitted by heat treated spruce and finishing. TVOC emitted by heat treated spruce and

poplar wood significantly increased after finishing. This phenomenon can be explained by the increase of Buthoxy-ethanol, the amount of which is shown in Figures 10 and 11.

Figures 10 and 11 show the influence of wood modification temperature and of time between VOC measurement and surface finishing. The amount of Buthoxy-ethanol can be measured 3 hours after finishing. This phenomenon can be explained by the use of waterborne lacquer for finishing of heat treated wood. Waterborne lacquer used for finishing of heat treated wood contains about ten percent of this chemical (product safety data sheet).

4 DISCUSSION
4. RASPRAVA

Based on the results of this paper, VOC emissions from natural and heat treated wood can be assessed.
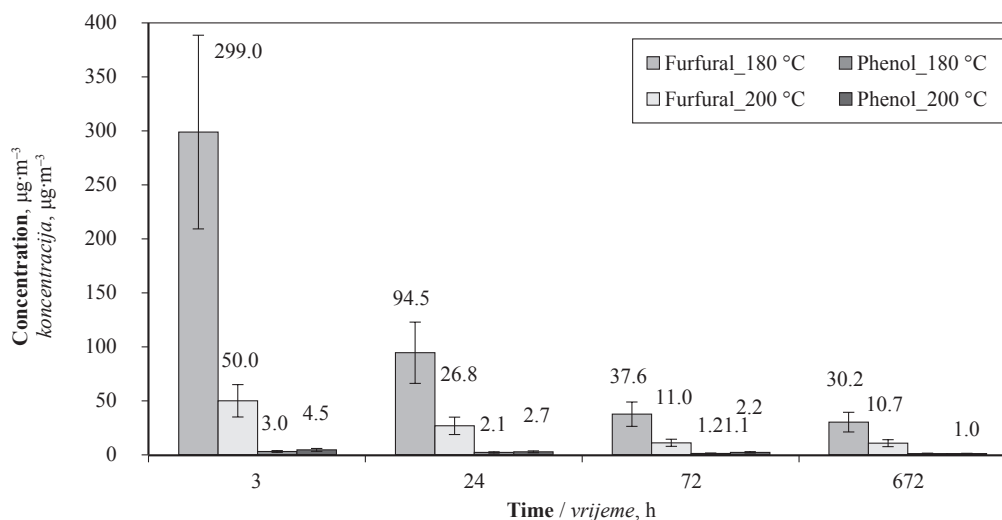
Figure 6 Amount of Furfural and Phenol emitted by heat-treated Spruce wood after finishing
Slika 6. Količina furfurala i fenola koju emitira toplinski obrađena smrekovina nakon završne obrade vodenim lakom

Figure 7 Comparison of TVOC from Norway Spruce – heat treated wood at 180 °C and 200 °C, before and after finishing
Slika 7. Usporedba TVOC-a koji emitira smrekovina – toplinski obrađena pri 180 i 200 °C, prije i nakon završne obrade vodenim lakom

Figure 8 Amount of Furfural and Phenol emitted by heat-treated Poplar wood after finishing
Slika 8. Količina furfurala i fenola koju emitira toplinski obrađena topolovina nakon završne obrade vodenim lakom

Figure 9 Comparison of TVOC from White Poplar – heat treated wood at 180 °C and 200 °C, before and after finishing
Slika 9. Usporedba TVOC-a koji emitira topolovina – toplinski obrađena pri 180 i 200 °C, prije i nakon završne obrade vodenim lakom

Figure 10 Amount of ButoxyEthanol emitted by heat-treated Spruce wood after finishing
Slika 10. Količina butoksietanola koji emitira toplinski obrađena smrekovina nakon završne obrade vodenim lakom
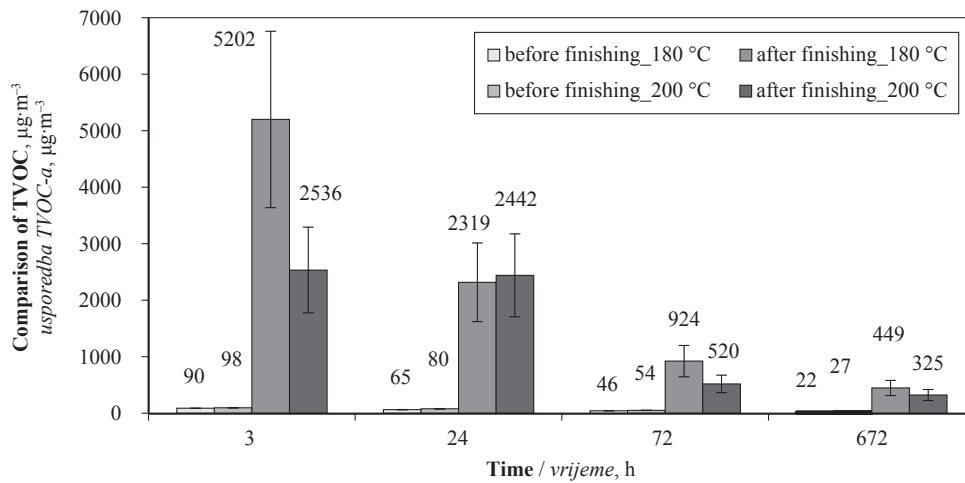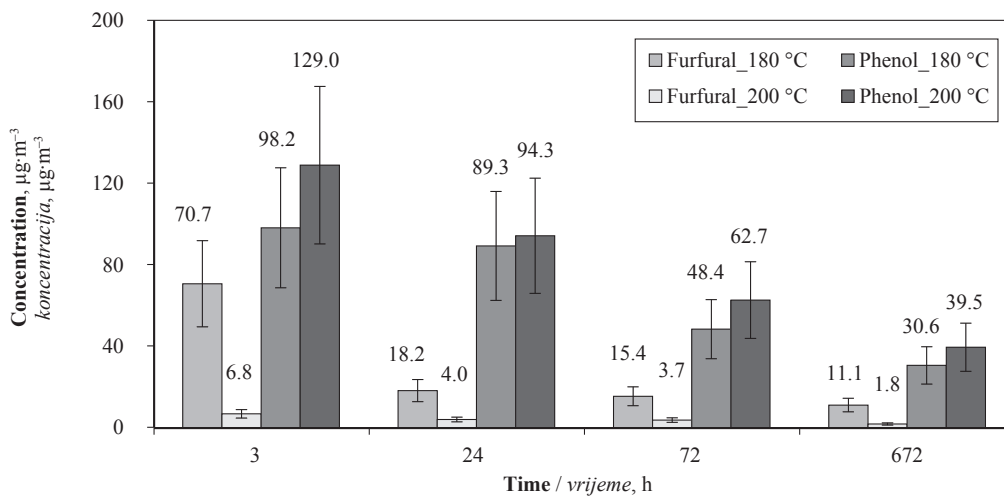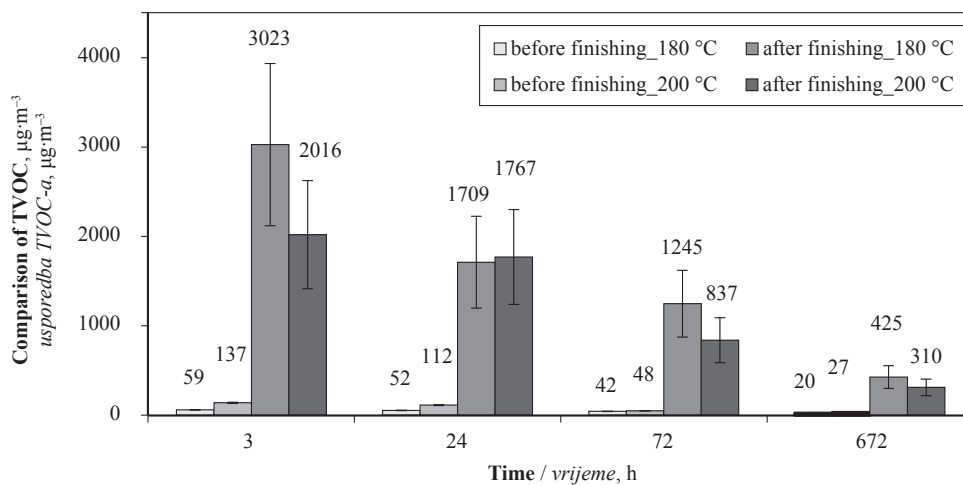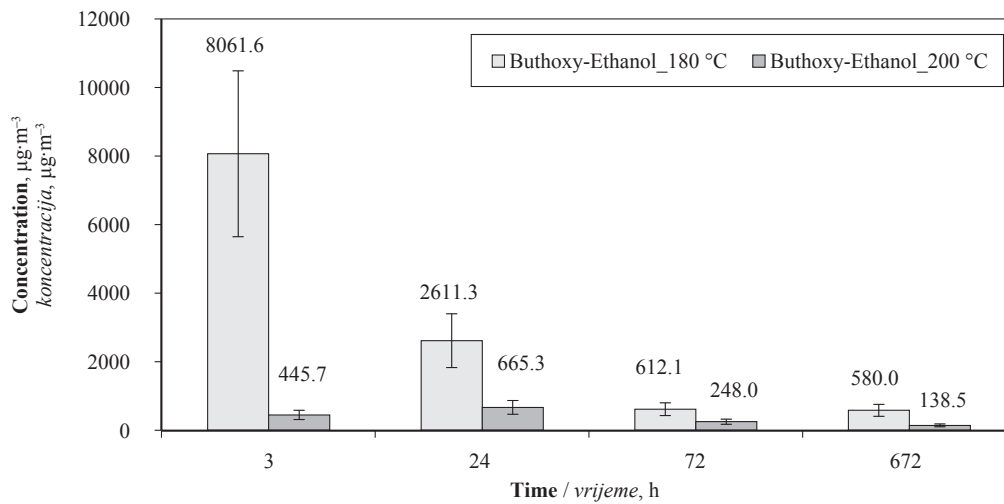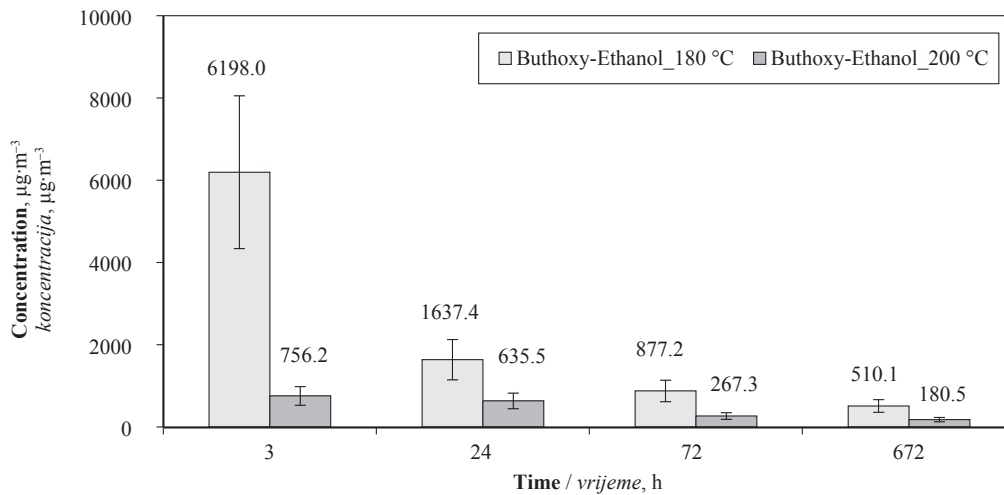

Figure 11 Amount of Buthoxy-Ethanol emitted by heat-treated Poplar wood after finishing
Slika 11. Količina butoksietanola koji emitira toplinski obrađena topolovina nakon završne obrade vodenim lakom

Natural wood

Tables 1 and 2 show the concentrations of VOCs emitted by natural, untreated, spruce and poplar wood. One of the major compounds found in our VOC collection from air-dried wood, hexanal, is known to be formed by oxidation of unsaturated fatty acids (Risholm-Sundman *et al*., 1998). Hexanal has also been a frequently analysed compound in the emissions of parquets and other wood products (Saarela, 1999).

Concentrations of other individual volatile organic compounds (VOCs) are very low and their values are comparable to background values (from 0.1 $\mu g \cdot m^{-3}$ for terpenes to almost 8 $\mu g \cdot m^{-3}$ for furfural).

Values of TVOC (Total Volatile Organic compounds) are very low; however, values decrease depending on measurement time (Hyttinen *et al.*, 2010).

Heat treated wood before finishing

The temperature of heat-treatment has a great influence on the amount of furfural emitted by tested heat-treated wood. The higher the temperature during spruce heat-treatment, the higher is the furfural emis-

sion. However, during poplar heat treatment, the phenol emission is higher compared to furfural. Furfural and phenol are typical chemicals produced as a result of thermal degradation of wood components.

Furfural and 5-hydroxymethylfurfural (HMF) are common degradation products from monosugars, where HMF is formed from hexoses, whereas furfural mainly originates from pentoses (Fengel and Wegener, 1983, Alén *et al*., 2002; Peters *et al*., 2008). Heat treated process used for thermally modified wood emitted more VOC emissions at the temperature of 200 °C than at 180 °C (Manninen *et al*., 2002). The highest amount of Furfural emitted by heat treated spruce wood at 200 °C amounted to 227 $\mu g \cdot m^{-3}$ after 3 hours, while the highest amount of Phenol emitted by heat treated poplar wood amounted to 185 $\mu g \cdot m^{-3}$, measured at the same time. Heat treated wood (spruce and poplar) emitted a very small amount of terpenes (from 0.1 to 0.7 $\mu g \cdot m^{-3}$).

Heat treated wood after finishing

The surface finished by waterborne lacquer does not decrease the amount of emissions escaping from

heat-treated spruce and poplar wood. Finished heat treated wood emitted high amounts of Butoxy-ethanol, especially by heat treated process at 180 °C (spruce emitted more than 8 000 μg·m⁻³, poplar more than 6 000 μg·m⁻³). This effect has a significant impact on the value of TVOC.

TVOC emissions were significantly higher from heat-treated than from normal, air-dried wood samples. Terpenes were the main compounds emitted from softwood (spruce) and heat-treatment decreased their emissions. Terpenes partly evaporate and partly degrade during the heat-treatment process (McGraw *et al.*, 1999). 4-Methyl-1-(1-methylethenyl)-benzene (p-cymenene) and 1-methyl-2-(1-methylethyl)-benzene (o-cymene) were detected to a higher degree in air-dried than in heat-treated softwood samples. These compounds are degradation products of camphene, delta-carene, and limonene (McGraw *et al.*, 1999).

Emissions of aldehydes (furfural and hexanal) and carboxylic acids (acetic acid) were the most dominating compounds in heat treated softwood samples. In agreement with (Peters *et al.*, 2008), emissions of furfural increased and those of hexanal decreased in heat-treated wood samples when compared to the air-dried ones. This phenomenon was observed in all wood species. This was to be expected, because hexanal belongs to the prevailing aldehydes in natural wood, whereas furfural is a major degradation product of hemicelluloses.

VOC emission profile changed dramatically during the heat treatment process. Although VOC emissions from the heat-treated samples were lower than from air-treated wood, oxidised organic compounds were also formed during the treatment. These have more unpleasant odour and are typically more irritating than terpenes, which dominate in the emissions of native softwoods. However, air-dried wood samples also emitted oxidised organic compounds, and terpenes might be oxidised to aldehydes and acids during the usage of the wood product (especially when ozone is preset in the air). In the present study, emissions of wood species were tested for a month. Actually, VOC emissions from wood (as any other materials) under constant conditions keep decreasing at least for one year. However, TVOC emissions from heat-treated wood products were relatively low already in the first days of testing.

5 CONCLUSIONS
5. ZAKLJUČAK

Based on the obtained results (Figures 2-11), it is concluded that the heat-treatment of wood increases the quantity of VOC emissions emitted by tested samples. The main difference was found in the amount of emitted furfural and phenol in the gaseous blend evaporated by heat-treated poplar under normal conditions.

The temperature of heat-treatment has a great influence on the amount of phenol and furfural emitted by tested heat-treated wood. Heat treated spruce emitted the highest amount of Furfural. The higher the temperature during the poplar heat-treatment, the higher is the phenol emission. Furfural and phenol are typical chemicals produced as a result of thermal degradation of wood components.

The surface finished by waterborne lacquer does not decrease the amount of emissions escaping from heat-treated spruce and poplar wood. Surprisingly, waterborne lacquers even elevated the amount of VOCs.

In the next step of this research, focus should be placed on the study of the influence of heat treatment on VOC emissions emitted by different kinds of wood and influence of finished surfaces of heat treated wood. It would also be important to find the correlation between the type of surface finishing and VOC emissions, i.e. to study the effect of the quality and quantity of VOC emissions emitted by heat treated wood on the way of finishing the heat-treated wood.

6 REFERENCES
6. LITERATURA

1. Alén, R.; Kotilainen, R.; Zaman, A., 2002: Thermochemical behavior of Norway spruce (*Picea abies*) at 180-225 °C. Wood Science and Technology, 36 (2): 163-171. http://dx.doi.org/10.1007/s00226-001-0133-1.
2. Banerjee, S.; Su, W.; Wild, M. P.; Otwell, L. P.; Hittmeier, M. E.; Nichols, K. M., 1998: Wet line extension reduces VOCs from softwood drying. Environmental science & technology, 32 (9): 1303-1307. http://dx.doi.org/10.1021/es970849o.
3. Čermák, P.; Rautkari, L.; Horáček, P.; Saake, B.; Rademacher, P.; Sablík, P., 2015: Analysis of Dimensional Stability of Thermally Modified Wood Affected by Re-Wetting Cycles. BioResources, 10 (2): 3242-3253. http://dx.doi.org/10.15376/biores.10.2.3242-3253.
4. Fengel, D.; Wegener, G. (eds.) 1983: Wood: chemistry, ultrastructure, reactions. Walter de Gruyter. https://books.google.cz/books?hl=cs&lr=&id=x1B4uITKnt0C&oi=fnd&pg=PA1&dq=Wood:+chemistry,+ultrastructure,+reactions.+&ots=ece_45Qs1Z&sig=HItPHZKXVSnVQvgi3Ei-l72jg6s&redir_esc=y#v=onepage&q=Wood%3A%20chemistry%2C%20ultrastructure%2C%20reactions.&f=false.
5. Hill, C. A., 2007: Wood modification: chemical, thermal and other processes (Vol. 5). John Wiley & Sons. http://dx.doi.org/10.1002/0470021748.
6. Hyttinen, M.; Masalin-Weijo, M.; Kalliokoski, P.; Pasanen, P., 2010: Comparison of VOC emissions between air-dried and heat-treated Norway spruce (*Picea abies*), Scots pine (*Pinus sylvesteris*) and European aspen (*Populus tremula*) wood. Atmospheric Environment, 44 (38): 5028-5033. http://dx.doi.org/10.1016/j.atmosenv.2010.07.018.
7. Kamdem, D. P.; Pizzi, A.; Triboulot, M. C., 2000: Heat-treated timber: potentially toxic byproducts presence and extent of wood cell wall degradation. European Journal of Wood and Wood Products, 58 (4): 253-257. http://dx.doi.org/10.1007/s001070050420.
8. Kamdem, D. P.; Pizzi, A.; Jermannaud, A., 2002: Durability of heat-treated wood. European Journal of Wood and Wood Products, 60 (1): 1-6.

http://dx.doi.org/10.1007/s00107-001-0261-1.

9. Kotilainen, R., 2000. Chemical changes in wood during heating at 150 – 260 °C. PhD Thesis, Jyvaskyla University. Research report 80, Finland. https://books.google.cz/books/about/Chemical_changes_in_wood_during_heating.html?id=EF-djwEACAAJ&redir_esc=y.

10. Lavery, M. R.; Milota, M. R., 2000: VOC emissions from Douglas-fir: Comparing a commercial and a laboratory kiln. Forest Products Journal, 50 (7/8): 39. http://search.proquest.com/docview/214640257?pq-origsite=gscholar.

11. Long, L.; Wang, J. L., 2007: Aldehyde and terpene emissions from four species of wood at normal temperature. China Wood Industry, 21 (3): 14-17. http://dx.doi.org/10.15376/biores.11.2.3550-3560.

12. Manninen, A. M.; Pasanen, P.; Holopainen, J. K., 2002: Comparing the VOC emissions between air-dried and heat-treated Scots pine wood. Atmospheric Environment, 36 (11): 1763-1768. http://dx.doi.org/10.1016/S1352-2310(02)00152-8.

13. McGraw, G. W.; Hemingway, R. W.; Ingram Jr., L. L.; Canady, C. S.; McGraw, W. B., 1999. Thermal degradation of terpenes: camphene, Δ^3-carene, limonene, and a-terpinene. Environmental Science and Technology 33: 4029-4033. http://dx.doi.org/10.1021/es9810641.

14. Militz, H., 2002. Thermal treatment of wood: European processes and their background. In: 33rd Annual Meeting, 12 – 17 May, Cardiff-Wales, IRG/WP 02-40241, 4, pp. 1-17. http://www.irg-wp.com/irgdocs/details.php?f6f6ffad-b3c3-433d-aaaa-647a154fd4c7.

15. Miller, D. D., 1998: Food chemistry – A laboratory manual, Wiley-Interscience, John Wiley & Sons, New York, Chichester, Weinhiem, Brisbane, Singapore, Toronto.

16. Milota, M. R., 2000: Emissions from wood drying: the science and the issues. Forest Products Journal, 50 (6): 10. http://search.proquest.com/docview/214640755?pq-origsite=gscholar.

17. Peters, J.; Fischer, K.; Fischer, S., 2008: Characterization of emissions of thermally modified wood and their reduction by chemical treatment. BioResources, 3 (2): 491-502. https://ojs.cnr.ncsu.edu/index.php/BioRes/article/view/BioRes_03_2_0491_Peters_FF_Emissions_Thermal_Wood.

18. Sandermann, W.; Augustin, H., 1964: Chemische Untersuchungen über die thermische Zersetzung von Holz-Dritte Mitteilung: Chemische Untersuchung des Zersetzungsablaufs. European Journal of Wood and Wood Products, 22 (10): 377-386. http://dx.doi.org/10.1007/BF02628346.

19. Risholm-Sundman, M.; Lundgren, M.; Vestin, E.; Herder, P., 1998: Emissions of acetic acid and other volatile organic compounds from different species of solid wood. Holz als Roh-und Werkstoff, 56: 125-129. https://link.springer.com/content/pdf/10.1007/s001070050282.pdf.

20. Saarela, K., 1999: Emission from floor coverings. In: Salthammer, T. (ed.). Organic Indoor Air Pollutants. Occurrence, Measurement, Evaluation. Wiley-VCH, Weinheim, pp. 185-202. https://doi.org/10.1002/9783527613663.ch14.

21. Sjöström, E., 1993: Wood chemistry. Fundamentals and Applications, second ed. Academic Press, Inc., San Diego, pp. 1-293. https://books.google.cz/books?hl=cs&lr=&id=NCkXBQAAQBAJ&oi=fnd&pg=PP1&ots=eKjlSUuE22&sig=uj1m8SzUutePmlVnpVV3hEgkA0Y&redir_esc=y#v=onepage&q&f=false.

22. Sivonen, H.; Maunu, S. L.; Sundholm, F.; Jämsä, S.; Viitaniemi, P., 2002: Magnetic resonance studies on thermally modified wood. Holzforschung, 56: 648-654. https://www.degruyter.com/view/j/hfsg.2002.56.issue-6/hf.2002.098/hf.2002.098.xml.

23. Syrjanen, T.; Oy, K., 2001: Production and classification of heat treated wood in Finland, Review on heat treatments of wood. In: Proceedings of the special seminar held in Antibes, France. http://projects.bre.co.uk/ecotan/pdf/Heat_treatment_processes_Andreas_Rapp%20.pdf.

24. Su, W.; Boerner, J. R.; Hooda, U.; Yan, H.; Banerjee, S.; Shmulsky, R.; Conners, T. E., 1999: VOC extraction from softwood through low-headspace heating. Holzforschung, 53 (6): 641-647. http://dx.doi.org/10.1515/HF.1999.105.

25. Tjeerdsma, B. F.; Militz, H., 2005: Chemical changes in hydrothermal treated wood: FTIR analysis of combined hydrothermal and dry heat-treated wood. Holz als roh-und Werkstoff, 63 (2): 102-111. http://dx.doi.org/10.1007/s00107-004-0532-8.

26. Westin, M.; Simonson, R.; Östman, B., 2001: Kraft lignin wood fiberboards – The effect of kraft lignin addition to wood chips or board pulp prior to fiberboard production. European Journal of Wood and Wood Products, 58 (6): 393-400. http://dx.doi.org/10.1007/s001070050451.

27. Windeisen, E.; Strobel, C.; Wegener, G., 2007: Chemical changes during the production of thermo-treated beech wood. Wood Science and Technology, 41 (6): 523-536. http://dx.doi.org/10.1007/s00226-007-0146-5.

28. Windeisen, E.; Wegener, G., 2009: Chemical characterization and comparison of thermally treated beech and ash wood. In Materials Science Forum, Vol. 599, pp. 143-158, Trans Tech Publications. http://dx.doi.org/10.4028/www.scientific.net/MSF.599.143.

29. Wu, J.; Milota, M. R., 1999: Effect of temperature and humidity on total hydrocarbon emissions from Douglas-fir lumber. Forest products journal, 49 (6): 52. http://search.proquest.com/docview/214624706?pq-origsite=gscholar.

30. ***ISO International Standardisation Organisation 2007: ISO 16000-1. General aspects of sampling strategy. Geneva: International Organization for Standardization.

31. ***ISO International Standardisation Organisation 2007: ISO 16000-5. Sampling strategy for volatile organic compounds (VOCs). Geneva: International Organization for Standardization.

32. ***ISO International Standardisation Organisation 2007: ISO 16000-6. Determination of volatile organic compounds indoor and test chamber air by active sampling on Tenax TA® sorbent, thermal desorption and chromatography using MS/FID. Geneva: International Organization for Standardization.

33. ***ISO International Standardisation Organisation 2007: ISO 16000-9. Determination of emissions of volatile organic compounds from building materials and furniture – test chamber method. Geneva: International Organization for Standardization.

Corresponding address:

Ing. PETR ČECH, Ph.D.

Department of Furniture, Design and Habitation
Faculty of Forestry and Wood Technology
Mendel University in Brno – Zemědělská 3,
Brno, 613 00, CZECH REPUBLIC
e-mail: Cech.P007@seznam.cz

↳in Laboratorij za ispitivanje namještaja i dijelova za namještaj

Dobra suradnja s proizvođačima, uvoznicima i distributerima namještaja čini nas prepoznatljivima

Kvaliteta namještaja se ispituje i istražuje, postavljaju se osnove normi za kvalitetu, razvijaju se metode ispitivanja, a znanost i praksa, ruku pod ruku, kroče naprijed osiguravajući dobar i trajan namještaj s prepoznatljivim oznakama kvalitete. Kvalitete koja je temelj korisniku za izbor namještaja kakav želi. Taj pristup donio je Laboratoriju za ispitivanje namještaja pri Šumarskom fakultetu međunarodno priznavanje i nacionalno ovlaštenje te članstvo u domaćim i međunarodnim asocijacijama, kao i suradnju s vodećim europskim institutima i laboratorijima.

Laboratorij je član udruge hrvatskih laboratorija CROLAB čiji je cilj udruživanje hrvatskih ispitnih, mjeriteljskih i analitičkih laboratorija u interesu unaprjeđenja sustava kvalitete laboratorija te lakšeg pridruživanja europskom tržištu korištenjem zajedničkih potencijala, dok je Šumarski fakultet punopravni član udruženja INNOVAWOOD kojemu je cilj doprinijeti poslovnim uspjesima u šumarstvu, drvnoj industriji i industriji namještaja s naglaskom na povećanje konkurentnosti europske industrije.

Istraživanje kreveta i spavanja, istraživanja dječjih krevetića, optimalnih konstrukcija stolova, stolica i korpusnog namještaja, zdravog i udobnog sjedenja u školi, uredu i kod kuće neka su od brojnih istraživanja provedena u Zavodu za namještaj i drvne proizvode, kojima je obogaćena riznica znanja o kvaliteti namještaja.

---

akreditirani laboratorij za ispitivanje kvalitete namještaja i dijelova za namještaj prema HRN EN ISO/IEC 17025

56 akreditiranih metoda u području ispitivanja namještaja, dječjih igrališta i opreme, boja i lakova

ispitivanje materijala i postupaka površinske obrade

istraživanje drvnih konstrukcija i ergonomije namještaja

ispitivanje zapaljivosti i ekologičnosti ojastučenog namještaja

sudska stručna vještačenja

Znanje je naš kapital

CROLAB   INNOVAWOOD   LGA   AIDIMA

Jaroslav Kljak, Nikola Španić, Vladimir Jambreković

Comparison of Finite Element Models for Particle Boards with Homogenous and Three-Layer Structure

Usporedba simulacijskih modela za ploče iverice homogene i troslojne strukturne građe

ABSTRACT • *This paper shows the results of finite element (FE) models of three-layer particle boards. Two particle board FE models were made with differently defined structures. In the first model, the structure of commercial three-layer particle board is defined as single-layer with isotropic (PB-1L) properties, while in the second model, it is defined as three-layer with orthotropic properties (PB-3L). The results of FE models were compared with values obtained by testing the commercial particle board. Dimensions of FE models and applied loads were prepared according to bending strength testing mode defined according to EN 310:1993. Model comparison is based on comparison of sample deflection and von Mises stress in the middle of the sample. The analysis was done only in linear elastic region. The obtained results show that models with homogenous material (PB-1L) achieved greater agreement with measured results (deviation app. 2 %), while models with three-layer material (PB-3L) displayed deviation of app. 7 %. Lower agreement of results obtained for PB-3L model and measured values of commercial particle board is due to a greater number of approximations (elastic characteristics) involved in the simulation model. Despite the greater deviation, the preparation of a three-layer model would be more acceptable for the analysis of strain distribution across the cross-section of the particle board.*

Key words: particle board, structure, finite element (FE) model, bending properties

SAŽETAK • *U radu su prikazani rezultati ispitivanja simulacijskih modela troslojne ploče iverice. Izrađena su dva simulacijska modela iverice različito definirane strukturne građe. U prvom je modelu strukturna građa komercijalne troslojne ploče iverice definirana kao jednoslojna, s izotropnim (PB-1L) svojstvima, a u drugom je modelu definirana kao troslojna ploča ortotropnih svojstava (PB-3L). Vrijednosti simulacijskih modela uspoređene su s komercijalnom pločom ivericom. Dimenzije i opterećenja simulacijskih modela izrađeni su prema načinu ispitivanja savojnog opterećenja definiranoga normom EN 310:1993. Usporedba modela temelji se na usporedbi veličine progiba te von Misesovih naprezanja na sredini dužine uzorka. Analiza je provedena samo u linearno elastičnom području. Dobiveni rezultati pokazuju da je za model homogene građe (PB-1L) zabilježena veća podudarnost s mjernim rezultatima (odstupanje je iznosilo približno 2 %), dok je za modela troslojne građe (PB-3L) odstupanje bilo nešto veće (približno 7 %). Manja podudarnost rezultata dobivenih za model PB-3L nego za mjerne rezultate komercijalne ploče posljedica je većeg broja aproksimacija pri definiranju elastičnih svojstava ploče. Unatoč većem odstupanju, izrada troslojnih modela bila bi prihvatljivija za analizu raspodjele naprezanja po poprečnom presjeku ploče iverice.*

Ključne riječi: ploča iverica, strukturna građa, simulacijski model, savojna svojstva

---

[1] Authors are associate professor, assistant professor and professor at University of Zagreb, Faculty of Forestry, Department of Material Technologies, Zagreb, Croatia.
[1] Autori su izvanredni profesor, docent i redoviti profesor Zavoda za tehnologije materijala, Šumarski fakultet Sveučilišta u Zagrebu, Zagreb, Hrvatska.

1 INTRODUCTION
1. UVOD

Particle boards are most commonly made as three-layer boards, where face layers are made from wood chips with smaller dimensions (passing through sieves with openings from approx. 0.125 to 2.0 mm), with core layer made from slightly larger wood chips (approx. 0.355 to 4.0 mm). Using different types of wood chips, different layers are formed according to physical and mechanical properties such as density, porosity, strength, modulus of elasticity, etc. However, in standard practice, only the properties of the entire particle board are stated, regardless of the composition of its layers. Based on such expression of properties, the particle board is often viewed as a homogeneous and one-layer material, ignoring the differences in their layers, which in standard use does not represent a significant problem. On the other hand, when determining, optimizing or analysing the structure, the difference between the layers has an important role and their properties are determined by various non-destructive or destructive methods (Archanowicz *et al.*, 2013; Kazemi Najafi *et al.*, 2005; Standfest *et al.*, 2009; Standfest *et al.*, 2010). Wong *et al.*, (1999) gave a detailed analysis and comparison of the properties of particle boards with homogeneous distribution of profile density and classical U-distribution of profile density. They have concluded that commercial boards have better properties than homogeneous boards, because of their U-distributions. In further study, the effect of profile density on particle board properties was analysed by means of the finite element method (FEM) using a 2D finite element (FE) model (Wong *et al.*, 2003). A FE model was created, based on which particle board properties can be predicted. However, in order to carry out further research, that is to make a more realistic 3D particle board analysis, it is necessary to determine all nine elastic characteristics on the assumption that the particle board is a material with orthotropic properties. This is shown in the papers (Wilczyński and Kociszewski, 2011, 2012), where all nine elastic characteristics were experimentally determined, their values being based on commercial type P4 particle boards. All nine elastic characteristics are specifically determined for face and core layers. The elastic characteristics for the whole particle board were experimentally determined for type P2 board (Archanowicz *et al.*, 2013), where particular characteristics from the literature were used. The data obtained from the conducted researches are very useful for the development of 3D FE models, but the problem arises because the standard division (according to EN 312:2010) classifies the particle boards in seven different classes of use (P1 to P7) and eight to ten thickness classes (as depending on class of use). Experimental determination of elastic characteristics for all classes of use and all thickness classes is a very demanding job seen either from a technical or economic aspect. However, to make the results of previous researches appropriate for the analysis of other particle boards, it would be necessary to define the ratios between the individual elastic characteristics and to apply

them to other types of boards. The principle of calculating individual elastic characteristics based on their mutual ratios for solid wood is reported by Kretschmann (2010). However, the question is whether the principles that apply to solid wood could be successfully applied to particle boards, especially in the analysis of particle board of different use class with different thickness. Various authors have reported that, in case of layered wood based panels, the thicknesses and properties of individual layers as well as their mutual ratios have significant influence on changes of bending properties such as deflection, force at the proportional limit and point of rupture. Additionally, it is stated that ratios of individual layers also contribute to changes of bendability and bending coefficient (Gaff *et al.*, 2015a; Gaff *et al.*, 2015b; Ruman *et al.*, 2017; Svoboda *et al.*, 2017). Such results confirm the importance of particle board analysis as multi-layered material and partially explain the influence that individual layers have on the properties of the entire board. The results obtained for layered wood based materials could be used to predict particle board tensile properties (Gašparík *et al.*, 2017). However, the data regarding the elongation of individual particle board layer (outer or core layer) and ratios of their proportionality limits and fracture forces should not be neglected. No data that would define the elasto-plastic behaviour of particle boards have been found in available literature and this significantly complicates the prediction of their properties. Unlike particle boards, when predicting elasto-plastic behaviour of solid wood, useful data could be obtained regardless whether the tensile, compression or bending load is applied, with 16% deviation between the FE model and experimentally obtained values (Milch *et al.*, 2016). If only the predictions of the results in elastic portion of the load-deflection curve and in the field of shear behaviour are determined, the deviations are even smaller as they are only around 7 % for Norway spruce and 0.5 % for European beech (Milch *et al.*, 2017).

Based on the above, the objectives of this paper have been set:

1. Define the elastic characteristics of 10 mm thick, three-layer type P2 particle board, retaining the experimentally determined elastic characteristics on the basis of the results of previous researches (Wilczyński and Kociszewski, 2012), and (Archanowicz *et al.*, 2013)

2. Create a 3D FE model for a one-layer particle board with isotropic properties (PB-1L) and a three-layer particle board with orthotropic properties (PB-3L),

3. Compare the values of the FE models with the experimental results of the commercially available 10 mm thick type P2 particle bord (PB-com).

2 MATERIALS AND METHODS
2. MATERIJALI I METODE

Physical properties of commercial three-layer type P2 particle board used in the experiment were as follows: thickness = 10.76 mm (determined according to EN 325:2012), density = 0.622 g·cm⁻³ (EN 323:1993)
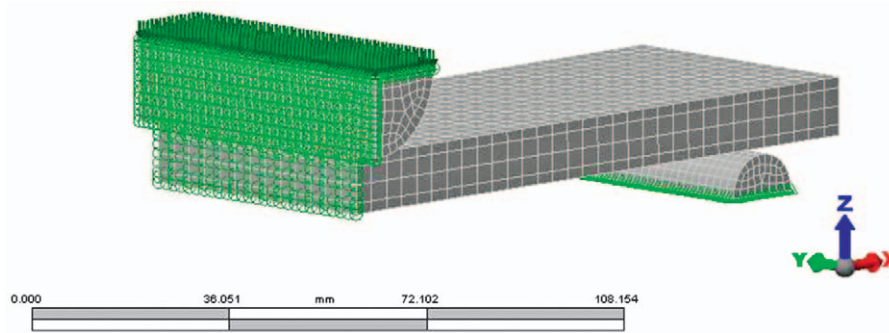
Figure 1 Finite element (FE) model for determination of bending properties according to EN 310:1993 (only half of the test sample is shown due to load symmetry)
Slika 1. Simulacijski model za određivanje savojnih svojstava prema EN 310:1993 (zbog simentričnosti opterećenja prikazano je samo pola ispitnog uzorka)

and water content = 9.02 % (EN 322:1993). Mechanical properties (bending strength (f_m) and modulus of elasticity (MOE)) were determined in accordance with EN 310:1993 and were as follows: f_m = 13.2 N·mm^{-2} and MOE = 2167 N·mm^{-2}. In total, 12 particle board samples were experimentally tested (F_{mean} = 264.6 N; F_{min} = 201.6 N; F_{max} = 311.2 N; COV = 13.85 %). However, in order to obtain a more realistic FE model, it was created based on actual dimensions (width = 51.0 mm; thickness = 10.8 mm) of a single randomly chosen sample. For the same reason, the value of force used in developing the FE model was 130 N as obtained for individually chosen sample. Half of the actual value was used as, due to load symmetry, only half model was created.

To create FE model, software package Autodesk Simulation mechanical 2015 – Educational Institution Version was used. The 3-point bending numerical model was created as a half model with definition of symmetrical boundary conditions, see Figure 1. Brick elements with midside nodes were used to create a FE model. 3D mesh size was generated automatically by simulation software. The force used to make the model and load-deflection curves (Figure 2) was up to 40 % of the fracture force (i.e. 0.1 F_{max}, 0.2 F_{max}, 0.3 F_{max} and 0.4 F_{max}) so as to perform the analysis only within the limits of the linear elastic region. The thickness of each face layer was 2.0 mm and of the core layer 6.8 mm. To avoid the effect of different meshing techniques on the result, both FE models had the same layout of the elements. FE models differed only in the values of elastic characteristics. The geometry of the FE model with the support and the force layout is shown in Figure 1. The model was loaded by force (130 N) applied vertically in negative z direction. Lower fixed point (support) had fixed degree of freedom (DOF), while upper support and particle bord sample had plane of symmetry to allow their movement in the z direction. The marks x-, y-, z- indicate the direction of the boards - length, - width, - thickness and the directions of the elastic characteristis E_x, E_y and E_z, respectively.

The elastic characteristics of the commercial particle board were unknown except for the global modulus of elasticity measured on the universal testing machine (MOE = 2167 N·mm^{-2}).

This value of MOE was the basic value for determining other elastic characteristics. Determination of elastic characteristics was based on results of previous measurements (Wilczyński and Kociszewski, 2012) by retaining the ratio between individual elastic characteristics. The face and core layer ratios (Table 1) were adopted according to Wilczyński and Kociszewski (2012), and then the elastic characteristics values were calculated (Table 2). The principle of defining the values of the ratio between individual elastic characteristics was adapted from Kretschmann (2010), taking into consideration that these values refer to the orthotropic properties of solid wood rather than those of particle boards.

Poisson ratios were not calculated but were considered as constants. The basis for this approach is found in the fact that the difference in Poisson ratios between the face and core layers is only a few percent (Wilczyński and Kociszewski, 2012). Nonetheless, these differences may vary considerably as shown for the MDF board (Sebera *et al.*, 2014). Although the differences in the Poisson ratios are undoubtedly present, they are relatively small if compared with the differences in the structure of the layers (the type and size of wood chips, density and porosity), where these differences are more noticeable. So a small percentage difference between Poisson ratios was also the basis for introducing an approximation (assumption) that the Poisson ratios values remain unchanged for all board types. When creating a second FE model, i.e. one-layer (homogeneous) particle board with isotropic properties, the usual value of 0.3 was used for the Poisson ratio.

In addition to determining the ratio of elastic characteristics, it was necessary to determine the MOE (in x- direction) for each layer. The measured MOE value (2167 N·mm^{-2}) referred to the properties of the entire board, where MOE values for the face and core layers were not known. To determine the MOE of each layer, ratios of previous research results were used (Archanowicz *et al.*, 2013). In the above research, MOE values are specified for the entire board (MOE = 2680 N·mm^{-2}) as well as for its individual layers (face layer MOE = 3050 N·mm^{-2}; core layer MOE = 1490 N·mm^{-2}). This difference in percentage values was used to determine the properties of experimentally examined commercial type 2 particle board. So, the MOE

Table 1 Elastic constants ratios for the particle board
Tablica 1. Omjeri elastičnih konstanti za ploču ivericu

Elastic ratio[a] *Elastični omjer*	Face layer *Vanjski sloj*	Core layer *Središnji sloj*
E_T/E_L	0.862	0.874
E_R/E_L	0.111	0.126
G_{LT}/E_L	0.363	0.410
G_{LR}/E_L	0.077	0.104
G_{TR}/E_L	0.074	0.099
Poisson ratio[b] / *Poissonov broj*		
ν_{xy}	0.27	0.28
ν_{yx}	0.23	0.23
ν_{xz}	0.35	0.34
ν_{yz}	0.35	0.30
ν_{zx}	0.04	0.04
ν_{zy}	0.05	0.05

[a] Elastic ratios were adopted from Wilczyński and Kociszewski (2012) (e.g. $E_T = 3.82$; $E_L = 4.43$) and after that calculated (e.g. $E_L/E_T = 3.82/4.43 = 0.862$) / *elastični omjeri preuzeti su iz rada Wilczyński i Kociszewski (2012) (e.g. $E_T = 3,82$; $E_L = 4,43$) i nakon toga izračunani (e.g. $E_L/E_T = 3,82/4,43 = 0.862$);*
[b] Poissons ratios were adopted from Wilczyński and Kociszewski (2012) / *Poissonovi brojevi preuzeti su iz rada Wilczyński i Kociszewski (2012.)*

Table 2 Elastic constants (calculation values) used in creating of FE model
Tablica 2. Elastične konstante (proračunske vrijednosti) za izradu simulacijskog modela FEM

Elastic ratio *Elastični omjer*	Orthotropic model *Ortotropni model* (Calculated values) *(proračunske vrijednosti)*		Isotropic model *Izotropni model*
	Face layer *Vanjski sloj*	Core layer *Središnji sloj*	Entire board *Cijela ploča*
E_L	2465	1204	
E_T	2125	1052	
E_R	273	152	
G_{LT}	895	493	$E_L = 2167$[a]
G_{LR}	190	125	
G_{TR}	182	119	
Poisson ratio / *Poissonov broj*			
ν_{xy}	0.27	0.28	
ν_{yx}	-	-	
ν_{xz}	0.35	0.34	
ν_{yz}	0.35	0.30	$\nu_{xy} = 0.3$
ν_{zx}	-	-	
ν_{zy}	-	-	

[a] Measured value / *izmjerena vrijednost*

of the core layer is 55.6 % lower than the MOE of the entire board, while the MOE of the face layer is 13.8 % higher than the MOE of the entire board (Table 2).

3 RESULTS AND DISCUSSION
3. REZULTATI I RASPRAVA

The results of the deflection for the control particle board and the FE models are shown in Figure 2 and Table 3. From load-deflection curves made based on data obtained from 0.1 to 0.4 F_{max} (Figure 2), it is apparent that the values of both FE models match the values of control (commercial) particle board with high-accuracy. Table 3 clearly shows that the FE model PB-1L has fewer and almost insignificant deviations (app. 2 %) than the control particle board, while the PB-3L model has slightly larger deviations (app. 7 %), both of which are significantly lower than the obtained COV value (13.85 %). This is because PB-1L modelling used the actual (measured) value of the MOE, while the MOE of the PB-3L model was calculated. The uncertainty of the calculation values stems from the fact that the literature values of the elastic characteristics are determined on different types of particle boards of different thickness. Additional reason of larger deviation of the results for the PB-3L board is the approximation of the structure in the creation of this model. Namely, the actual distribution of the profile density is carried out gradually, whereby the density of the board gradually decreases from the face layer towards the core layer. In the FE model, the transition from the face

to the core layer is stepwise, i.e. there is no transition area in the middle. Due to the larger share of the core layer compared to the actual particle board, a model with a slightly larger deflection (less stiff) is obtained. Although models of the profile density and density predictions of particle boards can be found in the literature (Suo and Bowyer, 1994; Zhou *et al.*, 2011; Gamage and Setunge, 2015), it is necessary to define the correlation ratios of density and MOE to define the elastic properties of each layer.

Examining the stress values in the particle board, it is evident that there is a significant difference only in the distribution of stress. In the three-layer orthotropic model, the role of face layers is more distinct as, due to their higher mechanical properties, they take more stress and thus relieve the core layer. Von Mises stress values at
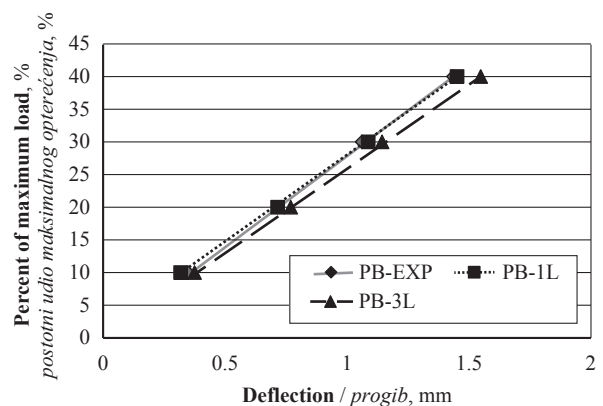

Figure 2 Load-deflection curves within the region of elastic deformation (EN 310:1993)
Slika 2. Krivulje progiba – opterećenja unutar raspona elastične deformacije (EN 310:1993)
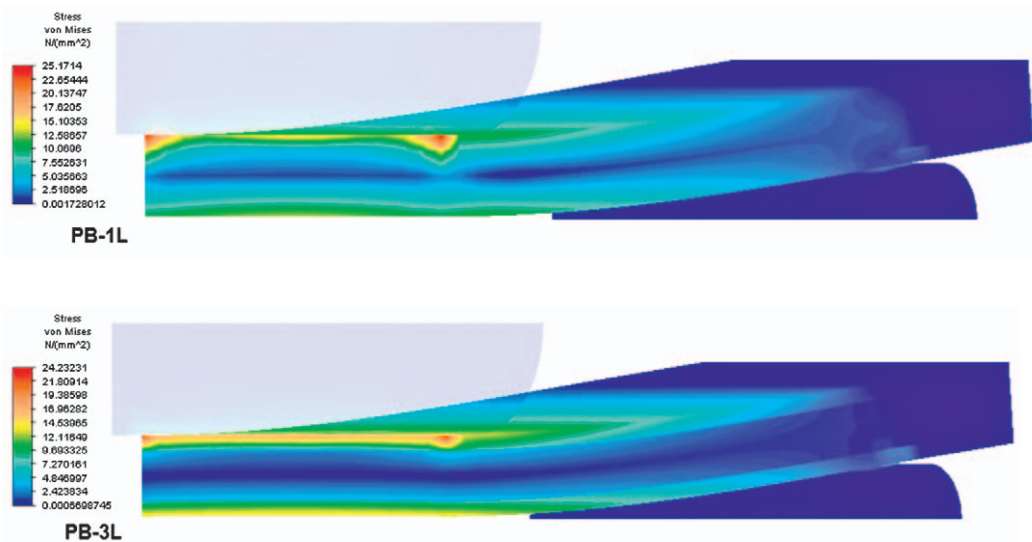
Figure 3 Values and distribution of von Mises stresses for PB-1L and PB-3L boards (Upper support surfaces are shaded for better stress display)
Slika 3. Vrijednosti i raspodjela von Misesovih naprezanja za ploče PB-1L i PB-3L (površine gornjeg oslonca osjenčane su radi boljeg prikaza naprezanja)

Table 3 Deflection values for examined particle board and FE models
Tablica 3. Vrijednosti progiba ispitivane ploče iverice i simulacijskih modela

Percentage of max load	Deflection / *Progib*, mm		
Postotni udio maksimal-nog opterećenja %	**PB-EXP**	**PB-1L**	**PB-3L**
10	0.35	0.32	0.37
20	0.71	0.72	0.77
30	1.06	1.09	1.14
40	1.44	1.45	1.55

F_{max} are shown in Figure 3. The maximum values of the von Mises stresses are not significantly different (24.2 N·mm⁻² for PB-3L and 25.17 N·mm⁻² for PB-1L) and occur on the upper side of the experimental sample directly below the central support, where in actual measurement local retraction of face layer forms.

For the analysis of bending strength, stresses from the underside of the sample were observed at the middle of the length, where in reality the fracture of the test sample was formed. The control particle board (PB-EXP) had a bending strength of (f_m = 13.2 N·mm⁻²) as determined at F_{max}. In the FE model, the values determined at F_{max} were similar to PB-1L (f_m = 13.0 N·mm⁻²), while for the PB-3L model, it was slightly higher (f_m = 14.8 N·mm⁻²). Although the results of the FE model are only based on the linear analysis, it is evident that the particle board strength can be predicted with satisfactory accuracy.

Based on these results, it can be concluded that the literature data for one type of particle board can be used to predict the properties of the other type and other thickness of particle board. It is also evident that the average deviation of the simulation values from the actual values is about 7 %, which is acceptable considering a small number of known (measured) elastic characteristics. However, the variability of experimental results (COV = 13.85 %) and the fact that the FE model was only based on literary values (except the global MOE) must be taken in consideration.

4 CONCLUSIONS
4. ZAKLJUČAK

Based on the results of the FE model and the standardized method of determining the bending properties of the particle board, it can be concluded that modelling can achieve satisfactory results in solving real (practical) problems as to whether the particle board is defined as a one-layer board with isotropic properties or three-layer board with orthotropic properties. More precise results were achieved using a one-layer isotropic model (app. 2 % deviation), while a slightly higher deviation from the control sample was observed in the three-layer orthotropic model (app. 7 %). The reason for a higher deviation in the three-layer orthotropic model is the introduction of a greater number of approximations of particular properties. Based on the MOE value of the entire board, it is not possible to precisely determine the MOE values of individual layers (face and core), the transition layer properties between these two layers are not yet defined, and a more significant approximation of Poisson ratios is also performed. However, in spite of the greater number of approximations, the deviation of the obtained results from the realistic results is about 7 %, which can be considered acceptable. However, for a more realistic stress distribution analysis, the three-layer (or multilayer) model should be a priority because the inhomogeneity of the three-layer particle board is very noticeable both from the aspect of mechanical and physical properties.

It can also be concluded that by retaining the elasticity properties ratio of the type P4 particle board (18 mm) and using the same Poisson ratios, it is possi-

ble to relatively successfully predict the properties of particle board from different class of use (P2) and of different thickness (10 mm).

5 REFERENCES
5. LITERATURA

1. Archanowicz, E.; Kowaluk, G.; Niedziński, W.; Beer, P., 2013: Properties of particleboards made of biocomponents from fibrous chips for FEM modeling. BioResources, 8 (4): 6220-6230.
http://doi.org/10.15376/biores.8.4.6220-6230.

2. Gaff, M.; Gašparík, M.; Borůvka, V.; Haviarová, E., 2015a: Stress simulation in layered wood-based materials under mechanical loading. Materials and Design, 87: 1065-1071.
http://dx.doi.org/10.1016/j.matdes.2015.08.128.

3. Gaff, M.; Gašparík, M.; Borůvka, V.; Babiak, M., 2015b: Simulating stresses associated with the bending of wood using a finite element method. BioResources, 10 (2): 2009-2019.
http://doi.org/10.15376/biores.10.2.2009-2019.

4. Gamage, N.; Setunge, S., 2015: Modelling of vertical density profile of particleboard, manufactured from hardwood sawmill residue. Wood Material Science & Engineering, 10 (2): 157-167.
http://dx.doi.org/10.1080/17480272.2014.923043.

5. Gašparík, M.; Gaff, M.; Babiak, M., 2017: Tension stress simulations of layered wood using a finite element method. Wood research, 62 (4): 517-528.

6. Kazemi Najafi, S.; Bucur, V.; Ebrahimi, G., 2005: Elastic constants of particleboard with ultrasonic technique. Materials Letters, 59: 2039-2042.
http://dx.doi.org/ 10.1016/j.matlet.2005.02.013.

7. Kretschmann, D. E., 2010: Mechanical properties of wood. U: R. J. Ross (ed.): Wood handbook – Wood as an engineering material. Madison, Wisconsin, Forest Products Society, pp. 86-88.

8. Milch, J.; Tippner, J.; Sebera, V.; Brabec, M., 2016: Determination of the elasto-plastic material characteristics of Norway spruce and European beech wood by experimental and numerical analyses. Holzforschung, 70 (11): 1081-1092. https://doi.org/10.1515/hf-2015-0267.

9. Milch, J.; Sebera, V.; Brabec, M.; Tippner, J., 2017: Verification of the elastic material characteristics of Norway spruce and European beech in the field of shear behaviour by means of digital image correlation (DIC) for finite element analysis (FEA). Holzforschung, 71 (5): 405-414. https://doi.org/10.1515/hf-2016-0170.

10. Ruman, D.; Záborský, V.; Svoboda, T.; Kašičková, V.; Rodrová, V., 2017: Identifying the characteristics of laminated wood based on the values of deflection measured during its bending. BioResources, 12 (2): 2592-2608.
http://doi.org/10.15376/biores.12.2.4146-4165.

11. Sebera, V.; Tippner, J.; Šimek, M.; Šrajer, J.; Děcký, D.; Klímová, H., 2014: Poisson's ratio of the MDF in respect to vertical density profile. European Journal of Wood and Wood Products, 72 (3): 407-410.
http://dx.doi.org/10.1007/s00107-014-0780-1.

12. Standfest, G.; Petutschnigg, A.; Dunky, M.; Zimmer, B., 2009: Rohdichtebestimmung von Holzwerkstoffen mit-

tels Computertomographie. European Journal of Wood and Wood Products, 67 (1): 83-87.
http://dx.doi.org/10.1007/s00107-008-0289-6.

13. Standfest, G.; Kranzer, S.; Salaberger, D.; Plank, B.; Petutschnigg, A.; Dunky, M., 2010: 3D microstructure characterization of wood based panels. U: Teischinger, A.; Barbu, M. C.; Dunky, M.; Harper, D.; Jungmeier, G.; Militz, H.; Musso, M.; Petutschnigg, A.; Pizzi, A.; Wieland, S.; Young, T. M. (eds.): Processing Technologies for forest and biobased products industries. Kuchl, Austria, Salzburg University of Applied Sciences, pp. 96-101.

14. Suo, S.; Bowyer, J. L., 1994: Simulation modelling of particleboard density profile. Wood and Fiber Science, 26(3): 397-411.

15. Svoboda, T.; Gaffová, Z.; Rajnoha, R.; Šatanová, A.; Kminiak, R., 2017: Bending forces at the proportionality limit and the maximum – technological innovations for better performance in wood processing companies. BioResources, 12 (2): 4146-4165.
http://doi.org/10.15376/biores.12.2.4146-4165.

16. Wilczyński, A.; Kociszewski, M., 2011: Determination of elastic constants of particleboard layers by compressing glued layer specimens. Wood Research, 56 (1): 77-91.

17. Wilczyński, A.; Kociszewski, M., 2012: Elastic properties of the layers of three-layer particleboards. European Journal of Wood and Wood Products, 70 (1-3): 357-359.
http://dx.doi.org/10.1007/s00107-010-0497-8.

18. Wong, E. D.; Yang, P.; Zhang, M.; Wang, Q.; Nakao, T.; Li, K. F.; Kawai, S., 2003: Analysis of the effects of density profile on the bending properties of particleboard using finite element method (FEM). Holz als Roh-und Werkstoff, 61 (1): 66-72.
http://dx.doi.org/10.1007/s00107-002-0350-9.

19. Zhou, C.; Dai, C.; Smith, G. D., 2011: Modeling vertical density profile formation for strand-based wood composites during hot pressing: Part 1. Model development. Composites Part B: Engineering, 42(6): 1350-1356.
http://doi.org/10.1016/j.compositesb.2011.05.036.

20. *** EN 310, 1993: Wood based panels – Determination of modulus of elasticity in bending and of bending strength.

21. *** EN 312, 2010: Particleboards – Specifications.

22. *** EN 322, 1993: Wood based panels – Determination of moisture content.

23. *** EN 323, 1993: Wood-based panels – Determination of density.

24. *** EN 325, 2012: Wood based panels – Determination of dimension of test pieces.

Corresponding address:

Assist. prof. NIKOLA ŠPANIĆ, Ph.D.

Department of Material Technologies
University of Zagreb, Faculty of Forestry
Svetošimunska 25, p.o. box 422
10002 Zagreb, CROATIA
e-mail: nspanic@sumfak.hr

Morteza Nazerian[1], Hossin Assadolahpoor Nanaii[2], Rahiim Mohebbi Gargarii[2],

Influence of Nano-Silica (SiO$_2$) Content on Mechanical Properties of Cement-Bonded Particleboard Manufactured from Lignocellulosic Materials

Utjecaj sadržaja nanočestica silicijeva dioksida (SiO$_2$) na mehanička svojstva cementne ploče iverice proizvedene od lignoceluloznih materijala

ABSTRACT • *The influence of Nano-SiO$_2$ (NS) content and lignocellulosic material addition on hydration behavior of cement paste was studied through measurement of hydration temperature, initial and final setting time of cement paste and compressive strength of hardened cement paste. Besides, the amount of NS, particle size of reed and bagasse as lignocellulosic materials and bagasse to reed particles weight ratio were selected as manufacturing variables for cement-bonded particleboard (CBPB) each at five levels. The relationships between independent parameters and output variables (modulus of rupture (MOR), modulus of elasticity (MOE) and internal bonding (IB)) were modeled using response surface methodology (RSM) based on mathematical model equations (second-order multiple linear regression model) by computer simulation programming. The results indicated that cement pastes containing 3 wt.% Nano-SiO$_2$ content mixed with milled reed or bagasse particles enhanced maximum hydration temperature; however, the time of reaching the main rate peak shortened. Besides, the increase of SiO$_2$ replacement shortened the setting time. On the other hand, using reed particles, initial and final setting times of cement prolonged, while bagasse particles shortened initial and final setting times. Analysis of variance (ANOVA) was performed to determine the adequacy of the mathematical model and its respective variables. The interaction effect curves of the independent variables obtained from simulations showed a good agreement between the measured MOR, MOE and IB of CBPB and predicted values obtained by the developed models, and hence, the proposed concept was verified.*

Key words: cement-bonded particleboard, Nano-Silica, reed, bagasse, hydration, RSM

---

[1] Author is associate professor at Department of Lignosellulosic Composites, Faculty of Energy Engineering and New Technology, Shahid Beheshti University, Iran. [2]Authors are graduate student and lecturer at Department of Wood and Paper Science, University of Zabol, Iran.
[1] Autor je izvanredni profesor Odjela za lignocelulozne kompozite, Fakultet za proizvodnju energije i nove tehnologije, Sveučilište *Shahid Beheshti*, Iran. [2]Autori su student diplomskog studija i predavač Odjela za znanost o drvu i papiru, Sveučilište u Zabolu, Iran.

SAŽETAK • *Utjecaj sadržaja nanočestica silicijeva dioksida (NS) i dodatka lignoceluloznih tvari ispitivan je na temelju hidratacijskog ponašanja cementne paste uz pomoć mjerenja temperature hidratacije, početnoga i završnog vremena vezanja cementne paste te tlačne čvrstoće očvrsnute cementne paste. Od varijabli koje utječu na svojstva cementnih ploča iverica (CBPB) ispitivana je količina NS-a, veličina čestica lignoceluloznih materijala (trske i otpadaka u preradi šećerne trske) te težinski omjer različitih lignoceluloznih materijala. Za svaku varijablu odabrano je pet vrijednosti. Odnos između nezavisnih parametara i izlaznih varijabli – modula loma (MOR), modula elastičnosti (MOE) i čvrstoće raslojavanja (IB) – modeliran je s pomoću metodologije odziva površine (RSM-a) i računalnim simulacijskim programiranjem utemeljen na jednadžbama matematičkih modela (model višestruke linearne regresije drugoga reda). Rezultati su pokazali da cementne paste koje (težinski) sadržavaju 3 % čestica NS-a pomiješanih s mljevenim česticama trske ili otpadaka u preradi šećerne trske pokazuju povećanje maksimalne temperature hidratacije, no skraćeno je vrijeme postizanja maksimuma. Osim toga, s povećanjem udjela NS-a skraćeno je vrijeme vezanja cementne paste. Nasuprot tome, primjenom čestica trske produljeno je početno i završno vrijeme vezanja cementa, a primjenom čestica od otpadaka u preradi šećerne trske skraćuje se početno i završno vrijeme vezanja cementa. Kako bi se utvrdila adekvatnost matematičkog modela i njegovih odgovarajućih varijabli, provedena je analiza varijance (ANOVA). Krivulje interakcije nezavisnih varijabli dobivenih iz simulacija pokazale su dobru podudarnost izmjerenih vrijednosti MOR-a, MOE-a i IB-a cementnih ploča iverica s pretpostavljenim vrijednostima dobivenim razvijenim modelima, te je stoga predloženi koncept potvrđen.*

Ključne riječi: *cementna iverica, nanočestice silicijeva dioksida, trska, ostatci pri preradi šećerne trske, hidratacija, RSM*

1 INTRODUCTION
1. UVOD

Cement-bonded particleboard is used widely in wall lining in public buildings, external cladding, protective elements for fireproofing, specialized flooring, etc. It is a wood-based composite manufactured from wood-based materials or other lignocellulosic materials and a mineral binder under high pressure. Large quantities of lignocellulosic-based material are produced every year in the world. These materials are investigated to produce cement-bonded particleboards. In the last decade, research has beeb carried out on a wide range of annual plants species and agricultural residues including reed stalk (Alpar *et al.,* 2012), wheat straw (Soroushian *et al.,* 2004), coconut (Olorunnisola, 2009; Almeida *et al.,* 2002), bagasse (Aggarwal, 1995; Nazerian and Hosiny Eghbal, 2013), oil palm (Hermawan *et al.,* 2001), flax (Aamr-Daya *et al.,* 2008), rice husk (Ciannamea *et al.,* 2010), bamboo (Das *et al.,* 2012), corn (Jarabo *et al.,* 2013), groundnut hulls (Ayobami *et al.,* 2013), vine stalk (Rangavar *et al.,* 2014), tea (Sapuan *et al.,* 2011) etc.

All of these materials, such as giant reed (*Arundo donax L.*), can be applied for producing different types of composite materials. However, these materials have some negative effects on the properties of composites. Due to a rather high concentration of extractives compared to wood materials, higher inhibitory effects of available extractives in non-wood materials or agricultural residues can be expected on the hydration process of cement paste. Presence of these compounds increases the proportion of unhydrated cement particles and decreases the strength of the cement-bonded particleboard (Wei *et al.,* 2003). Different treatments can be used to minimize the effects of the inhabiting substances, including hydrothermal treatment (Asasutjarit *et al.,* 2007; Sutigno 2000; Ferraz *et al.,* 2011), immersion of lignosellulosic-based materials in different so-

lutions (Ferraz *et al.,* 2012), addition of accelerating agent (Wei *et al.,* 2000; Latorraca *et al.,* 2000; Olorunnisola, 2008; Ferraz *et al.,* 2012), and substitution of part of the cement by silica particles (Del Menezzi *et al.,* 2007).

Giant reed is a perennial herbaceous species that grows in different environments with different ranges of pH, salinity, and drought and trace element bioaccumulator, due to its capacity of absorbing contaminants such as metals without any symptom of stress, especially with phytoremediation processes. The growth of this plant is not inhibited by increasing bauxite (red mud) doses because of alkalinity, salt and metal toxicity, so that it is tolerant of the abiotic stresses and can decontaminate the polluted soil (Alshaal *et al.,* 2013). The presence of bauxite can improve the strength properties and workability of cementituos system due to its Pozzolanic reactivity, reacting with calcium hydroxide and producing additional gel (Soroshian and Won, 1995). According to Ribeiro *et al.* (2013), addition of bauxite changed the hydration process, setting time, and workability, and significantly altered important properties of Portland cement.

It is well known that the hydration temperature and the time duration until this temperature is reached give information on the suitability of a specific species to be bonded with cement (Frybort *et al.,* 2008). In this way, various additives at Nano scale can affect these parameters, such as mineral SiO$_2$ nanoparticle. As known, calcium silicate hydrate (C-S-H) is the main compound that increases the strength of the concrete paste (Qing *et al.,* 2007). According to Birgisson *et al.* (2012), a small amount of SiO$_2$ nanoparticles dispersed uniformly in a cement paste makes hydrated products of cement deposit on the nanoparticles due to their higher surface energy, i.e., they act as nucleation sites. Nucleation of hydration products on nanoparticles further promotes and accelerates cement hydration (Lin *et al.,* 2008). As colloidal silica is added, it reacts with the

released calcium hydroxide, and tricalcium silicate (C3S) dissolution is accelerated, so that the C-S-H gel in cement+water mixture is formed rapidly (Bjornstrom *et al.,* 2004).

Wood- or lignocellulosic-cement complex is prepared easily and is fabricated from available resources and, therefore, it is widely used in many various types of panel systems. Permanent reduction of wood resources and environmental hazards posed by formaldehyde emission from wood panel products have reached the alarming limit, so that using waste materials is necessary in cement complex manufacturing. In this regard, extensive research is conducted using several types of waste materials. However, none of the researches dealt with the application of abundant giant reeds in cement mixes and improvement of this complex by adding mineral additive at Nano scale.

The aim of the present research was to study the basic strength properties of the giant reed-cement mix. Hence, the effect of using giant reed, as the replacement of the bagasse in cement system, and also of adding SiO₂, as additive at Nano scale to the complex of giant reed particle-cement, on the hydration behavior of cement and properties of the cement-bonded particleboard was examined. Analysis was made of the modulus of rupture (MOR), modulus of elasticity (MOE) and internal bonding (IB) of CBPB by using mathematical model equations (second-order response functions).

2 MATERIAL AND METHODS
2. MATERIJAL I METODE

2.1 Hydration test
2.1. Test hidratacije

Commercial grade Portland cement (ASTM C150, 2009) and hammer-milled bagasse and reed (*Arundo donax* L.) were used to prepare cement pastes. Fifteen cement paste mixtures were designed, batched, and tested to establish the quantitative and qualitative evidence. One control mixture with pure cement was used to have a basis of comparison with other mixtures. Fourteen specimens were batched, cast, and tested with different amounts of NS particles in each mix combined with milled bagasse and reed particles sieved through a 42 wire mesh or without them. For this purpose, different weight ratios were used including 200 g binder with or without NS, 90.50 ml water and 15 g powder of lignocellulosic material for the treatments G, H, I, J, K, L, M, N and O, respectively, and 200 g cement and 90.50 ml distilled water for the treatments A, B, C, D, E and F, respectively (Table 1).

Nanosilica particles were used with specific surface area of 200.1 m²/g and average particle size of 5-20 nm. Type II commercial grade Portland cement was used in batches and was mixed with Nanosilica at different levels (0, 1.5, 3, 4.5 and 6 %). Distilled water (90.5 ml) was added to the mixture of cement+Nanosilica (200 g) and reed/bagasse (15 g oven dry basis) in a blender and stirred for 3 min. The cement–Nanosilica-reed/bagasse–water mixture was placed in a wide-

Table 1 Treatments for determination of hydration behavior of cement pastes
Tablica 1. Opis tretmana cementnih pasta za koje je istraženo hidratacijsko ponašanje

Treatment code *Kod tretmana*	Treatment *Oznaka*	Treatment type *Opis tretmana*
CW	A	cement paste
C1.5	B	cement p.+1.5% NS
C3.0	C	cement p.+3.0% NS
C4.5	D	cement p.+ 4.5% NS
C6.0	E	cement p.+ 6.0% NS
CB	F	cement p.+ bagasse
C1.5B	G	cement p.+1.5% NS+ bagasse
C3.0B	H	cement p.+3.0% NS+ bagasse
C4.5B	I	cement p.+4.5% NS+ bagasse
C6.0B	J	cement p.+6.0% NS+ bagasse
CR	K	cement p.+ reed
C1.5R	L	cement p.+ 1.5% NS+ reed
G3.0R	M	cement p.+ 3.0 NS+ reed
C4.5R	N	cement p.+ 4.5% NS+ reed
C6.0R	O	cement p.+ 6% NS+ reed

mouth insulated flask with a thermocouple wire and then it was covered with styrofoam. The flask was sealed with a wrapping tape. The temperature of the mixture was measured and plotted against time. Preliminary work indicated that the hydration temperature started to change after 30 min of testing. The time to attain the maximum temperature was the required setting time of the cement paste mixture. Also, Vicat apparatus was used to obtain the same workability of the mentioned cement pastes by determining initial and final seting times. To determine the effect of adding bagasse and reed particles on the compressive strength and find the correlation between compressive strength and hydration behavior, the mixtures were moulded into one inch cubic stainless steel moulds, and were vibrated on a mechanical vibrator for 4 minutes. The moulds were stored inside a humidity cabinet at 21±3 °C and 100 % RH. Under these conditions, the moulds were preserved for 1, 3, 7 and 28 days. After these periods, they were demoulded and compressive strength test was carried out.

2.2 Board preparation and strength measurement
2.2. Priprema ploče i mjerenje **čvrstoće**

Giant Reed stalks, 3m high, were cut above the water line (collected from a suburb near Zabol City in Sistan-Baloochestan Province of Iran) and split along the grain by a local harvester with the dimensions of 100-200mm (length) × 1-5mm (width) × 0.1-1 mm (thickness). Bagasse particles were purchased from a local market. Crashed reed stalk and bagasse were milled into particles using a hammer mill, and then they were sieved using the sieves with the mesh size >8mm, 6-8, 4-6, 2-4 and <2 mm, separately. The particles were further oven dried to 5 % moisture content (MC) at 90 °C. Commercial Portland cement (type II)

was purchased from Sistan Cement Industry Co., Ltd., Iran, to be used as a binder for making panels. CBPBs were produced at nominal board density of 1150 kg/m³ from the following weight ratios of bagasse/reed particle: 2.55:97.45, 6.94:93.06, 13.38:86.62, 19.81:80.19 and 24.20:75.80. In order to determine the effect of the mineral Nano-particles on the properties of panels, cement was blended with SiO₂ Nano-particles at five levels (0.48, 1.5, 3, 4.5 and 5.52 wt% based on composition by cement weight) in a laboratory mixer with a high rotation speed (2000rpm). The lignocellolosic particle/cement+ Nanosilica/ water weight ratio was set at 1:4:1. Calcium chloride (5 % of cement weight) was dissolved in water and added to the mixture to accelerate cement curing. Particles-cement-water slurry was blended for 10 min in a rotary blender and manually formed into a mat with an approximate moisture content of 20 %. Mat was cold pressed at 4.0 MPa for 48 h. After that, the boards were put into polyethylene bags for 20 days to complete the hydration process as soon possible. Then, they were kept for 6 days in the laboratory to ensure full curing and uniform drying.

After 28 days of curing, the panels were trimmed and subjected to the following tests: internal bonding strength and flexural tests.

2.3 Statistical analysis
2.3. Statistička analiza

In this study, response surface methodology (RSM) is used to evaluate the effect of some main process variables and their levels on MOR, MOE and IB values of CBPB. This method finds an appropriate model for predicting the dependent variables as responses. A standard RSM analysis, known as central composite rotatable design (CCRD), is used to create runs according to a logical experimental design and also describe the interaction between the independent variables. The quadratic equation model is used to develop regression equations related to response variable of CBPB production process, as shown by equation (1) below:

$$y = \beta_0 + \sum_{i=1}^{k}\beta_i x_i + \sum_{i<}^{k}\sum_{j}^{k}\beta_{ij}x_i x_j + \sum_{i=1}^{k}\beta_{ii}x_i^2 + \varepsilon.$$

Where x_i and x_j are inputs or independent factors, β_0 is the free term of the equation, coefficients β_1, β_2, β_i

Table 2 Range of process parameters
Tablica 2. Raspon procesnih parametara

Parameters / *Parametri*	**Coded factor** *Kodirani faktor*	**Symbol** *Oznaka*	**Units** *Jedinica*	**Lower limit** *Donja granica*	**Upper limit** *Gornja granica*
Nano-Silica content in cement / *sadržaj nanočestica silicijeva dioksida*	(X_1)	NS	%	1.5	4.5
Particle size of reed and bagasse / *veličina čestica trske i čestica otpada u preradi šećerne trske*	(X_2)	PS	mm	4	8
Weight ratio of bagasse to reed particles / *težinski omjer čestica otpada u preradi šećerne trske i čestica trske*	(X_3)	WR	%	6.94	19.81

Table 3 Experiment design and results
Tablica 3. Dizajn eksperimenta i rezultati

Run	Coded values / *Kodirane vrijednosti*			Actual values / *Stvarne vrijednosti*			MOR MPa	MOE MPa	IB MPa
	X_1	X_2	X_3	NS	PS	WR			
1	1	1	1	4.50	8.00	19.81	12.45	2350	0.43
2	0	0	1.68	3.00	6.00	24.20	16.34	2780	0.65
3	-1.68	0	0	0.48	6.00	13.38	7.9	1367	0.21
4	-1	1	-1	1.50	8.00	6.94	4.9	789	0.18
5	1.68	0	0	5.52	6.00	13.38	11.56	2246	0.33
6	1	-1	-1	4.50	4.00	6.94	9.6	1678	0.25
7	-1	-1	-1	1.50	4.00	6.94	6.6	845	0.2
8	0	0	0	3.00	6.00	13.38	11.2	2050	0.47
9	0	-1.68	0	3.00	2.64	13.38	8.8	1456	0.26
10	1	-1	1	4.50	4.00	19.81	12	2456	0.52
11	0	1.68	0	3.00	9.36	13.38	3.75	456	0.19
12	0	0	0	3.00	6.00	13.38	10.87	1998	0.48
13	0	0	0	3.00	6.00	13.38	11	2089	0.49
14	0	0	-1.68	3.00	6.00	2.55	6.65	768	0.32
15	0	0	0	3.00	6.00	13.38	12	2134	0.495
16	-1	-1	1	1.50	4.00	19.81	8.56	1546	0.42
17	0	0	0	3.00	6.00	13.38	9.98	1867	0.493
18	-1	1	1	1.50	8.00	19.81	9.56	1784	0.32
19	1	1	-1	4.50	8.00	6.94	6	589	0.22
20	0	0	0	3.00	6.00	13.38	11.88	1879	0.5

are linear terms; β_{11}, β_{22}, β_{ii} are quadratic terms; β_{12}, β_{13}, $\beta_{i-1,j}$ are the interaction terms and ϵ denotes random error.

The CCRD offers n^2 factorial runs, $2n$ axial runs and n center runs (six replicates), with n as number of variables. The axial points were added to estimate the quadratic terms of the model and collected at ($\pm\alpha$, 0, 0), (0, $\pm\alpha$, 0), and (0, 0, $\pm\alpha$). α is defined depending on the region of operability and region of interest. In this research, α value was selected as 1.68, and 20 experimental design points were considered including 6 center points. It was assumed that the design is rotatable when the value of α is determined. Table 2 shows three production parameters, i.e. Nano-Silica content in cement (X_1), size of reed and bagasse particles (X_2) and weight ratio of bagasse to reed particles (X_3) and their five levels.

A total of 20 experiments were required according to the CCRD design. The sequence of the experiment was randomized to minimize the effect of the uncontrolled factor (Table 3). For evaluating the statistical significance of the generated regression model, the analysis of variance (ANOVA) for the model was also performed at 5 % significance level incorporated in Expert Design software.

3 RESULTS AND DISCUSSION
3. REZULTATI I RASPRAVA

3.1 Hydration temperature
3.1. Temperatura hidratacije

In order to study the effect of the NS content as additive on hydration of cement based composites, the hydration temperature of the pure cement paste, cement-bagasse-based- and cement-reed-based-composites containing different levels of NS particles was monitored by isothermal calorimetric analysis. As shown in Figs. 1, 2 and 3, there is a significant difference between the heat of the hydration of one gram cement evolved during its hydration, cement-bagasse and cement-reed particles during the first 12 hours at a constant water to cement ratio.

While 6 wt.% additives decreased the hydration temperature, hydration temperature curves indicated that the addition of 1.5-4.5 wt.% NS particles to pure cement resulted in an increase of T_{max} in all samples (Figure 1). Moreover, the addition of NS shortened the initial and final setting times of the paste compared to the initial and final setting times of pure cement paste. When the hydration process begins, hydrate products diffuse and coat nanoparticles so that the cement hy-
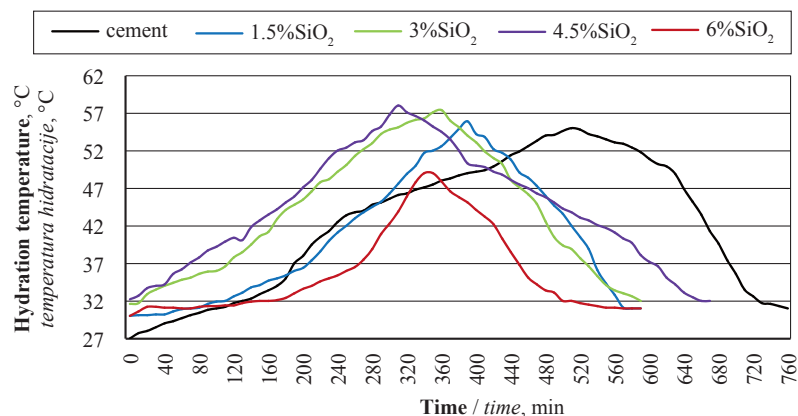

Figure 1 Exothermic curves of NS–cement mixtures as compared to neat cement
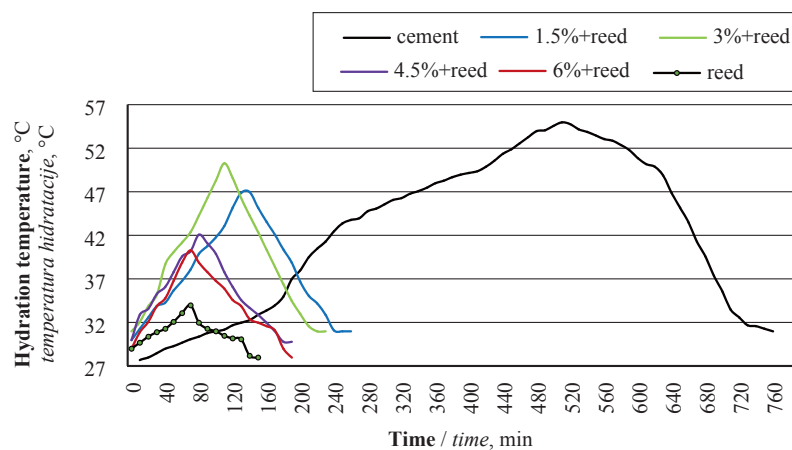**Slika 1.** Egzotermne krivulje smjesa cementa s česticama NS-a u usporedbi s čistim cementom

Figure 2 Exothermic curves of reed particles+NS+cement mixtures as compared to neat cement
Slika 2. Egzotermne krivulje smjesa cementa s česticama NS-a i trske u usporedbi s čistim cementom
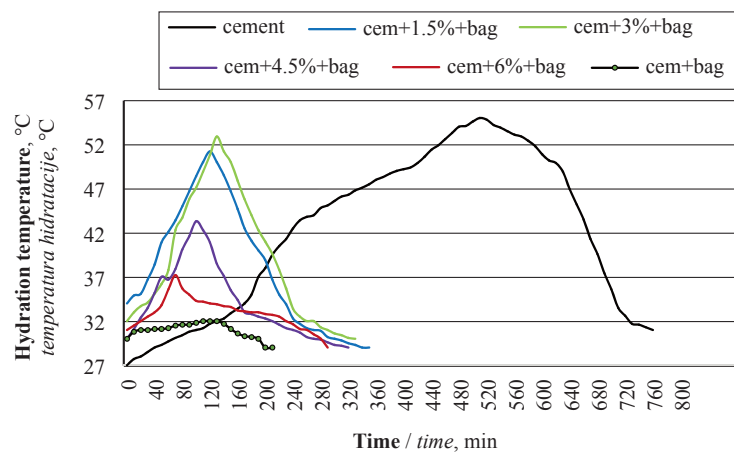
Figure 3 Exothermic curves of bagasse particles+NS+cement mixtures as compared to neat cement
Slika 3. Egzotermne krivulje smjesa cementa s česticama NS-a i česticama otpada u preradi šećerne trske u usporedbi s čistim cementom

dration speed rises, and the cement paste becomes more homogeneous and compact (Jalal *et al.,* 2012). Besides, the time of reaching the main rate peak (t$_{max}$) changes significantly due to more pozzolanic reaction creating an earlier peak. Therefore, with an increase of the Nanosilica amount from 3 to 4.5%, more reactive nuclei are created during the hydration, and t$_{max}$ decreases correspondingly. However, the values of water absorption and apparent porosity of Nanosilica particles are high (Senff *et al.,* 2010) so that the water to binder ratio becomes low due to the absorption process. As a result, a large amount of cement particles are still dehydrated at the end of cement hydration process in the sample containing 6% Nano-silica. Hence, although Nano-particles can accelerate cement hydration to a great extent in the early ages, the later hydration of cement is hindered.

In cement+Nano-Silica + reed/bagasse mixture, the addition of 3 % Nanosilica increased maximum heat of hydration (Figures 2 and 3). Compared to the analysis results of pure cement samples (510 min), the induction period reduced to 110 min for reed component (Figure 2) and 130 min for bagasse component, respectively (Figure 3), when 3 wt.% cement was replaced by Nanosilica. Besides, during the hydration, all of the cement samples that contained reed or bagasse showed lower maximum hydration temperature in comparison with pure sample or samples containing only Nanosilica as an additive. This is consistent with the results obtained by (Bilba *et al.,* 2003; Xie *et al.,* 2016), which showed that hemicellulose and lignin in plant fiber component have a negative effect on cement hydration process. Moreover, this phenomenon is related to the partial substitution of cement with lignocellulosic particles, causing excessive use of water and absorption of a part of the water for hydration. Sudin and Swamy (2006) and Alpar et al. (2011) stipulated that the delayed setting time of Portland cement matrix was caused by high content of carbohydrates, such as sugars in the fiber. The dissolution of these soluble sugar compounds forms calcium mixtures in the cement paste. These mixtures decrease hydration tem-

perature of cement matrix and delay the formation of hydration products. It was also observed that using bagasse prolonged the initial and final setting times and raised the T_{max} of the paste, compared to the initial and final setting times and T_{max} of cement paste containing reed.

3.2 Vicat test and compressive strength
3.2. *Vicat* test i tlačna čvrstoća

The influence of reed and bagasse on the initial and final setting times of the pure cement paste, 1.5 %, 3 %, 4.5 % and 6 % SiO$_2$ Nano-particle systems are shown in Figure 4.

The results indicate that an increased level of SiO$_2$ replacement results in shortened setting time. Shortening effect is probably due to higher volume fraction of Nano-particles, higher specific surface area in comparison with cement, and hence more absorption of water by these particles. Moreover, adding NS particles to hydrating cement increases formation of calcium silicate hydrate (C–S–H) gel due to reaction of Nano-SiO$_2$ with Ca(OH)$_2$ (calcium hydroxide, CH), accelerates the hydration of tricalcium silicate (C$_3$S) and dicalcium silicate (C$_2$S) and fills pores in the C–S–H crystal net (Biricik and Sarier, 2014; Senff *et al.,* 2009). Then, SiO$_2$ decreases the setting time of the cement paste and reduces water leakage, while improving the cohesiveness of fresh cement mixtures (Senff *et al.,* 2009).

Results also showed that using reed particles increases initial and final setting times of cement with or without NS, while bagasse particles reduce initial and final setting times of the cement mixture. This is likely because the addition of bagasse particles in cement increases the water demand to obtain a plastic mix of cement due to its spongy structure; however, the addition of reed particles minimizes water demand to obtain a plastic mix of the cement due to the existence of smooth outer surface and also hydrophobic waxy layer coating the outer surface of reed stalks. The presumable reason behind this phenomenon is the decrease in fluidity and increase in stiffness of cement that in-
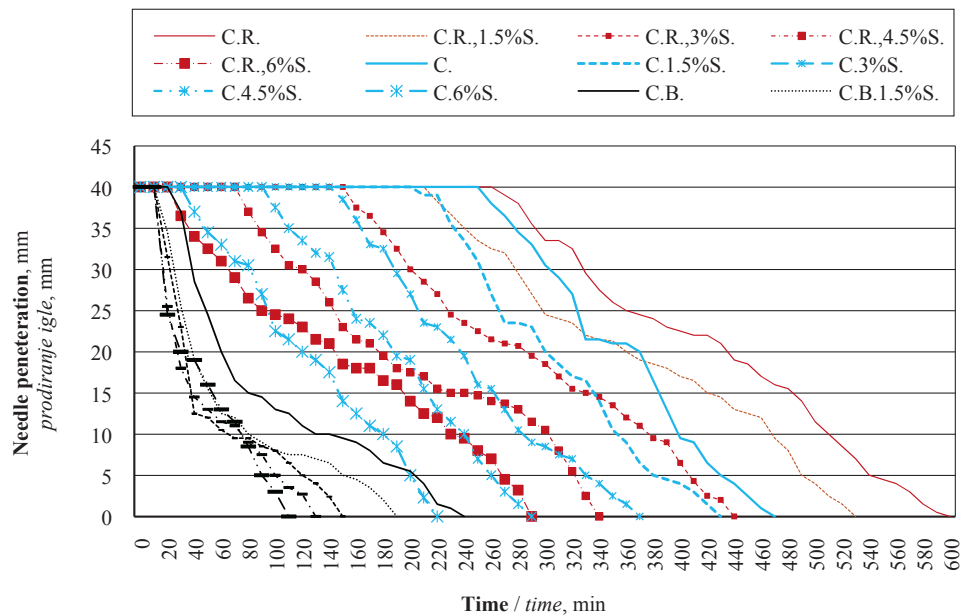
Figure 4 Initial and final hydration curves of lignocellulosic particles+ NS+ cement mixtures as compared to neat cement
Slika 4. Krivulje početne i završne hidratacije različitih smjesa cementa s česticama lignoceluloznog materijala i nanočesticama silicijeva dioksida u usporedbi s čistim cementom

crease the water demand due to higher absorption of water by hygroscopic particles (Byung-Wan *et al.,* 2014). However, the reed exerts a smoothing effect on the cement particles, thus decreasing the interior attrition coefficient, which in turn promotes the fluidity of cement paste.

According to Figure 5, not only additives (NS) but also lignocellulosic content differently influenced the compressive strength of cementitious samples during different periods. The addition of NS from 0 to 6 % significantly increased the compressive strength of the pure cement paste in the hardening stages (after 1, 3 and 7 days), while this variable decreased after 28 days for samples containing more than 4.5 % of NS. This is related to hydrophilic characteristics of silicates and silica gel formation, which strongly bound to portlandite compound formed in the early ages of cement paste hydration. Due to the

excess NS content and the subsequent high water absorption of the NS and formation of silica gel, hardening process of the paste is accelerated at early ages (as shown in Figure 5), while a loose coagulation of cementitious structure may form at later ages, because of the lack of enough water for completion of cement particles hydration; so the strength of samples decreases (Kotsay, 2013).

Besides, due to the addition of a high amount of Nano-silica to cement complex and the resulting increase in its viscosity, a large amount of air can be trapped into the system increasing the porosity of hardened concrete (Yu *et al.,* 2014). In the presence of the optimal amount of Nanosilica, the resulting positive effect of the nucleation and the negative influence of the entrapped air can be equal. Therefore, using a specified content of Nano silica, the porosity of the hardened cement can be decreased.
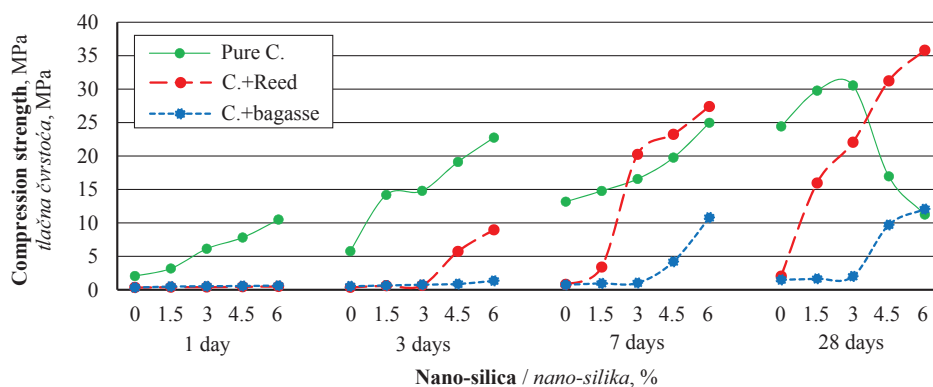

Figure 5 Compression strength development in pure cement pastes, reed+cement paste and bagasse+cement paste during 1 day, 3 days, 7 days and 28 days of hydration
Slika 5. Promjena tlačne čvrstoće čiste cementne paste, cementne paste s česticama trske i cementne paste s česticama otpada u preradi šećerne trske tijekom jednog dana, 3 dana, 7 dana i 28 dana hidratacije

3.3 Mechanical properties of CBPB
3.3. Mehanička svojstva cementnih iverica

Mechanical properties were optimized by the response surface methodology (RSM). The CCRD was used to develop the correlation between the process variables, including Nanosilica content (NS), reed and bagasse particle size (PS) and weight ratio of bagasse/reed particles (WR) (coded as X_1, X_2, and X_3, respectively) and responses, MOR, MOE and IB. The quadratic models of the responses are presented in Equations (2, 3 and 4) in terms of the coded factors according to their significance:

The results of the analysis of variance (ANOVA) for quadratic models are shown in Table 4 for MOR, MOE and IB. According to Table (4), the weight ratio of R/B particles (WR) is the most important factor affecting not only MOR but also MOE and IB, followed by Nano silica content (NS) and particle size (PS) (because F values of WR are higher than NS and PS for all responses). Besides, interaction effect of PS and WR ($X_2 X_3$) on MOR, MOE and IB, NS and PS ($X_1 X_2$) on MOE, and NS and WR ($X_1 X_3$) on IB are significant; however, the effect of the quadratic value of WR (X_3^2) on MOR and IB and NS (X_1^2) and WR (X_3^2) are not significant. Coefficients of determination (R^2) for MOR, MOE and IB showed that 93.4 %, 94.6 % and 99.7 of all variations are explained by the model, respectively.

R^2 values obtained after adjusting the terms of the model for MOR, MOE and IB are 90.4 %, 92.1 % and 99.5 %, respectively. The comparison of R^2_{Adj} = 0.9040, 0.9214 and 0.9952 with R^2_{Pred}=0.8053, 0.8190 and 0.9916 shows that both terms are in good agreement with each other and the models can explain 80.53 %, 81.90 % and 99.16 % variance of the new data.

The "Lack of Fit F-value" of 0.237, 0.07 and 0.74 for MOR, MOE and IB, respectively, imply that the Lack of Fit is not significant relative to the pure error. Hence, the models should fit the data. Improved precision and reliability of test results are shown below the values of coefficient of variation (C.V.) for MOR, MOE and IB; they are 9.73 %, 11.28 % and 2.6 %, respectively.

The influence of three factors including NS, PS and WR are shown in three-dimensional response of contour (Figures 6, 7 and 8). Figure 6, 7 (left) and 8 (left) illustrate the effect of two variables including PS

Table 4 Analysis of variance of MOR, MOE and IB
Tablica 4. Analiza varijance MOR-a, MOE-a i IB-a

Source / *Izvor varijacije*		Sum of squares *Zbroj kvadrata*	df	Mean Square *Srednja vrijednost kvadrata*	*F* Value *F-vrijednost*	*p*-Value *p-vrijednost* prob > F	Sig.
Model:		160.67	6	26.78	30.81	< 0.0001	**
		7.991E+006	6	1.332E+006	38.14	< 0.0001	**
MOR		160.67	6	26.78	30.81	< 0.0001	**
MOE		7991	6	61332	38.14	<0.0001	**
IB		0.37	7	0.018	197.24	<0.0001	**
X_1	MOR	20.14	1	20.14	23.17	0.0003	**
	MOE	9.423E+005	1	9.423E+005	26.99	0.0002	**
	IB	0.018	1	0.018	197.24	< 0.0001	**
X_2	MOR	11.16	1	11.16	12.83	0.0033	**
	MOE	5.317E+005	1	5.317E+005	15.23	0.0018	**
	IB	9.370E-003	1	9.370E-003	100.23	< 0.0001	**
X_3	MOR	73.89	1	73.89	85.01	< 0.0001	**
	MOE	4.250E+006	1	4.250E+006	121.73	< 0.0001	**
	IB	0.14	1	0.14	1524.21	< 0.0001	**
X_1^2	MOR	4.89	1	4.89	5.63	0.0338	*
	IB	0.086	1	0.086	919.53	< 0.0001	**
X_2^2	MOR	47.23	1	47.23	54.33	< 0.0001	**
	MOE	1.825E+006	1	1.825E+006	52.28	< 0.0001	**
	IB	0.13	1	0.13	1339.66	< 0.0001	**
AB	MOE	2.370E+005	1	2.370E+005	6.79	0.0218	*
BC	MOR	5.70	1	5.70	6.55	0.0238	*
	MOE	2.038E+005	1	2.038E+005	5.84	0.0311	*
	IB	2.450E-003	1	2.450E-003	26.21	0.0003	**
AC	IB	1.800E-003	1	1.800E-003	19.25	0.0009	**
MOR	Lack of Fit	8.57	8	1.07	1.96	0.2370	ns
MOE	Lack of Fit	3.932E+005	8	49155.15	4.05	0.0700	ns
IB	Lack of Fit	5.118E-004	7	7.312E-005	0.60	0.7405	ns
	MOR			MOE		IB	
Std. Dev.=0.93, R^2=0.9343, Adj R^2=0.9040, C.V.= 9.73 Pred R^2=0.8053,			Std. Dev.=186.86, R^2=0.9462, Adj R^2=0.9214,C.V.=11.28, Pred R^2=0.8190			Std. Dev.=9.669E-003, R^2=0.9970, Adj R^2=0.9952, C.V.=2.6, Pred R^2=0.9916	

(X_2) and WR (X_3) on MOR, MOE and IB when NS (X_1) is held at center level. MOR, MOE and IB increase as bagasse content increases at both (i.e. lower and higher) values of PS. Maximum MOR, MOE and IB are achieved at maximum level of WR (>19.81 %) and 6 mm PS.

The boards with the highest content of reed particles had the lowest MOR and MOE values. The outer surface of reed is believed to be richly covered by silica and wax (Perdue *et al.,* 1958). Smooth, hard and waxy surface of these types of lignocellulosic material may be one of the likely reasons of difficulty and failure of adhesion between the cement and reed particles.

With hydration of cement, the metal-hydroxyl groups, such as -Ca-OH, -Si- OH, -Al-OH and Fe-OH (due to hydration and hydrolysis of silicates, aluminates and to a lesser extent ferrites of calcium in the cement paste) are present at the surface of reed particles to form chemical bonding; however, according to Wei and Tomita (2001), the bonding strength does not benefit from the presence of silica at the surface of lignocellulosic particles. According to observations during the IB test, the adhesive disconnection mainly took place between hardened cement and reed particles rather than on bagasse particles. In fact, the presence of wax and surface properties of reed particles may affect adversely the bonding of CBPB.

It was determined that the content of silica and lignin in the reed (1.18-1.97 % and 25 %, respectively) (Wang *et al.,* 2013) is higher than that of bagasse particles 0.98 % and 21 %, respectively (Agnihotri *et al.,* 2010). Increasing lignin content might contribute to a higher compressive strength and hardness values (as shown in Figure 5) and consequently brittleness. Higher silica content in reed stalks results in higher stiffness and lower flexibility (Wu *et al.,* 2010), simultaneously. This means that the compaction ratio of panels and
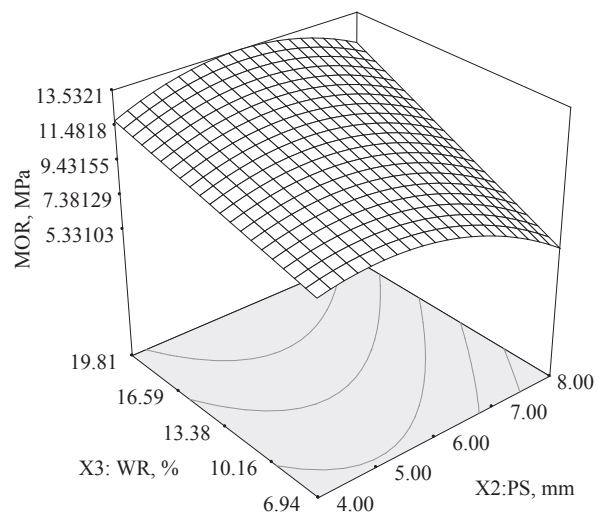

Figure 6 Three dimensional surface plots predicting MOR from the equation model: effect of particle size and weight ratio of bagasse to reed particles at center level of Nano SiO$_2$ content
Slika 6. Prikaz trodimenzionalnih površina koje predviđaju MOR iz jednadžbe modela: učinak veličine čestica i težinskog omjera čestica otpada u preradi šećerne trske i čestica trske na središnjoj razini sadržaja nanočestica silicijeva dioksida

consequently the contact between particles during pressing decrease, so the bending strength decreases.

Figure 7 (right) shows 3D surface graphs for the interaction effects of NS content and particle size (X_1X_2) on MOE. It can be seen that maximum value of MOE is achieved with the combination of highest NS and almost center level of PS (at 5.52 % NS and 6-5.25 mm particle size). Increasing NS at both (i.e. lower and higher) values of PS, MOE values increased, but as it can be seen in Figure 7 (right) and as noted in the ANOVA table, increase in NS has more influence on the increase in MOE.
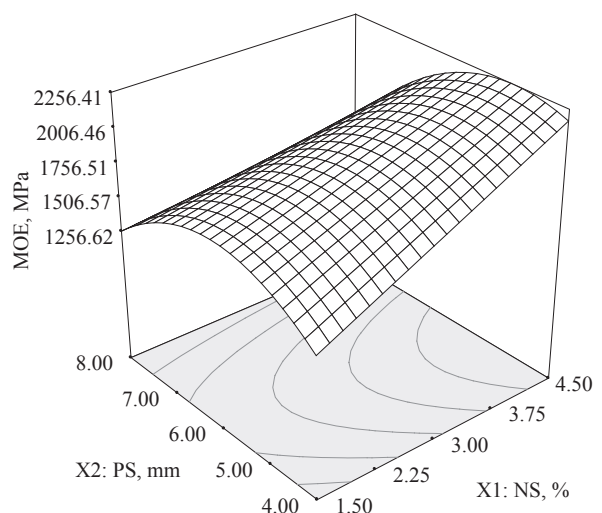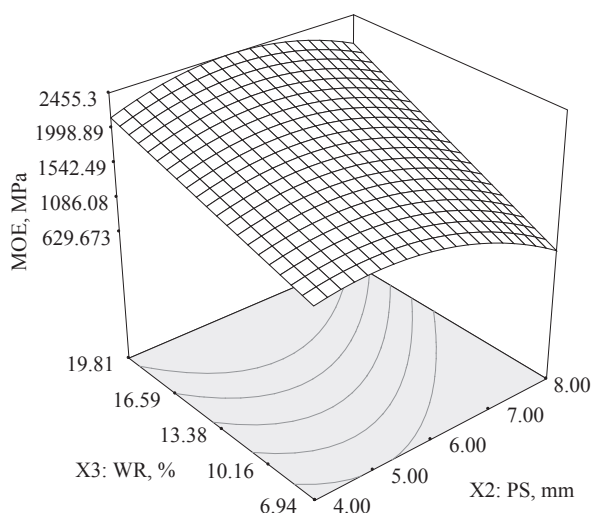

Figure 7 Three dimensional surface plots predicting MOE from the equation model: effect of particle size and weight ratio of bagasse to reed particles at center level of NS content (left); effect of NS content and particle size at center level of weight ratio of bagasse to reed particles (right)
Slika 7. Prikaz trodimenzionalnih površina koje predviđaju MOE iz jednadžbe modela: učinak veličine čestica i težinskog omjera čestica otpada u preradi šećerne trske i čestica trske na središnjoj razini sadržaja nanočestica silicijeva dioksida (lijevo); učinak sadržaja nanočestica silicijeva dioksida i veličine čestica na središnjoj razini omjera čestica otpada u preradi šećerne trske i čestica trske (desno)
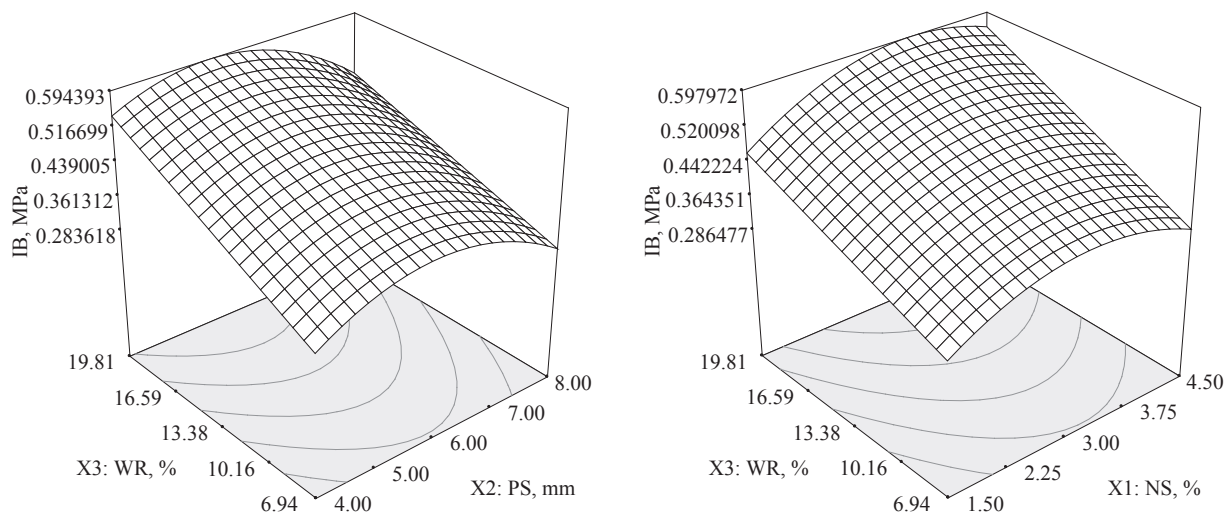
Figure 8 Three dimensional surface plots predicting IB from the equation model: effect of particle size and weight ratio of bagasse to reed particles at center level of NS content (left); effect of NS content and weight ratio of bagasse to reed particles at center level of particle size (right)

Slika 8. Prikaz trodimenzionalnih površina koje predviđaju IB iz jednadžbe modela: učinak veličine čestica i težinskog omjera čestica otpada u preradi šećerne trske i čestica trske na središnjoj razini sadržaja nanočestica silicijeva dioksida (lijevo); učinak sadržaja nanočestica silicijeva dioksida i omjera čestica otpada u preradi šećerne trske i čestica trske na središnjoj razini veličine čestica (desno)

Due to using NS, important effects for the hydration kinetics and the microstructure of the cement paste are revealed, such as (a) an increase in the initial hydration rate (as shown in Figures 1 and 2), (b) an increase of the amount of C-S-H gel in the paste through pozzolanic reaction due to the reaction of NS with CH during the hydration process, (c) reduction of porosity through the pore size refinement in the early ages, so NS acted as a core that strongly sticks to the hydrated cement, and finally, (d) improvement in the mechanical properties of the C-S-H gel itself by increasing the average chain length of C-S-H gel (Gaitero *et al.,* 2010). Besides, addition of additives as a pozzolanic mineral to cement mixtures decreases the inhibitory influence of extractives. Due to higher specific surface area of these additives than cement and higher sorption of these materials, the adsorption of water-soluble extractives occurs on the surface of NS first, while the concentration of extractives and their negative effects on hydration process decreases.

The influence of varying two factors of NS and WR (X_1X_3) on IB at a constant particle size, i.e. 6 mm, is depicted in Figure 8 (right). It can be observed from the figure that higher WR at both (i.e. lower and higher) values of NS results in lower IB. Since a large amount of cement has already been replaced by NS powder, the water to cement ratio is relatively stable. However, the water amount of samples containing high level of NS is still relatively low. Since the water used can be significantly absorbed by the hydrophilic materials, the amount of hydrated cement particles is fixed at lower limits. Finally, to further decrease the IB of the CBPB around 4.5 % and higher, NS is added into the lignocellulosic particles-cement matrix. On the other hand, 0.48 % to 3 % NS increased IB despite the increased demand for water in the matrix. In fact, Nano-scale SiO$_2$ plays a role not only as a filler to improve microstructure (which is a fac-

tor affecting the increase in cohesiveness of the paste and IB), but also as an accelerator of pozzolanic reaction in cement matrix (Qing *et al.,* 2007; Jo *et al.,* 2007).

4 CONCLUSION
4. ZAKLJUČAK

More effective utilization of wood and forest resources and uses of agricultural products in many valuable fields can be achieved by using reed and bagasse as lignocellulosic sources and alternative raw materials in cement-bonded particleboard industry. Thus, the effect of Nanosilica content, particle size of bagasse and reed and weight ratio of bagasse to reed particle were evaluated using RSM model. The major conclusions based on the data obtained in this paper can be summarized as follows:

1. NS makes cement paste thicker and accelerates the cement hydration process, while addition of ligno-sellulosic particles remarkably delayed the hydration process of the cement paste with or without NS.
2. Addition of reed and bagasse into the cement past had positive effect on the compressive strengths of hardened cement, especially at the end of the hydration ages.
3. While MOR, MOE and IB increased with increasing the particle size of bagasse and reed to a certain value and then decreased as the particle size of bagasse and reed increased more than a certain value, as the weight ratio of bagasse to reed increased, MOR, MOE and IB increased directly. Moreover, as NS content increased, MOE increased directly; however, IB enhanced as NS content increased to a certain value and then it decreased as NS content increased more than the certain value.
4. The mathematical model of MOR, MOE and IB developed by RSM presents desirable information with a small number of experimentations. The mod-

el is rationally appropriate and can predict the values of responses within the studied limit of parameters. It is determined from ANOVA that WR has a maximum effect on MOR, MOE and IB compared to other selected variables.

5. It is also concluded from the ANOVA that the developed model can be effectively used to predict the MOR, MOE and IB of the CBPB at 95 % confidence level. The values of R^2 and adjusted R^2 are 93.43 % and 90.40 % for MOR, 94.62 % and 92.14 % for MOE, and 99.70 % and 99.52 % for IB, respectively, and hence, the repeatability of the results is reasonable.

5 REFERENCES
5. LITERATURA

1. Aamr-Daya, E.; Langlet, T.; Benazzouk, A.; Queneudec, M., 2008: Feasibility study of lightweight cement composite containing flax by-product particles: Physico-mechanical properties. Cement and Concrete Composites, 30 (10): 957-963.
https://doi.org/10.1016/j.cemconcomp.2008.06.002.

2. Aggarwal, L. K., 1995: Bagasse-reinforced cement composites. Cement and Concrete Composites, 17 (2): 107-112. https://doi.org/10.1016/0958-9465(95)00008-Z.

3. Agnihotri, S.; Dutt, D.; Tyagi, C. H., 2010: Complete characterization of bagasse of early species *Saccharum officinarum* CO 89003 for pulp and paper making: Bio-Resources, 5 (2): 1197-1214.
http://dx.doi.org/10.15376/biores.5.2 1197-1214.

4. Almeida, R. R.; Del Menezzi, C. H. S.; Teixeira, D. E., 2002: Utilization of the coconut shell of babaçu (*Orbignya* sp.) to produce cement-bonded particleboard. Bioresource Technology, 85 (2): 159-163.
https://doi.org/10.1016/S0960-8524(02)00082-2.

5. Alpar, T. L.; Schlosser, M.; Hajdu, I.; Bejo, L., 2012: Developing building materials from cement-bonded reed composite based on waste materials. International Scientific Conference on Sustainable Development & Ecological Footprint. March 26-27, 2012. Sopron, Hungary.

6. Alpar, T. L.; Pavlekovics, A. A.; Csoka, L.; Horvath L., 2011: Wood wool cement boards produced with Nano minerals. Proceedings of the 3rd International Scientific Conference on Hardwood Processing (ISCHP³2011) I: Peer reviewed contributions October 16 – 18, 2011 Blacksburg, Virginia, USA.

7. Alshaal, T.; Domokos-Szabolcsy, E.; Marton, L.; Czako, M.; Katai, J.; Balogh, P.; Elhawat, N.; El-Ramady, H.; Fari, M., 2013: Phytoremediation of bauxite-derived red mud by giant reed. Environmental Chemistry Letters, 11 (3): 295-302. https://doi.org/10.1007/s10311-013-0406-6.

8. Asasutjarit, C.; Hirunlabh, J.; Khedari, J.; Charoenvai, S.; Zeghmati, B.; Shin, U. C., 2007: Development of coconut coir-based lightweight cement board. Constriction and Building Materials, 21 (2): 277-288.
https://doi.org/10.1016/j.conbuildmat.2005.08.028.

9. Ayobami, O. O.; Laja, O. S.; Emmanuel, O. S., 2013: Effect of Calcereous cow horn and storage on the physicochemical properties of cement-bonded particleboards from groundnut hulls. Journal of Chemistry, 1-8.
http://dx.doi.org/10.1155/2013/521763.

10. Bilba, K.; Arsene, M. A.; Ouensanga, A., 2003: Sugar cane bagasse fibre reinforced cement composites. Part I. Influence of the botanical components of bagasse on the setting of bagasse/cement composite. Cement and Concrete Composites, 25: 91-96.
https://doi.org/10.1016/S0958-9465(02)00003-3.

11. Birgisson, B.; Mukhopadhyay, A. K.; Geary, G.; Khan, K.; Sobolev, K., 2012: Nanotechnology in Concrete Materials: A Synopsis. Transportation Research Circular, E-C170 December.

12. Biricik, H.; Sarier, N., 2014: Comparative study of the characteristics of Nanosilica, silica fume – and fly ash-incorporated cement mortars. Materials Research, 17 (3): 570-582. http://dx.doi.org/10.1590/S1516-14392014005000054.

13. Bjornstrom, J. A.; Martinelli, A.; Matic, A.; Borjesson, L.; Panas, I., 2004: Accelerating effects of colloidal Nanosilica for beneficial calcium-silicate-hydrate formation in cement. Chemical Physics Letters, 392 (1-3): 242-248. https://doi.org/10.1016/j.cplett.2004.05.071.

14. Byung-Wan, J.; Chakraborty, S.; Yoon, K. W., 2014: A hypothetical model based on effectiveness of combined alkali and polymer latex modified jute fibre in controlling the setting and hydration behavior of cement. Construction and Building Materials, 68: 1-9.
https://doi.org/10.1016/j.conbuildmat.2014.06.043.

15. Ciannamea, E. M.; Stefani, P. M.; Ruseckaite, R. A., 2010: Medium-density particleboard from modified rice husks and soybean protein concentrate-based adhesives. Bioresource Technology, 101: 818-825.
https://doi.org/10.1016/j.biortech.2009.08.084.

16. Das, A. K.; Billha, M.; Shams, M. I.; Hannan, M. O., 2012: Physical and mechanical properties of bamboo wastage cement bonded board. Journal of the Indian Academy of Wood Science, 9 (2): 170-175.
https://doi.org/10.1007/s13196-012-0084-1.

17. Del Menezzi, C. H. S.; De Castro, V. G.; De Souza, M. R., 2007: Production and properties of a medium density wood cement boards produced with oriented strands and silica fume. Maderas. Ciencia y tecnología, 9 (2): 105-115. http://dx.doi.org/10.4067/S0718-221X2007000200001.

18. Ferraz, J. M.; Del Menezzi, C. H. S.; Teixeira, D. E.; Martins, S. A., 2011: Effects of treatment of coir fiber and cement/fiber ratio on properties of cement bonded composites. BioResources, 6 (3): 3481-3492. DOI: 10.15376/biores.6.3.3481-3492.

19. Ferraz, J. M.; Del Menezzi, C. H. S.; Souza, M. R.; Okino, E. Y. A.; Martins, S, A., 2012: Compatibility of pretreated coir fibres (*Cocos nucifera* L.) with Portland cement to produce mineral composites. International Journal of Polymer Science, 1-7.
http://dx.doi.org/10.1155/2012/290571.

20. Frybort, S.; Maurita, R.; Teischinger, A.; Muller, U., 2008: Cement bonded composites-a mechanical review. BioResources, 3 (2): 602-626. DOI: 10.1007/s00107-004-0501-2.

21. Gaitero, J. J.; Campillo, I.; Mondal, P.; Shah, S. P., 2010: Small changes can make a great difference. In Transportation Research Record: J Transportation Research Board, No. 2141, Transportation Research Board of the National Academies, Washington, D.C., pp. 1-5.

22. Hermawan, D.; Subiyanto, B.; Kawai, S., 2001: Manufacture and properties of oil palm frond cement-bonded board. Journal of Wood Science, 47 (3): 208-213.
https://doi.org/10.1007/BF01171223.

23. Jalal, M.; Mansouri, E.; Sharifipour, M.; Pouladkhan, A. R., 2012: Mechanical, rheological, durability and microstructural properties of high performance self-compacting concrete containing SiO₂ micro and nanoparticles. Materials & Design, 34: 389-400.
https://doi.org/10.1016/j.matdes.2011.08.037.

24. Jarabo, R.; Monte, M. C.; Fuente, E.; Santos, S. F.; Negro, C., 2013: Corn stalk from agricultural residue used as reinforcement fiber in fiber-cement production. Ind Crop Prod, 43: 832-839.
https://doi.org/10.1016/j.indcrop.2012.08.034.

25. Jo, B. W.; Kim, C. H.; Tae, G.; Park, J. B., 2007: Characteristics of cement mortar with Nano-SiO$_2$ particles. Constriction and Building Materials, 21 (6): 1351-1355. https://doi.org/10.1016/j.conbuildmat.2005.12.020.

26. Kotsay, G., 2013: Effect of synthetic nanodispersed silica on the properties of Portland cement based mortars. Chemistry & Chemical Technology, 7 (3): 335-338.

27. Latorraca, J. V. F.; Iwakiri, S., 2000: Efeitos do tratamento das part´ıculas de Eucalyptus dunnii (Maid), da variac¸˜ao da relac¸˜ao madeira-cimento e do uso de aditivos sobre as propriedades f´ısicas e mecˆanicas de chapas de madeira-cimento. Cerne, 6 (1): 68-76.

28. Lin, K. L.; Chang, W. C.; Lin, D. F.; Luo, H. L.; Tsai, M. C., 2008: Effects of Nano-SiO$_2$ and different ash particle sizes on sludge ash-cement mortar. Journal of Environmental Management, 28 (6): 708-714. https://doi.org/10.1016/j.jenvman.2007.03.036.

29. Nazerian, M.; Hosiny-Eghbal, S., 2013: The influence of additive content and particle size of bagasse on some properties of cement-bonded particleboard. Journal of Indian Academy of Wood Science, 10 (2): 86-94. https://doi.org/10.1007/s13196-013-0099-2.

30. Olorunnisola, A. O., 2008: Effects of pre-treatment of rattan (*Laccosperma secundiflorum*) on the hydration of Portland cement and the development of a new compatibility index. Cement and Concrete Composites, 30 (1): 37-43. https://doi.org/10.1016/j.cemconcomp.2007.08.002.

31. Olorunnisola, A. O., 2009: Effects of husk particle size and calcium chloride on strength and sorption properties of coconut husk-cement composites. Industrial Crops and Products, 29 (2-3): 495-501. https://doi.org/10.1016/j.indcrop.2008.09.009.

32. Perdue, R. E., 1958: Arundo donax-source of musical reeds and industrial cellulose. Economic Botany, 12: 368-404. https://doi.org/10.1007/BF02860024.

33. Ferraz, J. M., Del Menezzi, C. H. S., Souza, M. R., Okino, E. Y. A., Martins, S. A., 2012: Compatibility of pretreated coir fibres (*Cocos nucifera* L.) with portland cement to produce mineral composites. International Journal of Polymer Science, 2012: 1-7. http://dx.doi.org/10.1155/2012/290571.

34. Qing, Y. Z.; Zenan, K. D.; Rongshen, C., 2007: Influence of Nano-SiO$_2$ addition on properties of hardened cement paste as compared with silica fume. Construction and Building Materials, 21 (3): 539-545. https://doi.org/10.1016/j.conbuildmat.2005.09.001.

35. Rangavar, H.; Khosro, S. K.; Payan, M. H.; Soltani, A., 2014: Study on the possibility of using vine Stalk waste (*Vitis Vinifera*) for producing gypsum particleboards. Mechanics of Composite Materials , 50 (4): 501-508. https://doi.org/10.1007/s11029-014-9436-9.

36. Ribeiro, D. V.; Silva, A. S.; Labrincha, J. A.; Morelli, M. R., 2013: Rheological properties and hydration behavior of Portland cement mortars containing calcined red mud. Canadian Journal of Civil Engineering, 40 (6): 557-566. https://doi.org/10.1139/cjce-2012-0230.

37. Sapuan, S. M.; Mustapha, F.; Majid, D. L.; Leman, Z.; Ariff, A. H. M.; Ariffin, M. K. A.; Zuhri, M. Y. M.; Ishak, M. R.; Sahari, J., 2011: Mechanical and physical properties of cement-bonded particleboard made from tea residues and hardboards. Composite Science and Technology, 471-472: 572-577. DOI: 10.4028/www.scientific.net/KEM.471-472.572.

38. Senff, L.; Hotza, D.; Repette, W. L.; Ferreira, V. M.; Labrincha, J. A., 2010: Mortars with Nano-SiO$_2$ and micro-SiO$_2$ investigated by experimental design. Construction and Building Materials, 24: 1432-1437. https://doi.org/10.1016/j.conbuildmat.2010.01.012.

39. Senff, L.; João, A. L.; Victor, M. F.; Dachamir, H.; Wellington, L. R., 2009: Effect of nano-silica on rheology and fresh properties of cement pastes and mortars. Construction and Building Materials, 23 (7): 2487-2491. https://doi.org/10.1016/j.conbuildmat.2009.02.005.

40. Soroshian, P.; Won, J. P., 1995: Statistical evaluation of mechanical and physical properties of cellulose fiber reinforced cement composites. ACI Materials Journal, 92 (2): 172-180.

41. Soroushian, P.; Aouadi, F.; Chowdhury, H.; Nossoni, A.; Sarwar, G., 2004: Cement-bonded straw board subjected to accelerated processing. Cement and Conceret Composites, 26 (7): 797-802. https://doi.org/10.1016/j.cemconcomp.2003.06.001.

42. Sudin, R.; Swamy, N., 2006: Bamboo and wood fibre cement composites for sustainable infrastructure regeneration. Journal of Material Science, 41 (21): 6917-6924. https://doi.org/10.1007/s10853-006-0224-3.

43. Sutigno, P., 2000: Effect of aqueous extraction of woodwool on the properties of wood-wool cement board manufactured from teak (*Tectona grandis*). In Proceedings of the Wood-Cement Composites in the Asia-Pacific Region Proceedings. Canberra-Australia, pp. 24-28.

44. Wang, X.; Deng, Y.; Wang, S.; Liao, C.; Meng, Y.; Pham, T., 2013: Nanoscale characterization of reed stalk fiber cell walls. BioResources, 8 (2): 1986-1996. DOI: 10.15376/biores.8.2.1986-1996.

45. Wei, Y. M.; Tomita, B.; Hiramatsu, Y.; Miyatake, A.; Fujii, T.; Yoshinage, S., 2003: Hydration behavior and compressive strength of cement mixed with exploded wood fiber strand obtained by the water-vapor explosion process. Journal of Wood Science, 49: 317-326. https://doi.org/10.1007/s10086-002-0479-5.

46. Wei, Y. M.; Zhou, Y.G.; Tomita, B., 2000: Study of hydration behavior of wood cement-based composite II: effect of chemical additives on the hydration characteristics and strengths of wood-cement composites. Journal of Wood Science, 46 (6): 444-451. https://doi.org/10.1007/BF00766220.

47. Wei, Y. M.; Tomita, B., 2001: Effects of five additive materials on mechanical and dimensional properties of wood cement-bonded boards. Journal of Wood Science, 47: 437-444. https://doi.org/10.1007/BF00767895.

48. Wu, Y.; Wang, S.; Zhou, D.; Xing, C.; Zhang, Y.; Cai, Z., 2010: Evaluation of elastic modulus and hardness of crop stalks cell walls by nano-indentation. Bioresource Technology, 101 (8): 2867-2871. https://doi.org/10.1016/j.biortech.2009.10.074.

49. Xie, X.; Gou, G.; Wei, X.; Zhou, Z.; Jiang, M.; Xu, X.; Wang, Z.; Hui, D., 2016: Influence of pretreatment of rice straw on hydration of straw fiber filled cement based composites. Construction and Building Materials, 113: 449-455. https://doi.org/10.1016/j.conbuildmat.2016.03.088.

50. Yu, R.; Spiesz, P.; Brouwers, H. J. H., 2014: Effect of Nano-silica on the hydration and microstructure development of Ultra-High Performance Concrete (UHPC) with a low binder amount. Construction and Building Materials, 65: 140-150. https://doi.org/10.1016/j.conbuildmat.2014.04.063.

Corresponding address:

Assoc. Prof. MORTEZA NAZERIAN, Ph.D.

Department of Lignosellulosic Composites
Faculty of Energy Engineering and New Technology
Shahid Beheshti University, IRAN
e-mail: morteza17172000@yahoo.com

Pantea Omrani, Hamid Reza Taghiyari, Mostafa Zolghadr[1]

Effects of Nano-Clay on Physical and Mechanical Properties of Medium-Density Fiberboards Made from Wood and Chicken-Feather Fibers and Two Types of Resins

Utjecaj nanogline na fizička i mehanička svojstva ploča vlaknatica srednje gustoće izrađenih od drva, vlakana pilećeg perja i dviju vrsta smola

ABSTRACT • *Medium-density fiberboards (MDF) were produced, using two different resins of urea-formaldehyde (UF) and phenol-formaldehyde (PF) at 10 % and 8 % contents, respectively. In order to find new source of raw material to satisfy the increasing need of composite manufacturing industry, 10 % of chicken feather was added to the furnish. Moreover, nano-clay was added to investigate its potential improving effects on MDF panel properties. Results showed that panels with PF resin demonstrated significantly lower water absorption and thickness swelling values in comparison to the panels with UF resin. However, mechanical properties of panels containing UF resin were generally higher; this was partially attributed to the higher resin content. It was concluded that panels with PF resin are recommended for applications where panels may be more exposed to water and vapor. In cases where the mechanical properties are of prime importance, panels with UF resin are more preferable. NC can be recommended in panels containing UF-resin to improve the properties, while it is not recommended in panels with PF-resin. Moreover, chicken feather can be included in MDF furnish to provide part of raw materials, though its addition can have diminishing effect on the properties to some extent.*

Key words: *feather fibers, mineral materials, nano-composites, clay nanofibers, wood fiber*

SAŽETAK • *Ploče vlaknatice srednje gustoće (MDF) izrađene su uz dodatak dviju različitih smola, ureaformaldehidne (UF) i fenolformaldehidne (PF), i to u udjelu od 10 odnosno 8 %. Kako bi se pronašao novi izvor sirovine i pritom zadovoljile povećane potrebe industrije kompozitnih materijala, smjesi sirovine za izradu ploča vlakna-*

---

[1] Authors are assistant professor, associate professor and MS student of Wood Science & Technology Department, Faculty of Materials Engineering and New Technologies, Shahid Rajaee Teacher Training University, Tehran, Iran.
[1] Autori su docent, izvanredni profesor i student diplomskog studija Odsjeka za znanost o drvu i tehnologiju, Fakultet strojarstva i novih tehnologija, Učiteljsko sveučilište *Shahid Rajaee*, Teheran, Iran.

tica dodano je 10 % pilećeg perja. Nadalje, dodana joj je i nanoglina da bi se istražilo moguće poboljšanje MDF ploča. Rezultati su pokazali da su ploče s PF smolom znatno slabije upijale vodu i da im je debljinsko bubrenje u odnosu prema pločama s UF smolom bilo manje. Međutim, mehanička svojstva ploča koje su sadržavale UF smolu u osnovi su bila bolja, što je djelomično povezano s većim udjelom smole. Zaključeno je da se ploče s PF smolom preporučuju za primjenu u uvjetima veće izloženosti vodi i pari. Kada su, pak, važnija mehanička svojstva ploča, pogodnije su one s UF smolom. Nanoglina se preporučuje za poboljšanje svojstava ploča koje sadržavaju UF smolu, a ne preporučuje se za ploče s PF smolom. Nadalje, pileće se perje može dodati sirovini za izradu MDF ploča iako ono može donekle pridonijeti pogoršanju svojstava ploče.

Ključne riječi: *vlakna od perja, mineralni materijali, nanokompoziti, nanovlakna gline, drvna vlakna*

1 INTRODUCTION
1. UVOD

Wood is a renewable material for many applications that helped mankind keep a sustainable development over centuries of civilization (Daly-Hassan *et al.*, 2014; Fernandez *et al.*, 2014 and 2017; Arce and Moya, 2015). Fast-growing species provide an opportunity to provide the raw materials necessary for wood industries and composite products (Behling *et al.*, 2011; Gbetoho *et al.*, 2017); however, the wood produced of these trees is usually of low quality and density and it is usually more susceptible to wood deteriorating bio-agents (Schmidt, 2006; de Medeiros *et al.*, 2016; Schmidt *et al.*, 2016; Ayata *et al.* 2017). Therefore, many modification techniques were used to improve its properties (Hill, 2006). However, it is mostly used in composite panels, engineered wood, and paper manufacturing industries (Candan and Akbulut, 2014; Bastani *et al.*, 2016; Andrade *et al.*, 2016; Behr *et al.*, 2017; Hubbe *et al.*, 2017). In this connection, composite panels not only provide a homogeneous material but they also offer boards with large length and width (Eshaghi *et al.*, 2013; Mendes *et al.*, 2013; Tajvidi *et al.*, 2016; Altuntas *et al.*, 2017) and therefore, there have been many studies elaborating on composite panels (Malanit *et al.* 2005; Valenzuela *et al.*, 2012). However, for a steady production of composite panels, a continuous flow of raw materials is essential. Iran is short of woody materials and therefore, many other substitutes have been considered (Hosseinkhani, 2015).

Feather fibers were reported to be used in some materials including concrete (Hamoush & El-Hawary, 1994; Koch, 2006; Acda, 2010). In an official report by the Ministry of Jihad-e-Agriculture of Iran, the chicken feather produced in 2012 was about 80,000 metric tons in Iran. This amount of chicken feather would be enough to manufacture more than 20 million composite panels with standard size of $366 \times 183 \times 16$ mm with 5 % feather content. Other countries also produce immense amount of chicken feather on a monthly basis. Chicken feathers from poultry farms used to be a valuable filling for blankets and matrices. However, synthetic materials substituted this natural substance and now chicken feathers are considered waste materials in Iran. Application of a percentage of chicken feathers in composite panels were studied before and the results were promising (Winandy *et al.*, 2003 and 2007; Taghiyari *et al.*, 2014ab; Taghiyari and Sarvari, 2016). However, the cited authors (Winandy *et al.*

2003 and 2007) only used phenol-formaldehyde (PF) resin in their study. Though PF is very practical in many applications, it is not popular in composite-manufacturing countries in Iran and some South-East Asian countries like Malaysia. Therefore, urea-formaldehyde (UF) resin was used here along with PF for comparison purposes. In addition, previous studies used quill-free feathers, that is, quills were removed from feathers. The process of removing quills is costly, adding to the final cost of the composite panels produced. Therefore, in the present study, the whole feather was used in the production of composite panels.

Moreover, nanomaterials have been successful in improving properties in many materials (Majidi, 2016; Harsini *et al.*, 2017; Matinise *et al.*, 2016; Pethig, 2017; Sandeep *et al.* 2017; Suganya *et al.*, 2017). In wood science and technology, different metal and mineral nanomaterials were used to decrease hot-pressing in wood-composite panels, to improve biological resistance of solid wood and composites, and to ameliorate the negative effects of thermal modification. In the present research project, nano-clay was also added as an additive to the resins to investigate its effects.

2 MATERIALS AND METHODS
2. MATERIJALI I METODE

2.1 Specimen procurement
2.1. Nabava uzoraka

Composite panels were manufactured from a mixture of five species of poplar, alder, hornbeam, maple and beech. The final thickness of panels was 16 mm with a density of 0.67 g/cm³. Two types of resins were separately used for panels, namely urea-formaldehyde (UF) and phenol-formaldehyde (PF) resins. Specifications of the resins are given in Table 1.

Urea-formaldehyde (UF) and phenol-formaldehyde (PF) resins were procured from Dehghani Co. and Iran Composite Co. in Iran, respectively. The temperature and duration of hot press was 175 °C and 8 minutes, and 200 °C and 6 minutes for UF and PF resins, respectively. Once produced, panels were kept in conditioning chamber (25 °C, and 40±3 % relative humidity) for four weeks before being cut, ready for tests. The moisture content of the specimens were measured at the time of testing to be 7.4 % in all treatments, because wood has a thermo-hygromechanical behavior and its properties depend on the combined action of temperature, relative humidity, and mechanical load variations (Figueroa *et al.*, 2012). Five replicate boards

Table 1 Specifications of urea-formaldehyde (UF) and phenol-formaldehyde (PF) resins
Tablica 1. Specifikacija ureaformaldehidne (UF) i fenolformaldehidne (FF) smole

Resin type *Vrsta smole*	Color *Boja*	Solid content, % *Sadržaj suhe tvari, %*	Solvent *Otapalo*	Producer *Proizvođač*	Country of origin *Država podrijetla*
UF	Transparent *prozirna*	0.58	Water / *voda*	Dehghani Co.	Iran
PF	Red / *crvena*	0.78	Thinner / *razrjeđivač*	Iran Composite Co.	Iran

Table 2 Molecular specifications of serine (Taghiyari and Sarvari, 2016)
Tablica 2. Molekularna specifikacija serina (Taghiyari i Sarvari, 2016.)

Molecular formula / *Molekularna formula*	$C_3H_7NO_3$
Molecular weight / *Molekularna masa*	105.09 g mol $^{-1}$
Isoelectric point (pH) / *Izoelektrična točka (pH)*	5.68
pK$_a$ values / *pK$_a$ vrijednost*	2.21, 9.15
Density / *Gustoća*	1.603 g/cm³ (22 °C)
Melting point / *Talište*	246 °C
Acidity (pK_a) / *Kiselost (pK_a)*	2.21 (carboxyl), 9.15 (amino)

were produced for each treatment. From each board, two specimens were cut for each kind of test.

Chicken feathers were bought from a chicken farm located in Ghazvin city, Ghazvin Province. Only the feathers of the chicken body were used because the quills of the wing feathers were thick and inflexible. Moreover, the process of removing the quills of wing feathers is not commercially competitive for composite manufacturing factories. The chemical combinations of chicken feathers are given in Table 2. As can be observed, they are mostly comprised of serine ($C_3H_7NO_3$).

2.2 Nano-clay application
2.2. Nanošenje nanogline

Nano-clay (NC) powder was produced in cooperation with Mehrabadi Manufacturing Company in Tehran, Iran. The size range of nanoparticles was 30-110 nm. NC composition is given in Table 3. NC was mixed with the resins and sprayed on to the wood fibers in a rotary drum-mixer before the hot press. A magnetic mixer stirred the resin-nanoclay mixture for 25-30 minutes for each production batch before being sprayed on the furnish. Consumption level of NC powder was 10 % based on the dry weight of the composite mat.

Table 3 Composition of the nano-clay used in the present research project
Tablica 3. Sastav nanogline primijenjene u istraživanju

Component *Komponenta*	Proportion (% w/w) *Udio (%* w/w*)*
CaO	1.97
SiO_2	50.95
Al_2O_3	19.60
Fe_2O_3	5.62
TiO_2	0.62
K_2O	0.86
MgO	3.29
Na_2O	0.98
LOI	15.45

2.3 Physical and mechanical tests
2.3. Fizička i mehanička ispitivanja

Physical and mechanical tests, as well as number and location of the specimens, were carried out in accordance with the Iranian National Standard ISIRI 9044 PB Type P2 (compatible with ASTM D1037-99) specifications, using INSTRON 4486 test machine, with five kN capacity. Figures 1 and 2 show thickness swelling and MOR specimens, ready for measurement.

Figure 1 Water absorption and thickness swelling specimens after being immersed in distilled water for 24 hours
Slika 1. Uzorci za određivanje upijanja vode i bubrenja nakon 24-satnog potapanja uzoraka u destiliranoj vodi

Figure 2 Surface of MOR specimens with feather content
Slika 2. Površina uzoraka s perjem za određivanje modula loma

2.4 Statistical analysis
2.4. Statistička analiza

Statistical analysis was conducted using SAS software program, version 9.2 (2010). One-way ANO-VA was performed to discern significant difference at the 95 % level of confidence. Grouping was made between treatments, using the Duncan's multiple range test. Hierarchical cluster analysis, including dendrogram and using Ward methods with squared Euclidean distance intervals, was carried out by SPSS/18 (2010). Cluster analysis was performed to find similarities and dissimilarities between treatments based on more than one property simultaneously. The scaled indicator in each cluster analysis shows how much treatments are similar or different; lower scale numbers show more similarities, while higher ones show dissimilarities (Taghiyari *et al.*, 2014ab). Surface and contour plots were made by Minitab software, version 16.2.2 (2010).

3 RESULTS AND DISCUSSION
3. REZULTATI I RASPRAVA

Results showed that MOR values of panels produced with UF-resin were higher when the composite furnish was comprised only of wood fibers (Figure 3). This was attributed to the higher UF-resin content (10 %) in comparison to PF-resin content (8 %). Addition of chicken feathers resulted in a decrease in MOR values in all treatments, though the decreases were not statistically significant in some cases. The decrease was partially attributed to the incompatibility of resins with the chemical components of feather. Similar chemical incompatibility between UF-resin and chicken feather components were reported to decrease biological resistance of composite panels (Taghiyari *et al.*,

2014ab), and to increase liquid permeation (Taghiyari & Sarvari, 2016). Addition of NC to the composite furnish reacted differently in each treatment. In panels with 100 % wood fibers and UF resin, NC improved MOR values by 10.7 %. This was because NC acted as a filler in UF resin, improving the overall strength of the composite matrix. Similar improvement was reported by addition of other minerals. However, in panels produced with PF-resin, resin content was lower (8 %) and part of the resin was absorbed by NC particles, avoiding this portion to be actively involved in the process of sticking the fibers together; ultimately MOR values decreased, though the amount of decrease was not significant. No significant difference was observed by addition of NC to panels with 10 % feather-content. It was concluded that NC can act as a filler and improve MOR values only in panels produced with UF-resin.

Modulus of elasticity (MOE) values illustrated somehow different trends in comparison to MOR values. Addition of chicken feather to the furnish generally improved MOE values in the produced MDF panels (Figure 4). This was a result of higher flexibility of feather fibers in comparison to wood fibers. Addition of NC to the furnish significantly decreased MOE values only in panels with PF-resin and feather content, similar to the decrease that occurred in MOR value of this treatment.

Results of water absorption (WA) measurements showed significant difference between panels produced with UF-resin and those produced with PF-resin (Figure 5). Panels with PF-resin generally showed lower WA values. This was due to the BWP (boil and water proof) nature of this resin. To be specific, lower WA values were achieved in panels produced with PF-resin
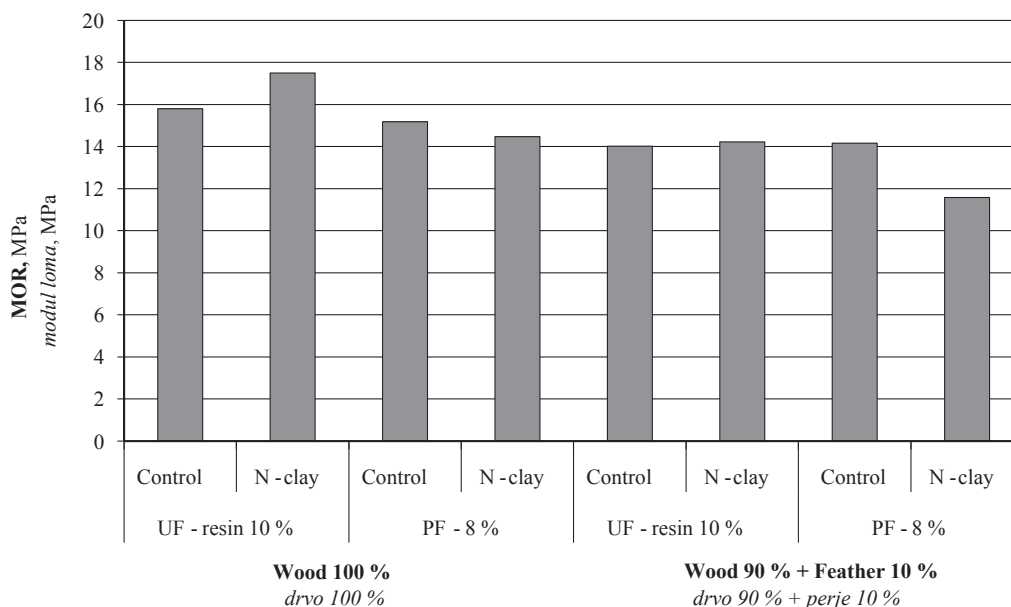

Figure 3 Modulus of rupture (MOR) values (MPa) in eight treatments of medium-density fiberboard (N – Nano; UF – urea-formaldehyde resin; PF – phenol-formaldehyde resin)
Slika 3. Vrijednosti (u MPa) modula loma (MOR) osam različitih ploča vlaknatica srednje gustoće (N – nanočestice; UF – ureaformaldehidna smola; PF – fenolformaldehidna smola)
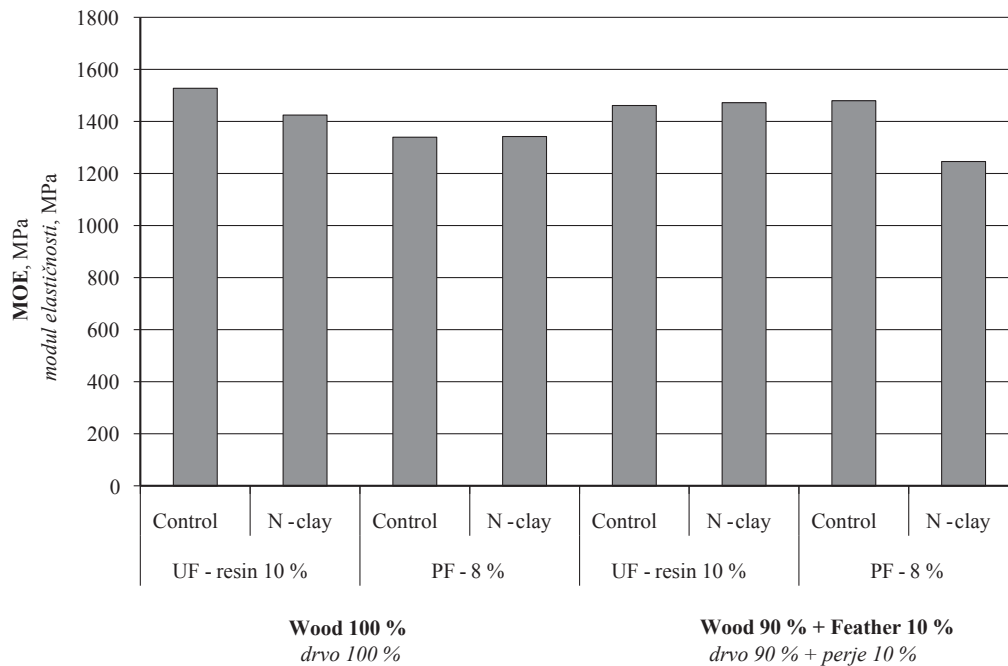
Figure 4 Modulus of elasticity (MOE) values (MPa) in eight treatments of medium-density fiberboard (N – Nano; UF – urea-formaldehyde resin; PF – phenol-formaldehyde resin)
Slika 4. Vrijednosti (u MPA) modula elastičnosti(MOE) osam različitih ploča vlaknatica srednje gustoće (N – nanočestice; UF – ureaformaldehidna smola; PF – fenolformaldehidna smola)

although PF-resin content (8 %) was 2 % lower than UF-resin content (10 %), and this was because of water resistance nature of PF-resin. Addition of feather did not have statistically significant effect on WA values.

Thickness swelling (TS) values generally followed the same trend as WA values, though the improving effects of PF-resin were more conspicuous on TS values in comparison to WA values (Figure 6). Addition of NC generally did not affect TS values, though

there were some fluctuations. It was concluded that in MDF composite panel production, when water resistance is of prime importance, PF-resin is more preferable than UF-resin, though lower PF-resin provided an edge of commercial competition over UF-resin.

Results of the surface analysis showed clear inverse relationship between MOR values versus both WA and TS values in panels produced with PF-resin (Figure 7). In panels produced with UF-resin, no clear
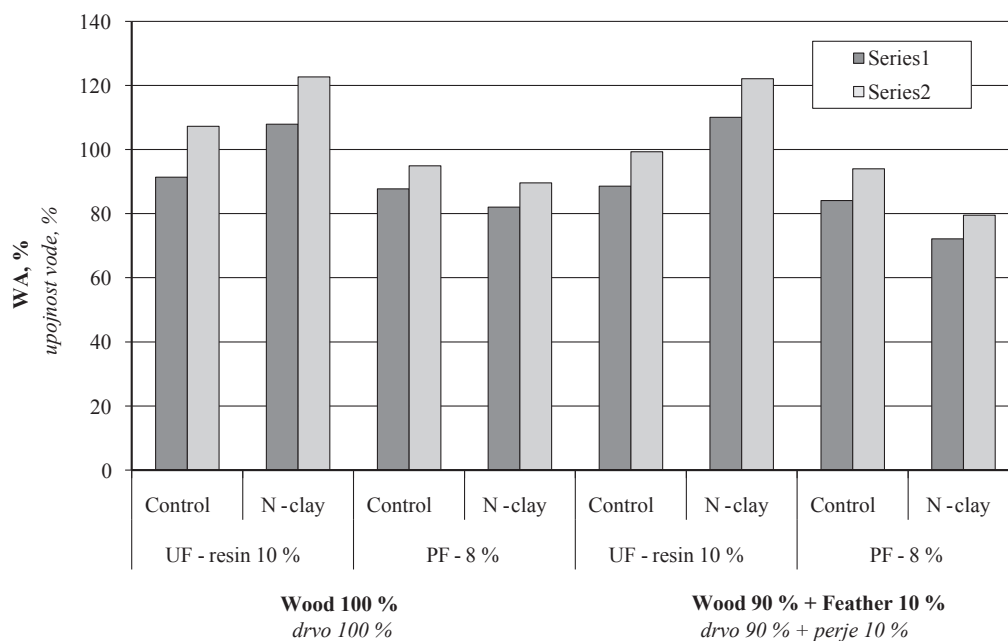

Figure 5 Water absorption (WA) values (%) in eight treatments of medium-density fiberboard (N – Nano; UF – urea-formaldehyde resin; PF – phenol-formaldehyde resin)
Slika 5. Postotak upijanja vode (WA) osam različitih ploča vlaknatica srednje gustoće (N – nanočestice; UF – ureaformaldehidna smola; PF – fenolformaldehidna smola)
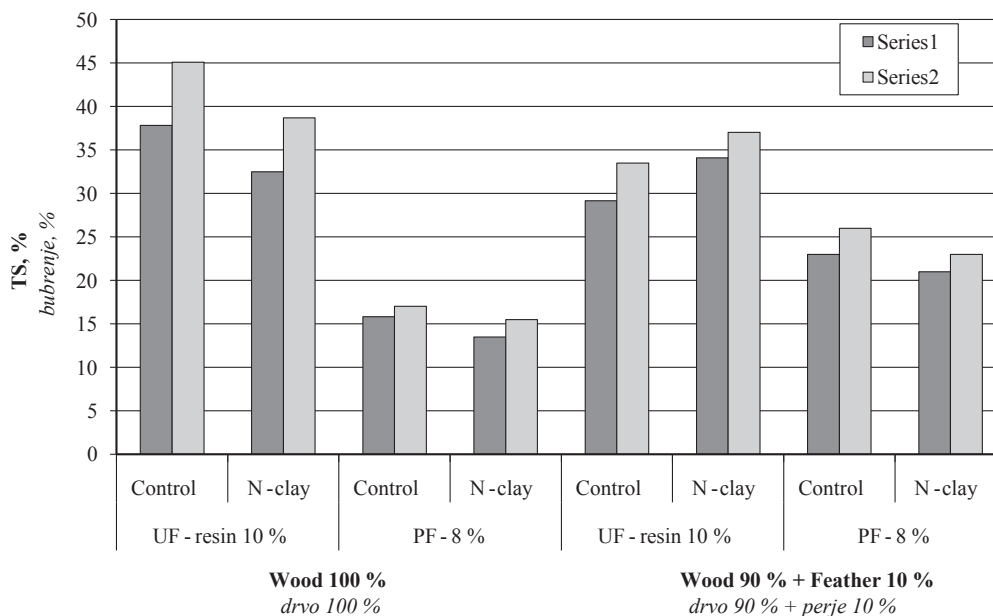
Figure 6 Thickness swelling (TS) values (%) in eight treatments of medium-density fiberboard (N – Nano; UF – urea-formaldehyde resin; PF – phenol-formaldehyde resin)
Slika 6. Postotak bubrenja (TS) osam različitih ploča vlaknatica srednje gustoće (N – nanočestice; UF – ureaformaldehidna smola; PF – fenolformaldehidna smola)

relationship was found between MOR versus WA and TS. The inverse relationship indicated that, in panels containing PF-resin, physical stability of MDF panels can easily be anticipated with regard to their mechanical property of MOR values. However, in panels produced with UF-resin, the interactions between different production factors of NC-content and feather-content were so high, varying from treatment to treatment, that ultimately it made no clear anticipation possible.

Contour plots clearly demonstrated inverse relationship between MOE versus WA and TS values in panels produced with PF-resin (Figure 8A). Contour plot between MOR versus WA and TS demonstrated direct relationship between MOR versus WA values, but inverse relationship versus TS (Figure 8B). The in-
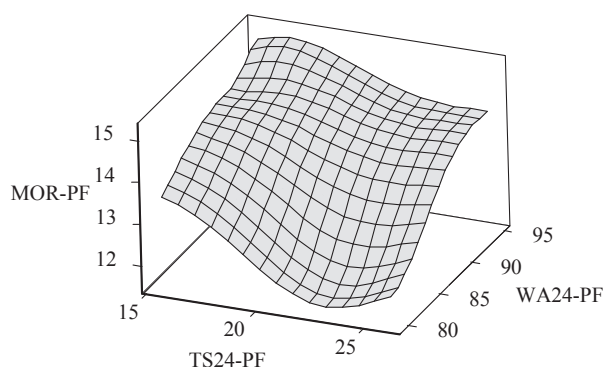

Figure 7 Surface plot between MOR versus WA and TS values in panels produced with phenol-formaldehyde (PF) resin (MOR – modulus of rupture; TS – thickness swelling; WA – water absorption)
Slika 7. Površinski prikaz odnosa MOR, WA i TS vrijednosti na pločama proizvedenima uz dodatak fenolformaldehidne smole (PF) (MOR – modul loma; TS – bubrenje; WA – upijanje vode)

verse relationship indicated that both MOR and TS values were in close agreement with the overall strength of the matrix; that is, the higher strength and integrity among wood fibers can be translated into higher MOR values, and consequently lower TS values. However, WA values cannot necessarily be related to the strength of material, but it is closely related to other factors such as porous structure/system of the composite.

Cluster analysis based on the properties studied in the present project demonstrated remote clustering of panels produced with feather and PF-resin containing NC, that is, treatment WF-P-NC (Figure 9). Therefore, based on the properties discussed above and the cluster analysis, it was concluded that addition of feather and NC to panels produced with PF resin would not be recommended due to the unsatisfactory physical and mechanical properties. Close clustering of the two panel treatments produced with PF-resin and 100 % wood fibers with or without NC content (W-P and W-P-NC treatments) indicated that in these panels, the improvement by NC was so low that extra expenses for addition of NC would not be commercially recommendable. The same decision was true about panels with feather content and produced with UF resin (WF-U and WF-U-NC treatments).

4 CONCLUSIONS
4. ZAKLJUČAK

Wood composite industry is in constant need for raw materials to keep up a continuous production line. Therefore, in the present research project, 10 % of chicken feathers was added to medium-density fiberboard (MDF) furnish to investigate if chicken feathers can be used as part of the mat. Two different resins of urea-formaldehyde (UF) and phenol-formaldehyde (PF)
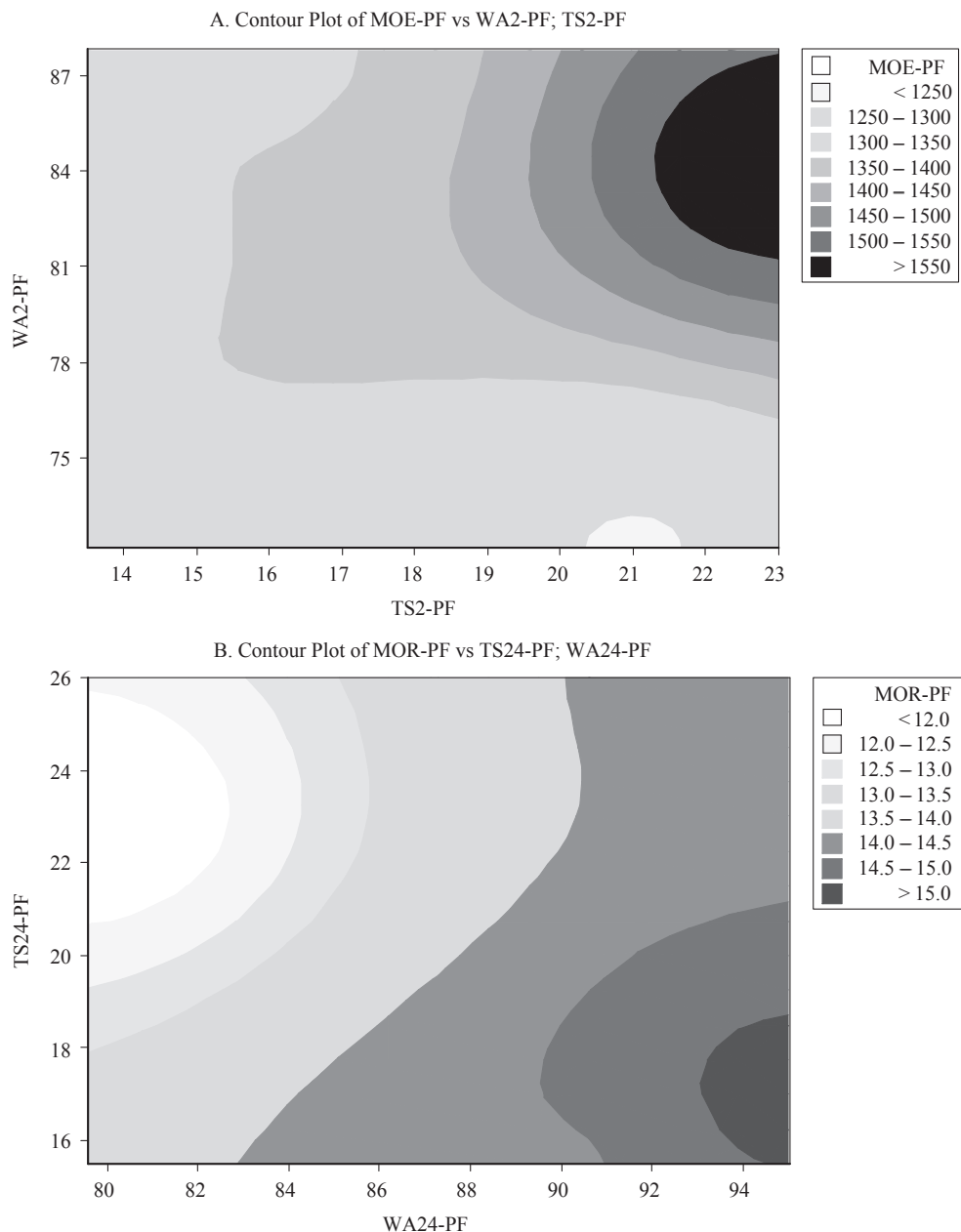
A. Contour Plot of MOE-PF vs WA2-PF; TS2-PF

B. Contour Plot of MOR-PF vs TS24-PF; WA24-PF

Figure 8 Contour plots between MOE (A) and MOR (B) values versus WA and TS values in panels produced with phenol-formaldehyde (PF) resin (MOR – modulus of rupture; TS – thickness swelling; WA – water absorption)
Slika 8. Kontrastni prikaz vrijednosti MOE (A) i MOR (B) u odnosu prema WA i TS za ploče proizvedene s dodatkom fenolformaldehidne smole (PF) (MOR – modul loma; TS – bubrenje; WA – upijanje vode)
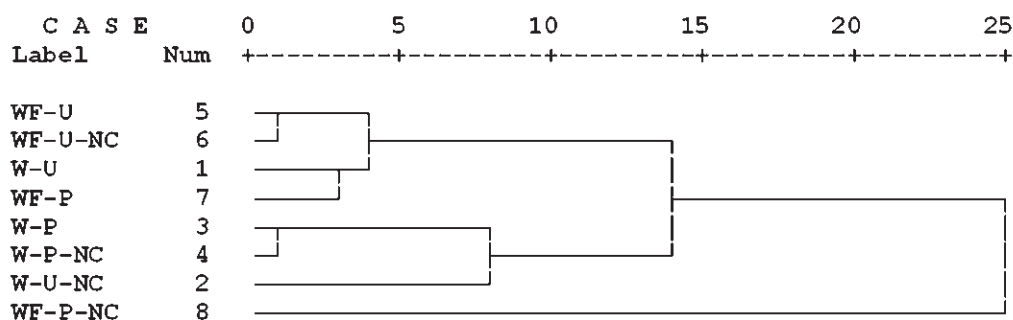
Figure 9 Cluster analysis based on physical and mechanical properties in the present research project (W – wood fibers; F – chicken-feather fibers; U – urea-formaldehyde resin; PF – phenol-formaldehyde resin; NC – nano-clay)
Slika 9. Klasterska analiza napravljena na osnovi fizičkih i mehaničkih svojstava određenih ovim istraživanjem (W – drvna vlakna; F – vlakna od pilećeg perja; U – ureaformaldehidna smola; PF – fenolformaldehidna smola; NC – nanoglina)

were used at 10 % and 8 % contents, respectively. Nano-clay was mixed with the above mentioned resins and sprayed on the furnish to investigate its potential improving effects on physical and mechanical properties. Panels containing PF-resin demonstrated better stability towards water. However, mechanical properties of panels containing UF resin were generally higher; this was partially attributed to the higher UF-resin content (10 %). It was concluded that NC can be recommended only in panels with UF-resin to improve the properties, while in panels with PF-resin, the improvements are not so high to compensate for the accompanying expenses. Moreover, chicken feathers to be added in MDF panels as part of the furnish demonstrated promising results, though they reduced the properties to some extent.

5 REFERENCES
5. LITERATURA

1. Ayata, U.; Akcay, C.; Esteves, B., 2017: Determination of decay resistance against *Pleurotus ostreatus* and *Coniophora puteana* fungus of heat-treated scotch pine, oak and beech wood species. Maderas Ciencia y tecnologia, 19 (3): 309-316. doi.org/10.4067/S0718-221X2017005000026.

2. Acda, M. N., 2010: Waste chicken feather as reinforcement in cement-bonded composites. Philippine Journal of Science, 139 (2): 161-166.

3. Altuntas, E.; Narlioglu, N.; Alma, M. H., 2017: Investigation of the fire, thermal, and mechanical properties of zinc borate and synergic fir retardants on composites produced with PP-MDF wastes. BioResources, 12 (4): 6971-6983.

4. Andrade, A. C. D. A.; Silva, J. R. M. D.; Braga Junior, R. A.; Moulin, J. C., 2016: Distinction of mechanically processed wood surfaces with similar qualities using sunset laser technique. CERNE, 22 (2): 159-162.

5. Arce, N.; Moya, R., 2015: Wood characterization of adult clones of *Tectona grandis* growing in Costa Rica. CERNE, 21 (3): 353-362.

6. ASTM D1037-99, Standard Test Methods for Evaluating Properties of Wood-Base Fiber and Particle Panel Materials, ASTM International, West Conshohocken, PA, 1999.

7. Bastani, A.; Adamopoulos, St.; Militz, H., 2016: Shear strength of furfurylated, N-methylol melamine and thermally modified wood bonded with three conventional adhesives. Wood Material Science & Engineering, 12 (4): 236-241.

8. Behling, M.; Piketty, M. G.; Morello, T. F.; Bouillet, J. P.; Mesquita Neto, F.; Laclau, J. P., 2011: Eucalyptus plantations and the steel industry in Amazonia – A contribution from the 3-PG model. Bois et Forets Des Tropiques, 309 (3): 37-49.

9. Behr, G.; Bollmus, S.; Gellerich, A.; Militz, H., 2017: Improvement of mechanical properties of thermally modified hardwood through melamine treatment. Wood Material Science & Engineering, 12 (1): 14-23.

10. Candan, Z.; Akbulut, T., 2014: Nano-engineered plywood panels: Performance properties. Composites: Part B, 64: 15-161.

11. Daly-Hassen, H.; Kasraoui, M.; Karra, C., 2014: Industrial timber production in Tunisia: Despite reforestation, dependence on imports is increasing. Bois et Forets Des Tropiques, 324 (4): 29-37.

12. de Medeiros, F. C. M.; Gouveia, F. N.; Bizzo, H. R.; Vieira, R. F.; Del Menezzi, C. H. S., 2016: Fungicide activity of essential oils from Brazilian Cerrado species against wood decay fungi. International Biodeterioration & Biodegradation, 114: 87-93.

13. Eshaghi, S.; Faezipour, M.; Taghiyari, H. R., 2013: Investigation on lateral resistance of joints made with drywall and sheet metal screws in bagasse particleboard and comparison with that of commercial MDF. Maderas Cienca y tecnologia, 15 (2): 127-140.

14. Fernandez-Puratich, H.; Oliver-Villanueva, J. V., 2014: Quantification of biomass and energetic value of young natural regenerated stands of *Quercus ilex* under Mediterranean conditions. BOSQUE, 35 (1): 65-74.

15. Fernandes, C.; Gaspar, M. J.; Pires, J.; Alves, A.; Simoes, R.; Rodrigues, J. C.; Silva, M. E.; Carvalho, A.; Brito, J. E.; Lousada, J. L., 2017: Physical, chemical and mechanical properties of *Pinus sylvestris* wood at five sites in Portugal. iForest Biogeosciences and Forestry, 10: 669-670.

16. Figueroa, M.; Bustos, C.; Dechent, P.; Reyes, L.; Cloutier, A.; Giuliano, M., 2012: Analysis of rheological and thermo-hygro-mechanical behaviour of stress-laminated timber bridge deck in variable environmental conditions. Maderas Ciencia y tecnologia, 14 (3): 303-319.

17. Gbetoho, A. J.; Aoudji, A. K. N.; Roxburgh, L.; Ganglo, J. C., 2017: Assessing the suitability of pioneer species for secondary forest restoration in Benin in the context of global climate change. Bois et Forets des Tropiques, 332 (2): 43-55.

18. Hamoush, S. A.; El-Hawary, M. M., 1994: Feather fiber reinforced concrete. Concrete international, 16 (6): 33-35.

19. Harsini, I.; Matalkah, F.; Soroushian, P.; Balachandra, A. M., 2017: Robust, carbon nanotube/polymer nanolayered composites with enhanced ductility and strength. Journal of Nanomaterials & Molecular Nanotechnology, 6 (3):1-6. http://dx.doi.org/10.4172/2324-8777.1000218.

20. Hill, C. A. S., 2006: Wood Modification: Chemical, Thermal, and Other Processes. John Wiley & Sons Ltd., pp 260. ISBN: 978-0-470-02172-9.

21. Hosseinkhani, H., 2015: MDF production from date palm pruning residues in pilot plant scale. Iranian Journal of Wood and Paper Science Research, 29 (4): 591-604.

22. Hubbe, M. A.; Smith, R. D.; Zou, X.; Katuscak, S.; Potthast, A.; Ahn, K., 2017: Deacidification of acidic books and paper by means of non-aqueous dispersions of alkaline particles: A review focusing on completeness of the reaction. BioResources, 12 (2): 4410-4477.

23. ISIRI 9044, Wood – Wood-based panels – Particleboards – Specifications. Institute of Standards and Industrial Research of Iran, Iran.

24. Koch, J. W., 2006: Physical and mechanical properties of chicken feather materials. A thesis presented in partial fulfillment of the requirements for the degree of Master of Science in the School of Civil Environmental Engineering; Georgia Institute of Technology, May, 2006.

25. Majidi, R., 2016: Electronic properties of graphyne nanotubes filled with small fullerenes: A density functional theory study. Journal of Computational Electronics, 15: 1263-1268.

26. Malanit, P.; Kyokong, B.; Laemsak, N., 2005: Oriented strand lumber from rubberwood residues. Walailak Journal of Science & Technology 2 (2): 115-125.

27. Matinise, N.; Fuku, X.; Maaza, M., 2016: Fabrication of Mixed Phase Bimetallic Zinc Cobaltite Nanocomposite

via Moringa Oleifera Green Synthesis. Journal of Nano-material & Molecular Nanotechnology, 5 (6): 1-7. http://dx.doi.org/10.4172/2324-8777.1000197.

28. Mendes, R. F.; Junior, G. B.; De Almeida, N. F.; Surdi, P. G.; Barbeiro, I. N., 2013: Effects of thermal pre-treatment and variables of production on properties of OSB panels of *Pinus taeda*. Maderas. Ciencia y tecnologia, 15 (2): 141-152.

29. Pethig, R., 2017: Review – Where is dielectrophoresis (DEP) going? Journal of The Electrochemical Society, 164 (5): B3049-B3055.

30. Sandeep, N.; Sulochana, C.; Kumar, B. R., 2017: Flow and heat transfer in MHD dusty nanofluid past a stretching/shrinking surface with non-uniform heat source/sink. Walailak Journal of Science and Technology, 14 (2): 117-140.

31. Schmidt, O., 2006: Wood and Tree Fungi: Biology, damage, protection, and use. Berlin: Springer; 334 pp. doi: 10.1007/3-540-32139-X.

32. Schmidt, O.; Magel, E.; Frühwald, A.; Glukhykh, L.; Erdt, K.; Kaschuro, S., 2016: Influence of sugar and starch content of palm wood on fungal development and prevention of fungal colonization by acid treatment. Holzforschung, 70 (8): 783-791.

33. Suganya, S.; Kumar, P. S.; Saravanan, A., 2017: Construction of active bio-nanocomposite by inseminated metal nanoparticles onto activated carbon: probing to antimicrobial activity. IET Nanobiotechnology, 11 (6): 746-753.

34. Taghiyari, H. R.; Bari, E.; Schmidt, O.; Tajick Ghanbary, M. A.; Karimi, A.; Tahir, P. M. D., 2014a: Effects of nanowollastonite on biological resistance of particleboard made from wood chips and chicken feather against *Antrodia vaillantii*. International Biodeterioration & Biodegradation, 90: 93-98.

35. Taghiyari, H. R.; Bari, E.; Schmidt, O., 2014b: Effects of nanowollastonite on biological resistance of medium-density fiberboard against *Antrodia vaillantii*. European Journal of Wood and Wood Products, 72: 399-406.

36. Taghiyari, H. R.; Sarvari Samadi, Y., 2016: Effects of wollastonite nanofibers on fluid flow in medium-density fiberboard. Journal of Forestry Research, 27 (1): 209-217.

37. Tajvidi, M.; Gardner, D. J.; Bousfield, D. W., 2016: Cellulose Nanomaterials as Binders: Laminate and Particulate Systems. Journal of Renewable Materials, 4: 365-376.

38. Valenzuela, J.; von Leyser, E.; Pizzi, A.; Westermeyer, C.; Gorrini, B., 2012: Industrial production of pine tannin-bonded particleboard and MDF. European Journal of Wood and Wood Products, 70: 735-740.

39. Winandy, J. E.; Muehl, J. H.; Micales, J. A.; Raina, A.; Schmidt, W., 2003: Potential of chicken feather fiber in wood MDF composites. Proceedings EcoComp, P20: 1-6.

40. Winandy, J. E.; Muehl, J. H.; Glaeser, J. A.; Schmidt, W., 2007: Chicken feather fiber as an additive in MDF composites. Journal of Natural Fibers; 4 (1): 35-48. http://dx.doi.org/10.1300/J395v04n01_04.

Corresponding address:

Assoc. prof. HAMID REZA TAGHIYARI, Ph.D.

Faculty of Materials Engineering & New Technologies
Shahid Rajaee Teacher Training University (SRTTU)
Lavizan, Shabanloo St.
Tehran, IRAN
e-mail: htaghiyari@sru.ac.ir; htaghiyari@yahoo.com

Jacek Kluska[1], Paweł Kazimierski[1,2], Mateusz Ochnio[1], Dariusz Kardaś[1]

Influence of Bed Movement and Amount of Supplied Air on Updraft Gasification of Hardwood Pellet

Utjecaj pomaka tepiha materijala i dobave zraka na protusmjerno rasplinjavanje peleta od drva listača

ABSTRACT • *This work presents the results of hardwood pellet gasification with different amounts of air as a gasification medium. The effects of bed movement and the equivalence ratio (ER) on the temperature profile, gas composition, carbon conversion efficiency and the energy balance were taken into account. Slow movement of the bed promotes high combustion and reduction zones, while fast bed movement leads to high pyrolysis zones and higher caloric values of syngas. When the amount of air increased from 12 to 23 Nm^3/h, the gas yield increased from 1.4 to 1.6 $Nm^3/kg_{biomass}$ for slow bed movement, and from 1.0 to 1.3 $Nm^3/kg_{biomass}$ for fast bed movement. These results show that in both Cases similar specific energy values were obtained. However, in Case 1 lower fuel consumption was reached. Chemical energy in the syngas represents 80 % of the output energy for slow bed movement (265 MJ/h) and 75 % for fast bed movement (295 MJ/h). A significant effect of bed movement in the reactor suggests that the gasifier could be considered as a flow reactor, and additionally the fast movement of the bed with 20 Nm^3/h of supplied air yielded the highest-quality gasification process. Moreover, fast bed movement in the reactor leads to a high amount of generated char with high energy potential.*

Keywords: gasification, updraft gasifier, hardwood, carbon conversion, bed movement

SAŽETAK • *U radu su prikazani rezultati rasplinjavanja peleta od drva listača različitim količinama zraka kao sredstvom za rasplinjavanje. U ispitivanju je uzet u obzir utjecaj pomaka tepiha materijala i omjera ekvivalencije (ER) na temperaturni profil, sastav plina i učinkovitost pretvorbe ugljika te na energetsku ravnotežu. Usporeni pomak tepiha materijala pospješuje zone dobrog izgaranja i redukcije, dok brzi pomak tepiha materijala rezultira visokim zonama pirolize i višim kalorijskim vrijednostima sintetskog plina. Kada je količina zraka porasla s 12 na 23 Nm^3/h, prinos plina povećao se s 1,4 na 1,6 $Nm^3/kg_{biomase}$ pri laganom pomaku tepiha materijala, a od 1,0 do 1,3 $Nm^3/kg_{biomase}$ pri brzom pomaku tepiha materijala. Ti rezultati pokazuju da su u oba primjera dobivene slične vrijednosti specifične energije. Međutim, u prvom je primjeru postignuta niža potrošnja goriva. Kemijska energija u sintetskom plinu čini 80 % izlazne energije pri laganom pomaku tepiha materijala (265 MJ/h) i 75 % pri brzom pomaku tepiha materijala (295 MJ/h). Znatan učinak pomaka tepiha materijala u reaktoru sugerira da se rasplinjač*

---

[1] Authors are researcher at Institute of Fluid-Flow Machinery, Polish Academy of Sciences, Gdańsk, Poland. [2]Author is PhD student at Gdańsk Univeristy of Technology, Faculty of Mechanical Engineering Gdańsk, Poland.
[1] Autori su istraživači Odsjeka za hidrauličke strojeve, Poljska akademija znanosti, Gdansk, Poljska. [2]Autor je doktorand Tehnološkog sveučilišta u Gdanjsku, Strojarski fakultet, Gdanjsk, Poljska.

može smatrati protočnim reaktorom, a dodatno brz pomak tepiha materijala s 20 Nm³/h dobave zraka omogućio je najkvalitetniji proces rasplinjavanja. Štoviše, brzi pomak tepiha materijala u reaktoru dovodi do nastanka velike količine pougljenjenog materijala s visokim energetskim potencijalom.

Ključne riječi: *rasplinjavanje, protusmjerni rasplinjač, drvo listača, pretvorba ugljika, pomak tepiha materijala*

1 INTRODUCTION
1. UVOD

The gasification process, which is recognized as one of the most effective in terms of thermal utilization of biomass and municipal waste, is a very popular topic in global research (Arena, 2012). This process is typically classified based on the type of gasification system. A common construction is a fixed-bed gasifier working in the downdraft or updraft configuration (McKendry, 2002). Downdraft gasification systems generate gas with a lower tar content than updraft gasifiers. Therefore, many studies focused on different types of downdraft gasifiers can be found in the literature (Balu and Chung, 2012; Phuphuakrat *et al.*, 2010; Nisamaneenate *et al.*, 2012; Zainal *et al.*, 2002; Erlich *et al.*, 2011). In the case of updraft reactors, the high tar content in the produced gas has significantly slowed the development of this technology (Dudyński *et al.*, 2012). However, studies based on updraft gasification are described in the literature. Blasi *et al.* (1999) used beechwood biomass in an updraft fixed-bed gasification process, which resulted in gas with a content of 28 % CO, 7 % CO_2, 7 % H_2 and 2 % CH_4.

Chen *et al.* (2011) studied the operating conditions of updraft gasification of mesquite and juniper and found that the heating value of syngas increased from 3.5 to 3.9 MJ/Nm³ for juniper and from 2.4 to 3.5 MJ/Nm³ for mesquite when the equivalence ratio (ER) decreased from 0.37 to 0.22. For both types of fuel, the maximum temperature in the combustion zone was above 1000 °C.

Pedroso *et al.* (2013) studied wood chip gasification in bottom-feed updraft gasification and showed that the gas produced contained 27 % CO and 4 % CH_4 and, relative to a typical updraft gasification system, a lower concentration of H_2 (6 %). The temperature of the bed in the reactor decreased from 885 °C in the combustion zone to 100 °C in the drying zone.

Recent research has focused on methods to clean the producer gas, optimize the updraft gasification process to decrease the high content of tar in the syngas, and obtain high-quality biochar (Taupe *et al.*, 2016). Ismail and El-Sala (2017) carried out numerical simulations and experimental studies of the influence of temperature in the gasifier and ER on syngas composition and tar yields during updraft gasification of wood pellets. It was reported than the ER had a significant impact on bed temperature and gas quality. A higher ER ratio corresponds to a larger amount of oxygen in the combustion zone, which leads to a lower concentration of carbon monoxide and hydrogen and also increases the carbon dioxide content of the syngas. On the other hand, more oxygen supplied to the gasifier promotes oxidization reactions and leads to more heat generation and higher

temperatures in the gasifier. These aspects were also presented by Ayyadurai *et al.* (2017), who studied large (1 m in length and 0.06 m in diameter) woody biomass gasification in a 60 kW_{th} updraft gasifier. These authors found that the gasification process with ER=0.6 producer syngas attained a heating value of 4.5 MJ/Nm³ and that the gasification temperature reached a temperature of 955 °C in the oxidation zone.

Another interesting issue related to updraft biomass gasification has been presented by Huang *et al.* (2017). These authors studied the characteristics of residual carbon in biomass, including structure and gasification activity. These aspects were investigated using Raman spectroscopy. Residual carbon in the ash is the result of char particles spending only a short amount of time in the gasifier.

Based on current literature, there are no available works that provide detailed information about the influence of time that the fuel spends in the gasifier or rate of bed movement and the amount of supplied air on the gasification temperature and syngas characteristics. The primary objective of this work was to investigate an alternative way to stimulate the updraft gasification process by forcing different rates of bed movement at different amounts of supplied air. The main parameters presented in this work include the temperature profile along the gasifier (e.g., the characteristics of the temperature zones, gas composition and caloric value, carbon conversion rate and energy balance).

2 MATERIALS AND METHODS
2. MATERIJALI I METODE

2.1 Proximate and ultimate analysis of fuel
2.1. Neposredna i krajnja analiza goriva

The hardwood pellets particles are a cylinder with diameter of 8 mm and length of up to 15 mm. The bulk density of hardwood pellets during experiments was 646 kg/m³. To conduct the proximate and ultimate analyses, the hardwood samples were first dried using a moisture analyzer (RADWAG) to determine their moisture content. The analysis of elementary composition was carried out using a CHNS-O Flash 2000 analyzer. The determination and calculation of the calorific value was executed using a KL-11 calorimeter. The results of the proximate and ultimate analyses are presented in Table 1.

2.2 Gasification stand
2.2. Postrojenje za rasplinjavanje

The experimental setup for the updraft gasification is shown in Figure 1. The gasifier was constructed using boiler steel and clad on mineral wool isolation. The total height of the reactor was 135 cm and its internal radius was 22 cm. The air inlet (three axially spaced
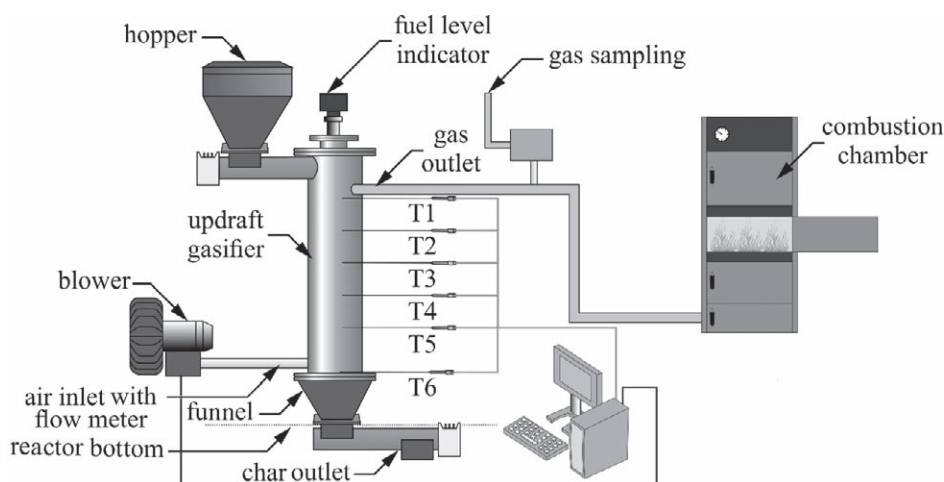
Figure 1 Schematic diagram of the experimental setup
Slika 1. Shematski prikaz istraživačkog postrojenja

Table 1 Duncan's test results for main effects
Tablica 1. Rezultati Duncanova testa za glavne utjecajne činitelje

	Hardwood pellets *Peleti od drva listača*
HHV, MJ/kg	19.6
Moisture, wt.%. as delivered	6.1
Proximate, wt.%$_{db}$[a] *Neposredno, wt.%$_{db}$*[a]	
Volatiles / *hlapljive komponente*	76.3
Fixed Carbon / *fiksni ugljik*	21.4
Ash / *pepeo*	2.3
Ultimate, wt.%$_{db}$[a] *Krajnje, wt.%$_{db}$*[a]	
C	48.5
H	5.3
O[b]	45.8
N	0.4

[a] db – oven-dry basis / *na bazi standardno suhe tvari*
[b] by difference / *prema razlici*

nozzles with a diameter of 8 mm) was installed 52 cm from the bottom of the reactor, ended with a funnel with 43 cm and it was connected with the char outlet tube with a diameter of 104 mm. The syngas outlet was installed 111 cm from the bottom.

During the experimental investigation, fuel from the hopper was loaded by a screw feeder, and tube with a diameter of 104 mm, to the reactor 10 cm below the syngas outlet. Six thermocouples (Type N and S) were installed in order to measure temperature within the gasifier. These thermocouples were placed 30, 55, 72, 88, 90 and 119 cm from the bottom of the reactor. The air was supplied to the gasifier via an electric blower and controlled using an inverter and a thermal mass flow meter. The syngas left the reactor and passed to the combustion chamber, through an outlet tube with a diameter of 54 mm. On the outlet tube, part of the produced gas was directed to the gas sampling system.

2.3 Experimental procedure
2.3. Postupak istraživanja

Prior to starting gasification, a batch of 3 kg feedstock was loaded into the gasifier in each experiment.

The initial level of the feedstock was maintained at the level of the air inlet nozzles until a high bed temperature was obtained. After a high bed temperature was obtained, the gasifier was filled to the level of the indicator. In each experiment, the height of the fuel bed was kept at the same level using a rotary fuel level indicator (i.e. 112 cm from the bottom). The amount of supplied air was set at 12, 17, 20 and 23 Nm³/h, and the duration of each experiment was 120 minutes from the point when the gasification process reached a steady-state condition (i.e. a constant temperature in each zone and a steady amount of received char). The gasification process was performed at atmospheric pressure in the range of 900-1100 °C. The solid residue (char and ash) was gathered from the bottom of the reactor using an inverter coupled with a cyclical screw at a frequency of 5 sec/5min (*Case 1*) and 10 sec/2.5 min (*Case 2*), which stimulated slow and fast bed movement in the reactor (char outlet velocity).

2.4 Measurements of gas composition
2.4. Mjerenje sastava plina

After steady-state conditions of gasification were achieved, the samples of syngas were sampled using tedlar bags. The analysis of the syngas content was performed using a SRI Instruments 310 gas chromatograph with a ShinCarbon ST 80-100 packed column and a thermal conductivity detector. The gas analyzer was pre-calibrated using a standard mixture of gas (CO, CO_2, CH_4 and H_2), and argon was used as a carrying medium.

3 RESULTS AND DISCUSSION
3. REZULTATI I RASPRAVA

3.1 Temperature profile in the gasifier
3.1. Temperaturni profil u rasplinjaču

Experimental investigations of hardwood pellet updraft gasification revealed a similar temperature profile trend in the gasifier, which is consistent with the literature (Chen *et al.*, 2012; Joseph *et al.*, 2016). The results indicated a significant impact of bed movement velocity in the gasifier on the height of individual pro-
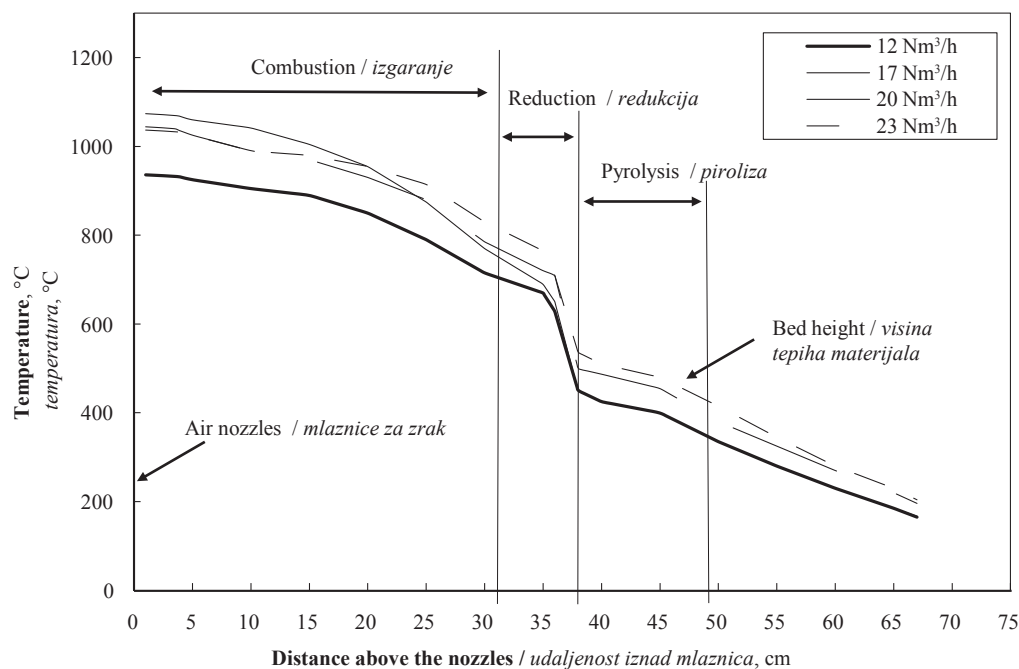
Figure 2 Characteristic temperature profile and gasifier zones in *Case 1*
Slika 2. Karakteristični temperaturni profil i zone rasplinjavanja u primjeru 1.

cess zones (Figure 2 and Figure 3). Based on the literature, the boundary of the combustion and reduction zone was established at 1000 °C and 750 °C (Chen *et al*., 2012; Sircar *et al*., 2014; Mani *et al*., 2011). Our results show that, in *Case 1* (slow bed movement in the reactor), the combustion zone attained a height of about 32 cm from the air nozzles and the reduction zone reached a maximum height of 7 cm.

Since the level of the fuel in the gasifier was set at 50 cm from the air nozzles, the pyrolysis zone attained a height of 11 cm. In *Case 2* (fast bed movement in the reactor), the height of the combustion (reduc-

tion) zone attained a maximum of 16 cm. *Case 2* promoted the pyrolysis process with a zone height of 17 cm. Lower temperatures in pyrolysis zone in *Case 2* are associated with the intensification of supplied fresh fuel and consumed heat, supplied by oxidation of biomass at the lower part of the reactor, in endothermic pyrolysis reactions (high temperature gradient between 35 and 40 cm from the air nozzles, Figure 3).

The results of the hardwood updraft gasification also indicated that the gradient of the bed temperature was about 6 °C/cm for 12 Nm³/h of supplied air and 10 °C/cm for all other amounts of air in *Case 1*. In *Case 2*,
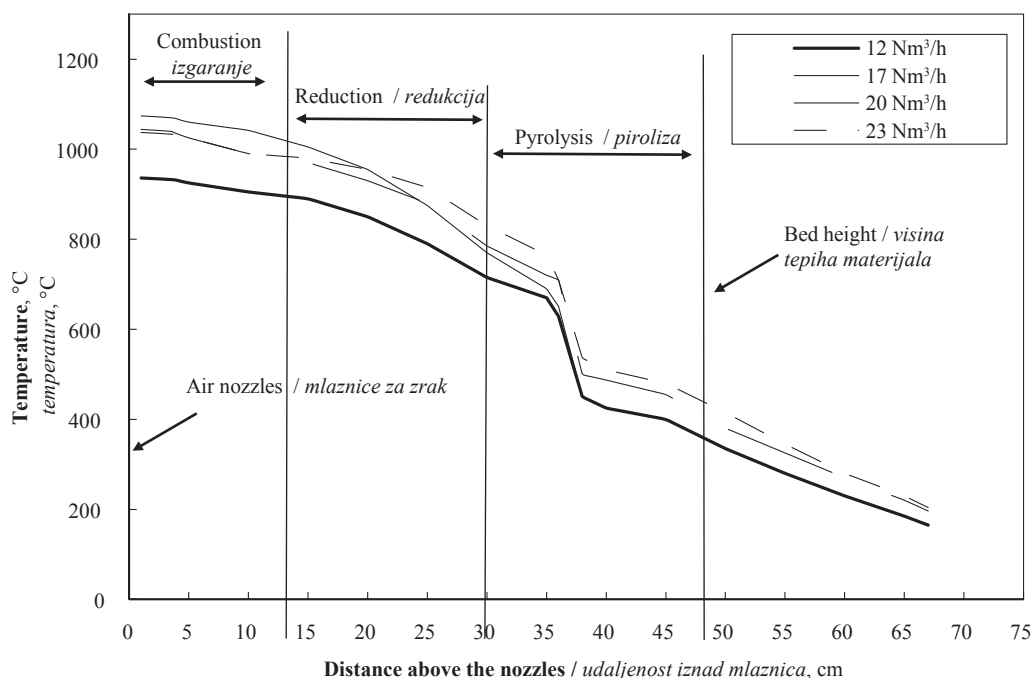

Figure 3 Characteristic temperature profile and gasifier zones in *Case 2*
Slika 3. Karakteristični temperaturni profil i zone rasplinjavanja u primjeru 2.

Table 2 Performance of the gasification process
Tablica 2. Obilježja procesa rasplinjavanja

Case *Primjer*	Air, Nm³/h *Zrak*, Nm³/h	Fuel consumption, kg/h *Potrošnja goriva*, kg/h	ER *ER*	Temperature, °C *Temperatura*, °C
Case 1 / *primjer 1.*	12	14.6	0.16	774
	17	19.61	0.16	1092
	20	23.0	0.16	1094
	23	27.0	0.16	1056
Case 2 / *primjer 2.*	12	26.2	0.09	936
	17	27.1	0.12	1074
	20	28.8	0.13	1044
	23	33.7	0.13	1038

the corresponding values were 12 °C/cm and 13 °C/cm. Faster bed movement in the reactor resulted in a slightly steeper temperature gradient.

3.2 Performance of the gasification process
3.2. Obilježja procesa rasplinjavanja

Experimental investigation showed the importance of comparing the amount of air supplied, fuel consumption, equivalence ratio and temperature. The results presented in Table 2 show similar temperature and fuel consumption trends as a function of the amount of air. However, in *Case 1* the same value of ER was rated (0.16) in each experiment. In *Case 2* ER value increased from 0.09 to 0.13, which is related to similar fuel consumption with the simultaneous increase in the amount of supplied air. It is noteworthy that, in *Case 2*, increasing of the amount of air supplied to 23 Nm³/h led to a significant increase in fuel consumption (from 28.8 to 33.7 kg/h), which may be caused by the increase of the intensity of oxidation/reduction processes.

3.3 Gas calorific value
3.3. Ogrjevna vrijednost plina

In an updraft gasifier, carbon dioxide is generated via the oxidation of wood pellets in the lower part of the reactor, and carbon monoxide is produced by a char reduction reaction (Boudouard reaction) in the reduction zone between the bottom and the middle parts of the reactor. Pyrolytic gas is produced in the pyrolityc zone at the lower-middle part of the gasifier (McKendry, 2002).

Different rates of bed movement, apart from variable amounts of supplied air, also affected significantly the generated zone heights and syngas composition. Fast bed movement in the gasifier (*Case 2*) promoted pyrolysis process with the height of the zone (Figure 3), which led to a slightly reduced production of pyrolytic gas and higher calorific value of the syngas (Table 3). In *Case 1*, slow movement of fixed bed resulted in the formation of a high zone of oxidation and reduction (Figure 2) that influenced the lower content of carbon dioxide, hydrogen and methane and increased the amount of generated syngas.

Based on the literature, the amount of produced gas was calculated using the nitrogen tracer method (Chen *et al.*, 2012; Thanapal, 2010), which relies on knowing the amount of nitrogen in the supplied air. The results revealed that the slow bed movement in the gasifier led to a larger gas yield per kg of biomass; the peak value was 1.6 Nm³/kg$_{biomass}$ for 23 Nm³/h of supplied air. At fast bed movement in the gasifier, the corresponding value was 1.3 Nm³/kg$_{biomass}$. Furthermore, an increase in the amount of air supplied to the gasifier resulted in an increase in the amount of gas yield per kg of biomass for both cases, which is consistent with the literature (Chen *et al.*, 2012;, Ismail and El-Sala, 2017).

Specific gas energy (MJ/kg) is an additional parameter representing the amount of energy obtained from a kilogram per hour of solid fuel in the form of gaseous fuel (Taupe *et al.*, 2016) and allows to determine the energy efficiency of the gasification process. For both Cases, experimental results showed that the specific gas energy reached similar value (Table 3). However, in *Case 1* these values were reached at lower fuel consumption (Table 2). It is caused by lower heating values of produced gas (4.8 - 6.2 MJ/Nm³) with a

Table 3 Syngas composition
Tablica 3. Sastav sintetskog plina

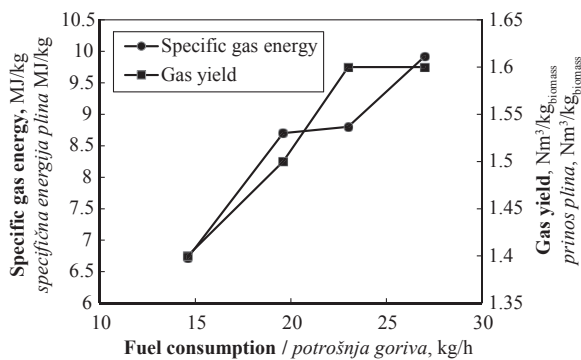| Case *Primjer*	Air / *Zrak* Nm³/h	ER *ER*	Syngas components, % *Sastav sintetskog plina*, %				LHV of gas *LHV plina* MJ/Nm³	Gas yield *Prinos plina* Nm³/kg$_{biomase}$	Specific energy *Specifična energija* MJ/kg
			CO	CO$_2$	H$_2$	CH$_4$			
Case 1 *primjer 1.*	12	0.16	25.3	5.6	6.9	2.4	4.8	1.4	6.72
	17	0.16	33.8	4.8	8.2	1.8	5.8	1.5	8.70
	20	0.16	32.2	5.7	8.4	1.3	5.5	1.6	8.80
	23	0.16	35.5	4.4	8.5	2.1	6.2	1.6	9.92
Case 2 *primjer 2.*	12	0.09	34.6	9.6	14.4	3.9	7.3	1.0	7.30
	17	0.12	33.4	7.1	12.1	3.1	6.7	1.2	8.04
	20	0.13	33.3	8.3	11.3	2.7	6.4	1.4	8.96
	23	0.13	36.8	7.5	11.5	2.6	6.8	1.3	8.84

Figure 4 Relation of fuel consumption and specific gas energy and gas yield in *Case 1*
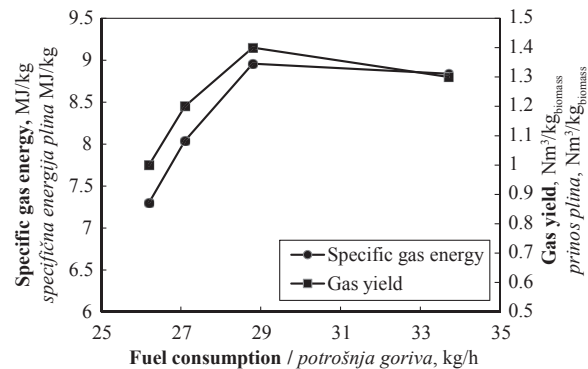**Slika 4.** Odnos potrošnje goriva i specifične energije plina te prinosa plina u primjeru 1.

Figure 5 Relation of fuel consumption and specific gas energy and gas yield in *Case 2*
Slika 5. Odnos potrošnje goriva i specifične energije plina te prinosa plina u primjeru 2.

higher gas yield (1.4 - 1.6 $Nm^3/kg_{biomass}$) in *Case 1*, and accordingly higher heating values of produced gas (6.4-7.3 MJ/Nm^3) with a lower gas yield (1.0-1.4 $Nm^3/kg_{biomass}$) in *Case 2*. Moreover, the results showed that, for the slow fuel motion in the reactor (*Case 1*), the gasification process reached the maximum gas yield with a fuel consumption of 23 kg/h (ER=0.21) (Figure 4). In *Case 2* (Figure 5) maximum gas yield was reached with a fuel consumption of 28.8 kg/h. This aspect indicates the potentially optimal process conditions for the presented Cases (char outlet velocity).

3.4 Char characteristic
3.4. Svojstva pougljenjenog materijala

Experimental investigations of hardwood pellet gasification revealed the impact of stimulated bed movement in the reactor on fuel consumption (Table 4). As the amount of supplied air increased from 12 to 23 Nm^3/h, the fuel consumption increased from 14.6 kg/h to 27 kg/h in *Case 1* and from 26.2 kg/h to 33.7 kg/h in *Case 2*. This relation was also presented by Pedroso *et al*. (2013), who showed that the increase in the amount of air from 21 to 28 Nm^3/h caused an increase in fuel consumption from 10 to 14 kg/h during updraft gasification of woodchips. Furthermore, a larger amount of oxygen supplied to the gasifier intensified the oxidization reaction, which led to an increase in the carbon conversion rate. In *Case 1*, an increase in the amount of supplied air from 12 to 23 Nm^3/h resulted in increased carbon conversion from 70 to 94 %. In *Case*

2, the corresponding data were 78 and 83 %, respectively. A larger amount of oxygen supplied to the gasifier promoted oxidization reactions and led to increased CO_2 generation. These aspects were presented by Kalström *et al*. (2015). These authors found that an increase in carbon dioxide concentration from 13 to 60 % significantly affected the char conversion rate during CO_2 gasification of char particles from torrefied fuels like pine shell, olive stones and straw.

The carbon conversion was calculated as the ratio of the carbon difference in biomass and char after gasification compared with the amount of carbon in the biomass. The theoretical amount of char was based on the difference in the mass of carbon in the fuel and the resulting syngas. These calculations did not take into account the tars. The experimental results revealed that optimum conditions were achieved for fast movement of fixed bed in the gasifier (*Case 2*) for 20 Nm^3/h, where the smallest difference between the received and calculated amount of produced char was obtained, which may indicate the high fuel conversion rate, lowest accumulation of carbon (char) in the reactor and low tar content.

3.5 Mass and energy balance
3.5. Masa i energetska bilanca

An important parameter for comparing the impact of the rate of bed movement in the gasifier and the amount of supplied air on the updraft gasification process is a mass and energy balance. The energy input

Table 4 Performance data of gasification process
Tablica 4. Podatci o procesu rasplinjavanja

|		**Case 1** / *Primjer 1.*				**Case 2** / *Primjer 2.*			
Amount of supplied air / *Količina dobave zraka*	Nm^3/h	12	17	20	23	12	17	20	23
Fuel consumption / *Potrošnja goriva*	kg/h	14.6	19.6	23.0	27.0	26.2	27.1	28.8	33.7
Carbon in the fuel / *Ugljik u gorivu*	kg/h	7.1	9.5	11.2	13.1	12.7	13.1	13.9	16.4
Char received / *Količina pougljenjenog materijala*	kg/h	2.6	1.1	0.8	0.8	3.4	3.2	3.5	2.9
Carbon content in the char / *Sadržaj ugljika u pougljenjenome materijalu*	%	84.0	87.4	97.5	97.8	82.3	87.3	92.8	96.8
Carbon conversion / *Pretvorba ugljika*	%	70	91	93	94	78	79	76	83
Mass of carbon in the gas / *Masa ugljika u plinu*	kg/h	3.5	6.2	8.1	9.5	6.5	7.2	9.1	10.3
Theoretical char / *Teorijska količina pougljenjenog materijala*	kg/h	4.2	3.8	3.2	3.6	7.9	6.8	5.2	7.5
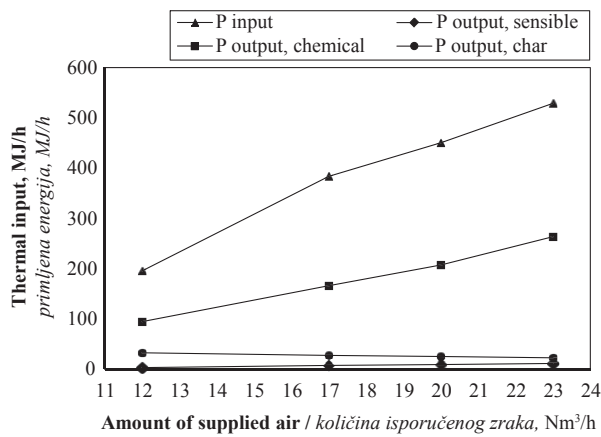
Figure 6 Characteristics of input and output energy during updraft gasification in *Case 1*
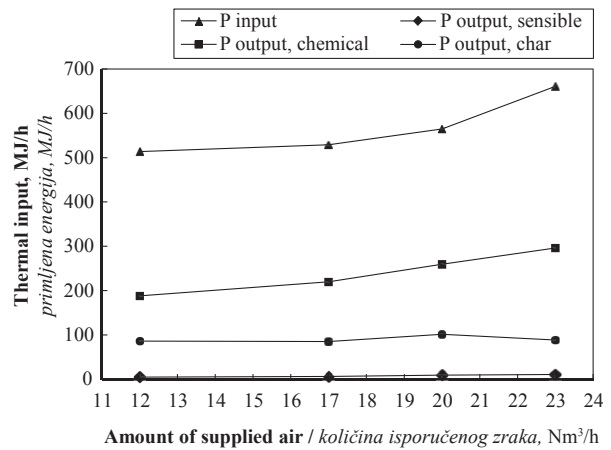**Slika 6.** Obilježja primljene i otpuštene energije tijekom protusmjernog rasplinjavanja u primjeru 1.

Figure 7 Characteristics of input and output energy during updraft gasification in *Case 2*
Slika 7. Svojstva primljene i otpuštene energije tijekom protusmjernog rasplinjavanja u primjeru 2.

flow was defined as the product of fuel consumption per unit time (Table 4) and the higher heating value of hardwood pellets (Table 1):

$$P_{input} = \dot{m}_{fuel} \cdot HHV_{fuel} \ (MJ \ / \ h) \qquad (1)$$

The energy output flow associated with chemical energy in the syngas was calculated from the volumetric composition of the combustible species contained in the syngas and their caloric value (Table 2):

$$P_{out,chemical} = \sum_i V_i \cdot HHV_i \ (MJ \ / \ h) \qquad (2)$$

The syngas produced at the outlet of the reactor was very hot and also carried a certain amount of heat (sensible heat), which can be defined as a product of the specific heat capacity, the molar flow of each component and the outlet temperature of the syngas:

$$P_{out,sensible} = \sum_i \dot{n}_i \int_{T_{ambient}}^{T_{gas,outlet}} c_{p,i} dT \ (MJ \ / \ h) \qquad (3)$$

The specific heat capacity $c_{p,i}$ at different temperatures is well known in the literature (Nederlandse Gasunie, 1988), and the molar flow of each component was calculated from the data given in Table 4. The syngas temperature at the outlet of the gasifier was no more than 230 °C.

A certain amount of char was collected during gasification of hardwood pellets in each experimental series (from 0.8 to 3.5 kg/h; Table 4). For this reason, the energy output contained in the char $P_{out,char}$ was also taken into account and was defined as the product of char received per unit time (Table 3) and its higher heating value:

$$P_{out,char} = \dot{m}_{char} \cdot HHV_{char} \ (MJ \ / \ h) \qquad (4)$$

Our experimental results revealed that the energy input contained in the hardwood pellets reached, at 23 Nm³/h of supplied air, 530 MJ/h in *Case 1* and 660 MJ/h in *Case 2* (Table 4). For both cases, the largest fraction of the calculated output energy was chemical energy in the syngas (Figure 4 and Figure 5), from 94 MJ/h (at 12 Nm³/h of supplied air) to 530 MJ/h (at 23 Nm³/h of supplied air) in *Case 1* (Figure 4) and from 513 to 660 MJ/h, respectively, in *Case 2*. The higher output energy in *Case 2* is associated with the promotion of the pyrolysis process and the production of syngas with a higher calorific value.

The analysis of heat input and output during updraft gasification of hardwood pellets revealed a deviation of 33-47 % in the heat balance (Table 5), which might be caused by our not taking into account the energy output of tars and the heat loss of the installation.

According to the findings of Ayyadurai *et al*. (2017), it is difficult to heat balance the gasification process. These authors showed that the deviation in the heat balance reached 22 %. They also found that the chemical energy contained in the syngas represented nearly 60 % of the output energy. In our study, the work chemical energy was balanced from 57-88 % in *Case 1* and from 67-74 % in *Case 2*.

The char was gathered from the bottom of the reactor using an inverter coupled with a cyclical screw at a frequency of 5 sec/5min (*Case 1*) and 10 sec/2.5 min (*Case 2*), which stimulated bed movement in the reactor.

Table 5 Energy balance
Tablica 5. Energetska bilanca

		Case 1 / *Primjer 1.*				**Case 2** / *Primjer 2.*			
Amount of supplied air / *Količina dobave zraka*	Nm³/h	12	17	20	23	12	17	20	23
Fuel consumption / *Potrošnja goriva*	kg/h	14.6	19.6	23.0	27.0	26.2	27.1	28.8	33.7
Thermal input / *Toplinski ulaz*	MJ/h	196	384	450	529	513	529	564	660
Thermal output / *Toplinski izlaz*	MJ/h	168	205	246	303	284	316	375	401
Deviation / *Odstupanje*	%	15	47	45	43	45	40	33	39

Table 6 Energy characteristics of char
Tablica 6. Energetska obilježja pougljenjenog materijala

	Case 1 / *Primjer 1.*				Case 2 / *Primjer 2.*			
Air / *Zrak,* Nm³/h	12	17	20	23	12	17	20	23
Fuel consumption / *Potrošnja goriva,* kg/h	14.6	19.6	23.0	27.0	26.2	27.1	28.8	33.7
Char received / *Količina pougljenjenog materijala,* kg/h	2.6	1.1	0.8	0.8	3.4	3.2	3.5	2.9
Carbon content in char / *Sadržaj ugljika u pougljenjenome materijalu,* %	84.0	87.4	97.5	97.8	82.3	87.3	92.8	96
$P_{out,char}$, MJ/kg	32.81	27.63	25.39	23.04	86.51	85.28	101.83	88.52

The energy output contained in the char P_{out} is also an important part of the output energy. As shown in Table 6, in *Case 2*, the thermal output reached 100 MJ/h with a fuel consumption of 28.8 kg/h (20 Nm*3*/h of air) and remained at a similar level (85 MJ/h) for the other cases. An increase in air supplied to the gasifier for the slow movement of the bed (*Case 1*) caused a decrease in the quantity of received char (from 2.6 to 0.8 kg/h) and a decrease in the char output energy from 66 to 23 MJ/h. This aspect shows that fast bed movement in the reactor, stimulated by char outlet velocity, leads to a high amount of the char with a high energy potential, which can react with steam and form clean energy gas.

Our experimental investigation revealed that sensible heat contained in the producer gas did not constitute a significant infraction of the output energy balance; the sensible heat reached 11 MJ/h in *Case 1* and 10 MJ/h in *Case 2* (Figure 4 and Figure 5).

4 CONCLUSIONS
4. ZAKLJUČAK

Updraft gasification of hardwood pellets with different bed movement in the reactor and for 12, 17, 20 and 23 Nm³/h of supplied air has been developed and evaluated. The following conclusions were drawn:
1. The results indicated a significant effect of bed movement in the reactor suggesting that the gasifier could be considered as a flow reactor.
2. Slow bed movement promotes a higher combustion and reduction zone, which leads to syngas maximum calorific value of about 6 MJ/Nm³, while fast movement of the bed promotes a higher pyrolysis zone and generates more calorific gas (6-7 MJ/Nm³).
3. The results indicate that slow bed movement, in comparison to fast bed movement, generated a higher syngas yield, with its lower caloric value. These results showed that in both Cases similar specific energy values were obtained. However, lower fuel consumption was reached in *Case 1*.
4. Fast bed movement in the reactor leads to a high amount of generated char with high energy potential.
5. An energy balance analysis was carried out for all considered cases. The total calculated input energy flow attained a maximum of 560 MJ/h for slow bed movement and 660 MJ/h for fast bed movement (at 23 Nm³/h of supplied air), and the output energy flow was 303 and 400 MJ/h, respectively. The devia-

tion of 30-40 % in heat balance was caused by not taking into account the tars and heat losses. Furthermore, it was noted that the chemical energy in the syngas represented 60-80 % of the output energy.
6. Both cases of updraft hardwood pellet gasification generated high-quality gas. However, based on the temperature characteristics, performance data, carbon conversion efficiency and energy balance analysis, it was found that the fast movement of the bed with 20 Nm³/h of supplied air yielded the highest-quality gasification process.

5 REFERENCES
5. LITERATURA

1. Arena, U., 2012: Process and technological aspects of municipal solid waste gasification. A review. Waste Manage, 32: 625-639.
   https://doi.org/10.1016/j.wasman.2011.09.025.
2. Ayyadurai, S.; Schoenmakers, L.; Hernández, J. J., 2017: Mass and energy analysis of a 60 kW$_{th}$ updraft gasifier using large size biomass. Fuel, 187: 356-366.
   https://doi.org/10.1016/j.fuel.2007.03.028.
3. Balu, E., Chung, N., 2012: System characteristics and performance evaluation of a trailer – scale downdraft gasifier with different feedstock. Bioresource Technol, 108: 264-273.
   https://doi.org/10.1016/j.biortech.2011.12.105.
4. Blasi, D. C.; Signorelli, G.; Portoricco, G., 1999: Countercurrent Fixed-Bed Gasification of Biomass at Laboratory Scale. Ind. Eng. Chem. Res., 38: 2571-2581. https://doi.org/10.1021/ie980753i.
5. Chen, W.; Annamalai, K.; Ansley, R. J.; Mirik, M., 2012: Updraft fixed bed gasification of mesquite and juniper wood samples. Energy, 41: 454-461.
   https://doi.org/10.1016/j.energy.2012.02.052.
6. Dudyński, M.; Kwiatkowski, K.; Bajer, K., 2012: From feathers to syngas – Technologies and devices. Waste Manage, 32: 685-691.
   https://doi.org/10.1016/j.wasman.2011.11.017.
7. Erlich, C.; Fransson, T. H., 2011: Downdraft gasification of pellets made of wood, palm-oil residues respective bagasse: Experimental study. Applied Energy, 88: 899-908.
   https://doi.org/10.1016/j.apenergy.2010.08.028.
8. Huang, S.; Wu, S.; Wu, Y.; Gao, J., 2017: Structure characteristics and gasification activity of residual carbon from updraft fixed-bed biomass gasification ash. Energy Conversation and Management, 36: 108-118.
   https://doi.org/10.1016/j.enconman.2016.12.091.
9. Ismail, T. M., El-Sala, M. A., 2017: Parametric studies on biomass gasification process on updraft gasifier high temperature air gasification. Applied Thermal Engineering, 112: 1460-1473.
   https://doi.org/10.1016/j.applthermaleng.2016.10.026.

10. Joseph, H.; Kihedu, J. H.; Yoshiie, R.; Naruse, I., 2016: Performance indicators for air and air-steam auto-thermal updraft gasification of biomass in packed bed reactor. Fuel Processing Technology, 141: 93-98. https://doi.org/10.1016/j.fuproc.2015.07.015.

11. Karlström, O.; Costa, M.; Brink, B.; Hupa, M., 2015: CO_2 gasification rates of char particles from torrefied pine shell. Fuel, 158: 753-763. https://doi.org/10.1016/j.fuel.2015.06.011.

12. Mani, T.; Mahinpey, N.; Murugan, M., 2011: Reaction kinetics and mass transfer studies of biomass char gasification with CO_2. Chemical Engineering Science, 66: 36-41. https://doi.org/10.1016/j.ces.2010.09.033.

13. McKendry, P., 2002: Energy production from biomass (part 3): gasification technologies. Bioresource Technology, 83: 55-63. https://doi.org/10.1016/S0960-8524(01)00120-1.

14. Nederlandse Gasunie, N. V., 1988: Physical properties of natural gases.

15. Nisamaneenate, J.; Aton, D.; Sornkade, P.; Sricharoenchaikul, V., 2012: Fuel gas production from peanut shell waste using a modular downdraft gasifier with the thermal integrated unit. Renewable Energy, 79: 45-50. https://doi.org/10.1016/j.renene.2014.09.046.

16. Pedroso, D. T.; Machín, E. B.; Silveira, J. S.; Nemoto, Y., 2013: Experimental study of bottom feed updraft gasifier. Renewable Energy, 57: 311-316. https://doi.org/10.1016/j.renene.2013.01.056.

17. Phuphuakrat, T.; Nipattummakul, N.; Namioka, T.; Kerdsuwan, S.; Yoshikawa, K., 2010: Characterization of tar content in the syngas produced in a downdraft type fixed bed gasification system from dried sewage sludge. Fuel, 89: 2278-2284. https://doi.org/10.1016/j.fuel.2010.01.015.

18. Sircar, I.; Sane, A.; Wang, W.; Gore, J. P., 2014: Experimental and modeling study of pinewood char gasification with CO_2. Fuel, 119: 38-46. https://doi.org/10.1016/j.fuel.2013.11.026.

19. Taupe, N. C.; Lynch, D.; Wnetrzak, R.; Kwapinska, M.; Kwapinski, W.; Leahy, J. J., 2016: Updraft gasification of poultry litter at farm-scale – A case study. Waste Management, 50: 324-333. https://doi.org/10.1016/j.wasman.2016.02.036.

20. Thanapal, S. S., 2010: Gasification of low ash partially composted dairy biomass with enriched air mixture. Master's thesis. Texas A&M University.

21. Ueki, Y.; Torigoe, T.; Ono, H.; Yoshiie, R.; Kihedu, J. H.; Naruse, N., 2011: Gasification characteristics of woody biomass in the packed bed reactor. Proceedings of the Combustion Institute, 33: 1795-1800. https://doi.org/10.1016/j.proci.2010.07.080.

22. Zainal, Z. A.; Rifau, A.; Quadir, G. A.; Seetharamu, K. N., 2002: Experimental investigation of a downdraft biomass gasifier. Biomass and Bioenergy, 23: 283-289. https://doi.org/10.1016/S0961-9534(02)00059-4.

Corresponding address:

JACEK KLUSKA

Institute of Fluid Flow Machinery
Fiszera 14
80-231 Gdańsk, POLAND
e-mail: jkluska@imp.gda.pl

LABORATORY FOR HYDROTHERMAL PROCESSING OF WOOD AND WOODEN MATERIALS

Testing of hydrothermal processes of wood and wooden materials

Thermography measurement in hydrothermal processes

Standard and nonstandard determination of moisture content in wood

Determination of climate and microclimate conditions in air drying and storage of wood, organization of lumber storage

Project and development of conventional and unconventional drying systems

Steaming chamber projects

Establishing and modification of kiln drying schedules

Consulting in selection of kiln drying technology

Introduction of drying quality standards

Determination of wood bending parameters

Detection and reducing of hydrothermal processes wood defects

Reducing of kiln drying time

Drying costs calculation

Kiln dryer capacity calculation

ZAGREB UNIVERSITY
FACULTY OF FORESTRY
WOOD SCIENCE AND TECHNOLOGY DEPARTMENT
Svetošimunska c. 25, p.p. 422
HR-10002 ZAGREB
CROATIA

385 1 235 2509 tel
385 1 235 2544 fax
hidralab@sumfak.hr
pervan@sumfak.hr
www.sumfak.hr

Aurel Lunguleasa[1], Nadir Ayrilmis[2], Cosmin Spirchez[1], Ferhat Özdemir[3]

Investigation of the Effects of Heat Treatment Applied to Beech Plywood

Istraživanje utjecaja toplinske obrade na svojstva uslojene ploče od bukovine

ABSTRACT • *The aim of this study is to determine the effects of heat treatment on some physical and mechanical properties of beech plywood boards. The 3-layered beech plywood boards with a thickness of 3.9 mm were subjected to heat treatment for 1, 2 and 3 hours at temperatures of 160, 180 and 200 °C. These beech plywood boards were tested for physical properties such as density, water absorption and thickness swelling, mechanical property tests such as modulus of rupture (MOR) and Brinell hardness, and mass loss rates according to the relevant standards. The results obtained show that the hydrophobicity of beech plywood boards is improved but the strength and weight loss are adversely affected, depending on the temperature and duration of heat treatment. It has been found that beech plywood boards heat-treated at 200 °C for 3 hours can be used in very humid environments for average mechanical stresses of wood parts with a reduced thickness swell of 4 % and a reduced water absorption rate of more than 12 %.*

Keywords: *plywood, heat treatment, mass loss, swelling, Brinell hardness, water absorption*

SAŽETAK • *Cilj istraživanja bio je utvrditi utjecaj toplinske obrade na neka fizička i mehanička svojstva uslojenih ploča od bukovine. Troslojne uslojene ploče od bukovine debljine 3,9 mm podvrgnute su toplinskoj obradi u trajanju jednoga, dva i tri sata pri temperaturama 160, 180 i 200 °C. Prema odgovarajućim standardima, ispitana su fizička svojstva tih ploča kao što su gustoća, apsorpcije vode i bubrenje, mehanička svojstva poput modula loma (MOR) i tvrdoće prema Brinellu te gubitka mase. Dobiveni su rezultati pokazali da se hidrofobnost ploča povećala, ali je njihova toplinska obrada negativno utjecala na čvrstoću i gubitak mase ovisno o trajanju i temperaturi obrade. Utvrđeno je da se uslojene ploče od bukovine, toplinski obrađene pri temperaturi od 200 °C u trajanju tri sata, mogu upotrebljavati u vrlo vlažnim uvjetima, pri prosječnome mehaničkom opterećenju drvnih dijelova, uz smanjenje bubrenja od 4 % i smanjenje apsorpcije vode veće od 12 %.*

Ključne riječi: *uslojeno drvo, toplinska obrada, gubitak mase, bubrenje, tvrdoća prema Brinellu, apsorpcija vode*

[1] Authors are professor and PhD student at Department of Wood Processing and Design of Wooden Products, Faculty of Wood Engineering, Transylvania University of Brasov, Brasov, Romania. [2]Author is professor at Department of Wood Science, Section of Mechanical Wood Composite Technology, Faculty of Forestry, Istanbul University-Cerrahpasa, Istanbul, Turkey. [3]Author is assistant professor at Department of Forest Industry Engineering, Faculty of Forestry, Kahramanmaras Sutcu Imam University, Kahramanmaras, Turkey.

[1] Autori su profesor i doktorand Odsjeka za obradu drva i dizajn drvnih proizvoda, Fakultet drvne industrije, Transilvanijsko sveučilište Brašov, Brašov, Rumunjska. [2]Autor je profesor Odsjeka za znanost o drvu, Zavod za mehaničku obradu drvnih kompozita, Šumarski fakultet, Sveučilište u Istanbulu-*Cerrahpasa*, Istanbul, Turska. [3]Autor je izvanredni profesor Odsjeka za industriju na bazi šuma, Šumarski fakultet, Kahramanmaras Sutcu Imam Sveučilište, Kahramanmaras, Turska.

1 INTRODUCTION
1. UVOD

Plywood is an ancient engineering product, known as a primary form since the times of the ancient Egyptians. It is made of three or more layers (usually an odd number) of veneer, disposed at 90^0 between them, glued and pressed. The odd number of veneers is given by the symmetry of the final board structure, i.e. the existence of a median layer, next to which other veneer layers are placed on one side and the other. The perpendicular layout of two adjacent veneer layers confers to the board a high uniformity of the properties, especially of fibers perpendicular and parallel with the wood. Although recently these boards have been increasingly replaced by fiberboards in the furniture manufacturing industry, or by oriented strand boards in the field of construction, they are still products demanded for various other uses. Among the board properties that make them preferable to massive wood, the following can be mentioned: board density is slightly higher than the one of massive wood from which veneer was made, due to the densification degree and the density of the adhesive in dry state; board higroscopicity is low i.e. approximately 10 times lower transversally as compared to massive wood, due to the presence of dry adhesive (not hygroscopic); the board has higher strength than massive wood and the quality index (the ratio between strength and density) makes the board superior to steel and aluminum alloys. At the same time, the board is a homogeneous product and reduces the effect of the natural defects of massive wood, spreading them on wide surfaces.

The purpose of heat treatment of wooden products (lumber, shredding, sawdust and chips, briquettes, pellets, straw, rice husk) at high temperatures is to improve properties (Lundborg, 1998; Demirbas, 2001; Jehlickova and Morris, 2007; Gavrilescu, 2008; Chen *et al.*, 2011; Wang *et al.*, 2011; Chen *et al.*, 2012; Omer, 2012; Vilcek, 2013; Chen *et al.*, 2014) such as absorption and thickness swelling, natural durability (especially the strength against attacks of xylophages fungi), caloric power (Kastanaki and Vamvuka, 2005), all these thanks to the degradation of the hemicelluloses in the wood (Prasertsan and Sajakulnukit, 2006; Jehlickova and Morris, 2007; Shulga *et al.*, 2008). The true revolution in the field of heat treatment started with the introduction of the European standard CEN/TS 15679 in 2007. The use of classic boards in outdoor environment involves the use of more expensive adhesives, or the increase of the paraffin or wax content, which increases considerably their price. These inconveniences can be avoided by heat treatment of the boards at high temperatures, taking care not to reduce drastically their strength. The question also arises whether it is adequate to subject the boards to heat streatment ard then to glue them (Zdravković *et al.*, 2013), or to apply heat treatment directly to the plywood. The opinions of the researchers in this respect are contradictory. The important fact is to provide an efficient manufacturing chain (as short as possible), lower costs and as many as possible benefits (Uslu, 2008; Batidzirai *et al.*, 2013). Feher *et al.* (2014) considers that it is simpler to apply heat treatment to the veneer. The heat treated board acquires a black color, the black degree depending on the intensity of the applied treatment. The darkening of the veneers and boards represents heat treatment deficiency (Tabarés *et al.*, 2000; Thomson *et al.*, 2005; Lovrić *et al.*, 2014; Salca *et al.*, 2016), but it does not reduce the quality of the products used in outdoor environment, as the wooden surface darkens anyway under the effects of bad weather. Due to heat degradation, all heat treated products have lower strength, regardless of whether these products are manufactured of wood glued veneers, or Laminated Veneer Lumber (Nazerian *et al.*, 2011; Nazerian and Ghalehno, 2011). However, at the beginning of the heat treatment between 150 and 160 °C, a part of the strength of heat treated products slightly increases, after which their strength is reduced with the intensification of the heat treatment (Percin *et al.*, 2016). Some authors found that heat treatment affects the reduction of formaldehyde emission, especially in the case of poplar boards (Murata *et al.*, 2013). Heat treatment has additional beneficial effects on veneers when it is combined with their pressing at the pressure of 2.7 MPa (Arruda and del Menezzi, 2016).

The main objective of this study is to obtain an optimal heat treatment of 3-layered beech plywood, in order to be used in outdoor environment. For this purpose, it is intended to increase the hydrophobicity of the boards i.e. to reduce their absorption and thickness swelling in the conditions in which the mechanical properties (modulus of rupture MOR for static bending and Brinell hardness) could remain constant or slightly decrease.

2 MATERIALS AND METHODS
2. MATERIJALI I METODE

3 layer beech (*Fagus Sylvatica* L.) plywood sheets with an average thickness of 3.9 mm were purchased from the local market. Samples with dimensions of 380 x 380 mm have been cut from various parts of the boards (edge, middle or median) for heat treatment. The heat treatment of the board was performed in a laboratory stove without oxygen admission. The heat treatment applied to the test samples is shown in Table 1.

First, all the samples were conditioned at 23 ± 2 °C and 65 ± 5 % relative humidity until they reached a constant weight. The heat treatments shown in Table 1 were applied to the test samples and the weight loss amounts were determined. Then, some physical and mechanical properties of the test specimens were investigated. Mechanical properties such as MOR (EN 310, 2000) and Brinell hardness (EN 1534, 2000) together with physical property tests such as density (EN 323, 1993), water absorption and thickness swelling (EN 317) tests were carried out according to the relevant standards. The tests were repeated 15 times per each test type and parameter. The relationship between the force and time applied in the Brinell

Table 1 Experimental parameters of heat treatment applied to beech plywood
Tablica 1. Parametri istraživanja toplinske obrade uslojene ploče od bukovine

Board type *Vrsta ploče*		**Temperature, °C** *Temperatura*, **°C**		
		160	180	200
Beech plywood (3.9 mm) / *uslojena ploča od bukovine (3,9 mm)*	Time, h *Vrijeme,* h	0	0	0
		1	1	1
		2	2	2
		3	3	3
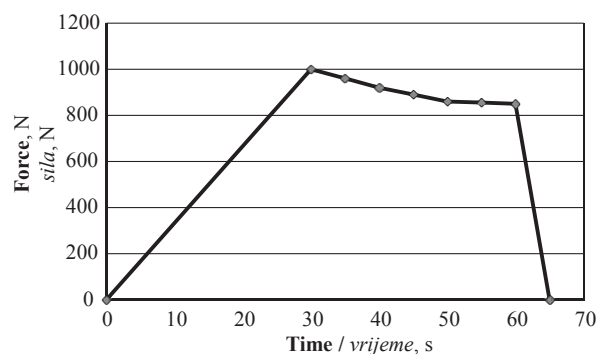
Figure 1 Force evolution in time of Brinell hardness testing
Slika 1. Promjena sile tijekom vremena pri ispitivanju tvrdoće prema Brinellu

hardness test is given in Figure 1. All data were processed by using Microsoft Excel with the application of a statistical analysis.

3 RESULTS AND DISCUSSION
3. REZULTATI I RASPRAVA

Following the laboratory determinations, the analyzed board (herein after referred to as control sample) had a thickness of 3.84 ± 0.11 mm, an average moisture content of 6.5 % and density of 749 ±12 kg/m³. After the heat treatment, each piece was visually checked and defect free samples were kept under study. The first analyzed parameter was mass loss, which linearly increased (by Pearson R^2 coefficients in majority over 0.99) with the increase of temperature and exposure time (Figure 2). Only at 160 °C, the mass loss linear variation is less accurate with the Pearson coefficient of 0.896. Maximum mass loss was 3.52 % at a temperature of 160 °C, 5.32 % at a temperature of 180 °C and 10.68 % at a temperature of 200 °C.

When the heat treatment is performed at a moisture content of 0 % (by drying at 103 °C in a lab oven), the board thickness slightly shrinks by losing moisture content from 6.5 to 0 %, with slight values of 0.8-1.9 %. This shrinkage does not have a big influence on the heat treatment process, being known the reversible absorption-desorption process of the water in the wooden products and their dimensional changes.

During the heat treatment process, the board degrades generally by degradation of the wood veneers, but also by degradation of the adhesive and consequently also the veneer adhesion.

The mechanical property that shows the highest board degradation is MOR (Windeisen *et al*., 2009), while the board surface degradation is shown by Brinell (Uslu *et al*., 2008). The modulus of rupture (MOR) was reduced significantly, depending on the torrefaction degree, from the value of 152.9 N/mm² to the minimum value of 120.8 N/mm² (a reduction of 20.9 %) at the temperature of 160 °C, to 108.6 N/mm² (a reduction of 28.9 %) at the temperature of 180 °C and to 66.3 N/mm² (a reduction of 56.6 %) at the temperature of 200 °C (Figure 3). Similar values of MOR have been found by other authors for the torrefaction of spruce massive wood (Beckta and Niemz, 2003) or beech and ash species (Windeisen *et al*., 2009).
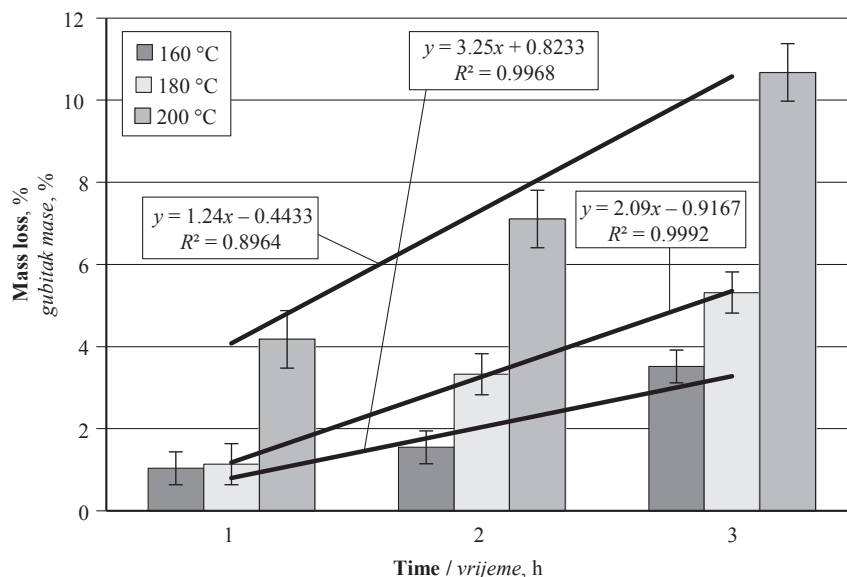

Figure 2 Influence of the heat treatment degree on mass loss
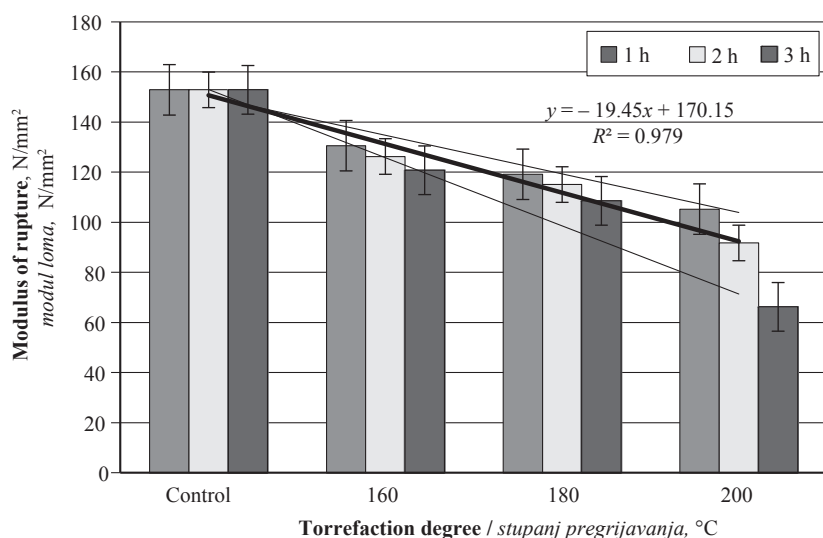**Slika 2.** Utjecaj toplinske obrade na gubitak mase

Figure 3 Influence of heat treatment degree on bending strength
Slika 3. Utjecaj toplinske obrade na čvrstoću na savijanje

Brinell hardness generally reduced depending on the treatment time, as well as depending on the heat treatment temperature (Figure 4). A slight increase in the Brinell hardness was found in the control sample (44.3 N/mm^2) as opposed to the sample treated at a temperature of 160 °C for 1 hour (44.5 N/mm^2), followed by its reduction of 8.1 % at the same temperature and 3-hour treatment. The same phenomenon was previously noticed on heat treated MDF, which showed that some hardening of the wooden surface treated at the temperature of 160 °C for 1 h can be obtained, regardless of the type of composite material. The maximum reduction of the Brinell hardness was 16 % at 180 °C and 40.6 % at 200 °C.

As shows in Figure 5, it was believed that the mass loss of the composite specimens was related to the decrease in Brinell hardness and tensile elastic modulus. Such trend confirmed that the mass loss increase leads to a proportional reduction of Brinell hardness and that it is almost proportional with the strength

modulus to static bending. At the same time, a significant reduction of the MOR in the first phase of the heat treatment at 160 °C was noticed as well. Similar results were obtained for the treatment repeated at 180 °C and 200 °C.

The absorption and thickness swelling of the boards were significantly lower than those of the control samples (Figure 6). After 2 hours of immersion, water absorption was reduced from 33.8 % for the control samples to 25.5 % for the 180/3 treatment degree, which represents a value reduction of 8.3 % or a percentage reduction of 24.5 %. The corresponding thickness swelling was reduced from 6.9 % to 3.1 %, namely a value reduction of 3.8 % or a percentage reduction of 55.07 %. As expected, the highest reductions were obtained for the maximum treatment degree 200/3, with a value of over 70 % of absorption and over 60 % of swelling.

Thickness swelling showed the same decreasing trend as water absorption (Figure 6), i.e. it reduced by
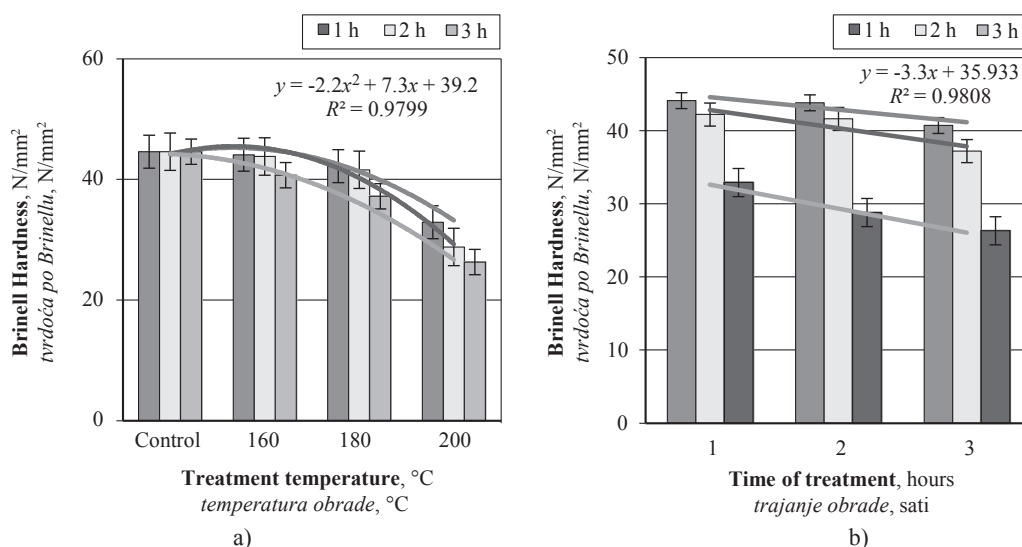

a)

b)

Figure 4 Influence of heat treatment degree by temperature (a) and treatment time (b) on Brinell hardness
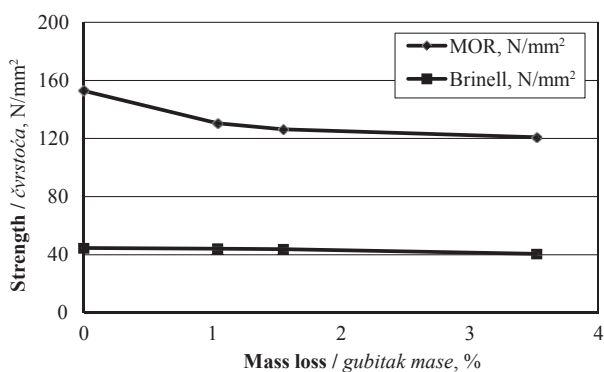**Slika 4.** Utjecaj temperature (a) i trajanja (b) toplinske obrade na tvrdoću prema Brinellu

Figure 5 Correlation between mass loss and strength of the board heat treated at 160 °C
Slika 5. Korelacija gubitka mase i čvrstoće ploče toplinski obrađene pri 160 °C

increase of the heat treatment. For example, values of 2h/TS for the samples treated at 160 °C for 1, 2, and 3 h were reduced by 2.51 %, 8.69 %, 30.35 %, respectively.

4 CONCLUSIONS
4. ZAKLJUČAK

1. The mass loss increased with the increase of heat treatment duration and temperature. The maximum loss of strength was determined as 10.68 % for the samples treated at 200 °C for 3 h heat exposure.
2. The modulus of rupture resistance was significantly reduced. The maximum loss of resistance was found to be 56.6 % at 200 °C and 3 h heat treated test specimens.
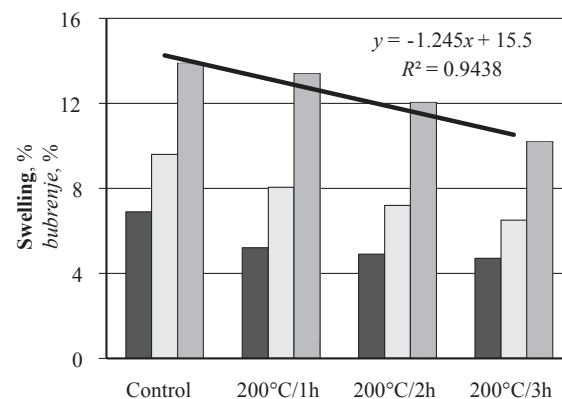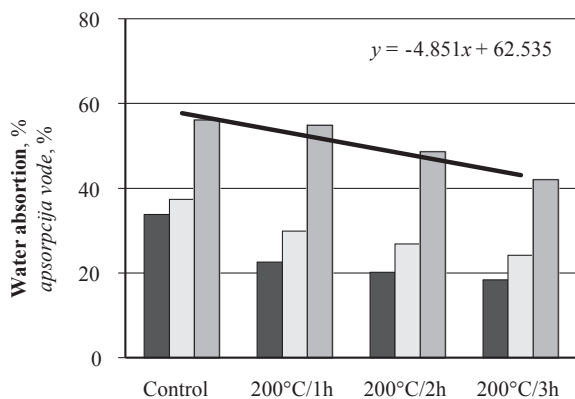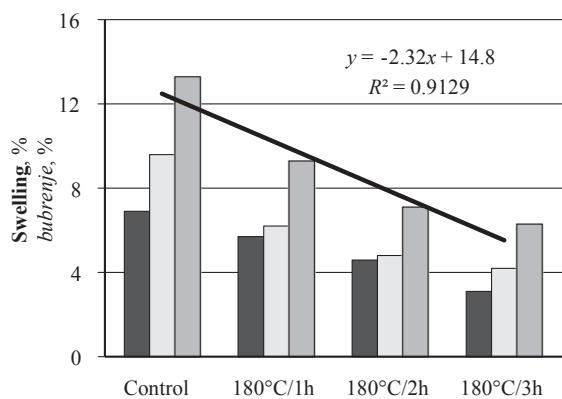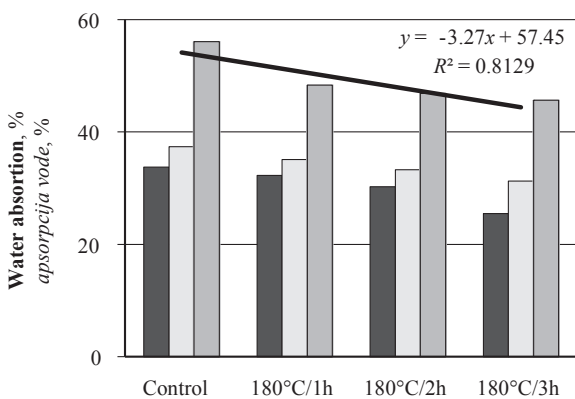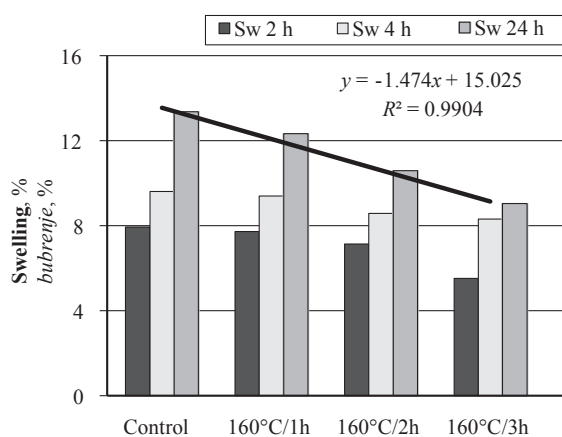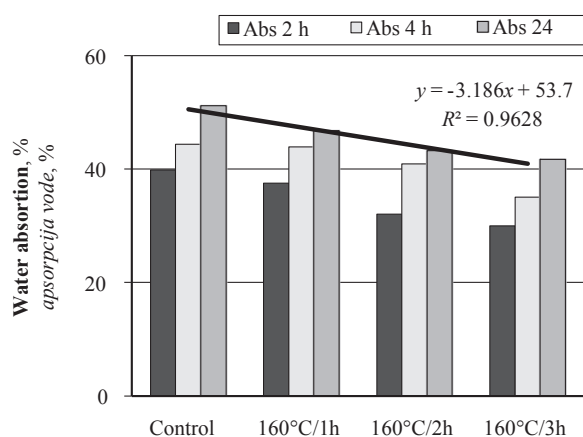
Figure 6 Water absorption and thickness swelling of the treated beech board
Slika 6. Apsorpcija vode i bubrenje toplinski obrađenih ploča od bukovine

3. The Brinell hardness was reduced due to the increase of heat treatment duration and temperature, but such decrease of about 40 % in test samples treated at 200 for 3 h was lower than the one obtained for MOR.

4. After being immersed in water for 2 h, water absorption and thickness swelling were positively affected and a significant decrease was detected. The reduction in water absorption and thickness swelling were determined to be 70 % and 60 %, respectively, for the samples treated at 200 °C for 3 h when compared to the control samples.

5. The heat treatment decreased the beech plywood density by 11 % and the strength to bending resistance by 57 %.

6. These beech plywood boards cannot be used for high stress support in construction.

5 REFERENCES
5. LITERATURA

1. Arruda, L.; Del Menezzi, C., 2016: Properties of a Laminated Wood Composite Produced with Thermo-mechanically Treated Veneers. Advances in Materials Science and Engineering. ID 8458065: 1-9. Hindawi Publishing Corporation. https://doi.org/10.1155/2016/8458065.

2. Batidzirai, B.; Mignot A. P. R.; Schakel, W. B.; Junginger, H. M.; Faaij, A. P. C., 2013: Biomass torrefaction technology: Techno-economic status and future prospects. Energy, 62: 162-214. https://doi.org/10.1016/j.energy.2013.09.035.

3. Bekhta, P.; Niemz, P., 2003: Effect of High Temperature on the Change in Color, Dimensional Stability and Mechanical Properties of Spruce Wood. Holzforschung, 57 (5): 539-546. https://doi.org/10.1515/HF.2003.080.

4. Chen, W. H.; Cheng, W. Y.; Lu, K. M.; Wuang, Y. P., 2011: An Evaluation on Improvement of Pulverized Biomass Property for Solid through Torrefaction. Applied Energy, 11: 3636-3644. https://doi.org/10.1016/j.apenergy.2011.03.040.

5. Chen, W. H.; Ye, S. C.; Sheen, H. K., 2012: Hydroheat Carbonization of Sugarcane Bagasse via Wet Torrefaction in Association with Microwave Heating. Bioresource Technology, 118: 195-203. https://doi.org/10.1016/j.biortech.2012.04.101.

6. Chen, D.; Zhou, J.; Zhang, Q.; Zhu, X.; Lu, Q., 2014: Upgrading of Rice Husk by Torrefaction and its Influence on the Fuel Properties. BioResources, 9 (4): 5895-5905. https://doi.org/10.15376/biores.9.4.5893-5905.

7. Demirbas, A., 2001: Biomass Resource Facilities and Biomass Conversion Processing for Fuels and Chemicals. Energy Conversation and Management, 42 (11): 1357-1378. https://doi.org/10.1016/S0196-8904(00)00137-0.

8. Gavrilescu, D., 2008: Energy from Biomass in Pulp and Paper Mills. Environmental Engineering Management Journal, 7(5): 537-546. https://doi.org/10.30638/eemj.2008.077.

9. Feher, S.; Kolman, S.; Borcsok, Z.; Taschner, R., 2014: Modification of Hardwood Veneers by Heat Treatment for Enhanced Colors. BioResources, 9(2): 3456-3465. https://doi.org/10.30638/eemj.2008.077.

10. Jehlickova, B.; Morris, R., 2007: Effectiveness of Policy Instruments for Supporting the Use of Waste Wood as a Renewable Energy Resource in the Czech Republic. Energy Policy, 35(1): 577-585. https://doi.org/10.1016/j.enpol.2005.12.024.

11. Kastanaki, E.; Vamvuka, D., 2005: Comparative Reactivity and Kinetic Study on the Combustion of Coal-biomass Char Blends. Fuel, 85 (9): 1186-1193. https://10.1016/j.fuel.2005.11.004.

12. Lovrić, A.; Zdravković, V.; Furtula, M., 2014: Influence of heat modification on color of poplar (Populus X Euramericana) rotary cut veneer. Wood Research, 59 (2): 661-670.

13. Lundborg, A., 1998: A Sustainable Forest Fuel System in Sweden. Biomass and Bioenergy, 15 (4-5): 399-406. https://doi.org/10.1016/S0961-9534(98)00046-4.

14. Murata, K.; Watanabe, Y.; Nakano, T., 2013: Effect of Heat Treatment of Veneer on Formaldehyde Emission of Poplar Plywood. Materials, 6: 410-420. https://doi.org/10.3390/ma6020410.

15. Nazerian, M.; Ghalehno, M. D., 2011: Physical and Mechanical Properties of Laminated Veneer Lumber Manufactured by Poplar Veneer. Journal of Agricultural Science and Technology, A1: 1040-1045.

16. Nazerian, M.; Ghalehno, M. D.; Kashkooli, X., 2011: Effect of Wood Species, amount of juvenile wood and heat treatment on mechanical and physical properties of Laminated Veneer Lumber. Journal of Applied Sciences, 11 (6): 980-987. https://doi.org/10.3923/jas.2011.980.987.

17. Omer, A. M., 2012: Biomass energy resources utilization and waste management. Agricultural Sciences, 3 (1): 124-145. https://doi.org/10.4236/as.2012.31016.

18. Percin, O.; Peker, H.; Atilgan, A., 2016: The effect of heat treatment on the some physical and mechanical properties of beech (Fagus Orientalis Lipsky) wood. Wood Research, 61 (3): 443-456.

19. Prasertsan, S.; Sajakulnukit, B., 2006: Biomass and Bioenergy in Thailand: Potential, Opportunity and Barriers. Renew Energy, 31 (5): 599-610. https://doi.org/10.1016/j.renene.2005.08.005.

20. Salca, E. A.; Kobori, H.; Inagaki, T.; Kojima, Y.; Suzuki S., 2016: Effect of heat treatment on color changes of black alder and beech veneers. Journal of Wood Science, 62: 297-304. https://doi.org/10.1007/s10086-016-1558-3.

21. Shulga, G.; Betkers, T.; Brovkina, J.; Aniskevicha, O.; Ozolinš, J., 2008: Relationship between Composition of the Lignin-based Interpolymer Complex and its Structuring Ability. Environmental Engineering and Management Journal, 7 (4): 397-400.

22. Tabarés, J. L. M.; Ortiz, L.; Granada, E.; Viar, F. P., 2000: Feasibility Study of Energy Use for Densificated Lignocellulosic Material (Briquettes). Fuel, 79 (10): 1229-1237. https://doi.org/10.1016/S0016-2361(99)00256-2.

23. Thompson, D.; Kozak, R.; Evans, P., 2005: Thermal modification of color in red alder veneer. Effects of temperature, heating time, and wood type. Wood and Fiber Science, 37 (4): 653-661.

24. Uslu, A.; Faaij, A. P. C.; Bergman, P. C. A., 2008: Pre-treatment technologies and their effect on international bioenergy supply chain logistics. Techno-economic evaluation of torrefaction, fast pyrolysis and pelletisation. Energy, 33: 1206-1223. https://doi.org/10.1016/j.energy.2008.03.007.

25. Vilcek, J., 2013: Bioenergetic potential of agricultural soils in Slovakia. Biomass and Bioenergy, 56: 53-61. https://doi.org/10.1016/j.biombioe.2013.04.030.

26. Wang, G. J.; Luo, Y. H.; Deng, J.; Kuang, J. H.; Zhang, Y. L., 2011: Pretreatment of biomass by torrefaction. Chinese Science Bulletin, 56 (14): 1442-1448. https://doi.org/10.1007/s11434-010-4143-y.

27. Windeisen, E.; Bächle, H.; Zimmer, B.; Wegener, G., 2009: Relations between chemical changes and mechanical properties of heatly treated wood. Holzforschung, 63: 773-778. https://doi.org/10.1515/HF.2009.084.

28. Zdravković, V.; Lovrić, A.; Stanković, B., 2013: Dimensional Stability of Plywood Panels Made from Heatly Modified Poplar Veneers in the Conditions of Variable Air Humidity. Drvna industrija, 64 (3): 175-181. https://doi.org/10.5552/drind.2013.1223.

29. ***CEN/TS 15679, 2007: Heat modified timber – definitions and characteristics. European Committee for Standardization (CEN).

30. ***EN 1534, 2000: Wood and parquet flooring. Determination of resistance to indentation (Brinell) – Test method. European Committee for Standardization.

31. ***EN 317, 1993: Particleboards and fiberboards. Determination of swelling in thickness after immersion in water. European Committee for Standardization (CEN).

32. ***EN 323, 1993: Wood-based panels. Determination of density. European Committee for Standardization.

33. ***EN 310, 2000: Wood-based panels. Determination of modulus of elasticity in bending and of bending strength. European Committee for Standardization.

Corresponding address:

Assist. Prof. FERHAT ÖZDEMİR, Ph.D.

Department of Forest Industry Engineering
Faculty of Forestry, Kahramanmaraş Sütçü Imam University
46100 Kahramanmaraş, TURKEY
e-mail: ferhatozd@hotmail.com

Melih Yucesan[1], Muhammet Gul[2], Erkan Celik[2]

Performance Comparison between ARIMAX, ANN and ARIMAX-ANN Hybridization in Sales Forecasting for Furniture Industry

Usporedba performansi modela ARIMAX, ANN i hibridizacije ARIMAX-ANN u predviđanju prodaje za industriju namještaja

ABSTRACT • *Manufacturing firms aim to increase their profits and reduce costs in a competitive and rapidly changing market. One of the most important ways to reach these goals is to forecast sales correctly. Furniture manufacturing, which is considered a prosperous and growing industry in Turkey, has an increasing trend related to the growth in construction and associated industries, increase in urban migration and increase in per capita income. Accuracy of sales forecasting in furniture industry is affected by external factors, such as consumer confidence index, producer price index, month of the year and number of vacation days as well as the time factor itself. This study aims to develop an Autoregressive Integrated Moving Average with external variables (ARIMAX) to forecast the total monthly sales of furniture products of a well-known manufacturer in Turkey. As a follow up study, a performance comparison between ARIMAX, artificial neural networks (ANNs) and ARIMAX-ANN hybridization is performed. In conclusion, results of performance measures demonstrate that hybrid model developed for each amount of product sales give better accuracy values than single methods. Overall, it is proved that using the ARIMAX and hybridization of this method with ANN are applicable for forecasting monthly sales of furniture products.*

Keywords: ARIMAX, ANN, hybrid method, sales forecasting, furniture industry

SAŽETAK • *Proizvodne tvrtke nastoje povećati dobit i smanjiti troškove na konkurentnom tržištu koje se brzo mijenja. Jedan od najvažnijih načina postizanja tih ciljeva jest što točnije predviđanje prodaje. Proizvodnja namještaja, koja se smatra perspektivnom i rastućom industrijom u Turskoj, bilježi sve veću potražnju, što se povezuje s rastom građevne industrije i s njom povezanih djelatnosti te s povećanjem urbanih migracija i povećanjem dohotka po stanovniku. Na točnost predviđanja prodaje u industriji namještaja utječu vanjski činitelji kao što su indeks povjerenja potrošača, indeks proizvođačkih cijena, mjeseci u godini i broj dana godišnjih odmora, kao i faktor vremena. Cilj ove studije jest razvoj modela integriranoga autoregresivnog pomičnog prosjeka (Autoregressive Integrated Moving*

---

[1] Author is assistant professor at Munzur University, Engineering Faculty, Department of Mechanical Engineering, Tunceli, Turkey. [2]Authors are assistant professors at Munzur University, Engineering Faculty, Department of Industrial Engineering, Tunceli, Turkey.
[1] Autor je docent Sveučilišta *Munzur*, Inženjerski fakultet, Odjel za strojarstvo, Tunceli, Turska. [2]Autori su docenti Sveučilišta *Munzur*, Inženjerski fakultet, Odjel za industrijsko inženjerstvo, Tunceli, Turska.

Average – ARIMAX) s vanjskim varijablama za predviđanje ukupne mjesečne prodaje namještaja poznatog proizvođača u Turskoj. U nastavku istraživanja provedena je usporedba performansi modela ARIMAX, umjetnih neuronskih mreža (ANNs) i hibridnog modela ARIMAX-ANN. Dobiveni rezultati pokazuju da hibridni model razvijen za prodaju svakog proizvoda daje bolju točnost od pojedinačnih modela. Zaključno, dokazano je da se za predviđanje mjesečne prodaje namještaja može primijeniti hibridizacija modela ARIMAX s ANN-om.

Ključne riječi: *ARIMAX, ANN, hibridna metoda, predviđanje prodaje, industrija namještaja*

1 INTRODUCTION
1. UVOD

The demand for furniture products in Turkey has increased rapidly with the recent development in construction industry, increase in urban population and personal income level (Hazır *et al.*, 2016; Turkey Furniture Products Council Industry Report, 2013). However, it is difficult to forecast this increase considering the multiplicity and internal interactions of the affecting factors. Statistical methods, such as regression or ARIMAX and data mining methods as ANNs have been frequently applied in sales forecasting by numerous researchers since they have the ability to solve complicated interactions affected by internal and external environments (Kuo *et al.*, 2002; Luxhøj *et al.*, 1996). Bearing this issue in mind, this study attempts to develop a time series model with external variables to forecast monthly sales of furniture products using ARIMAX, ANN and ARIMAX-ANN model.

In the related literature, researchers proposed new forecasting methods, evaluated the performance of existing ones or modified the existing ones depending on applications in sales forecasting (Arunraj and Ahrens, 2015). The methods include regression, time-series related methods and advanced machine learning related methods. Although sales forecasting in the context of all sectors has been studied by many researchers, in the area of furniture sales forecasting, the publications are very few when compared to other fields. Hazır *et al.* (2016) studied sales forecasting of Turkish furniture industry by ANN and multiple linear regression (MLR), and provided a road map for vision 2023. Data between 2004 and 2013 was used for analysis. As a result of the study, 24 billion dollars and 21 billion dollars demands were predicted by MLR analysis and ANN methodology, respectively. They stated that these results may be evaluated as the possible retail values for Turkish furniture industry within the target of vision 2023. Mahbub *et al.* (2013) proposed an ANN model to forecast the optimum demand considering time variables of the year, festival period, promotional programmes, holidays, number of advertisements, cost of advertisements, number of workers and availability. A feed-forward backpropagation ANN with 13 hidden neurons in one hidden layer as the optimum network was preferred. The model was confirmed with a furniture product data of a renowned furniture company. The model was compared with Brown's double smoothing. The results of the study show that ANN model performs much better than the linear Brown's double smoothing model. Oblak *et al.* (2012) applied two quantitative methods named Holt-Winters method

of exponent smoothing of higher orders and linear regression of the 1st order for forecasting of parquet sales. Parquet sales data by month in the years 2000 to 2009 was used in the models and the best result was obtained with the use of Holt-Winters multiplicative model of exponent smoothing of higher orders. In conclusion, it was suggested that the proposed model can be applied for forecasting optimum demand level of furniture products in any furniture company. As stated by Arunraj and Ahrens (2015), there is no common forecasting model that can be applied to different kinds of problems. Accuracy of the forecasting models can be improved by hybridized models rather than by a single model. Therefore, in this study, an ARIMAX model was developed to forecast the total monthly sales of furniture products of a well-known Turkish manufacturer and a performance comparison was performed between the models of ARIMAX, ANN and ARIMAX-ANN hybridization in order to improve the accuracy of the proposed framework.

Apart from forecasting sales in the furniture industry, the forecasting methods are used in different fields of application. Fabianová *et al.* (2016) presented a sale forecasting using the software tool for risk analysis. It was carried out based on time series analysis, forecasting and statistics analysis. Forecasting was performed using two different approaches: when considering simple seasonality of sales and when considering sale seasonality along with the impact of known events on demand. Subsequent forecasting is focused on the identification and analysis of risk factors using Monte-Carlo Simulation (MCS). Anggraeni *et al.* (2015) and Lee and Hamzah (2010) studied sales forecasting for clothing industry. While the first study made a performance comparison between ARIMA and ARIMAX in Moslem kids' clothes sales forecasting, the second one dealt with forecasting sales data with Ramadhan effect by ARIMAX modelling. Results of studies by Anggraeni *et al.* (2015) show that ARIMAX model is better than ARIMA model in accuracy level of training, testing and next time forecasting processes. In conclusion of the study by Lee and Hamzah (2010), it is observed that ARIMAX yields better forecast at out-sample data compared to the decomposition method and Seasonal Autoregressive Integrated Moving Average (SARIMA), and neural networks. Arunraj and Ahrens (2015) proposed hybridization of SARIMA-Quantile Regression (QR) model to food sales forecasting. The results show that the SARIMA-MLR and -QR models yield better forecasts at out-sample data when compared to seasonal naïve forecasting, traditional SARIMA, and multi-layered perceptron neural network models. Unlike the SARIMA-MLR model,

the SARIMA-QR model provides better prediction. Murlidharan and Menezes (2013) proposed a different concept in sales forecasting "*Frequent pattern mining-based sales forecasting*". In some studies, ANN was used in combination with Genetic Algorithm (GA) in order to select the appropriate input variables to the models (Doganis *et al.*, 2006; Kuo, 2001). Doganis *et al.* (2006) applied ANN-GA combination for short shelf-life food products sales forecasting. Kuo (2001) proposed a model based on fuzzy neural network with initial weights generated by GA. Similarly, Kuo *et al.* (2002) integrated ANNs and fuzzy neural networks

Table 1 Review of sales forecasting application studied in literature
Tablica 1. Pregled primjene metoda za predviđanje prodaje iz literature

Study *Literatura*	Application industry *Industrija primjene*	Methods used *Primijenjene metode*	Novelty *Novina*
Fabianová *et al.* (2016)	Retailing *maloprodaja*	ARIMA, MLR, MCS	Sales forecasting considering data uncertainty / *predviđanje prodaje uzimanjem nesigurnosti podataka u obzir*
Anggraeni *et al.* (2015)	Clothing *proizvodnja odjeće*	ARIMA, ARIMAX	Performance comparison between ARIMA and ARIMAX in Moslem kids' clothes sales forecasting / *usporedba performansi metoda ARIMA i ARIMAX u predviđanju prodaje odjeće za muslimansku djecu*
Oblak *et al.* (2012)	Forestry *šumarstvo*	Holt-Winters, Linear regression of the 1st order	Forecasting of parquet sales *predviđanje prodaje parketa*
Arunraj and Ahrens (2015)	Food *proizvodnja hrane*	SARIMAX, MLR, QR	Hybridization of SARIMA-QR model to food sales forecasting / *hibridizacija modela SARIMA-QR za predviđanje prodaje hrane*
Hazır *et al.* (2016)	Furniture *proizvodnja namještaja*	ANN, MLR	Sales forecasting in Turkey by ANN and MLR and providing a framework plan for 2023 vision *prognoza prodaje u Turskoj prema ANN-u i MLR-u te izrada okvirnog plana za viziju 2023.*
Mahbub *et al.* (2013)	Furniture *proizvodnja namještaja*	ANN, Brown's double smoothing	A neural approach to furniture product sales forecasting / *neuronski pristup predviđanju prodaje namještaja*
Murlidharan and Menezes (2013)	N/A	Frequent pattern mining	Frequent pattern mining-based sales forecasting / *procjena prodaje utemeljena na rudarenju podataka i pronalaženju čestih modela*
Lee and Hamzah (2010)	Clothing *proizvodnja odjeće*	ARIMAX	ARIMAX for forecasting sales data with Ramadhan effect / *ARIMAX za predviđanje podataka o prodaji Ramadhanovim učinkom*
Doganis *et al.* (2006)	Food *proizvodnja hrane*	ANN, GA	Sales forecasting for short shelf-life food products based on ANN-GA combination *predviđanje prodaje prehrambenih proizvoda s kratkim rokom trajanja na temelju kombinacije ANN-GA*
Kuo *et al.* (2002)	N/A	FNN, ANN	Integration of ANNs and fuzzy neural networks with fuzzy weight elimination / *integracija ANN i neizrazitih neuronskih mreža s neizrazitom eliminacijom težine*
Kuo (2001)	Convenience store *minimarket*	FNN, GA	A sales forecasting based on fuzzy neural network with initial weights generated by genetic algorithm / *prognoziranje prodaje utemeljeno na neizrazitoj neuronskoj mreži s inicijalnim težinama generiranima genetskim algoritmom*
Alon *et al.* (2001)	Retailing *maloprodaja*	ANN, MLR, Winters ES, Box-Jenkins ARIMA	A comparison of ANNs and traditional methods in forecasting aggregate retail sales / *usporedba ANN-ova i tradicionalnih metoda u predviđanju agregirane maloprodaje*
Yip *et al.* (1997)	N/A	ANN	Application of ANNs in sales forecasting *primjena ANN-ova u predviđanju prodaje*
Luxhøj *et al.* (1996)	Consumer goods *roba široke potrošnje*	ES, MLR, ANN	Hybrid econometric-neural network model for sales forecasting / *hibridni ekonometrijski neuronski model za prognozu prodaje*

Abbreviations: MLR (Multiple Linear Regression); QR (Quantile Regression); ES (Exponential Smoothing); FNN (Fuzzy neural network); GA (Genetic Algorithm); MCS (Monte-Carlo simulation); ARIMA (Autoregressive Integrated Moving Average); ARIMAX (Autoregressive Integrated Moving Average with external variables); SARIMAX (Seasonal Autoregressive Integrated Moving Average with external variables)
Kratice: MLR – višestruka linearna regresija; QR – kvantilna regresija; ES – eksponencijalno izravnavanje; FNN – neizrazita neuronska mreža; GA – genetički algoritam; MCS – Monte Carlo simulacija; ARIMA – integrirani autoregresivni pomični prosjek; ARIMAX – integrirani autoregresivni pomični prosjek s vanjskim varijablama; SARIMAX – sezonalni integrirani autoregresivni pomični prosjek s vanjskim varijablama

with fuzzy weight elimination for the first time in literature. According to the results of the study, the proposed model performs more accurately than the conventional statistical method and single ANN model. Alon *et al.* (2001) made a comparison of ANNs and traditional methods in forecasting aggregate retail sales. Yip *et al.* (1997) studied an application of ANNs in sales forecasting. Unlike Yip *et al.* (1997), Luxhøj *et al.* (1996) focused on a hybrid econometric-neural network model for sales forecasting. Using of this hybrid method yielded a modest 2.3 % reduction in the mean absolute percentage error (MAPE) when compared with the current qualitative approach used by the company. The above-mentioned literature review is summarized in Table 1.

2 MATERIAL AND METHODS
2. MATERIJAL I METODE

2.1 Data set
2.1. Set podataka

This study uses monthly sales of furniture products (dining room, bedroom, teen room, sitting group and armchair) measured in numbers from one of the biggest furniture factories as a case study from January 2009 to December 2015. The selected factory is located in Black sea region of Turkey. Figure 1 illustrates the monthly sales data of furniture products for a seven-year time period in a time series plot. The mean sales per month is about 140, 114, 60, 115 and 531, respectively, for the products of dining room, bedroom, teen room, sitting group and armchair. This time series is highly periodic, but it is easy to observe the monthly patterns. Especially in summer, the sales are observed at the peak point. This type of month effects can be recognized by considering the months from January to November as dummy variables (0 and 1). The refer-

ence month is December, so coefficients of other months may be interpreted relative to this month.

In Figure 2, the box plot displays the median monthly sales from January to December. From this figure, it is evident that the highest sales usually occur in August. May, June, July, September and October are the next highest sales months. The box-plot also shows information about extreme values and outliers, which occur mainly due to holidays and other variables. However, the median of monthly sales for May & June and September & October are similar; sales dispersion is higher in June than in July.

In addition to the month of the year affect, three variables are used as input parameters to forecast sales value of a furniture company. The first one is consumer confidence index (CCI). CCI is an aggregate of four sub-indices. Two of them are based on expectations regarding household finances, while the other two are based on expectations about economy-wide developments (Jansen and Nahuis, 2003). The second input variable is producer price index (PPI). PPI is an aggregate of over 1500 components. Each component is a monthly index of the national average price for some producer goods. The price pertains to the first transaction after production of the good. This is a transaction between firms rather than between businesses and consumers (Peltzman, 2000). Other input parameters are number of vacation days in the related month of the year in Turkey. Distribution of number of vacation days for the data set is given Figure 3.

The output parameters are monthly sales of dining room, bedroom, teen room, sitting group and armchair. Inputs, outputs and applied methods are shown in Figure 4.

Data about input and output variables were collected for 84 months from January 2009 to December 2015 from the furniture company. Descriptive statistics
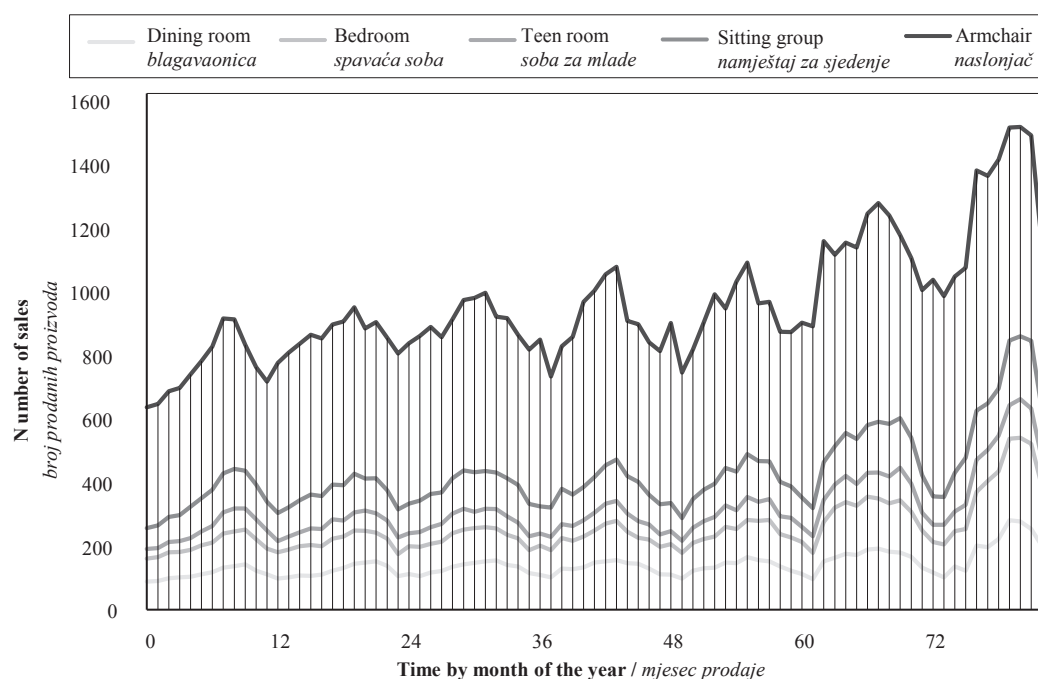

Figure 1 Sales of furniture products between 2009 and 2015
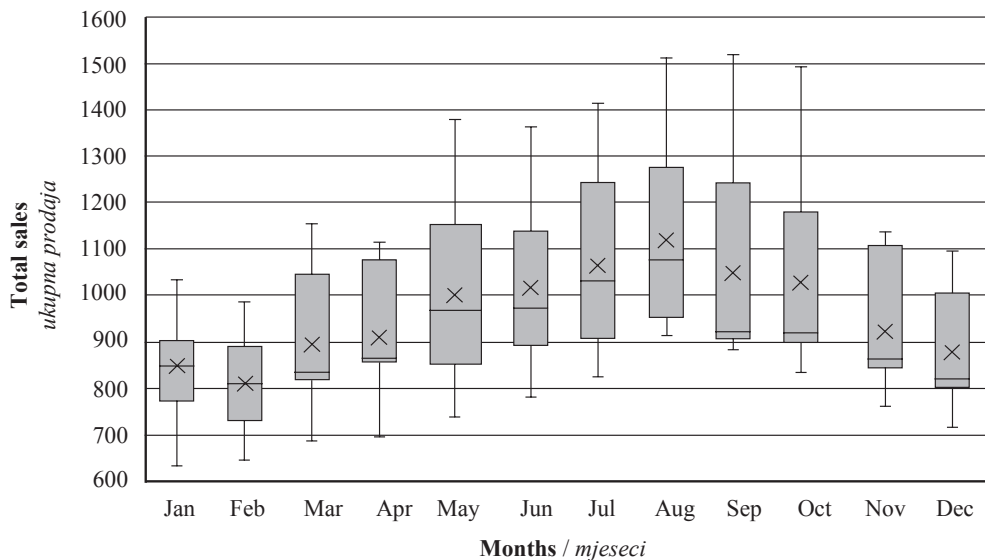**Slika 1.** Prodaja namještaja između 2009. i 2015. godine

Figure 2 Box-plot for total monthly sales of furniture products from January to December
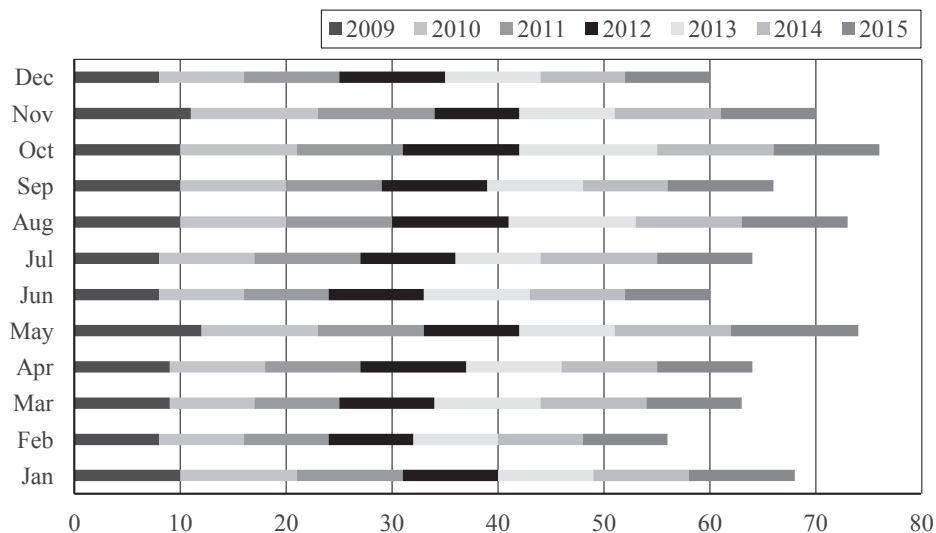**Slika 2.** *Box-plot* za ukupnu mjesečnu prodaju namještaja od siječnja do prosinca

Figure 3 Distribution of number of vacation days by year/month in Turkey
Slika 3. Raspodjela broja dana godišnjeg odmora po godini/mjesecu u Turskoj

Table 2 Descriptive statistics for total monthly sales (January 2009 – December 2015)
Tablica 2. Deskriptivna statistika ukupne mjesečne prodaje (siječanj 2009. – prosinac 2015.)

Output Variable *Izlazne varijable*	Count *Broj mjeseci*	Mean *Srednja vrijednost*	SE Mean *Srednja vrijednost stand. pogreške*	St. Dev *Standardna devijacija*	Variance *Varijanca*	Minimum *Minimum*	Q1	Median *Medijan*	Q3	Maximum *Maksimum*	Range *Raspon*
Dining room sales *prodaja blagovaonica*	84	140.39	4.17	38.18	1457.81	88	111.3	134	152	281	193
Bedroom sales *prodaja spavaćih soba*	84	114.17	4.53	41.56	1727.22	70	89.25	100	122	268	198
Teen room sales *prodaja soba za mlade*	84	60.44	2.09	19.15	366.85	29	47.25	57	66.75	122	93
Sitting group sales *prodaja namještaja za sjedenje*	84	115.24	3	27.51	756.98	65	95.75	111	124	212	147
Armchair sales *prodaja naslonjača*	84	530.98	9.4	86.13	7419.11	370	480.5	504.5	596.75	755	385

Furniture product sales forecasting: Sales influencing parameters (input variables), output variables and applied methods / *Predviđanje prodaje namještaja i utjecajni parametri na prodaju (ulazne varijable), izlazne varijable i primijenjene metode*

INPUTS *Ulazne varijable*	OUTPUTS *Izlazne varijable*	METHODS *Metode*
Month of the year *mjesec u godini*	Dining room sales *prodaja blagavaonica*	ARIMAX
Number of vacation days *broj dana godišnjeg odmora*	Bedroom sales *prodaja spavaćih soba*	ANN
CCI	Teen room sales *prodaja soba za mlade*	ARIMAX+ANN
PPI	Sitting group sales *prodaja namještaja za sjedenje*	
	Armchair sales *prodaja naslonjača*	

Figure 4 Presentation of inputs and output variables and applied methods
Slika 4. Prikaz ulaznih i izlaznih varijabli i primijenjenih metoda

for each output variable are presented in Table 2. The values of CCI and PPI are ratios that have a mean of 72.85 and 209.2, respectively. Mean number of vacation days in the studied data set is 9.45 per month. The reason for considering this input variable in our proposed comparative framework model stems from the fact that decision makers in furniture industry are of the opinion that sales increase in vacation days.

2.2 Research methods
2.2. Metode istraživanja

In this study, three forecasting methods including single (ARIMAX, ANN) and hybrid (ARIMAX-ANN) methods were investigated in order to find the best method that accurately fits the data. Detailed descriptions of each method are presented in the following subsections.

2.2.1 ARIMAX
2.2.1. ARIMAX

Recently, ARIMA has been studied by many researchers who used time series. However, when using ARIMA model, only one variable can be used, so it is not adequate to express real problems. Complex problems always need more the one variable in order to explain problems effectively. Therefore, it is necessary to build a multivariate ARIMAX model (Fan *et al.* 2009; Jalalkamali *et al.* 2015).

The ARIMAX model (Bierens, 1987) is a generalization of the ARIMA model, which is capable of incorporating an external input variable (*X*). The ARIMAX model assumes the form

$$\left(1-\sum_s^p \alpha_s L_s\right)\Delta y_t = \mu + \sum_{s=1}^q \beta_s L^s x_t + \left(1+\sum_{s=1}^r \gamma_s L^s\right)e^t \quad (1)$$

where *L* is usual lag operator. $\gamma_s L^s = y_{(t-s)}$, $\Delta y_t = y_t - y_{t-1}$, $\mu \in$, $\alpha_s \in R$, $\beta_s \in R^k$ and $\gamma_s \in R$ are the unknown param-

eters and $e_t's$ are the errors (Arya *et al.*, 2015). ARIMAX model consists of four parts. These parts are Auto Regressive (AR), Integrated (I), Moving Average (MA), and Exogenous Variable (X) (Sutthichaimethee and Ariyasajjakorn, 2017).

2.2.2 ANN
2.2.2. ANN

ANNs are machine learning algorithms that aim to solve the computational processes in specific areas by using a large number of interconnected processing elements (Gul and Guneri, 2015; 2016a; 2016b; Yucesan *et al.* 2017; Onat and Gul, 2018). They are applied to the problems on prediction, clustering, classification, and detection of abnormalities (Pusat *et al.* 2016). The computational elements used in different ANN models are known as artificial neurons (Guneri and Gumus, 2008; 2009). The model of an artificial neuron is given in Figure 5.

Where $x_1, x_2, \ldots, x_p$ are the input signals; $w_{k1}, w_{k2}, \ldots, w_{kp}$ are the weights of neuron *k*, and, u_k is the linear combiner output, while θ_k denotes the threshold. Furthermore, Φ () is the activation function; and y_k is the output of the neuron. The first layer known as the ''input'' layer and the last one, which is called the ''output'' layer, are used to get information from inside and outside the network, respectively. The middle layers considered as ''hidden'' layers are vital for the network to convert certain input patterns into appropriate output patterns (Akkoyunlu *et al.*, 2015; Somoza and Somoza, 1993). The flow of information is passed through the network by linear connections and linear or nonlinear transformations. The error between the actual and predicted values is calculated. Then, a minimization procedure is used to adjust the weights between two connection layers, i.e. for back
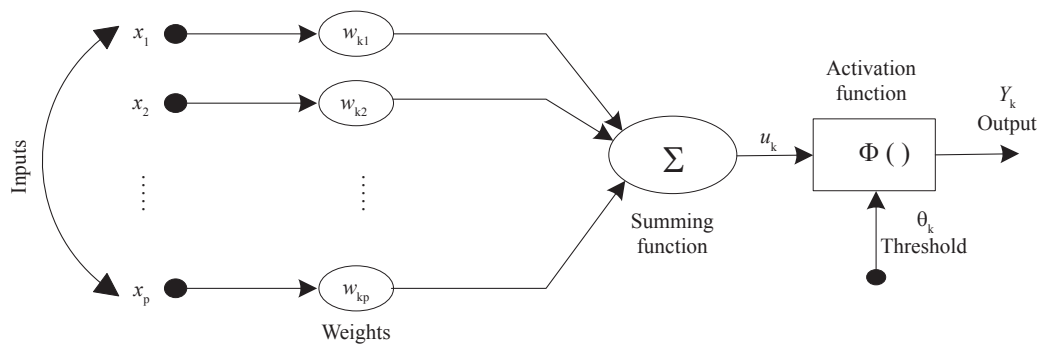
Figure 5 Flow chart of an artificial neuron (Yucesan *et al.* 2017)
Slika 5. Dijagram toka umjetnog neurona (Yucesan *et al.*, 2017.)

propagation model starting backwards from the output layer to input layer. There are many minimization procedures based on different optimization algorithms, such as Quasi-Newton, and Levenberg–Marquardt, gradient descent and conjugate gradient methods. In ANN models, there is a practical problem in network architecture (number of hidden layers and units in each layer) and network properties (error and activation functions). The design of hidden layer is dependent on the selected learning algorithm (Kröse *et al.*, 1993). The more layers and neurons, the more complex dependencies the network can model. One of the other important properties of an ANN model is the activation function for the hidden layer. Linear, logistic and hyperbolic tangent are the most common functions followed in the literature. In ANNs, some controllable factors are available in order to aid the learning of selected algorithm such as *Learning Rate* and *Momentum*. They are control parameters used by several learning algorithms, which affect the changing of weights. The higher learning rates cause higher weight changes during each iteration. The greater the momentum, the more the current weight change is affected by the weight change that took place during the previous iteration.

2.2.3 ARIMAX-ANN hybrid method
2.2.3. Hibridna metoda ARIMAX-ANN

In time series forecasting, hybrid models are developed apart from single models in order to reduce risk of failure and also obtain more accurate results (Khashei and Bijari, 2010). ARIMAX models are insufficient to solve complex nonlinear problems. On the other hand, using ANNs to solve problems yields dicey results. For that reason, if a distinctive framework of problems is not know, hybrid methodology that contains advance sides of ARIMAX and ANN models can be a good solution. Therefore, we combined ARIMAX and ANN model in sales forecasting for furniture industry. In the first step, ARIMAX model is used to calculate residual of the model. In the second step, ANN model is applied with independent variables including residuals of ARIMAX model as input variables.

Since ARIMAX model cannot capture the nonlinear structure of the data, the residuals of the linear model will contain information about nonlinearity. The

results from the neural network can be used as predictions of the error terms for the ARIMA model (Zhang 2003; Xu *et al.*, 2016).

Step 1: ARIMAX model is applied to analyze the linear part of the problem. First, model identification is performed by using graphs, statistics, autocorrelation function (ACF), partial autocorrelation function (PACF) and transformations. The dependent variable is determined as stationary. Least squares are used to determine the valid model and variables. Finally, forecast verification and reasonableness is performed in order to track performance and determine the validity of forecast, then fit (y_t, y_{t-1} ... y_{t-n}) and calculate residuals (e_t, e_{t-1} ... e_{t-n}) (Areekul *et al.*, 2010).

Step 2: ANN model is applied considering the variables of month of the year, number of vacation days, PPI, CCI and residuals which are calculated in ARIMAX model as input variables of the model. To measure performance of ANN model, mean squared error (MSE), network error (average train error and average test error), absolute relative error (ARE), mean absolute percentage error (MAPE) and *R*-squared (R^2) can be used. R^2 and MAPE are defined as in Eqs. (2)-(3).

$$R^2 = 1 - \frac{SS_{residuals}}{SS_{total}} \qquad (2)$$

where SS_{total} refers to the total sum of squares (proportional to the variance of the data), and $SS_{residuals}$ indicate the sum of squares of residuals, also called the residual sum of squares.

$$MAPE = \frac{100}{n} \sum_{i=1}^{n} \left| \frac{y_i - f_i}{y_i} \right| \qquad (3)$$

Where f_i is vector of *n* forecasting, and y_i is the vector of actual values.

2.2.4 Proposed comparative framework
2.2.4. Predloženi usporedbeni okvir

The proposed comparative framework used in this study consists of four stages as given in Figure 6. It includes a time series (ARIMAX), an ANN and a hybrid (ARIMAX-ANN) model. The "best" model for each stage was identified, and then these models were compared at the last stage of the framework. Measures of solution adequacy are evaluated under MAPE values. Moreover, plots regarding actual vs. predicted values for each furniture product are demonstrated.
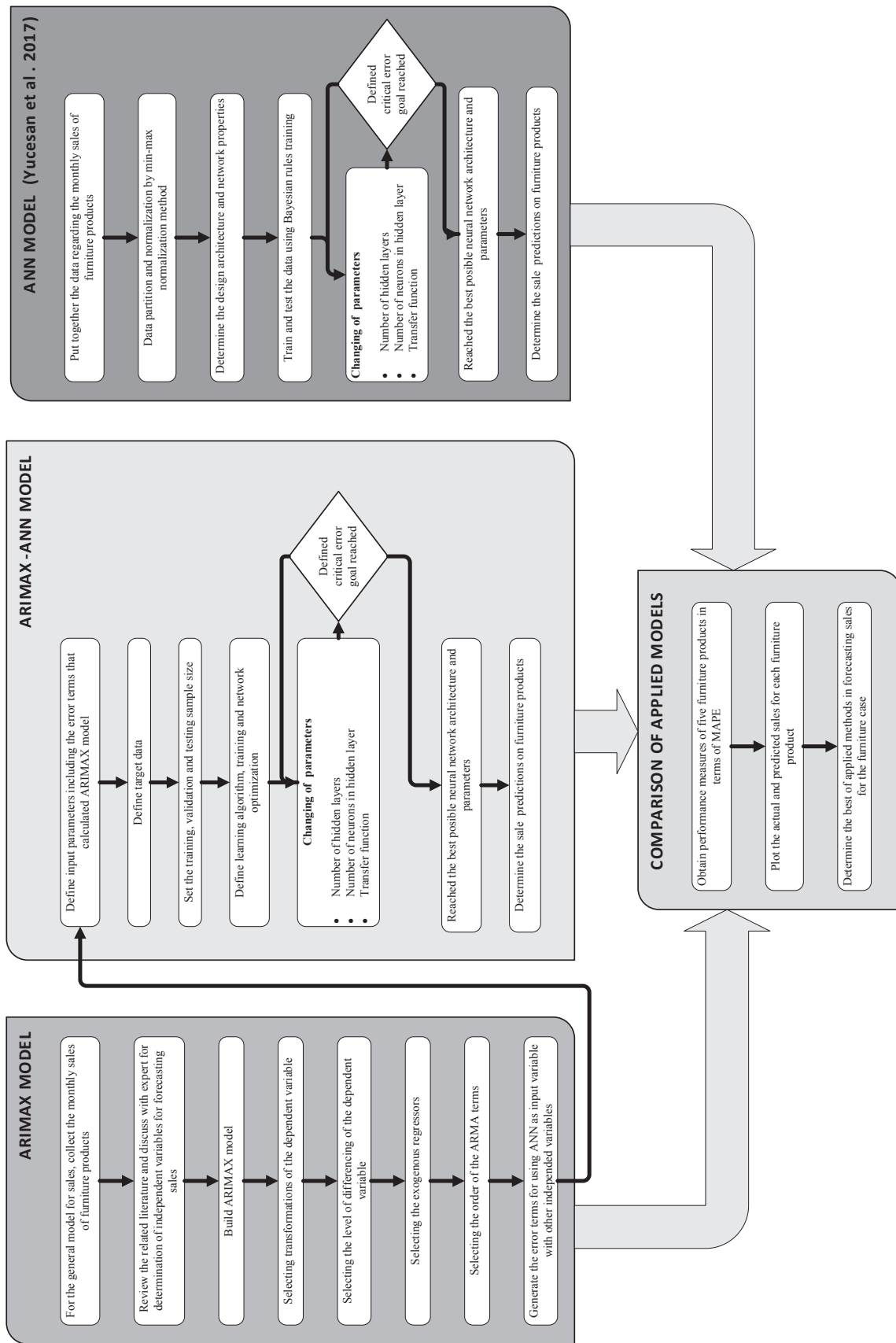
Figure 6 Flowchart of the proposed comparative framework for furniture product sales forecasting
Slika 6. Dijagram toka predloženoga usporedbenog okvira za predviđanje prodaje namještaja

3 RESULTS AND DISCUSSION
3. REZULTATI I RASPRAVA

3.1. Results of application case
3.1. Rezultati za promatranu tvrtku

In this study, a comparative framework to forecast total monthly sales of furniture products was developed. To achieve this aim, a case study was carried out in a furniture product manufacturing company located in Black Sea region of Turkey. In the first stage, an ARIMAX model is proposed. We collected the monthly sales data detailed above. It includes 84 data points for each output variable corresponding to seven-year data. For all of the ARIMAX modeling processes, EViews 10.0 was used. The ARIMAX model used for forecasting was split into three steps:

(1) Transformations of the dependent variables were made and the level of differencing was determined. Transformations of monthly sales of dining room, bedroom, teen room and armchair were made by differencing. The transformation of the sales of sitting group was arranged based on both logarithmic and differencing operations.

(2) The external independent variables were determined as mentioned in previous sub-sections (Subsection 2.2.1). The ARIMAX model developed to forecast teen room sales in our case study has the following external variables (Eq. 4).

$$D(y_t) = \sum_{i=1}^{12} c_j M_{j,t} + dCCI_t + ePPI_t + fV_t + \rho_1 \vartheta_{t-1} +$$
$$+ \rho_2 \vartheta_{t-2} + \rho_3 \vartheta_{t-3} + \theta_1 \epsilon_{t-1} + \theta_2 \epsilon_{t-2} \qquad (4)$$

where y_t refers to teen rooms sales, $M_{j,t}$ month of the year, CCI_t, CCI, PPI_t, PPI and V_t number of vacation days. ρ_p and θ_q are the model parameters for the autoregressive and moving average terms, respectively, and ε_t are the residual term representing random disturbances that cannot be predicted.

(3) The order of the autoregressive moving average (ARMA) terms was selected. EViews uses model selection to determine the appropriate ARMA order. The orders of AR and MA were limited to four. Model selection is a way of determining which type of model fits best a set of data and is often used to choose the best model for forecasting that data (EViews 10 tutorial, 2017). We used Akaike Information Criterion (AIC) in ARIMAX modeling process. As an example, the best ARMA terms for teen room sales were determined according to the AIC criteria. The results are given in Figure 7. The best ARMA term for this case is obtained as (3,2). The same steps were followed for each furniture product to make transformations and select ARMA terms based on AIC values. Best ARMA terms and related ARIMAX models with some model performance measures such as R^2, adjusted R^2 and AIC are given in Table 3.

The plots of actual versus forecasted values for ARIMAX models are provided by means of the EViews as shown in Figure 8. The results show that using the ARIMAX model is an applicable choice for forecasting monthly sales of the products in the observed furniture factory. The MAPE value of the armchair sales is calculated as 5.37 %, which means that a reasonable result is obtained (Çelik *et al.* 2016). On the other hand, MAPE values are also calculated for the sales of dining room, bedroom, teen room and sitting group as 10.36 %, 8.70 %, 10.67 % and 8.04 %, respectively.

The ARIMAX-ANN hybrid model integrated the ARIMAX model with the neural network model and tested with the raw data. We built the hybrid ARIMAX-ANN model with the following input layers: (1) the dependent variables used in ARIMAX modeling, (2) the residuals of the ARIMAX model. This process is followed by data partition and normalization by min-max normalization method. A training and testing model based on ANN is then employed after determining the design architecture and network properties. A logistic input and output activation function are used. Three layers which include input, hidden and output
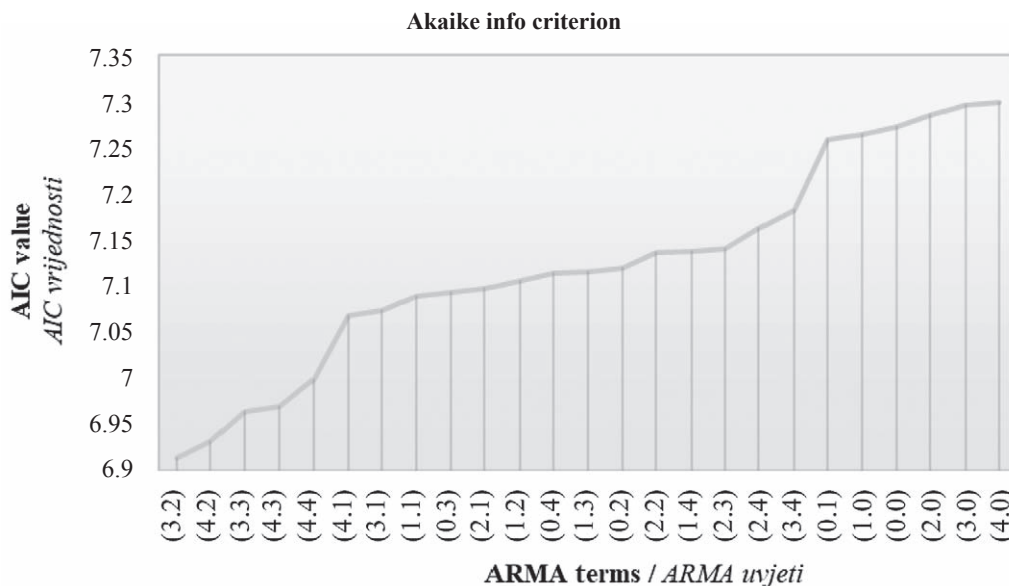

Figure 7 AIC values of ARMA terms proposed for teen room sales
Slika 7. AIC vrijednosti ARMA uvjeta predloženih za prodaju soba za mlade

Table 3 Performance measurement results of ARIMAX models
Tablica 3. Rezultati performansi ARIMAX modela

| Model name / *Model*	Selected dependent variable *Selektirana zavisna varijabla*	ARIMAX model representation *Prikaz modela ARIMAX*	*R*-Squared R^2	Adj. *R*-Squared *Prilagođeni* R^2	AIC
Dining room sales forecasting *predviđanje prodaje blagovaonica*	D(DININGROOM)	(2,1,4)	0.726288	0.632059	8.057243
Bedroom sales forecasting *predviđanje prodaje spavaćih soba*	DLOG(BEDROOM)	(3,1,4)	0.616559	0.475964	-1.552094
Teen room sales forecasting *predviđanje prodaje soba za mlade*	D(TEENROOM)	(3,1,2)	0.690860	0.591138	6.924504
Sitting group sales forecasting *predviđanje prodaje namještaja za sjedenje*	DLOG(SITTINGGROUP)	(0,1,3)	0.690440	0.603376	-2.015712
Armchair sales Forecasting *predviđanje prodaje naslonjača*	D(ARMCHAIR)	(2,1,4)	0.681010	0.571194	10.25667
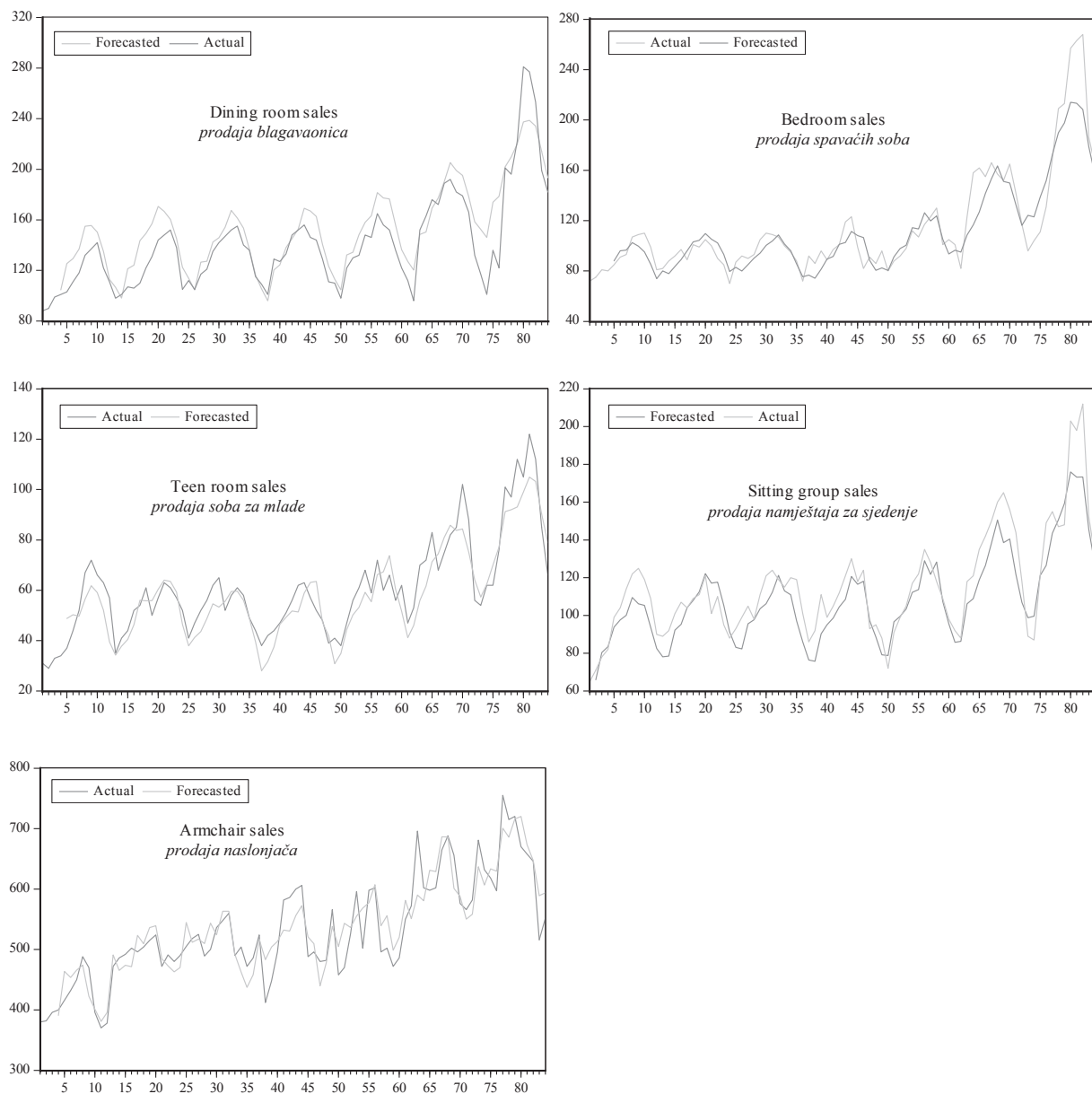
Figure 8 Comparison of actual and forecasted values for five furniture products by ARIMAX
Slika 8. Usporedba stvarnih i prognoziranih vrijednosti prodaje za pet proizvoda namještaja primjenom modela ARIMAX

16-8-1

"*N*" refers to numeric columns scaling parameters. "*C*" refers to categorical column encoding parameters.
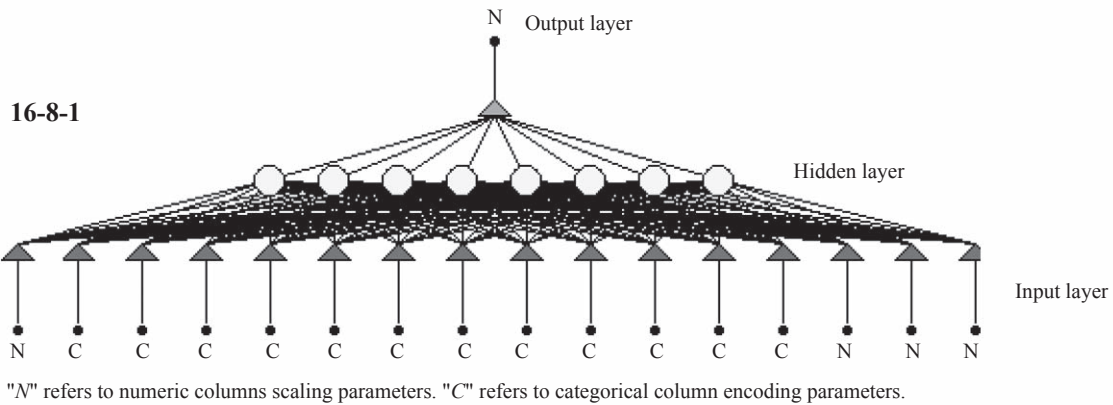
Figure 9 Network structure for teen room sales forecasting model (N refers to numerical columns scaling parameters, C refers to categorical column encoding parameters)
Slika 9. Struktura mreže za prognostički model prodaje soba za mlade (N se odnosi na parametre skaliranja numeričkih stupaca, C se odnosi na parametre za kodiranje kategoriziranih stupaca)

layers are constituted. The network structure for hybrid ARIMAX-ANN based teen room sales forecasting model is presented in Figure 9. While "16" in input layer represents number of inputs (12 for month of the year variable and one for each of the four variables: CCI, PPI, number of vacation days and residuals of the ARIMAX model), "8" in hidden layer shows number of neurons with best accuracy value. "1" in output layer shows number of outputs. The accurateness of the

model is directly related to the number of neurons in hidden layer. In this network, input and output activation functions are logistic. Output error function is sum-of-squares.

The performance indicator of R^2 is obtained as 98.97 %, which shows a good accurateness of the method. A commercial software, Alyuda NeuroIntelligence software, was used in developing the hybrid models. After the data entry to the software, it random-
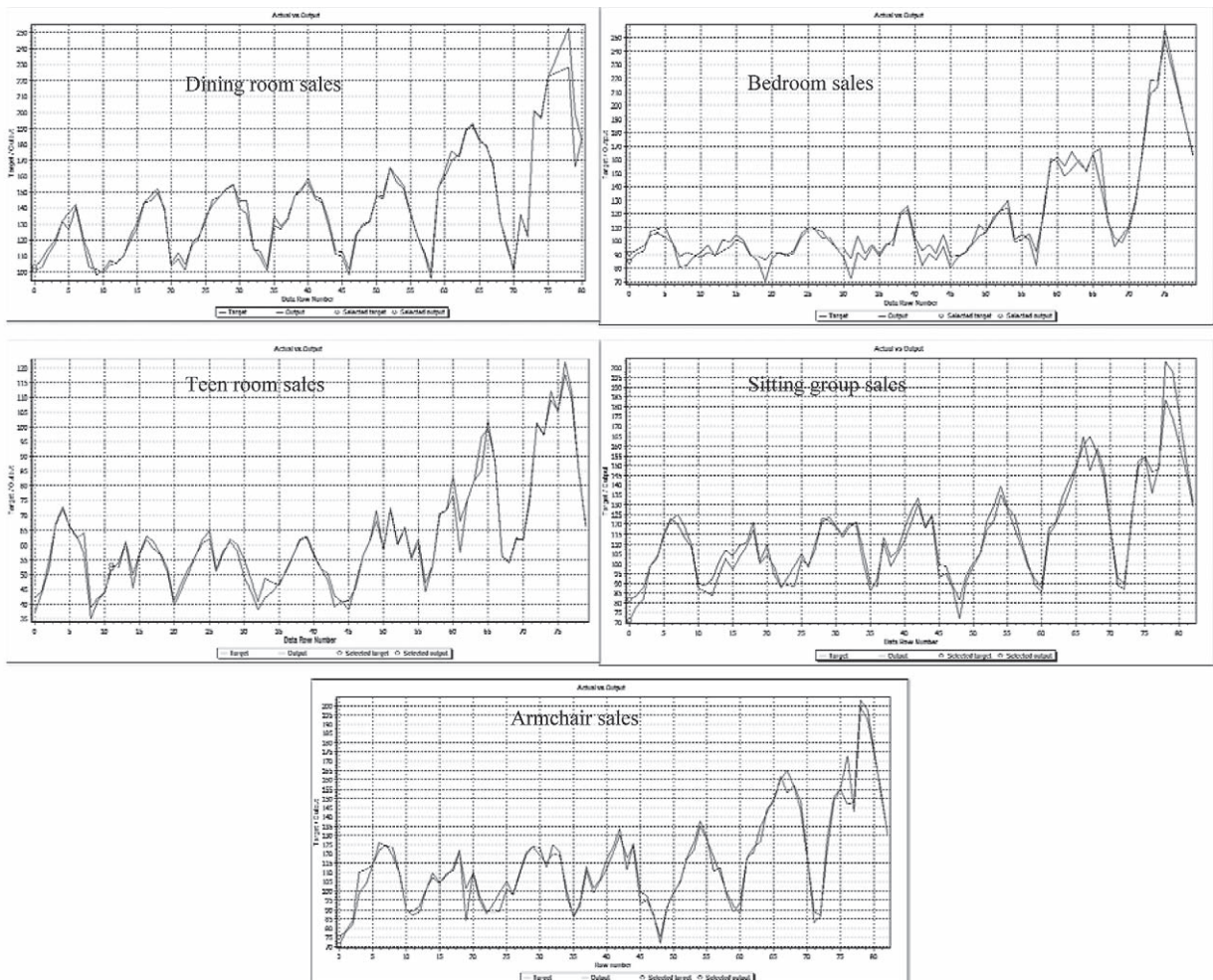
Figure 10 Comparison of actual and forecasted values for five furniture products by ARIMAX-ANN hybridization
Slika 10. Usporedba stvarnih i prognoziranih vrijednosti za pet vrsta namještaja primjenom hibridnog modela ARIMAX-ANN

ly selects 70:15:15 ratios for training, validation and testing. In some studies, this ratio may be 60:20:20 (Fu *et al.*, 2017). Experiments were run with various algorithms such as Quick Propagation, Quasi-Newton, Levenberg-Marquardt, Online Back Propagation and Conjugate Gradient Descent. The best network was obtained by Quick Propagation algorithm with some performance measures indicating as follows: while R^2 value is obtained as 0.9897 for all data set, the average test error is obtained as 3.621643. The MAPE value for overall and test data of this model was obtained as 3.22 % and 5.71 %, respectively.

The same steps were followed for each furniture product to develop hybrid models. The obtained MAPE values for overall and test data of the remaining four models (dining room, bedroom, sitting group and armchair) were obtained as, 1.99 % & 2.75 %, 4.42 % & 4.47 %, 3.66 % & 4.8 % and 1.05 % & 2.71 %, respectively. The actual versus fitted values for these five models are given in Figure 10.

Results of ANN models, which were compared to the ARIMAX and ARIMAX-ANN hybrid models through this study, were derived from Yucesan *et al.* (2017). That study was carried out by the authors of this study. They applied ANN modeling based on Bayesian rules training. They obtained MAPE values of each furniture product sales forecasting as 3.588%, 5.951%, 5.954%, 5.223% and 3.057%, respectively, for dining room, bedroom, teen room, sitting group and armchair.

3.2 Overall discussion
3.2. Rasprava rezultata

The best model for this study was the ARIMAX-ANN hybrid model in each furniture product sales forecasting (see Table 4). Çelik *et al.* (2016) reported that, in practical applications, MAPE < 10 % means high accuracy. Accordingly, it must be noted that MAPE values of ARIMAX-ANN hybridization and single ANN models for monthly furniture product sales figures are within the range reported by Çelik *et al.* (2016). Forecasting accuracy is dependent on the choice of forecasting model. ANN and ARIMAX models have different advantages and disadvantages. ARIMAX model is very flexible and it can also represent AR, MA, differencing and inclusion of external factors. ARIMAX model is very good when dealing with the linear part but it is weak when working with nonlinear data. ANN model is good at dealing with nonlinear parts. When using hybrid models, the residuals of the ARIMAX model as input variables can solve this problem. Also, the results show that a combination of ARIMAX and ANN models gives better forecasting accuracy.

4 CONCLUSION
4. ZAKLJUČAK

In this study, a comparative forecasting framework was developed and applied to solve the problem of sales forecasting for furniture products. The applied models include ARIMAX, ANN and ARIMAX-ANN hybridization. The models were used to forecast monthly sales figures of a corporate furniture manufacturing company located in Black Sea region of Turkey. In conclusion of this comparative study, the results of performance measures demonstrate that ARIMAX-ANN hybrid model, developed for each amount of product sales, gives better accuracy values than single models. Overall, it is proved that using the ARIMAX and hybridization of this method with ANN are applicable for forecasting monthly sales of furniture products.

The aim of sales forecasting is to determine the demand level of products in a certain time horizon and it is an important part of production planning. In aggregate production planning, sales forecasting is the starting point. This step is one of the most challenging problems for stakeholders in furniture industry. Decision makers should evaluate the costs and benefits of each model before choosing an appropriate forecasting method. In our opinion, the ARIMAX-ANN hybrid model was suitable for the observed company since this method gives effective solutions. This comparative framework can be adapted to any company competing in forestry industry or other industries. In addition to its methodological contributions, this study has some benefits for the forestry industry. First, it further encourages stakeholders to forecast sales figures in other forestry products such as timber, parquet, oriented

Table 4 MAPE values for five models with respect to three methodologies
Tablica 4. MAPE vrijednosti za pet modela s obzirom na tri metodologije

Model name / *Model*	MAPE values, %			
	ARIMAX	ANN (Yucesan *et al.* 2017)	ARIMAX-ANN	
			All data *Svi podatci*	Test data *Podatci testa*
Dining room sales forecasting *predviđanje prodaje blagovaonica*	10.36	3.58	1.99	2.75
Bedroom sales forecasting *predviđanje prodaje spavaćih soba*	8.70	5.95	4.42	4.47
Teen room sales forecasting *predviđanje prodaje soba za mlade*	10.67	5.95	3.22	5.71
Sitting group sales forecasting *predviđanje prodaje namještaja za sjedenje*	8.04	5.22	3.66	4.8
Armchair sales forecasting *predviđanje prodaje naslonjača*	5.37	3.06	1.05	2.71

standard board, plywood, etc. Secondly, advanced manufacturing methods have been increasingly employed in forestry sector due to today's technological development. Due to the possible demand for wood products, comprehensive and effective forecasting approaches are required for monitoring the trend. Therefore, a comparative forecasting outline has been developed, and it has been used to forecast the sales figures for furniture industry in Turkey.

By the current research, the model proposed by Yucesan *et al.* (2017) was improved by developing a more effective hybrid model. In future, the authors are planning to extend the hybrid model considering external factors to provide a more accurate result, although it has not been considered in this particular case study.

5 REFERENCES
5. LITERATURA

1. Akkoyunlu, M. T.; Akkoyunlu, M. C.; Pusat, S.; Özkan, C., 2015: Prediction of accurate values for outliers in coal drying experiments. Arabian Journal for Science and Engineering, 40 (9): 2721-2727.
http://dx.doi.org/ 10.1007/s13369-015-1746-2.

2. Alon, I.; Qi, M.; Sadowski, R. J., 2001: Forecasting aggregate retail sales: a comparison of artificial neural networks and traditional methods. Journal of Retailing and Consumer Services, 8 (3): 147-156.
http://dx.doi.org/10.1016/S0969-6989(00)00011-4.

3. Anggraeni, W.; Vinarti, R. A.; Kurniawati, Y. D., 2015: Performance Comparisons Between Arima and Arimax Method in Moslem Kids Clothes Demand Forecasting: Case Study. Procedia Computer Science, 72: 630-637.
https://doi.org/10.1016/j.procs.2015.12.172.

4. Areekul, P.; Senjyu, T.; Toyama, H.; Yona, A., 2010: Notice of violation of IEEE publication principles a hybrid ARIMA and neural network model for short-term price forecasting in deregulated market. IEEE Transactions on Power Systems, 25 (1): 524-530.
https://doi.org/10.1109/TPWRS.2009.2036488.

5. Arunraj, N. S.; Ahrens, D., 2015: A hybrid seasonal autoregressive integrated moving average and quantile regression for daily food sales forecasting. International Journal of Production Economics, 170: 321-335.
https://doi.org/10.1016/j.ijpe.2015.09.039.

6. Arya, P.; Paul, R. K.; Kumar, A.; Singh, K. N.; Sivaramne, N.; Chaudhary, P., 2015: Predicting pest population using weather variables: an ARIMAX time series framework. International Journal of Agricultural and Statistics Sciences, 11 (2): 381-386.

7. Bierens, H. J., 1987: ARMAX model specification testing, with an application to unemployment in the Netherlands. Journal of Econometrics, 35 (1): 161-190.
https://doi.org/10.1016/0304-4076(87)90086-8.

8. Çelik, Ö.; Teke, A.; Yıldırım, H. B., 2016: The optimized artificial neural network model with Levenberg – Marquardt algorithm for global solar radiation estimation in Eastern Mediterranean Region of Turkey. Journal of Cleaner Production, 116: 1-12.
http://dx.doi.org/10.1016/j.jclepro.2015.12.082.

9. Doganis, P.; Alexandridis, A.; Patrinos, P.; Sarimveis, H., 2006: Time series sales forecasting for short shelf-life food products based on artificial neural networks and evolutionary computing. Journal of Food Engineering, 75 (2): 196-204.

https://doi.org/10.1016/j.jfoodeng.2005.03.056.

10. Fabianová, J.; Kačmáry, P.; Molnár, V.; Michalik, P., 2016: Using a Software Tool in Forecasting: A Case Study of Sales Forecasting Taking into Account Data Uncertainty. Open Engineering, 6 (1): 270-279.
https://doi.org/10.1515/eng-2016-0033.

11. Fan, J.; Shan, R.; Cao, X.; Li, P., 2009: The analysis to tertiary-industry with ARIMAX model. Journal of Mathematics Research, 1 (2): 156.

12. Fu, Z.; Avramidis, S.; Zhao, J.; Cai, Y., 2017: Artificial neural network modeling for predicting elastic strain of white birch disks during drying. European Journal of Wood and Wood Products, 75: 949-955.
https://doi.org/10.1007/s00107-017-1183-x.

13. Gul, M.; Guneri, A. F., 2016a: Planning the future of emergency departments: Forecasting ED patient arrivals by using regression and neural network models. International Journal of Industrial Engineering: Theory, Applications and Practice, 23 (2): 137-154.

14. Gul, M.; Guneri, A. F., 2016b: An artificial neural network-based earthquake casualty estimation model for Istanbul city. Natural hazards, 84 (3): 2163-2178.
http://dx.doi.org/ 10.1007/s11069-016-2541-4.

15. Gul, M.; Guneri, A. F., 2015: Forecasting patient length of stay in an emergency department by artificial neural networks. Journal of aeronautics and space technologies (Havacilik ve uzay teknolojileri dergisi), 2 (8): 1-6.
http://dx.doi.org/ 10.7603/s40690-015-0015-7.

16. Guneri, A. F.; Gumus, A. T., 2008: Artificial neural networks for finite capacity scheduling: a comparative study. International Journal of Industrial Engineering: Theory, Applications and Practice, 15 (4): 349-359.

17. Guneri, A. F.; Gumus, A. T., 2008: The usage of artificial neural networks for finite capacity planning. International Journal of Industrial Engineering: Theory, Applications and Practice, 15 (1): 16-25.

18. Hazir, E.; Koç, K. H.; Esnaf, Ş., 2016: Türkiye mobilya satış değerlerinin örnek bir yapay zekâ uygulaması ile tahmini. Selçuk-Teknik Dergisi, 1172-1182.

19. Jalalkamali, A.; Moradi, M.; Moradi, N., 2015: Application of several artificial intelligence models and ARIMAX model for forecasting drought using the Standardized Precipitation Index. International Journal of Environmental Science and Technology, 12 (4): 1201-1210. https://doi.org/10.1007/s13762-014-0717-6.

20. Jansen, W. J.; Nahuis, N. J., 2003: The stock market and consumer confidence: European evidence. Economics Letters, 79 (1): 89-98.
http://dx.doi.org/10.1016/S0165-1765(02)00292-6.

21. Khashei, M.; Bijari, M., 2010: An artificial neural network (p, d, q) model for timeseries forecasting. Expert Systems with applications, 37 (1): 479-489.
https://doi.org/10.1016/j.eswa.2009.05.044.

22. Kröse, B.; Krose, B.; van der Smagt, P.; Smagt, P., 1993: An introduction to neural networks. CRC Press, London.

23. Kuo, R. J., 2001: A sales forecasting system based on fuzzy neural network with initial weights generated by genetic algorithm. European Journal of Operational Research, 129 (3): 496-517.
https://doi.org/10.1016/S0377-2217(99)00463-4.

24. Kuo, R. J.; Wu, P.; Wang, C. P., 2002: An intelligent sales forecasting system through integration of artificial neural networks and fuzzy neural networks with fuzzy weight elimination. Neural Networks, 15 (7): 909-925.
http://dx.doi.org/10.1016/S0893-6080(02)00064-3.

25. Lee, M.; Hamzah, N., 2010: Calendar variation model based on ARIMAX for forecasting sales data with Rama-

dhan effect. In Proceedings of the Regional Conference on Statistical Sciences, pp. 349-361.

26. Luxhøj, J. T.; Riis, J. O.; Stensballe, B., 1996: A hybrid econometric – neural network modeling approach for sales forecasting. International Journal of Production Economics, 43 (2): 175-192. https://doi.org/10.1016/0925-5273(96)00039-4.

27. Mahbub, N.; Paul, S. K.; Azeem, A., 2013: A neural approach to product demand forecasting. International Journal of Industrial and Systems Engineering, 15 (1): 1-18. http://dx.doi.org/10.1504/IJISE.2013.055508.

28. Murlidharan, V.; Menezes, B., 2013: Frequent pattern mining-based sales forecasting. Opsearch, 50 (4): 455-474. https://doi.org/10.1007/s12597-012-0119-9.

29. Oblak, L.; Stirn, L. Z.; Moro, M.; Hrovatin, J.; Mole, S.; Kuzman, M. K., 2012: Choice of Quantitative Method for Forecasting of Parquet Sales. Drvna industrija, 63 (4): 249-254. http://dx.doi.org/10.5552/drind.2012.1204.

30. Onat, O.; Gul, M., 2018: Application of Artificial Neural Networks to the prediction of out-of-plane response of infill walls subjected to shake table, 21 (4): 521-535. http://dx.doi.org/10.12989/sss.2018.21.4.521.

31. Peltzman, S., 2000: Prices rise faster than they fall. Journal of Political Economy, 108 (3): 466-502. http://dx.doi.org/ 10.1086/262126.

32. Pusat, S.; Akkoyunlu, M. T.; Pekel, E.; Akkoyunlu, M. C.; Özkan, C.; Kara, S. S., 2016: Estimation of coal moisture content in convective drying process using AN-FIS. Fuel Processing Technology, 147: 12-17. http://dx.doi.org/10.1016/j.fuproc.2015.12.010.

33. Somoza, E.; Somoza, J. R., 1993: A neural-network approach to predicting admission decisions in a psychiatric emergency room. Medical Decision Making, 13 (4): 273-280. http://dx.doi.org/ 10.1177/0272989X9301300402.

34. Sutthichaimethee, P.; Ariyasajjakorn, D., 2017: Forecasting Energy Consumption in Short-Term and Long-Term Period by Using Arimax Model in the Construction and Materials Sector in Thailand. Journal of Ecological Engineering, 18 (4). http://dx.doi.org/ 10.12911/22998993/74396.

35. Xu, Q.; Tsui, K. L.; Jiang, W.; Guo, H., 2016: A hybrid approach for forecasting patient visits in emergency department. Quality and Reliability Engineering International, 32 (8): 2751-2759. http://dx.doi.org/10.1002/qre.2095.

36. Yip, D. H.; Hines, E. L.; Yu, W. W., 1997: Application of artificial neural networks in sales forecasting. Proceedings of International Conference on Neural Networks (ICNN'97), IEEE, Vol. 4, pp. 2121-2124. http://dx.doi.org/ 10.1109/ICNN.1997.614233.

37. Yucesan, M.; Gul, M.; Celik, E., 2017: Application of artificial neural networks using bayesian training rule in sales forecasting for furniture industry. Drvna industrija: znanstveni časopis za pitanja drvne tehnologije, 68 (3): 219-228. http://dx.doi.org/10.5552/drind.2017.1706.

38. Zhang, G. P., 2003: Time series forecasting using a hybrid ARIMA and neural network model. Neurocomputing, 50: 159-175. https://doi.org/10.1016/S0925-2312(01)00702-0.

39. *** 2013: TOBB. Turkey Furniture Products Council Industry Report, TOBB Publication No: 2014/212, https://www.tobb.org.tr/Documents/yayinlar/2014/mobilya_sektor_raporu_tr_int.pdf.

40. *** 2017: EViews 10 tutorial., http://www.eviews.com/Learning/basics.html.

Corresponding address:

Asst. Prof. MELIH YUCESAN, Ph.D.

Munzur University
Engineering Faculty
Department of Mechanical Engineering
62000 Tunceli, TURKEY
e-mail: melihyucesan@munzur.edu.tr

Hadi Gholamiyan, Asghar Tarmian[1]

Weathering Resistance of Poplar Wood Coated by Organosilane Water Soluble Nanomaterials

Otpornost prema vremenskim utjecajima topolovine premazane vodenom otopinom organosilana u nanoveličinama

ABSTRACT • *The potential use of organosilane nanomaterials (nano-zycosil and nano-zycofil) for improving the weathering resistance of poplar wood was evaluated in comparison to common clear coatings (nitrocellulose and polyester lacquer). A 250 μm coating layer was applied by an automatic film applicator at the speed of 150 mm/s. The coated specimens were exposed to a 1000 W xenon arc light source at 65 % relative humidity and temperature of 20 °C inside a weather-o-meter for 1440 hrs. Among coating materials, nano-zycosil showed the best performance to improve the weathering resistance. Compared to the lacquer-coated samples, the roughness of nanoparticle-coated ones was less affected by weathering. Contact angle measurements indicated that nano-zycosil coating had a pronounced decreasing effect on the surface wettability. The combined analyses of SEM and EDX demonstrated that the nanoscale silane layer covered the whole wood surface homogeneously, whereas nitrocellulose and polyester coatings were deposited preferentially in the surface depressions.*

Keywords: clear coatings, organosilane nanomaterials, weathering, wood

SAŽETAK • *U radu je prikazano istraživanje mogućnosti uporabe organosilana u nanoveličinama (nano-zycosil i nano-zycofil) za povećanje otpornosti topolovine na vremenske utjecaje u usporedbi s uporabom klasičnih prozirnih premaznih materijala (nitroceluloznoga i poliesterskoga premaza). Sloj premaza od 250 μm nanesen je strojno, brzinom 150 mm/s. Premazani su uzorci 1440 sati bili izloženi izvoru svjetlosti ksenonske svjetiljke od 1000 W pri relativnoj vlazi zraka od 65 % i na temperaturi od 20 °C. Od premaznih materijala nano-zycosil se pokazao najboljim za povećanje otpornosti na vremenske utjecaje. U usporedbi s uzorcima obrađenim klasičnim premaznim materijalima, hrapavost nanopremaza bila je manje uvjetovana izlaganjem vremenskim utjecajima. Mjerenja kontaktnog kuta pokazala su da premaz nano-zycosilom znatno utječe na smanjenje kvašenja površine. Kombinirane analize SEM i EDX potvrdile su da sloj silana u nanoveličini ravnomjerno prekriva površinu drva, dok je sloj nitroceluloznoga i poliesterskog premaza u udubljenjima na površini deblji.*

Ključne riječi: prozirni premazi, organosilani nanoveličine, izlaganje vremenskim utjecajima, drvo

---

[1] Authors are assistant professor and associate professor at Department of Wood and Paper Science and Technology, Faculty of Natural Resources, University of Tehran, Karaj, I.R. Iran.
[1] Autori su docent i izvanredni profesor Odsjeka za znanost i tehnologiju drva i papira, Prirodoslovno matematički fakultet, Sveučilište u Teheranu, Karaj, IR Iran.

1 INTRODUCTION
1. UVOD

Wood surfaces exposed to outdoor conditions are rapidly degraded due to the combined action of weather factors, such as oxygen, ultraviolet light and relative humidity (RH). Several paints and varnishes are commonly used as coating materials to prevent the degradation. However, wood coated with common clear coatings is still susceptible to photo discoloration (Lung Chou *et al.*, 2008; Bulian *et al.*, 2017). The photo discoloration is unavoidable even if wood is coated with non-yellowing or durable clear coatings, such as aliphatic polyurethane ones (Chang and Chou, 1999). The coating performance depends on several factors, in particular the substrate, the coating system and the interactions between them (Bulian and Graystone, 2009). Nowadays, coating is an area of significant research in nanotechnology. Nanoparticle based coating systems can provide better weathering resistance (Clausen *et al.*, 2010; Nguyen-Tri *et al.*, 2018) and conservation than the conventional techniques because of very small pigment particles with very high specific surface. Some appropriate nanoparticles, such as silica (SiO_2), alumina (Al_2O_3) (Busseya *et al.*, 2018; Mori *et al.*, 1998; Powell *et al.*, 1997) and TiO_2 (Nanetti, 2006; Li *et al.*, 2005) have been previously used to improve the wood weathering resistance. For example, Veronovski *et al.* (2013) found that the surface treatment of wood with nano-TiO_2 (rutile) incorporated in water-based acrylic coatings improves the weathering resistance. Organosilane nanomaterials have been mainly developed for waterproofing of wood because they can block the pores by agglomeration and prevent the penetration of water into wood (Tshabalala and Gangstad, 2003; Godnjavec *et al.*, 2012). For concrete, Nano-zycosil with size of up to 6 nm can enhance the waterproofing property of the surfaces by filling the microcracks and nanopores (Taghiyari, 2013). Gholamiyan *et al.*, (2012, 2016) also reported that the organosilane nanomaterials (zycosil and zycofil) can be used as

water vapor diffusion retarders for wood. The present study was, therefore, conducted to evaluate if organosilane nanoparticles can significantly contribute to improvement of weathering resistance of wood.

2 MATERIALS AND METHODS
2. MATERIJALI I METODE

2.1 Wood sampling and coating materials
2.1. Uzorkovanje drva i premazni materijali

Flat-sawn boards of poplar wood (*Populous nigra*) with dimensions of 50 by 100 by 200 mm (T, R and L directions, respectively) at moisture content of 12 % were selected for the study. Sealer and nitrocellulose lacquer and polyester lacquer were used as clear coatings. They were purchased from Dorsa Chemistry (Brilliant) Co. The technical properties of the lacquers are summarized in Table 1. Organosilane water soluble nanomaterials (nano-zycosil and nano-zycofil) were purchased from Zydex Company. The most important properties of the nanomaterials are presented in Table 2.

2.2 Coating methods
2.2. Metode nanošenja premaznog materijala

The wood surfaces were sanded with 150-grade sandpaper before coating. Six different coating systems were applied as shown in Table 3. A 250 μm wet pre-cure coating layer was applied by an automatic film applicator at the speed of 150 mm/s. The nanomaterial-coated samples were oven dried at temperature of 103 ± 2 °C for 24 h, and the others were dried in a conditioned room (T = 25 °C and RH=65 %) for about 20 minutes. The lacquers were diluted by a lacquer thinner (1:2) before application.

2.3 Weathering test
2.3. Izlaganje vremenskim utjecajima

The coated specimens were exposed to a 1000 W xenon arc light source at 65 % RH and chamber temperature of 30 ºC in a weather-o-meter for 1440 hrs.

Table 1 Technical properties of nitrocellulose lacquer and polyester lacquer
Tablica 1. Svojstva nitroceluloznoga i poliesterskoga premaznog materijala

Coating type / *Vrsta premaznog materijala*	Viscosity at 25 °C / *Viskoznost pri 25 °C*	Percent solids *Udio suhe tvari*	Density at 25 ° C *Gustoća pri 25 °C*	Color (Gardner) / *Boja (Gardner)*	Flash point, °C *Točka zapaljenja,* °C
Nitrocellulose lacquer *nitrocelulozni premazni materijal*	16-38 Pa·s	21±1	0.94±0.01	3 max	≤20
Polyester lacquer *poliesterski premazni materijal*	10-25 Pa·s	30±1	0.94±0.01	3 max	≤20

Table 2 The most important information on used nanomaterials
Tablica 2. Najvažniji podatci o primijenjenim nanomaterijalima

Property / *Svojstvo*	Zycosil	Zycofil
Size / *veličina*	10-30 nm	90-300 nm
Color / *boja*	Pale yellow / *bljedožuta*	Yellow / *žuta*
Density / *gustoća*	1.7 (g/cm³) (25 °C)	2.5 (g/cm³) (25 °C)
Flash point / *točka zapaljenja*	More than / *iznad* 100 °C	More than / *iznad* 100 °C
Auto-ignition temperature / *temperatura samozapaljenja*	More than / *iznad* 200 °C	More than / *iznad* 150 °C
Viscosity / *viskoznost*	0.5-1 Pa·s (25 °C)	0.2-0.7 Pa·s (25 °C)

Table 3 Guide for coating systems
Tablica 3. Oznake sustava premaznih materijala

Coating type / *Vrsta premaznog materijala*	Coating materials *Premazni materijal*
Control	None
CZ	nano-zycosil
CZF	nano-zycofil
CZZF	nano-zycosil+ nano-zycofil
CPS	Clear polyester lacquer
CSC	sealer + nitrocellulose lacquer
CSC+CPS	sealer + nitrocellulose lacquer + polyester lacquer

2.4 Color measurement
2.4. Mjerenje boje

Spectrophotometry was applied to measure brightness ($L*$), redness ($b*$) and yellowness ($a*$) variables of specimens in the CIE-LAB system before and after exposure to the accelerated weathering. Ten boards were tested for each type of coating system. The spectrophotometry was performed using a miniscan EZ spectrophotometer with the aperture diameter of 25 mm and with a standard illuminant D65 and a 10° standard observer. The parameters of $\Delta E*$ (color difference), $C*$ (color saturation) and $h*$ were calculated using the following equations:

$$C* = \sqrt{(a*)^2 + (b*)^2} \qquad (1)$$

$$\Delta E* = \sqrt{(\Delta a*)^2 + (\Delta b*)^2 + (\Delta L*)^2} \qquad (2)$$

$$h* = \text{Arctan } (b*/a*) \qquad (3)$$

2.5 Measuring the surface roughness
2.5. Mjerenje hrapavosti površine

A Mitutoyo SJ-201P instrument was employed for measuring the surface roughness. Three roughness parameters characterized by ISO 4287 standard (1997), namely average roughness (Ra), mean peak-to-valley height (Rz), and maximum peak-to-valley height (Ry) were considered to evaluate the surface characteristics of coatings before and after weathering.

2.6 Determination of wettability
2.6. Ispitivanje kvašenja

The wetting behavior of coated samples conditioned at 65 % RH and 20 °C was characterized by static contact angle (CA) measurement and deionized water as test liquid. The CA values were determined by sessile drop method using a KSV Cam-101 Scientific Instrument (Helsinki, Gottingen University, Germany). The measurements were carried out for 1 and 10 seconds after deposition of the water drop on the surface. The average CA value was obtained with five drops for each sample.

2.7. SEM, EDX and ATR-FTIR studies
2.7. SEM, EDX i ATR-FTIR istraživanje

The surface morphology of coated samples was characterized by a scanning electron microscopy (SEM). The surface chemical composition of speci-mens was examined by energy dispersive X-ray analysis (EDX). Fourier transform infrared spectrophotometer (ATR-FTIR; Bruker model Confocheck) was also applied to identify the formed chemical bonds.

3 RESULTS AND DISCUSSION
3. REZULTATI I RASPRAVA

3.1 Color changes
3.1. Promjene boje

Table 4 shows $L*$, $a*$ and $b*$ values and their changes on various coated wood samples due to weathering. Before weathering, $L*$ for uncoated specimens was greater than that for all coated ones. The color parameters ($L*$, $a*$ and $b*$) of nano-zycofil (CZF)- and nano-zycosil (CZ)-coated specimens were found to be different. The color change of weathering for CZ was less than that for CZF. One of the main reasons for color change of clear coatings is the discoloration of wood substrate, affected by its individual chemical components, such as extractives (Fengel and Wegener, 1984). After coating, $b*$ and $a*$ decreased for all coatings, except CZ. Sigh *et al*. (2008) and Lung Chou *et al*. (2008) also reported a similar result for yellowing of clear coatings. After weathering, the least change in lightness index was observed for CZ and CZZF coatings. The lightness of CZ and CSC+CPS coatings dropped from 75.6 to 74.3 and from 78.1 to 67.5, respectively. After weathering, all coatings except CZ and CZZF were darker than the control sample as shown by the decreased $L*$ values (see Table 4). This $L*$ reduction is due to destruction of chemical bonds and photochemical degradation of cross-linking reactions at the surface coatings (Vlad Cristea *et al*., 2011). After weathering, all coatings are more reddish and yellowish (indicated by increased $b*$ and $a*$ values, respectively, in Table 4) than the control sample (Tsuchikawa *et al*., 2003 and Pastore *et al*., 2004). The least change in $a*$ and $b*$ parameters was observed for CZZF. After coating, CZ showed the least color change (ΔE). According to the measured color data, it can be noted that all coatings are more red, yellow and saturated ($c*$) than the uncoated wood both before and after weathering (Table 5). The color saturation after weathering ranged from 48.7 for sealer and nitrocellulose lacquer-coating to 35.6 for uncoated wood. Similar results were also found for hue angle ($h*$).

3.2 Surface roughness
3.2. Hrapavost površine

The surface roughness values (Ra, Rz and Rq) for each coating are depicted in Figure 1. After coating, the CSC+CPS and polyester (CPS) coatings were smoother than the other ones, probably due to rigid film formation on the wood surface (Gholamiyan *et al*., 2012). After weathering, the surface roughness increased for all coatings expect CZ. Increase in the surface roughness of wood after weathering is believed to be due to the erosion of primary cell wall caused by lignin degradation (Bulcke *et al*., 2007; Meincken and Evans, 2009). It is claimed that the surface roughness of nano-

Table 4 Guide for coating systems
Tablica 4. Oznake sustava premaznih materijala

Coating type /*Vrsta premaznog materijala*		Control	CZ	CZF	CZZF	CPS	CSC	CSC+CPS
L*	Before / *prije*	80.5 (1.5)	75.6 (1.8)	79 (1.3)	77.6 (2.2)	76.1 (3.9)	74.7 (2.5)	78.1 (1.0)
	After / *nakon*	73.2 (2.3)	74.2 (1.6)	70.7 (2.8)	73.3 (0.6)	69.3 (2.1)	65.4 (1.2)	67.5 (0.4)
	Mean changes / *prosječna promjena*	-7.2	-1.3	-8.2	-4.3	-6.7	-9.2	-10.5
a*	Before / *prije*	3.5 (0.3)	2.8 (0.8)	3.8 (0.9)	4 (0.7)	4.8 (0.5)	5.1 (0.8)	3.6 (0.6)
	After / *nakon*	9.5 (0.1)	9.8 (0.5)	11.4 (0.4)	8.7 (0.7)	11.7 (0.6)	13.8 (0.6)	13.1 (0.5)
	Mean changes / *prosječna promjena*	5.9	7	7.6	4.7	6.9	8.6	9.4
b*	Before / *prije*	19.1 (0.3)	20.8 (0.6)	20.4 (1.8)	22.5 (0.2)	25.6 (1.3)	25.7 (1.6)	23.2 (2.1)
	After / *nakon*	34.2 (0.7)	38.8 (2.6)	38.4 (0.3)	36.6 (0.8)	42.1 (2.6)	46.7 (1)	44.9 (1.0)
	Mean changes / *prosječna promjena*	15.1	17.9	17.9	14	16.42	20.9	21.7

Values in parentheses represent the standard deviation / *Vrijednosti u zagradama standardne su devijacije.*

Table 5 Changes of ∆*E*, *c** and *h** before and after weathering
Tablica 5. Promjene ∆*E*, *c** and *h** prije i nakon izlaganja vremenskim utjecajima

Coating type /*Vrsta premaznog materijala*		Control	CZ	CZF	CZZF	CPS	CSC	CSC+CPS
∆E*	Before / *prije*	…	2.1 (0.6)	2.2 (0.2)	4.5 (0.4)	8 (0.5)	9 (0.1)	4.7 (0.1)
	After / *nakon*	…	4.6 (0.5)	5.2 (0.8)	2.4 (0.8)	9 (0.7)	15.3 (0.9)	12.5 (0.8)
	Mean changes / *prosječna promjena*		2.4	3.1	-2	0.9	6.2	7.8
c*	Before / *prije*	19.4 (1.5)	21 (1.6)	20.8 (2.5)	22.9 (1.6)	26.1 (2)	26.3 (1.8)	23.5 (1.6)
	After / *nakon*	35.5 (2.1)	40.0 (2.9)	40.1 (3.2)	37.6 (2.1)	43.7 (2.5)	48.7 (3)	46.8 (3.6)
	Mean changes / *prosječna promjena*	16.1	18.9	19.2	14.7	17.5	22.4	23.2
h*	Before / *prije*	1.3 (0.3)	1.4 (0.1)	1.3 (0.1)	1.3 (0.2)	1.3 (0.2)	1. (0.13)	1.4 (0.2)
	After / *nakon*	1.2 (0.1)	1.3 (0.1)	1.2 (0.2)	1.3 (0.1)	1.2 (0.1)	1.2 (0.2)	1.2 (0.1)
	Mean changes *prosječna promjena*	-0.09	-0.1	-0.1	-0.06	-0.09	-0.09	-0.1

Values in parentheses represent the standard deviation / *Vrijednosti u zagradama standardne su devijacije.*

coatings is not significantly affected by weathering because of small size and high surface to volume ratio of nanoparticles (Li *et al.*, 2001). Thus, the smaller size of nano-zycosil particles (10-30 nm) compared to nano-zycofil (90-300 nm) ones may play an important role in the surface roughness.

3.3 Wettability
3.3. Kvašenje

The results showed that the wettability of wood decreased due to coating by all used coating systems (Figure 2), and the contact angle was increased significantly with the applied coatings. However, weathering had a decreasing effect on the contact angle for all coatings. The contact angle on the control sample dropped from 43º to 38º after 1440 h weathering and that of CZ from 87º to 67º. Among coatings, CZ and CSC+CPS exhibited the highest contact angle after the weathering exposure. In agreement with our results, waterproofing of organosilane nanomaterials has been reported, previously (Tshabalala and Gangstad, 2003; Godnjavec *et al.*, 2012).

3.4 SEM and EDX analysis
3.4. SEM i EDX analiza

Scanning electron microscopy (SEM) images of control and nano-zycosil coated films are shown in Figure 3. As can be seen in Figure 4, most particles are in nanometric dimensions (<100 nm). SEM images confirm that silane nanoparticles can effectively cover the wood surface after coating, which is similar to the results reported by a number of previous researchers (Li *et al.,* 2010; Da Silva *et al.*, 2012; Mahltig *et al.*, 2010). A significant silane peak in the EDX spectra of organosilane coated specimens confirms the presence of nano-zycosil or nano-zycofil particles (Figure 5).

3.5 Surface chemistry
3.5. Kemijska svojstva površine

The ATR-FTIR spectra of nano-zycosil coated and uncoated specimens are compared in Figure 6. The absorption bands at 1110-1090 cm^{-1}, 810-800 cm^{-1} and 480-470 cm^{-1} are attributed to the Si–O–Si asymmetric stretching, symmetric stretching and bending vibration, respectively. The spectrum of coated specimen
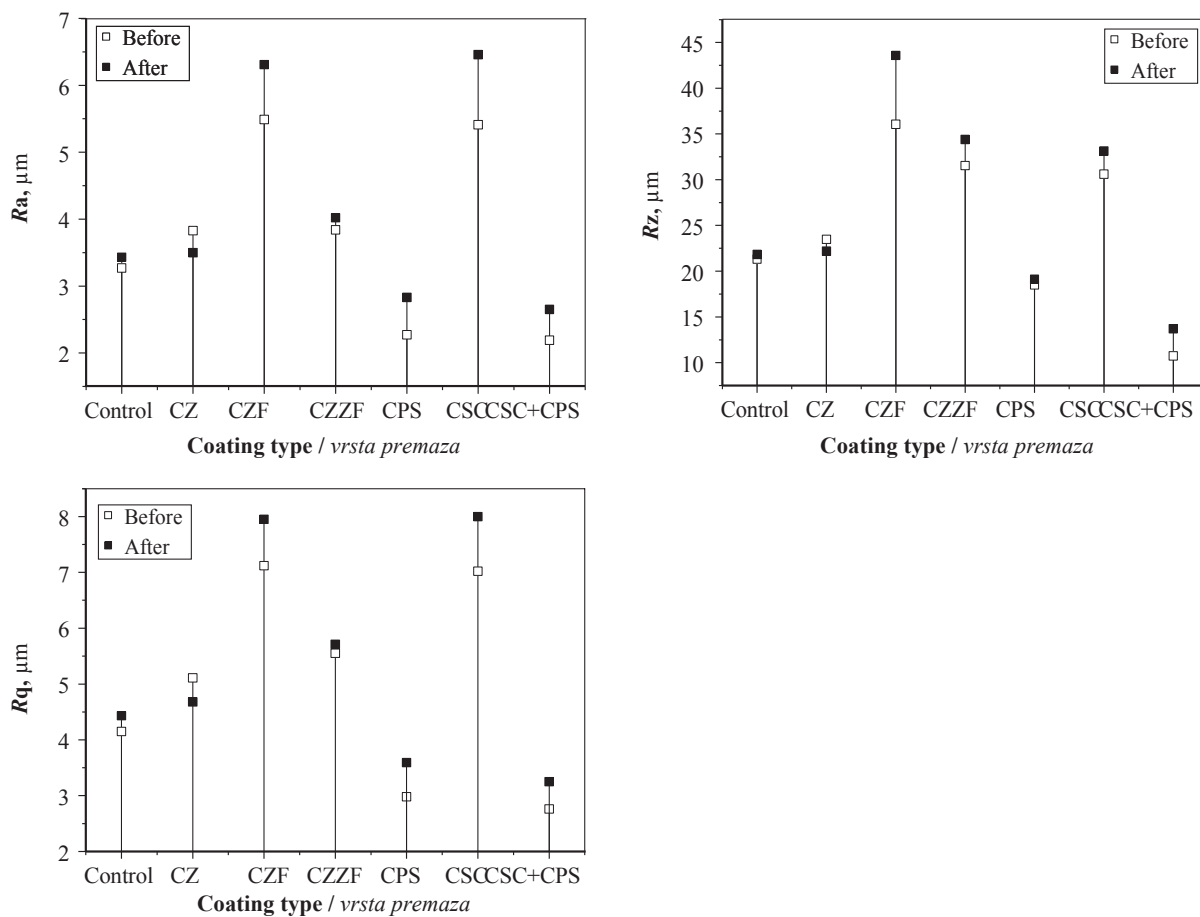
Figure 1 Surface roughness parameters for coated and uncoated specimens before and after weathering
Slika 1. Parametri hrapavosti površine premazanih i nepremazanih uzoraka prije i nakon izlaganja vremenskim utjecajima
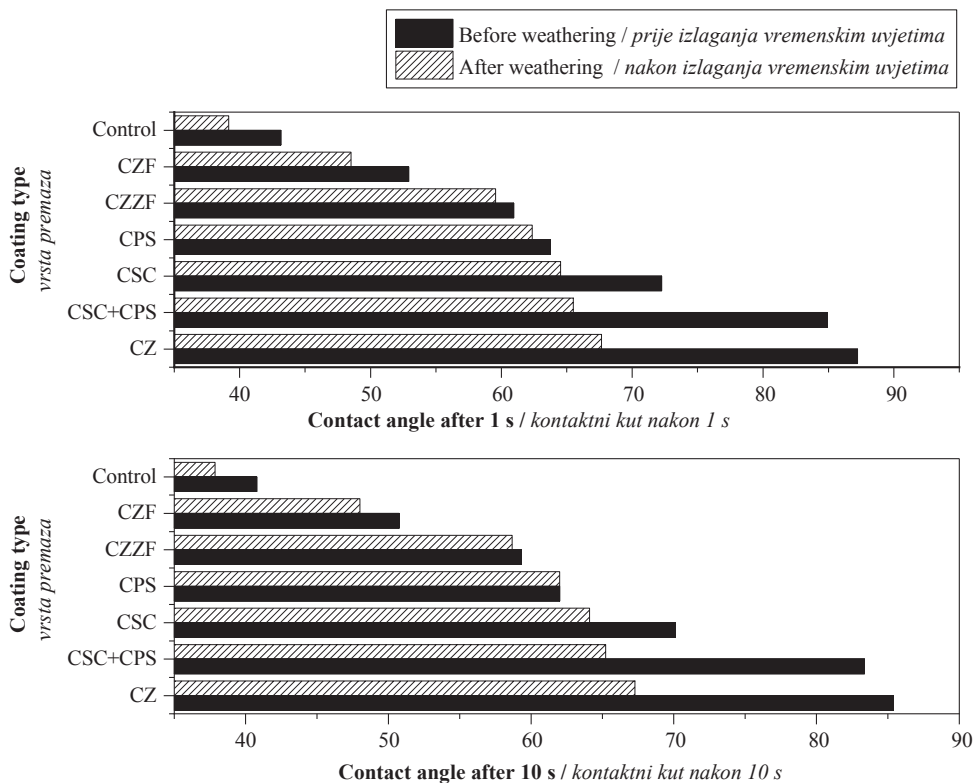

Figure 2 Contact angles for coated and uncoated specimens before and after weathering
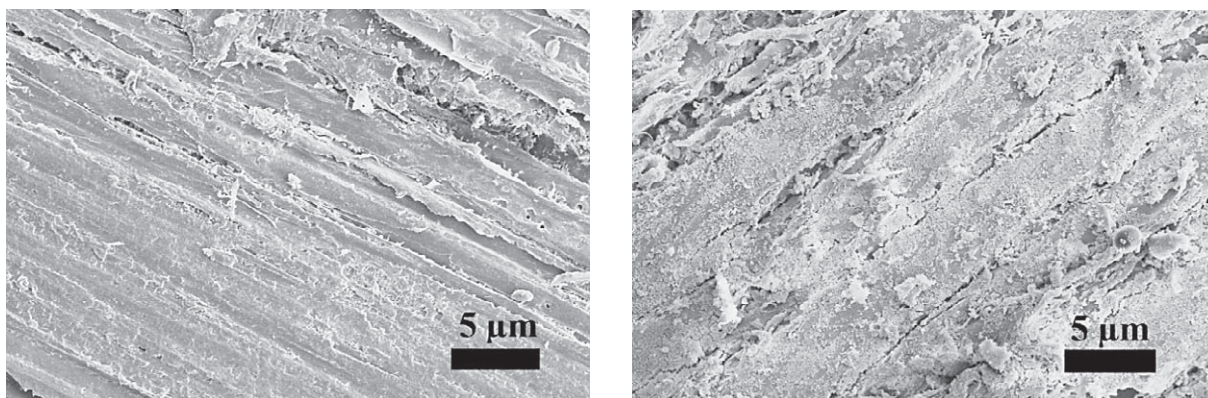**Slika 2.** Kontaktni kut premazanih i nepremazanih uzoraka prije i nakon izlaganja vremenskim utjecajima

Figure 3 SEM image of control (left) and nano-zycosil (right) coating
Slika 3. SEM fotografija kontrolnog premaza (lijevo) i premaza *nano-zycosilom* (desno)
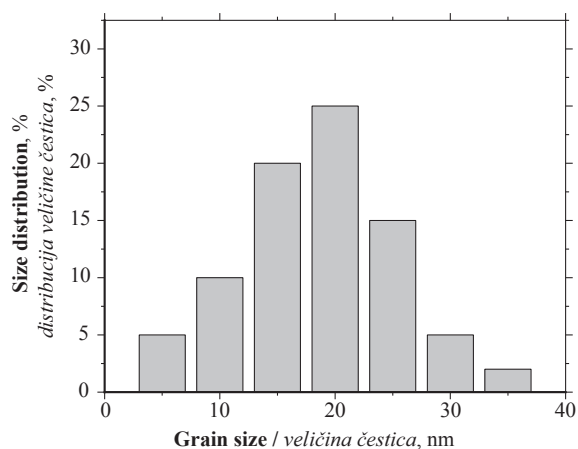
Figure 4 Particles size distribution of nano-zycosil
Slika 4. Raspodjela veličine čestica *nano-zycosila*

shows bands resulting from Si-CH$_3$ bonds (1269 cm^{-1}) (Tshabalala and Gangstad, 2003). The bands at broad absorption band of 3445-3425 cm^{-1} and 1640-1630 cm^{-1} are due to –OH groups of silane coatings (Rao *et al.,* 2010). In addition, the weak bands centered around 2880 cm^{-1} due to the C-H stretch and 1460 cm^{-1} due to the C-H bending vibrations of the wood components were replaced by sharper and much stronger bands at 2921 cm^{-1} due to the C-H bending vibrations of the long hydrocarbon chain bound to the wood by the nano-zycosil coating (Tshabalala and Gangstad, 2003 and Wang *et al.,* 2011).

4 CONCLUSIONS
4. ZAKLJUČAK

SEM images and EDX spectra showed that the wood surfaces can be effectively coated by the organosilane water soluble nanomaterials. SEM images revealed a significant surface coverage by the nanoparticles, and the EDX analysis also confirmed the presence of silane in the organosilane coated specimens. Among coating materials, nano-zycosil (CZ) exhibited the best performance for improving the weathering resistance of poplar wood. Different color parameters were observed between nano-zycosil and nano-zycofil coat-
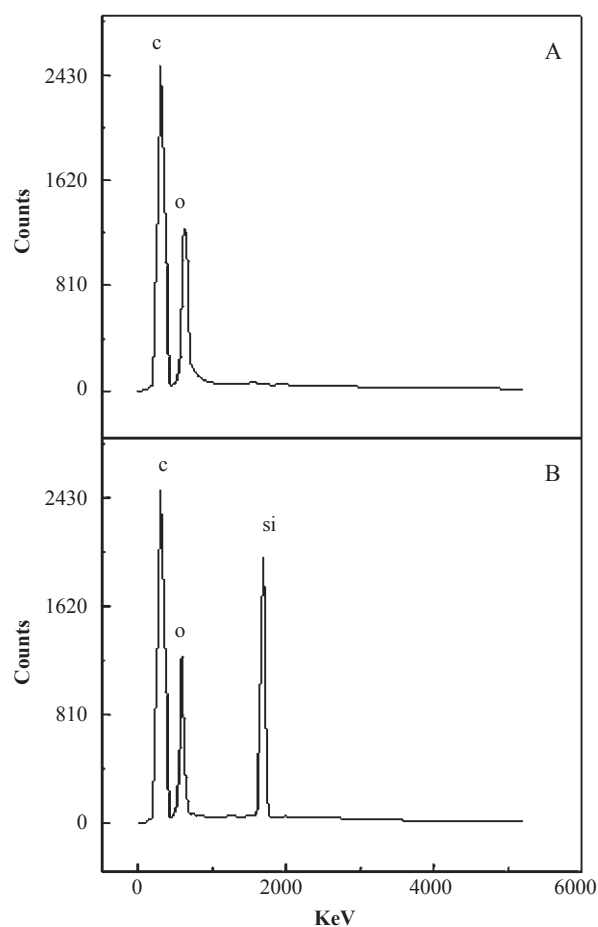
Figure 5 EDX spectra of (A) control and (B) nano-zycosil coated surfaces
Slika 5. EDX spektar (A) kontrolne površine i (B) površine premazane *nano-zycosilom*

ings. After weathering, all coatings except CZ and CZZF were darker than the uncoated wood. Compared to the clear coatings, the roughness of nano-zycosil and nano-zycofil was less affected by weathering, and the former showed a better performance. This can be due to the very small size and high surface to volume ratio of nanoparticles. Further researches on the nanofilm formation using sol-gel method are recommended for improving the weathering resistance of wood surfaces.
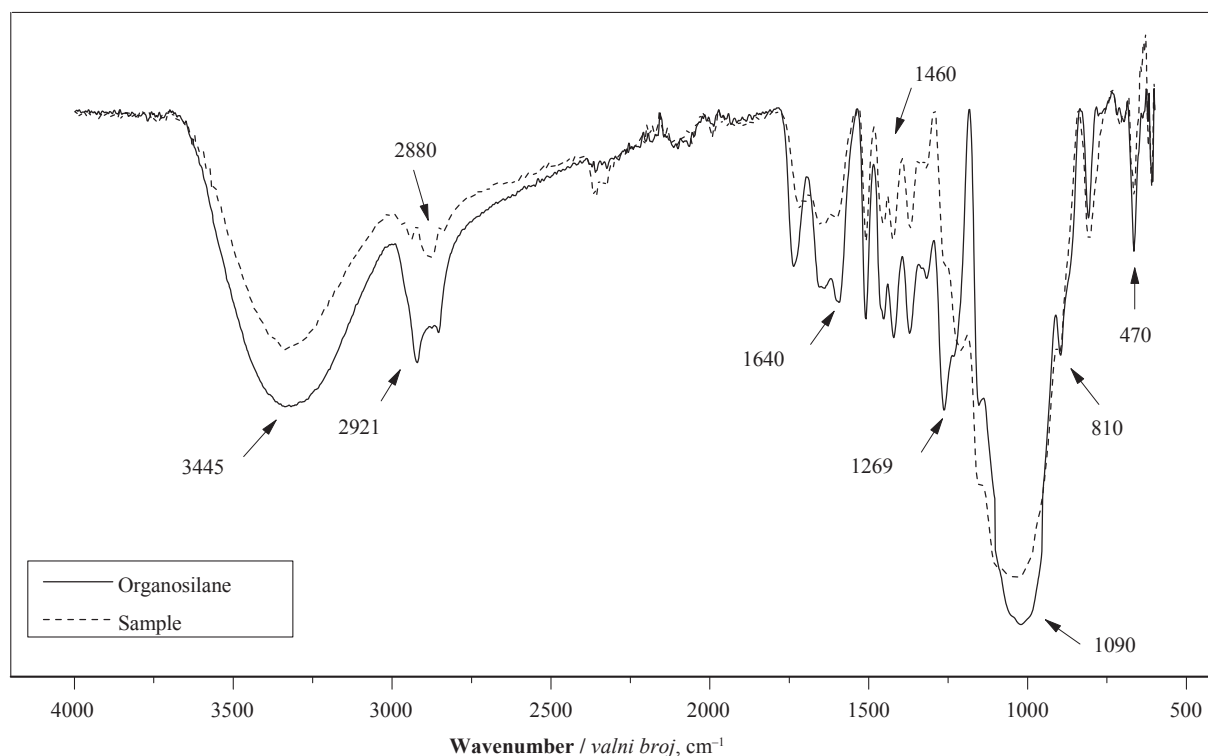
Figure 6 ATR-FTIR spectra for control and organosilane coated surfaces
Slika 6. ATR-FTIR spektar kontrolne površine i površine obrađene organosilanom

5 REFERENCES
5. LITERATURA

1. Bulcke, J.; Acker, J.; Saveyn, H.; Stevens, M., 2007: Modelling film formation and degradation of semi-transparent exterior wood coatings. Progress in Organic Coatings, 58: 1-12.
   https://doi.org/10.1007/s11998-007-9074-4.
2. Bulian, F.; Graystone, J., 2009: Wood Coatings Theory and Practice. Elsevier Science Ltd. 320.
3. Bulian, F.; Collavini, F.; Matellon, A., 2017: Investigating the effects of weathering on wood coatings. FME Transactions. 45, 405-411.
   https://doi:10.5937/fmet1703405B.
4. Busseya, D.; Perinab, V.; Jonesa, F.; Cechc, V., 2018: Effect of chemical modification on the mechanical properties of plasma-polymerized organosilicones. Progress in Organic Coatings, 119: 85-90.
   https://doi.org/10.1016/j.porgcoat.2018.02.020.
5. Chang, S. T.; Chou, P. L., 1999: Photodiscoloration of UV-curable acrylic coatings and the underlying wood. Polymer Degradation and Stability, 63: 435-444.
   https://doi.org/10.1016/S0141-3910(98)00124-4.
6. Clausen, C.; Green, F.; Kartal, S., 2010: Weatherability and Leach Resistance of Wood Impregnated with Nano-Zinc Oxide. Nanoscale Research Letters, 5: 1464-1467.
   https://doi.org/10.1007/s11671-010-9662-6.
7. Dasari, A.; Yu, Z.; Mai, Y., 2009: Fundamental aspects and recent progress on wear/scratch damage in polymer nanocomposites. Materials Science and Engineering: R: Reports, 63: 31-80.

   https://doi.org/10.1016/j.mser.2008.10.001.
8. Da Silva, M.; Santilli, C.; Pulcinelli, S., 2012: Wettability and photodegradation activity of sol-gel dip-coated zinc oxide films. Journal of Sol-Gel Science and Technology, 63: 230-234. https://doi.org/10.1007/s10971-012-2721-y.
9. Fengel, D.; Wegener, G., 1984: Wood: chemistry, ultrastructure, reactions. Berlin and New York, Walter de Gruyter, 613.
10. Gholamiyan, H.; Tarmian, A.; Doost Hosseini, K.; Azadfallah, M., 2012: Modification of moisture diffusion behavior of wood by clear coatings and nanoparticles. Maderas: Ciencia y Tecnología, 14: 43-52. https://doi.org/10.4067/S0718-221X2011000200004.
11. Gholamiyan, H.; Tarmian, A.; Ranjbar, Z.; Abdulkhani, A.; Azadfallah, M.; Mai, C., 2016: Silane nanofilm formation by sol-gel processes for promoting adhesion of waterborne and solvent-borne coatings to wood surface. Holzforschung, 70(5): 429-437. https://doi.org/10.1515/hf-2015-0072.
12. Godnjavec, J.; Znoj, B.; Vince, J.; Steinbucher, M.; Znidarsic, A.; Venturini, P., 2012: Stabilization of rutile TiO$_2$ nanoparticles with glymo in polyacrylic clear coating. Materials and Technology, 46 (1): 19-24.
13. International Organization for Standardization (ISO), 1997: Geometrical product specifications (GPS) – Surface texture: Terms definitions and surface texture parameters. Technical Report ISO 4287, International Organization for Standardization, Geneva.
14. Li, F.; Hu, K.; Li, J.; Zhao, B., 2001: The friction and wear characteristics of nanometer ZnO filled polytetrafluoroethylene. Wear, 249: 877-882.
   https://doi.org/10.1016/S0043-1648(01)00816-X.
15. Li, Q.; Chen, Y.; Zeng, D.; Gao, W.; Wu, Z., 2005: Photocatalytic characterization of silica coated titania nanoparticles with tunable coatings. Journal of Nanoparticle Research, 7: 295-299.
   https://doi.org/ 10.1007/s11051-004-5944-1.

16. Lung Chou, P.; Ting Chang, H.; Feng Yeh, T.; Tzen Chang, S. H., 2008: Characterizing the conservation effect of clear coatings on photodegradation of wood. Bioresource Technology, 99: 1073-1079. https://doi.org/ 10.1016/j.biortech.2007.02.027.

17. Mahltig, B.; Arnold, M.; Lothman, P., 2010: Surface properties of sol-gel treated thermally modified wood. Journal of Sol-Gel Science and Technology, 55: 221-227. https://doi.org/10.1007/s10971-010-2236-3.

18. Meincken, M.; Evans, P., 2009: Nanoscale characterization of wood photodegradation using atomic force microscopy. European Journal of Wood and Wood Products, 67: 229-231.
https://doi.org/10.1007/s00107-008-0305-x.

19. Mori, T.; Tanaka, K.; Inomata, T.; Takeda, A.; Kogoma, M., 1998: Development of silica coating methods for powdered pigments with atmospheric pressure glow plasma. Thin Solid Films, 316: 89-92.
https://doi.org/10.1016/S0040-6090(98)00395-2.

20. Nanetti, P., 2006: Coatings from A to Z. Vincentz Network, Germany, Hannover.

21. Pastore, T.; Santos, K.; Rubim, J. A., 2004: Spectro-colorimetric study on the effect of ultraviolet irradiation of four tropical hardwoods. Bioresource Technology, 93: 37-42. https://doi.org/10.1016/j.biortech.2003.10.035.

22. Nguyen-Tri, P.; Nguyen, T.; Carriere, P.; Ngo Xuan, C., 2018: Nanocomposite Coatings: Preparation, Characterization, Properties, and Application. International Journal of Corrosion, 2018: 1-19.
https://doi.org/10.1155/2018/4749501.

23. Powell, Q.; Fotou, G.; Kodas, T.; Anderson, B., 1997: Synthesis of alumina- and lumina/silica-coated Titania particles in an aerosol flow reactor. Chemistry of Materials, 9: 685-693. https://doi.org/10.1021/cm960334g.

24. Rao, A. V.; Gurav, A. B.; Latthe, S. S.; Vhatkar, R. S.; Kappenstein, C.; Wagh, P. B.; Gupta, S. C., 2010: Water repellent porous silica films by sol-gel dip-coating method. Journal of Colloid and Interface Science, 352: 30-35. https://doi.org/10.1016/j.jcis.2010.08.003.

25. Sigh, R.; Tomer, N.; Bhadraiah, S., 2001: Photo-oxidation studies on polyurethane coating: effect of additives on yellowing of polyurethane. Polymer Degradation and Stability, 73: 443-446.
https://doi.org/10.1016/S0141-3910(01)00127-6.

26. Taghiyari, H., 2013: Nano-zycosil in MDF: gas and liquid permeability. European Journal of Wood and Wood Products, 71: 353-360.
https://doi.org/ 10.1007/s00107-013-0691-6.

27. Tshabalala, M.; Gangstad, J., 2003: Accelerated Weathering of Wood Surfaces Coated with multifunctional Alkoxysilanes by Sol-Gel Deposition. Journal of Coatings Technology, 75: 37-43.
https://doi.org/ 10.1007/BF02730098.

28. Tsuchikawa, S.; Murata, A.; Kohara, M.; Itsui, K., 2003: Spectroscopic monitoring of biomass modification by light-irradiation and heat treatment. Journal of Near Infrared Spectroscopy, 11 (5): 401-405.
https://doi.org/10.1255/jnirs.391.

29. Veronovski, N.; Verhovsek, D.; Godnjavec, J., 2013: The influence of surface-treated nano-TiO2 (rutile) incorporation in water-based acrylic coatings on wood protection. Wood Science and Technology, 47: 317-328. https://doi.org/10.1007/s00226-012-0498-3.

30. Vlad Cristea, M.; Riedl, B.; Blanchet, P., 2011: Effect of addition of nanosized UV absorbers on the physico-mechanical and thermal properties of an exterior waterborne stain for wood. Progress in Organic Coatings, 72: 755-762. https://doi.org/10.1016/j.porgcoat.2011.08.007.

31. Wang, S.; Liu, C.; Liu, G.; Zhang, M.; Li, J.; Wang, C., 2011: Fabrication of superhydrophobic wood surface by a sol-gel process. Applied Surface Science, 258: 806-810. https://doi.org/10.1016/j.apsusc.2011.08.100.

32. Xu, B.; Cai, Z., 2008: Fabrication of a superhydrophobic ZnO nanorod array film on cotton fabrics via a wet chemical route and hydrophobic modification. Applied Surface Science, 254 (18): 5899-5904.
https://doi.org/10.1016/j.apsusc.2008.03.160.

Corresponding address:

Dr. HADI GHOLAMIYAN

Department of Wood and Paper Science & Technology
Faculty of Natural Resources
University of Tehran
4111 Karaj, IRAN
e-mail: Hadi_Gholamiyan@ut.ac.ir

Nadir Ayrilmis[1], Turgay Akbulut[1]

Screw Withdrawal Resistance and Surface Soundness of Three-Layer Fiberboard Having Coarse Fibers in Core Layer

Otpornost prema izvlačenju vijaka i međuslojna čvrstoća troslojne ploče vlaknatice s grubim vlaknima u središnjem sloju

ABSTRACT • *Screw withdrawal resistance (SWR) and surface soundness of three-layer MDF were investigated and the results were compared to the single-layer MDF. For this aim, effects of various formulation variables such as coarse fiber length (24.4 to 4.3 mm), resin content (10.5 to 6.5 wt%) in the core layer, average panel density (730 to 650 kg/m³), and surface/core layer ratio (70/30 to 30/70) were determined. The face and edge SWR and surface soundness of three-layer MDF panels were determined according to EN 320 and EN 311 standards, respectively. The results showed that the face SWR and edge SWR of MDF panels improved as the fiber length increased from 4.3 to 11.5 mm in the core layer. Similar results were determined for the surface soundness. The surface soundness of MDF panels improved with increasing fiber length in the core layer up to 17.8 mm. SWR and surface soundness improved with increasing resin content in the core layer, shelling ratio, and panel density.*

Keywords: *coarse fiber, resin, surface soundness, screw withdrawal resistance, three-layer fibreboard*

SAŽETAK • *U radu je prikazano istraživanje otpornosti prema izvlačenju vijaka i međuslojne čvrstoće troslojne MDF ploče, a rezultati su uspoređeni sa svojstvima jednoslojne MDF ploče. Za tu su svrhu istraživani učinci različitih parametara na pripremu ploče, primjerice duljina grubih vlakana (24,4 – 4,3 mm) i sadržaj smole (6,5 –10,5 %) u središnjem sloju, prosječna gustoća ploče (650 to 730 kg/m³) i omjer površinskoga i središnjeg sloja (70/30 – 30/70). Otpornost prema izvlačenju vijaka na licu i rubu ploče te međuslojna čvrstoća ispitivane su prema normama EN 320 i EN 311. Rezultati su pokazali da se otpornost prema izvlačenju vijaka na licu i rubu ploče povećala s povećanjem duljine vlakana u središnjem sloju s 4,3 na 11,5 mm. Slični su rezultati utvrđeni i za međuslojnu čvrstoću. Naime, međuslojna se čvrstoća MDF ploča također povećala s povećanjem duljine vlakana u središnjem sloju sve do 17,8 mm. Otpornost prema izvlačenju vijaka i međuslojna čvrstoća ploča povećale su se i s povećanjem udjela smole u središnjem sloju, omjera površinskoga i središnjeg sloja te gustoće ploče.*

Ključne riječi: *gruba vlakna, smola, međuslojna čvrstoća, otpornost prema izvlačenju vijaka, troslojna ploča vlaknatica*

---

[1] Authors are Professors at Department of Wood Mechanics and Technology, Forestry Faculty, Istanbul University-Cerrahpasa, Bahcekoy, 34473, Sariyer, Istanbul, Turkey.
[1] Autori su profesori Odsjeka za mehaniku drva i tehnologiju, Šumarski fakultet, Sveučilište u Istanbulu-*Cerrahpasa*, Istanbul, Turska.

1 INTRODUCTION
1. UVOD

Medium density fiberboard (MDF) is a wood-based panel made from fine wood fibers with resin under heat and pressure. It is one of the most commonly used wood-based panels in the furniture industry due to its favorable properties such as good mechanical properties and surface quality, and good machinability. In the traditional MDF production, surface and core layers are made from fine wood fibers. However, the core layer of the particleboard is mostly made from coarse wood particles, while the surface layers are made from fine wood particles. This technology can be applied to MDF production process. Due to a shortage in the supply of wood material and transportation costs, MDF manufacturers are forced to decrease panel density having acceptable technological properties.

Costs reduction in MDF production can be attained in two ways. The first possibility is the modernization and optimization of defibration process. The second one is the change of the structure of MDF boards (Danuta and Marcin, 2014). This study focused on the second way, i.e. the three-layer MDF production process. Three-layer wood-based panels having coarse fibers or particles in the core layer have some significant advantages as compared to single-layer panels such as lower resin consumption in the core layer and lower panel cost (Ayrilmis *et al*., 2017).

In this study, three-layer MDF panels were produced under laboratory conditions. Increasing fiber size in the core of MDF and optimizing the fiber size in the core could improve edge and surface SWR and surface soundness of MDF. The effects of various formulation variables such as coarse fiber length, resin content in the core layer, average panel density, and surface/core layer ratio on SWR and surface soundness of three-layer MDF panels were investigated.

2 MATERIALS AND METHODS
2. MATERIJALI I METODE

2.1 Wood fibers
2.1. Drvna vlakna

The pine (*Pinus sylvestris*) and beech (*Fagus orientalis* Lipsky) wood chips steamed in a digester at 170 °C and 8 bar for 4 min were converted to wood fibers using a thermo-mechanical refining process at Kastamonu Integrated Wood Company, Gebze, Turkey. The wet fibers in the plastic bags were transported to the Faculty of Forestry, Istanbul University-Cerrahpasa, where the boards were produced. The fibers were dried in a dryer until 2-3 % based on the oven-dry weight of wood fiber. Fine pine wood fibers were used in the face layers, while the coarse beech wood fibers were used in the core layer of MDF panels (Figure 1). The defibrator gap distance was adjusted to 0.4 mm for the surface layer fibers, while it was gradually increased to 1.2 mm for the core layer fibers. The length and thickness of 100 randomly selected fibers from core layer (five different sizes) and surface layers were measured using Brinell microscope 10X (Alfred J Amsler and Co).

2.2 Resin
2.2. Smola

A commercial liquid E1 grade urea-formaldehyde (UF) resin with 50 wt% solid content was supplied by Kastamonu Integrated Wood Company, Gebze, Turkey. The density, viscosity, and gel time of the UF resin were 1.208 g/cm^3, 26 cps, and 55 s, respectively. Ammonium chloride (NH_4Cl) solution with 20 wt% solid content was used as hardener for the UF resin.

2.3 Production of three-layer MDF panels
2.3. Proizvodnja troslojne MDF ploče

Three-layer MDF panels were produced under laboratory conditions (Figure 2). Different production parameters, effect of fiber size and resin content in the core layer, average panel density, and shelling ratio, were used in the production of three-layer MDF panels. (Table 1). The optimum fiber size in the core layer was determined based on the laboratory test results (panel types from A to E, Table 1). The size of surface fibers (pine fibers) was kept constant in all the panel types. As a hardener, 1 wt% ammonium chloride based on the solid content of the resin was added into the UF resin.

The surface and core layer fibers were separately glued with UF resin. First, the surface layer fibers were placed in a drum blender and then the UF resin based on the oven dry weight of the wood fiber was
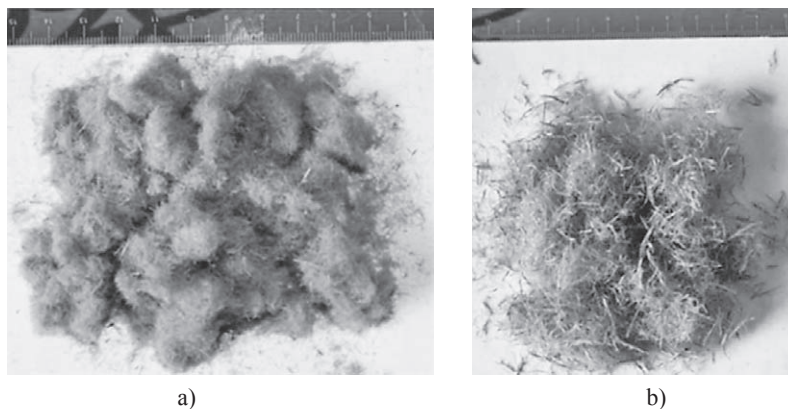

a)   b)

Figure 1 a) Fine wood fibers (pine) used in face layers of MDF; b) Coarse wood fibers (beech) used in core layer of MDF
Slika 1. a) Fina drvna vlakna (borovine) upotrijebljena u površinskom sloju MDF ploče; b) gruba drvna vlakna (bukovine) ugrađena u središnji sloj MDF ploče
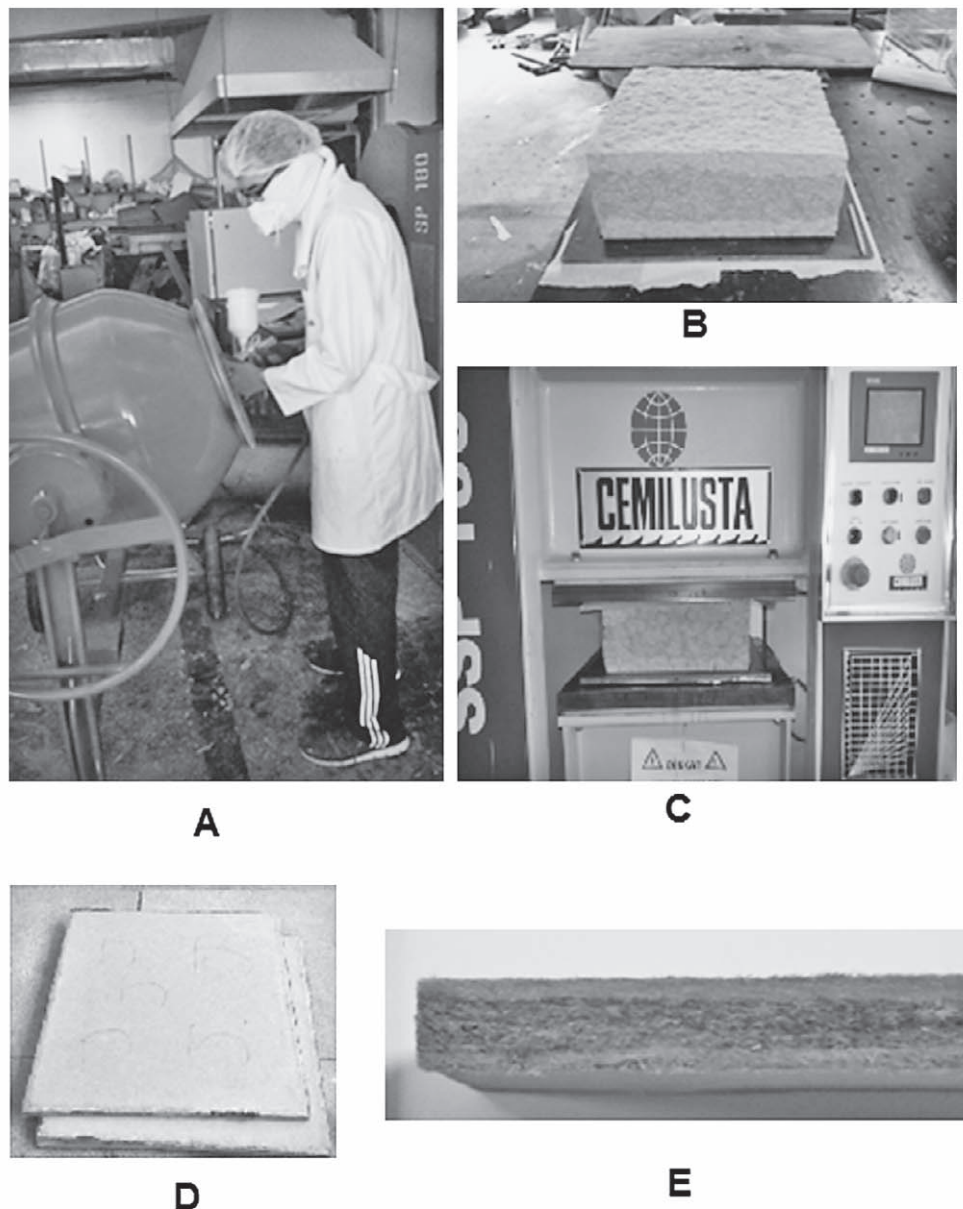
Figure 2 Process of production of three-layer MDF panels produced in laboratory, A – Resin application to wood fibers, B – Three layer-mat preparation, C – Hot pressing, D – Three-layer MDF panels, E – Cross section of three layer MDF panel
Slika 2. Postupak proizvodnje troslojne MDF ploče u laboratoriju: A – nanošenje smole na drvna vlakna, B – priprema slojeva, C – vruće prešanje, D – troslojna MDF ploča, E – presjek troslojne MDF ploče

applied with an air-atomized metered spray system for 5 min to obtain a homogenized mixture. This procedure was also applied to the core layer fibers. The surface and core fibers of three-layer boards were separately weighed and distributed evenly by hand into a 400 mm x 400 mm forming box. The mat was sandwiched between aluminum cauls with siliconized paper to prevent adherence between panel and caul. The mats were manually cold pressed and then transferred to the hot press operated in plate position control mode. Hot pressing temperature, maximum hot press pressure, and total press time for MDF panels having a density of 700 kg/m^3 were 190 °C, 3.5 N/mm^2, and 480 sec, respectively. The maximum hot press pressure was gradually decreased from 3.5 to 3.1 N/mm^2 to obtain 10 mm thick MDF panels having different densities (700 to 650 kg/m^3), while it was increased to 3.6 N/mm^2 to produce MDF panels having a density of 730 kg/m^3.

Three panels were prepared from each MDF type given in Table 1. The test specimens were conditioned in a climatic chamber at 20 °C and 65 % relative humidity until the specimens reached constant weight. The experimental design is presented in Table 1.

Table 1 Experimental design
Tablica 1. Plan istraživanja

Production parameters *Parametri proizvodnje*	Face layers ratio, wt% *Udio površinskih slojeva*, wt%		Core layer ratio, wt% *Udio središnjeg sloja*, wt%	Core layer / *Središnji sloj*		Target density of MDF, kg/m³ *Ciljana gustoća MDF ploče*, kg/m³	Resin content in core layer, wt% *Sadržaj smole u središnjem sloju*, wt%
				Coarse fiber length in core layer, mm *Duljina grubih vlakana u središnjem sloju,* mm	Coarse fiber thickness in core layer, mm *Debljina grubih vlakana u središnjem sloju,* mm		
Effect of fiber size in core layer of MDF *utjecaj veličine vlakana u središnjem sloju MDF ploče*	A	50	50	4.3 (0.5)	0.51 (0.03)	700	10.5
	B	50	50	7.9 (0.8)	0.65 (0.04)	700	10.5
	C	50	50	11.5 (0.8)	0.73 (0.04)	700	10.5
	D	50	50	17.8 (0.6)	0.79 (0.03)	700	10.5
	E	50	50	24.4 (1.1)	0.94 (0.05)	700	10.5
Effect of resin content in core layer of MDF *utjecaj sadržaja smole u središnjem sloju MDF ploče*	F	50	50	11.5 (0.8)	0.73 (0.04)	700	10.5
	G	50	50	11.5 (0.8)	0.73 (0.04)	700	9.5
	H	50	50	11.5 (0.8)	0.73 (0.04)	700	8.5
	I	50	50	11.5 (0.8)	0.73 (0.04)	700	7.5
	J	50	50	11.5 (0.8)	0.73 (0.04)	700	6.5
Effect of surface/core layer ratio *utjecaj omjera površinskoga i središnjeg sloja*	K	70	30	11.5 (0.8)	0.73 (0.04)	700	10.5
	L	60	40	11.5 (0.8)	0.73 (0.04)	700	10.5
	M	50	50	11.5 (0.8)	0.73 (0.04)	700	10.5
	N	40	60	11.5 (0.8)	0.73 (0.04)	700	10.5
	O	30	70	11.5 (0.8)	0.73 (0.04)	700	10.5
Effect of average panel density *utjecaj prosječne gustoće ploče*	P	50	50	11.5 (0.8)	0.73 (0.04)	725	10.5
	R	50	50	11.5 (0.8)	0.73 (0.04)	700	10.5
	S	50	50	11.5 (0.8)	0.73 (0.04)	675	10.5
	T	50	50	11.5 (0.8)	0.73 (0.04)	650	10.5

Note: The average length and thickness of the fibers used in the face layers of MDF were 4.3 mm and 0.51 mm, respectively.
Napomena: Prosječna duljina i debljina vlakana upotrijebljenih u slojevima lica MDF ploče iznosile su 4,3 mm i 0,51 mm.

2.4 Determination of screw withdrawal resistance and surface soundness of MDF
2.4. Određivanje otpornosti prema izvlačenju vijaka i međuslojne čvrstoće MDF ploče

The surface and edge SWR of MDF specimens with dimensions of 50 mm x 50 mm x 10 mm were determined according to EN 320 standard. Predrilling was applied to the face and edges of MDF specimens before inserting screws into MDF. 10 specimens for the surface SWR and 10 specimens for the edge SWR were used in the experiments. The densities of 15 MDF specimens with dimensions of 50 mm x 50 mm x 10 mm were measured according to EN 323. The surface soundness test of 10 specimens with dimensions of 50 mm x 50 mm x 10 mm was carried out according to EN 311.

2.5 Statistical analysis
2.5. Statistička analiza

The results were statistically analyzed by analysis of variance ($p < 0.05$) to evaluate the effects of material formulation on SWR and surface soundness of MDF specimens. Significant differences among the mean values of MDF types were determined using Duncan's multiple range test.

3 RESULTS AND DISCUSSION
3. REZULTATI I RASPRAVA

The surface and edge SWR results of MDF specimens depending on the material formulation are given in

Figure 3. As the wood fiber size in the core layer increased from 4.3 to 11.5 mm, the surface SWR increased from 652 to 719 N. As for the edge SWR, it increased from 490 to 575 N as the fiber length increased from 4.3 to 17.8 mm in the core layer. However, further increment in the fiber length decreased the surface and edge SWR of MDF specimens. A similar result was observed for the particleboards (García-Ortuño *et al*., 2011). They reported that SWR improved with increasing particles size up to a certain point. The surface and edge SWR of single-layer MDF (panel type A), having the same fiber size in the core and surface layers, were found to be 652 N and 490 N, respectively. The results showed that the face and edge SWR of three-layer MDF were better than single-layer MDF (Figure 3). The surface and edge SWR of three-layer MDF types C, D, and E showed significant difference ($p < 0.05$) with MDF type A (single-layer), while MDF type B did not show such a significant difference. The higher SWR of three-layer MDF panels having coarse fibers in the core layer as compared with single-layer MDF could be due to the ability of the coarse fibers to conform around the thread of the screw, allowing continuous load transfer along the thread.

The increases in the resin content and panel density improve bond performance between the fibers in the core layer of particleboards (Post, 1961; Warmbier *et al*., 2013; Benthien and Ohlmeyer, 2017) and MDF (Wold, 2010; Danuta and Marcin, 2014), thus improving SWR of MDF. There was no significant difference in SWR as the resin content decreased from 10.5 to 9.5 wt%. How-

ever, further decrement in the core layer significantly decreased SWR. As the panel density decreased from 730 to 650 kg/m³, the surface SWR of MDF panels decreased from 755 to 659 N. SWR improved with increasing surface layer ratio from 30 to 70 wt%. The surface of the fibers is well covered by the resin as the amount of the resin in the core layer is increased. In addition, the resin fills the micro voids in the core layer, which improves SWR. The weakness of the core layer of wood-based panels, such as MDF and particleboard, is mainly responsible for lower edge SWR due to its higher porosity than that of face layers. The edge and surface SWR of MDF panels were positively affected by the shelling ratio. Similar results were observed in previous studies (Akbulut, 1998; Istek *et al.*, 2017). The surface SWR increased from 675 to 791 N as the surface layer ratio increased from 30 to 70 wt%. A similar result was observed for the edge SWR, which increased from 515 to 584 N. There was no significant difference in SWR values between 30 wt% and 40 wt% surface layer ratios.

The results of surface soundness of MDF panels showed a similar trend to the results of SWR (Figure 4). The surface soundness of MDF specimens improved with increasing fiber size in the core layer. As the fiber length increased from 4.3 to 17.8 mm, the surface sound-

ness increased from 1.08 to 1.33 N/mm². However, further increment in the fiber size decreased the surface soundness. MDF type A showed no significant difference with MDF type B, but other panel types from C to E showed significant difference with the panel type A. The surface soundness of MDF specimens increased with increasing coarse fiber length (up to 17.8 mm) (Figure 4). The specific surface area of longer particles is lower than that of shorter particles of the same species at the same MDF density. More resin was required to sufficiently bond the fibers as the fiber size was decreased. Thus, the resin content per unit particle surface area is higher for long particles than for short ones at a given resin content, which improves the bond performance between the fibers (Benthien *et al.*, 2014).

The increase in the resin content in the core layer improved the surface soundness of MDF specimens. This was expected because the resin improved the bond strength between the surface layer (fine fibers) and core layer (coarse fibers). There was no significant difference in the surface soundness values of MDF specimens as the resin content decreased from 10.5 to 8.5 wt% in the core layer, this being resin saving that could be obtained. However, further decrement in the resin content significantly decreased the surface soundness. The contact area
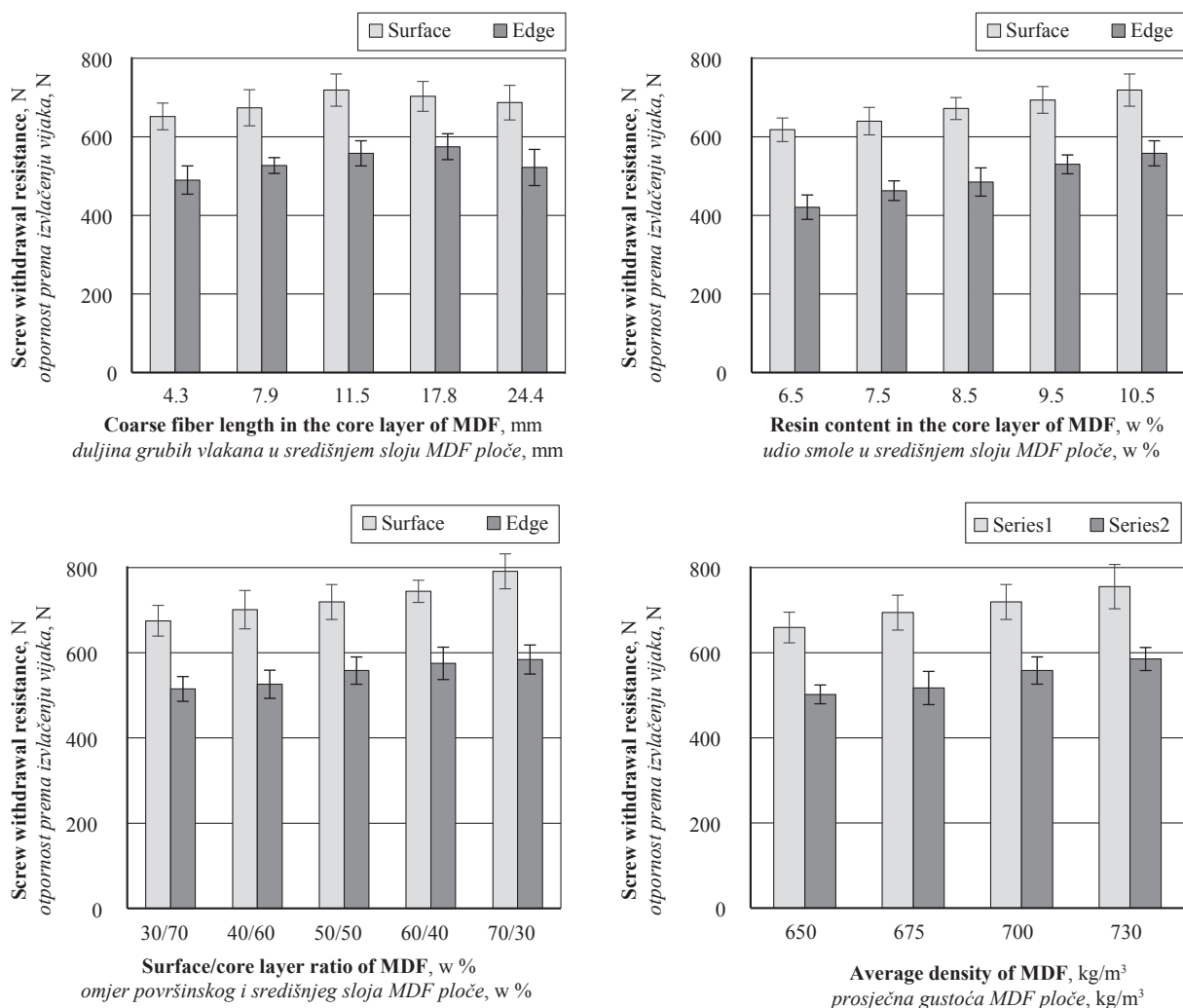

Figure 3 Screw withdrawal resistance of three-layer MDF depending on manufacturing conditions
Slika 3. Otpornost troslojne MDF ploče prema izvlačenju vijaka u ovisnosti o uvjetima proizvodnje
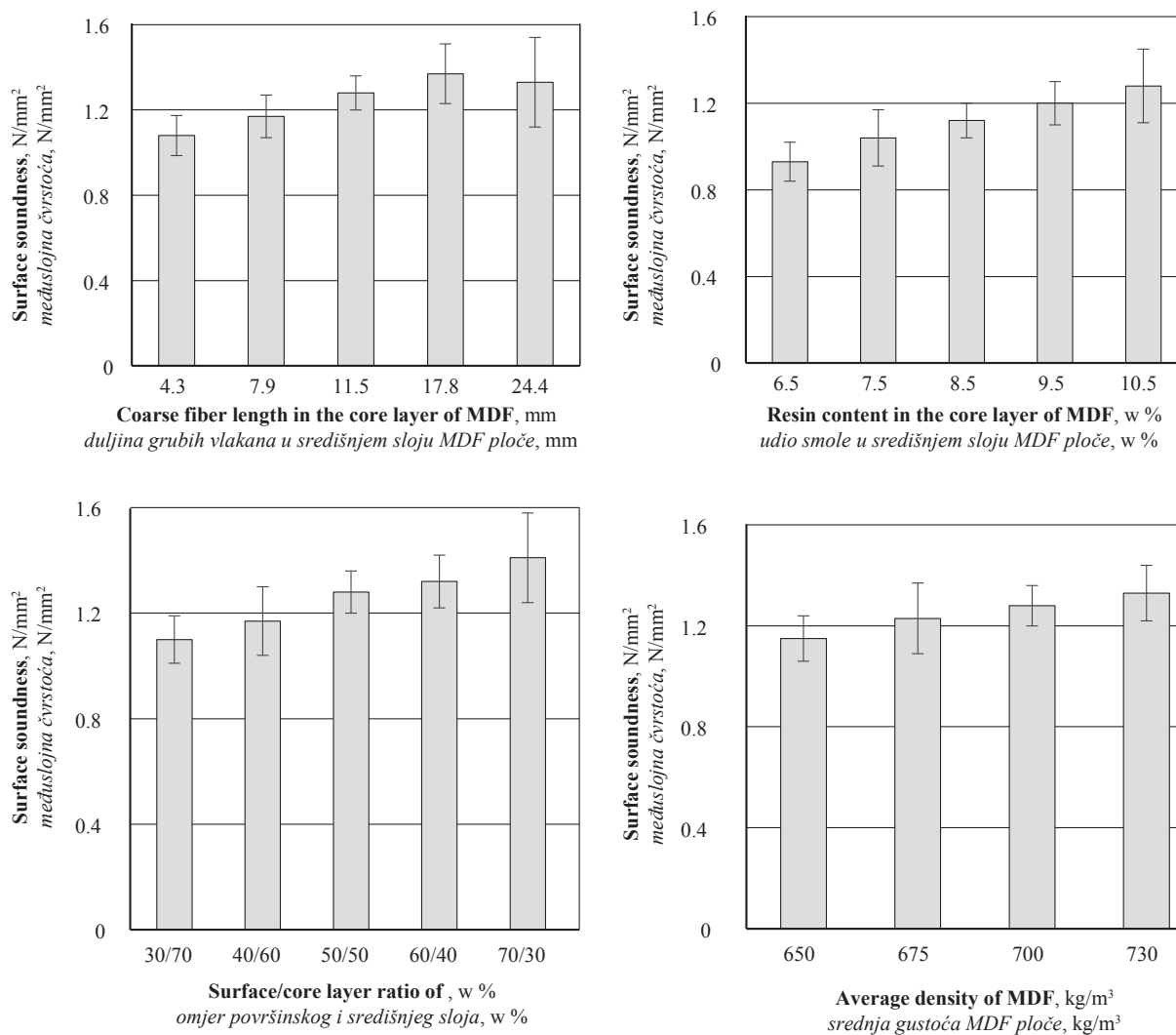
Figure 4 Surface soundness of three-layer MDF depending on manufacturing conditions
Slika 4. Međuslojna čvrstoća troslojne MDF ploče u ovisnosti o uvjetima proizvodnje

between the wood fibers increases with increasing density of MDF. This improves the bond performance of the connection area of the resin as compared to MDF having lower density, which increases the surface soundness and SWR. As the panel density is increased, stronger connections are produced due to the higher contact area between the fibers and their higher overlap (Suchsland and Woodson, 1986). Similar results were observed in previous studies (Hong *et al*., 2017).

The increase in the surface layer ratio from 30 to 70 wt% improved the surface soundness of MDF panels (1.10 to 1.41 N/mm²). Panel type N showed no significant differences with panel types O and P, but it showed significant differences with panel types R and S. As the amount of the surface layer made from fine fibers was increased, more compact structure was obtained. This may improve the delamination strength between surface and core layers.

4 CONCLUSIONS
4. ZAKLJUČAK

SWR and surface soundness of three-layer MDF was found better than single-layer MDF as the surface layers of the panels were made from softwood fine fibers

and the core layer was made from hardwood coarse fibers. The surface SWR increased as the fiber length increased from 4.3 to 11.5 mm and the edge SWR increased as the fiber length increased from 4.3 to 17.8 mm. The surface soundness of the wood fibers improved as the fiber length in the core layer was increased by 17.8 mm. There was no significant difference in SWR of MDF as the resin content decreased from 10.5 to 8.5 wt% in the core layer. SWR and surface soundness improved with increased shelling ratio and average panel density. The resin consumption in the three-layer MDF production can be reduced by 15% compared with the single-layer MDF. This was because the coarse fibers in the core layer decreased the resin consumption due to decreased surface area as compared to the fine fibers in the single layer MDF. Energy consumption and resin savings are important factors influencing MDF price. The decreases in the resin content and panel density can be significant advantages of three-layer MDF as compared to the single-layer MDF, resulting in a decrease in the production cost of MDF.

5 REFERENCES
5. LITERATURA

1. Akbulut, T., 1998: The effect of various manufacturing variables on technological properties of particleboard. Journal of Istanbul University Forest Faculty, 48: 91-116.

2. Ayrilmis, N.; Akbulut, T.; Yurttas, E., 2017: Effects of core layer fiber size and face-to-core layer ratio on the properties of three-layer fiberboard. BioResources, 12: 7964-7974. https://doi.org/10.15376/biores.12.4.7964-7974.

3. Benthien, J. T.; Ohlmeyer, M., 2017: Influence of face-to-core layer ratio and core layer resin content on the properties of density-decreased particleboards. European Journal of Wood and Wood Products, 75: 55-62. https://doi.org/10.1007/s00107-016-1059-5.

4. Danuta, N.; Marcin, K., 2014: Possibility of the production of three-layer MDF. Annals of Warsaw University of Life Sciences – SGGW Forestry and Wood Technology, 88: 162-169.

5. García-Ortuño, T.; Andréu-Rodríguez, J.; Ferrández-García, M. T.; Ferrández-Villena, M.; Ferrández-García, C. E., 2011: Evaluation of the physical and mechanical properties of particleboard made from giant reed (*Arundo donax* L.). BioResources, 6: 477-486.

6. Hong, M. K.; Lubis, M. A. R.; Park, B. D., 2017: Effect of panel density and resin content on properties of medium density fiberboard. Journal of Korean Wood Science and Technology, 45: 444-455. https://doi.org/10.5658/wood.2017.45.4.444.

7. Istek, A.; Kursun, C.; Aydemir, D.; Koksal, S. E.; Kelleci, O., 2017: The effect of particle ratios of surface layers on particleboard properties. Journal of Bartin University Foresty Faculty, 19: 182-186.

8. Post, P. W., 1961: Relationship of flake size and resin content to mechanical and dimensional properties of flake board. Forest Products Journal, 11 (9): 34-37.

9. Suchsland, O.; Woodson, G. E., 1987: Fiberboard Manufacturing Practices in the United States. U.S. Department of Agriculture, Forest Service, Madison WI, USA.

10. Warmbier, K.; Wilczyński, A.; Danecki, L., 2013: Effects of density and resin content on mechanical properties of particleboards with the core layer made from willow Salix viminalis. Annals of Warsaw University of Life Sciences – SGGW Forestry and Wood Technology, 84: 284-287.

11. Wold, D., 2010: The EVO 56 Defibrator system – the obvious choice at Medite; Metso Results Pulp & Paper 3/2010: 26-27 (www.metso.com/pulpandpaper).

12. *** 2012: EN 311. Wood-based panels. Surface soundness. Test method. European Committee for Standardization, Brussels, Belgium.

13. *** 2011: EN 320. Particleboards and fibreboards. Determination of resistance to axial withdrawal of screws. European Committee for Standardization, Brussels, Belgium.

14. *** 1993: EN 323. Determination of density. European Committee for Standardization, Brussels, Belgium.

Corresponding address:

Prof. dr. NADIR AYRILMIS, Ph.D.

Department of Wood Mechanics and Technology
Forestry Faculty, Istanbul University-Cerrahpasa.
Bahcekoy, Sariyer
34473, Istanbul, TURKEY
e-mail: nadiray@istanbul.edu.tr

Pavlo Bekhta[1], Tomasz Krystofiak[2], Stanislaw Proszyk[2], Barbara Lis[2]

Evaluation of Dynamic Contact Angle of Loose and Tight Sides of Thermally Compressed Birch Veneer

Procjena dinamičkoga dodirnog kuta površine toplinski komprimiranoga bukova furnira

ABSTRACT • *Rotary-cut veneer is characterised by two sides, namely loose and tight surface, which have different properties. The information concerning dynamic contact angle behaviour of veneer sides plays an important role in efficient use of veneer. Therefore, the objective of this study was to investigate the influence of different compression temperatures and pressures on various wetting behaviour of loose and tight sides of birch veneer. Veneer sheets were compressed in a hot press at temperatures of 150 and 180 °C using seven pressure levels from 0.5 to 3.5 MPa. Wettability of loose and tight sides of thermally compressed veneer was evaluated by measuring the dynamic contact angle with distilled water. The results showed that thermal compression decreased the surface wettability of both loose and tight sides of the samples, especially for veneer samples compressed at a temperature of 180 °C. Tight side of the samples had lower wettability than loose side, even after thermal compression. Therefore, adhesive or any kind of finishing can be applied to both sides of thermally compressed veneer sheets without having any adverse influence on not only the bonding quality but also the whole finishing process.*

Keywords: birch veneer, thermal compression, loose and tight sides, wettability, dynamic contact angle

SAŽETAK • *Za ljuštene je furnire karakteristično da njihove dvije površine, tzv. otvorena i zatvorena strana, imaju različita svojstva. Za učinkovitu uporabu furnira važni su podaci o ponašanju dinamičkoga dodirnog kuta površina furnira. Stoga je cilj istraživanja bio ispitati utjecaj različitih temperatura i tlakova kompresije na ponašanje površina furnira pri kvašenju. Listovi furnira komprimirani su u vrućoj preši pri temperaturi 150 i 180 °C te uz primjenu sedam različitih tlakova, od 0,5 do 3,5 MPa. Ispitana je sposobnost kvašenja površine na obje strane toplinski komprimiranog furnira mjerenjem dinamičkoga dodirnog kuta primjenom destilirane vode. Rezultati su pokazali da toplinsko komprimiranje smanjuje površinsko kvašenje na obje strane furnira, posebice na uzorcima furnira koji su komprimirani pri temperaturi 180 °C. Zatvorena strana uzoraka furnira pokazala je manju sposobnost kvašenja nego otvorena, čak i nakon toplinske kompresije. Stoga se ljepilo ili neko drugo sredstvo za završnu obradu furnira može nanositi na obje strane toplinski komprimiranog furnira bez ikakve opasnosti od nepovoljnog utjecaja na kvalitetu lijepljenja i završnu obradu furnira.*

Ključne riječi: bukov furnir, toplinska kompresija, otvorena i zatvorena strana furnira, sposobnost kvašenja, dinamički dodirni kut

---

[1] Author is professor at Department of Wood-Based Composites, Cellulose and Paper, Ukrainian National Forestry University, Lviv, Ukraine. [2]Authors are associate professor, professor and associate professor at Department of Wood Based Materials, Poznan University of Life Sciences, Poznan, Poland

[1] Autor je profesor Odsjeka za kompozite na bazi drva, celulozu i papir, Ukrajinsko nacionalno šumarsko sveučilište, Lavov, Ukrajina. [2]Autori su izvanredni profesor, profesor i izvanredni profesor Odsjeka za materijale na bazi drva, Poznanjsko sveučilište bioloških znanosti, Poznanj, Poljska.

1 INTRODUCTION
1. UVOD

In general, the thermal compression process is used to improve the properties of wood and wood-based materials to facilitate their versatile applications. For example, densified wood veneers may potentially be used in various products in wooden building, furniture, flooring, and numerous other applications (Candan *et al.*, 2010; Diouf *et al.,* 2011). In addition to the advantageous effect on properties such as strength, surface hardness and durability (Kutnar *et al.,* 2008; Büyüksari *et al.,* 2012; Büyüksari, 2013; Rautkari *et al.,* 2013), surface quality of their aesthetic-decorative features could also be improved. The colour of wood becomes more attractive (Diouf *et al.,* 2011), surface roughness decreases (Candan *et al.,* 2010; Arruda and Del Menezzi, 2013; Bekhta *et al.,* 2014), and the surface becomes glossier and smoother, while minimising the need for sanding. Despite the fact that thermal compression is an environmentally friendly process, after this treatment, the surface of the member becomes hydrophobic, which could result in serious problems during gluing or finishing.

Surface qualities of veneer are decisive to surface wettability and bonding quality between veneer sheets. Wood wettability is an important parameter that provides information on physical and chemical affinity between wood surface and adhesives/coatings (Gray, 1962; Elbez, 1978; Gindl *et al.,* 2004), while it also has a great influence on bonding strength and mechanical properties of veneer-based products. Clearly, wetting of wood surfaces is a complex process influenced by many factors (Piao *et al.,* 2010; Bekhta and Krystofiak, 2016).

Although many studies have been conducted on the evaluation of wettability of solid wood, fewer studies have been performed on wood veneer. As well known, rotary-cut veneer sheets are characterised by the presence of small lathe checks on the loose side of the veneer, while there are no checks on the reverse tight side of the sheet (Kollmann *et al.*, 1975). Since properties including morphology, porosity, roughness, density, hardness, and moisture content of these veneer sides show variation, they will behave differently due to the absorbtion of adhesive or finishing products. The depth of penetration and the area of adhesive spreading will vary between rough and smooth veneer. This leads to an uneven thickness of the adhesive layer, resulting in increased concentration of stresses in the adhesive layer, and consequently adversely influencing overall bonding quality. Hse (1972) concluded that surface roughness and possibly surface chemical properties of the tight side differed from those of the loose side and that these differences may affect the contact angle. Moreover, in most of the previous studies on wood wettability, instantaneous or equilibrium contact angles were used (Liptakova and Kudela, 1994; Scheikl and Dunky, 1998; Kutnar *et al.,* 2012), neglecting adhesive penetration and the spreading process. However, studying the wetting process may be more meaningful than evaluating only the initial equilibrium contact angle on the surface of the sample (Liptakova and Kudela, 1994).

Currently, despite some studies related to surface roughness (Fang *et al.*, 2012), aesthetic features and wettability (Arruda and Del Menezzi, 2013; Diouf *et al.,* 2011; Bekhta *et al.,* 2015; Bekhta and Krystofiak, 2016) of compressed veneer, there is still insufficient information on surface characteristics, especially dynamic contact angle, wettability processes of different veneer sides under the process of thermal compression, which directly influence the bonding quality of veneer-based composites. Veneer may be used not only in the production of plywood or LVL, but also for veneering of particleboards and MDF in the furniture industry. It is essential to gain specific data on surface characteristics of thermally compressed birch veneer, including its wettability, to optimise gluing or coating processes. Therefore, the objective of this study was to investigate the effect of thermal compression treatment at various temperatures and pressures and the treated veneer side (loose and tight) on dynamic contact angle of birch veneer to provide guidelines for an appropriate application of compressed veneer in veneer-based composites.

2 MATERIALS AND METHODS
2. MATERIJALI I METODE

2.1 Wood veneer samples
2.1. Uzorci furnira

Birch is one of the most commonly used raw materials for plywood production in Ukraine. Therefore, rotary-peeled birch (*Betula verrucosa* Ehrh.) wood veneer with the nominal thickness of 1.5 mm and moisture content of 5 % were used in this study. Defect free tangential sheets of veneer were cut in 300 mm by 300 mm pieces for thermo-mechanical densification and subsequent measurements.

2.2 Short-term thermo-mechanical compression
2.2. Kratkoročna toplinsko-mehanička kompresija

Veneer sheets were compressed using an automatically controlled single-opening hot press. To avoid surface contamination during compression, veneer samples were placed between smooth and cleaned thin stainless steel press caul. Then, the veneer samples held between steel sheets were placed between heated press plates and when the pressure reached 0.5, 1.0, 1.5, 2.0, 2.5, 3.0 or 3.5 MPa, it was held under compression perpendicular to the grain (thickness direction) at the temperatures of 150 or 180 °C for 1 min. After this period, the press was opened, the densified veneer was removed from the press and allowed to cool at room temperature. The weight and dimensions of the samples were measured before and after compression. Afterwards, each veneer sheet was cut to strips of 100 mm in length and 15 mm in width for dynamic contact angle measurements. Ten replications for each variant of short-term thermo-mechanical compression were prepared.

2.3 Dynamic contact angle measurements
2.3. Mjerenje dinamičkoga dodirnog kuta

Droplets having distilled water volume *V*=3.5 µL, were placed on the loose and tight side of birch veneer using the sessile drop method and were determined using a PG-3 goniometer. The measurements were conducted at a temperature of 20±1 °C and relative humidity of 65±2 %. Fifteen images per second of the liquid drop shape on the veneer surface along the grain were captured by a camera. The contact angles were measured directly from the images using an integrated imaging software package. Twenty contact angle measurements were taken per droplet for each birch veneer sample.

2.4 Analysis of variance (ANOVA)
2.4. Analiza varijance (ANOVA)

Analysis of variance (ANOVA) at a 0.05 significance level was carried out using IBM SPSS Statistics software to estimate the relative importance of the effects of the experimental variables, such as compression temperature and pressure, on the dynamic contact angle of veneer. Duncan's multiple range tests were also conducted for multiple comparisons between the means of the measured properties for different sides of veneer and various compression temperature and pressure. ANOVA analysis and Duncan test were carried out at 60 s deposition because water droplets fully penetrate across the surface of veneer on the loose side after 60 s deposition for certain thermal compression conditions.

3 RESULTS AND DISCUSSION
3. REZULTATI I RASPRAVA

The behaviour of the contact angle in both loose and tight sides as function of time of non-densified and densified veneer for different thermal compressions is shown in Figs.1 and 2. As can be seen in these figures, the contact angle decreased as a function of wetting time. Spreading is the dominant process on the tight side for non-densified veneer, while penetration is the dominant process on the loose side of veneer (Fig. 1). After about 60 seconds, a drop of water completely penetrates into the wood surface on the loose side. As can be seen in Fig. 1, there is a distinct and substantial difference between the loose and tight sides of non-densified veneer. Therefore, in practice, this is usually taken into account and adhesive is applied on the loose side of veneer and its loose side is turned in the middle position in the process of forming a veneer package.

Similar behaviour of a drop of water on the surface of wood is observed for densified veneer (Fig. 2). However, the time required to penetrate the drop into the wood surface on the loose side of veneer increases to 60-80 seconds. In addition, under certain compression pressures, the drop of water on the loose side spreads without penetration into the wood, similar to the tight side of the samples, especially those compressed at the temperature of 180 °C. However, no clear dependence on the behaviour of a drop of water on the surface of wood, depending on the compression pressure, was established. Probably, this is because it is very difficult to pick up veneer sheets that would have identical properties such as morphology, porosity, roughness, density, hardness, and moisture content.

The difference between the contact angles on the loose and tight side was significant for non-densified veneer (Table 1). As can be seen in Fig. 1, contact angle decreased more rapidly on the loose side than on the tight side. This difference is largely due to the deeper lathe checks on the loose side of veneer. As a result, water will easily penetrate the wood surface on the loose side, increasing wettability. Therefore, the loose
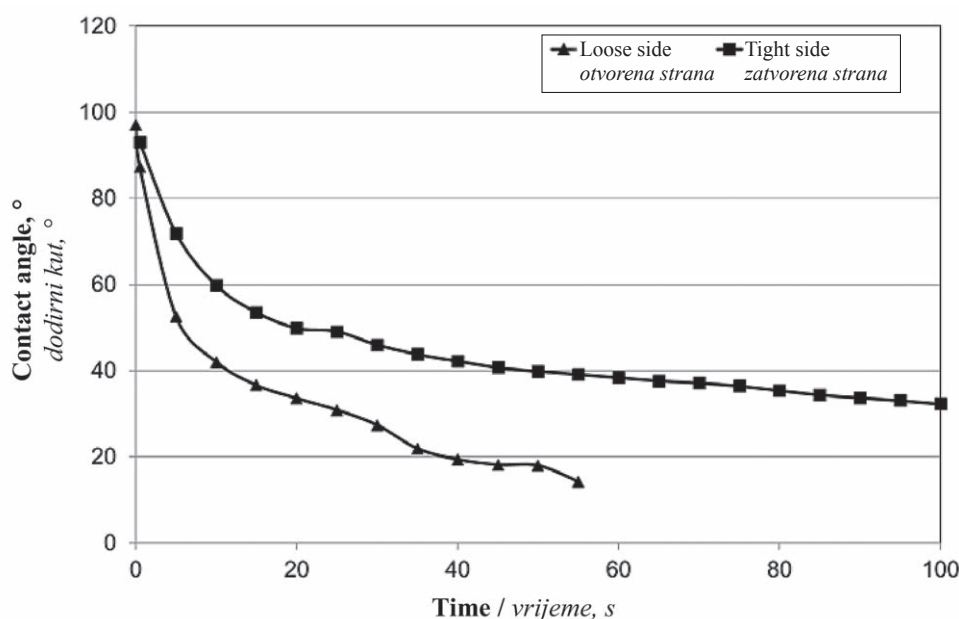

Figure 1 Changes in dynamic contact angle of distilled water as a function of time on non-densified veneer surfaces
Slika 1. Promjene dinamičkoga dodirnog kuta destilirane vode kao funkcija vremena na nekomprimiranim površinama furnira
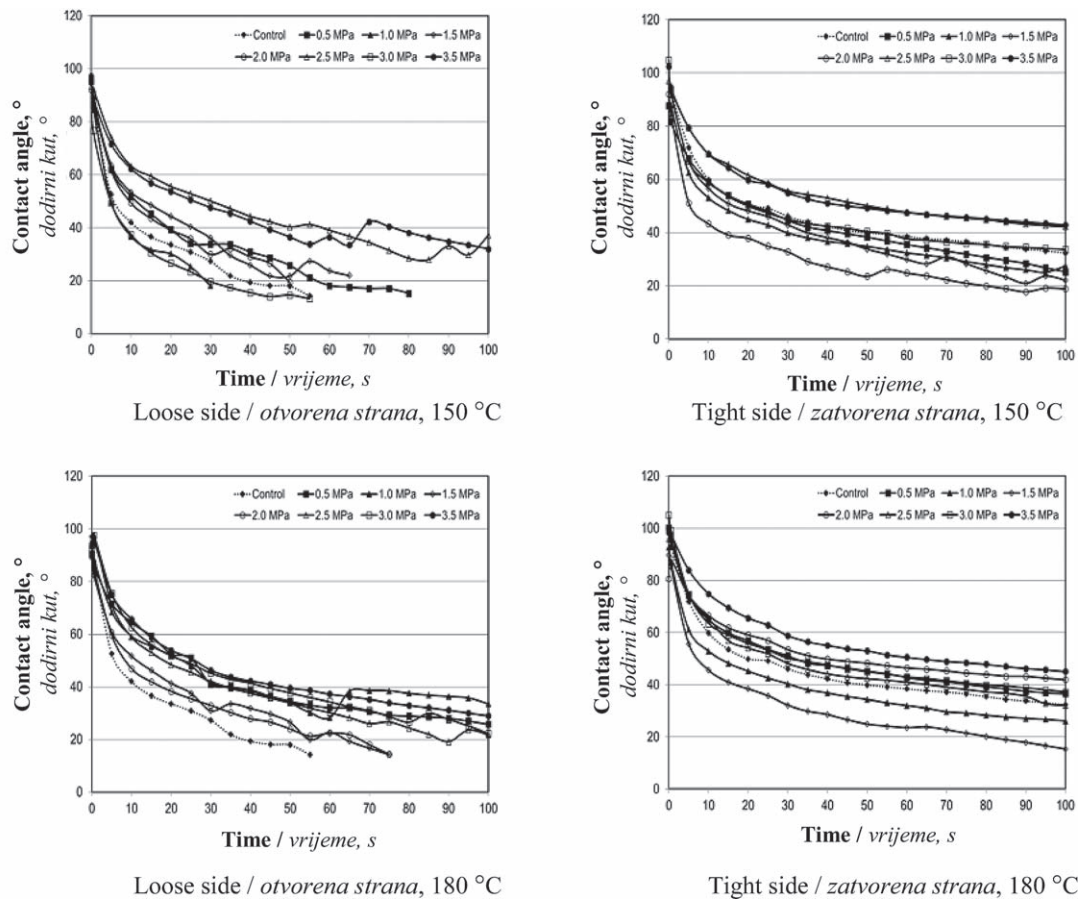
Figure 2 Changes in dynamic contact angle of distilled water as a function of time on densified surfaces of birch veneer at various compression temperature and pressure values
Slika 2. Promjene dinamičkoga dodirnog kuta destilirane vode kao funkcija vremena na površinama bukova furnira komprimiranoga pri različitim temperaturama i tlakovima

Table 1 Duncan's test results for main effects
Tablica 1. Rezultati Duncanova testa za glavne utjecajne činitelje

Variable / *Varijable*	Contact angle (degrees) / *Dodirni kut (u stupnjevima)*			
	Loose side / *Otvorena strana*		Tight side / *Zatvorena strana*	
	Mean	SG	Mean	SG
Temperature / *temperatura*, °C				
non-densified (control) / *nekomprimirani kontrolni uzorak*	39.56	aA	57.28	abB
150	47.61	bA	55.91	aB
180	54.51	cA	59.08	bB
Pressure / *tlak*, MPa				
non-densified (control) / *nekomprimirani kontrolni uzorak*	39.56	aA	57.28	cB
0.5	52.49	cA	58.80	cB
1.0	46.97	bA	50.60	abA
1.5	48.34	bA	48.77	aA
2.0	45.37	bA	52.85	abB
2.5	58.11	dA	63.69	dB
3.0	46.63	bA	59.08	cB
3.5	59.48	dA	68.63	eB

Different letters denote a significant difference. The means followed by the same letter do not statistically differ from each other ($p \leq 0.05$). Lower case letters regard the analysis between temperatures and pressures within each loose and tight side and capital letters regard the analysis (*t*-test) between the loose and tight sides within each temperature and pressure. SG: statistical group.
Različita slova označavaju značajnu razliku. Srednje vrijednosti obilježene istim slovom međusobno se statistički ne razlikuju ($p \leq 0,05$). Mala slova znače da je uzeta u obzir analiza između vrijednosti dobivenih na svakoj strani furnira pri različitim temperaturama i tlaku a velika znače da je uzeta u obzir analiza (t-test) između srednjih vrijednosti za različite strane furnira pri svakoj temperaturi i tlaku kompresije; SG – statistička skupina.

side of non-densified veneer surface is more wettable. Shupe *et al.* (1998) found that loose-side values were much smaller than tight-side values for both earlywood and latewood. Vazquez *et al.* (2003) also showed that the presence of lathe checks on the loose sides favours wettability, with the contact angle decreasing more rapidly on these sides than on tight sides.

According to Fig. 2, the contact angle of birch veneer changed after the thermal compression process. The statistical analysis identified that significant changes (p<0.05) occurred at various compression temperatures and pressures on both loose and tight sides. It was found that, with an increase of compression temperature and pressure, the contact angle increased on the loose and tight sides of veneer compared to the loose and tight sides of non-densified veneer. For example, the compression at 150 °C caused an average increase of 16.9 % and compression at 180 °C caused an average increase of 27.4 % in the contact angle of
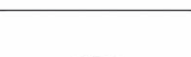
the loose side, respectively. However, insignificant difference in the contact angle values was observed between samples compressed at temperatures of 150 and 180 °C for the tight side (Table 1).

The change in contact angle values especially on the tight side for the investigated pressure range of 0.5-3.5 MPa was irregular probably because of the complex morphology of the veneer surface. As mentioned above, it is very difficult to pick up veneer sheets that would have identical characteristics.

Factor analysis showed that the effect of compression temperature and pressure on changes in contact angle was significant (*p*<0.05) for both sides of veneer. Regarding the temperature, a clear dependence was found on the effect of compression temperature on wettability. In particular, if the compression temperature increases, wettability worsens. With respect to the compression pressure, no clear dependence of the effect of this factor on wettability was found. Contact

Table 2 Drop shape changing on non-densified and densified surfaces of birch veneer specimens as a function of time at different thermal compression
Tablica 2. Promjena oblika kapljice na površini uzoraka nekomprimiranoga i komprimiranog furnira kao funkcija vremena pri različitim toplinskim kompresijama

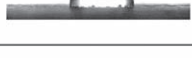| Side of veneer and compression conditions / *Strana furnira i uvjeti kompresije*	Wetting period / *Vrijeme kvašenja*		
	5 sec	30 sec	60 sec
Loose side (non-densified) / *otvorena strana (nekomprimirana)*			
Tight side (non-densified) / *zatvorena strana (nekomprimirana)*			
Loose side (densified at 150 °C/0.5MPa) / *otvorena strana (komprimirana pri 150 °C / 0,5 MPa)*			
Tight side (densified at 150 °C/0.5MPa) / *zatvorena strana (komprimirana pri 150 °C / 0,5 MPa)*			
Loose side (densified at 150 °C/3.5MPa) / *otvorena strana (komprimirana pri 150 °C / 3,5 MPa)*			
Tight side (densified at 150 °C/3.5MPa) / *zatvorena strana (komprimirana pri 150 °C / 3,5 MPa)*			
Loose side (densified at 180 °C/0.5MPa) / *otvorena strana (komprimirana pri 180 °C / 0,5 MPa)*			
Tight side (densified at 180 °C/0.5MPa) / *zatvorena strana (komprimirana pri 180 °C / 0,5 MPa)*			
Loose side (densified at 180 °C/3.5MPa) / *otvorena strana (komprimirana pri 180 °C / 3,5 MPa)*			
Tight side (densified at 180 °C/3.5MPa) / *zatvorena strana (komprimirana pri 180 °C / 3,5 MPa)*			

angle values on the tight side are higher than on the loose side for the same thermal compression conditions. Therefore, the tight side presents lower wettability than the loose side. Moreover, contact angle values of densified veneer are higher than those of non-densified veneer. This difference is significant for the loose side (Table 1). For the tight side, this difference is not clear as displayed in Table 1. The changes in the contact angle values for a tight side of veneer densified at temperature levels of 150 and 180 °C, as compared to non-densified veneer, are negligible. The contact angles on the tight side of veneer thermally compressed at 150 and 180 °C were found as 55.91° and 59.08°, respectively. It appears that these values were close to 57.28°, which was found on the tight side of non-densified veneer. However, this difference in the contact angle values on the tight side between compression temperatures of 150 and 180 °C was significant (Table 1).

Table 2 shows the reduction in drop volume as a function of time due to the penetration of water into the porous structure of wood. Slower absorption of water by capillaries on a smooth (tight) surface justifies the observed differences. At higher compression temperature, the shape of water drop on the loose and tight sides of veneer surface remains unchanged.

For non-densified veneer, the surface on the tight side is more homogeneous than on the loose side. The penetration of water into the tight side is more homogeneous, with the exception of penetration into the area of veneer heterogeneous, while penetration into the loose side is both deeper and less homogeneous. Compression of veneer homogenises the surface and reduces the influence of wood anatomical characteristics on wetting behaviour. After compression, the surface characteristics of the loose and tight sides become comparable. The difference between the loose and tight sides of densified veneer is reduced, although it still remains significant. The difference between the values of the contact angle for the loose and tight sides is 30.9 % for non-densified veneer, 14.8 % for the veneer densified at 150 °C and 7.7 % for the veneer densified at 180 °C (Table 1).

The contact angle decreases faster on the loose side than on the tight side of the veneer (Table 3). On the loose side, due to the existence of lathe checks, the horizontal flow on the veneer surface was mainly responsible for decreasing the contact angle (Vazquez *et al.*, 2003). On the tight side, the speed of changing the values of the contact angle for non-densified veneer and veneer compressed at different temperatures remains practically the same. This may indicate that the tight side surface, both in non-densified and densified veneer, is homogeneous. The speed with which the contact angle changes for non-densified veneer is greater than for the veneer compressed at different temperatures. The smallest rate of changes in the contact angle was observed at the compression temperature of 180 °C.

There are several possible reasons for the decreased wettability of surface densified wood veneers.

Table 3 Contact angle changes on non-densified and densified birch veneer specimens at different wetting period (T – compression temperature; P – compression pressure; LS – loose side; TS – tight side)
Tablica 3. Promjene dodirnih kutova na uzorcima nekomprimiranoga i komprimiranog bukova furnira pri različitom vremenu kvašenja (*T* – temperatura kompresije, *P* – tlak kompresije, LS – otvorena strana, TS – zatvorena strana)

T, °C	*P*, MPa	Initial angle *Početni kut*		Angle after 30 s *Kut nakon 30* s		Angle after 60 s *Kut nakon 60* s		Percent decrease of angle after 30 s *Postotno smanjenje dodirnog kuta nakon 30* s		Percent decrease of angle after 60 s *Postotno smanjenje dodirnog kuta nakon 60* s	
		LS	TS	LS	TS	LS	TS	LS	TS	LS	TS
Control (non-densified) *Kontrolni nekomprimirani uzorak*		87.2	93.1	27.3	46.0	13.0	38.4	68.7	50.6	85.1	58.7
150	0.5	86.0	81.6	37.2	44.6	18.1	35.5	56.8	45.4	78.9	56.5
	1.0	84.6	87.9	18.1	39.8	-	32.4	78.6	54.7	-	63.2
	1.5	87.4	91.9	36.1	42.8	23.7	29.9	58.7	53.4	72.9	65.7
	2.0	89.5	85.0	29.9	32.8	17.0	24.8	66.6	61.5	81.0	70.9
	2.5	92.4	93.6	50.1	55.6	39.1	47.6	45.8	40.6	57.7	49.1
	3.0	76.6	93.5	19.7	45.1	12.5	37.7	74.4	51.8	83.7	59.7
	3.5	88.9	94.5	47.6	54.9	36.4	47.7	46.5	41.9	59.1	49.8
180	0.5	85.6	96.0	41.0	51.0	32.1	42.8	52.1	46.9	62.5	55.5
	1.0	88.5	87.1	41.3	40.3	28.2	32.0	53.4	53.7	68.2	63.3
	1.5	82.3	85.3	30.9	32.1	22.7	23.5	62.4	62.3	72.5	72.5
	2.0	84.9	88.1	33.0	53.5	22.5	46.5	61.2	39.3	73.5	47.3
	2.5	97.7	94.6	42.0	48.3	30.1	41.0	57.0	49.0	69.2	56.7
	3.0	97.5	99.3	45.2	50.1	34.3	42.9	53.7	49.5	64.8	56.8
	3.5	95.2	97.8	46.3	58.8	37.2	50.5	51.4	39.8	60.9	48.3

This may be attributed to surface roughness and chemical indices of wood surfaces that are changed with thermal compression (Diouf *et al.,* 2011; Fang *et al.,* 2012; Kutnar *et al.,* 2012; Arruda and Del Menezzi, 2013). When analysing the anatomical characteristics of densified veneer, it was shown that wood morphology changed significantly in the compression process. Earlier studies (Arruda and Del Menezzi, 2013; Bekhta *et al.,* 2014) indicated that thermo-mechanical densification improved surface quality of veneers with the surface becoming smoother, and roughness values decreasing significantly. Roughness is closely related to wettability: the higher the roughness, the higher the surface hydrophilicity (Piao *et al.,* 2010; Arnold, 2011). A contrary result was found by Stehr *et al.* (2001) in the case of southern pine. It was found that a smoother wood surface provided enhanced wetting and penetration properties for high-viscosity liquids such as adhesives. Our findings are in good agreement with the results obtained by Stehr *et al.* (2001). An increase in contact angle values on the loose side of densified veneer was also due to the decreased wood surface porosity during thermal compression. Smoother surfaces have lower porosity, which results in lower penetration characteristics. This increase was higher on the tight side of surface when compared to that of the loose side, since the loose surface (with more lathe checks) was more affected by compression compared to the tight side.

Liptakova *et al.* (1995) found that mechanical treatments not only change the morphological structure of wood, but also the chemical composition of the wood surface layer. The decreased wettability might also be caused by increased hydrophobicity. It has been reported that extractives that migrate to wood surface create hydrophobic properties and reduce its wettability (Nussbaum and Sterley, 2002). The degradation of the most hygroscopic components of wood, namely cellulose, hemicelluloses and lignin, which probably occurs during thermal compression (Kocaefe *et al.,* 2008; Diouf *et al.,* 2011; Bekhta and Krystofiak, 2016), reduces water absorption of wood. Changes in lignin occur at these temperatures. Lignin softens and blocks the cell pores contributing to the reduction in water absorption (Rowell *et al.,* 2000).

4 CONCLUSIONS
4. ZAKLJUČAK

Based on the findings presented in this paper, wettability of the loose and tight sides of veneer was decreased significantly by thermal compression treatment at all studied temperatures and pressures. For non-densified veneer, the dynamic contact angle values for the loose-side were much smaller than for the tight-side. It was also observed that, in the case of distilled water, there was no clear trend distinguishing the loose and tight sides of veneer after thermal compression treatment, whose mean values, considering all the temperatures and pressures studied, were very similar. On the other hand, the loose side showed a slight trend to-

wards better wettability than the tight side for densified veneer compared to non-densified veneer. Thermal compression of veneer homogenises the surface and, as a result, its wettability of the loose and tight sides is comparable. Based on the obtained results, it can be argued that the difference between the loose and tight sides of the veneer is significantly reduced due to the compression process. For example, the difference between mean values of the contact angle for the loose and tight sides of non-densified veneer is 30.9 %. For the veneer compressed at the temperature of 150 °C, this difference is already 14.8 %, and for the veneer compressed at the temperature of 180 °C, this difference is only 7.7 %. In general, at the higher compression temperature, the wettability on the densified wood surface worsens as compared to non-densified veneer. At the same time, however, the difference between the loose and tight sides of the veneer is reduced. It seems that the main reason for the changes in dynamic contact angle are connected with the difference in the anatomical structure of loose and tight sides of veneer, since the thermal compression time was only 1 min. However, an accurate explanation of this phenomenon requires further study.

5 REFERENCES
5. LITERATURA

1. Arnold, M., 2011: Planing and Sanding of Wood Surfaces – Effects on Surface Properties and Coating Performance. In: Proceedings PRA's 7th International Woodcoatings Congress "Reducing the Environmental Footprint", The Netherlands, 12-13 October 2010; Middlesex: Hampton, p.12.

2. Arruda, L.; Del Menezzi, C. H. S., 2013: Effect of thermo-mechanical treatment on physical properties of wood veneers. International Wood Products Journal, 4 (4): 217-224. https://doi.org/10.1179/2042645312Y.0000000022.

3. Bekhta, P.; Krystofiak, T., 2016: The influence of short-term thermo-mechanical densification on the surface wettability of wood veneers. Maderas-Ciencia y tecnologia, 18 (1): 79-90.
https://doi.org/10.4067/S0718-221X2016005000008.

4. Bekhta, P.; Proszyk, S.; Krystofiak, T.; Mamonova, M.; Pinkowski, G.; Lis, B., 2014: Effect of thermomechanical densification on surface roughness of wood veneers. Wood Material Science and Engineering, 9 (4): 233-245. https://doi.org/10.1080/17480272.2014.923042.

5. Bekhta, P.; Proszyk, S.; Lis, B.; Krystofiak, T., 2015: Surface wettability of short-therm thermo-mechanically densified wood veneers. European Journal of Wood and Wood Products, 73: 415-417.
https://doi.org/10.1007/s00107-015-0902-4.

6. Büyüksari, U.; Hiziroglu, S.; Ayrilmis, N.; Akkilic, H., 2012: Mechanical and physical properties of medium density fiberboard panels laminated with thermally compressed

veneer. Composites Part B: Engineering, 43 (2): 110-114. https://doi.org/10.1016/j.compositesb.2011.11.040.

7. Büyüksari, U., 2013: Surface characteristics and hardness of MDF panels laminated with thermally compressed veneer. Composites Part B: Engineering, 44: 675-678.
https://doi.org/10.1016/j.compositesb.2012.01.087.

8. Candan, Z.; Hiziroglu, S.; Mcdonald, A. G., 2010: Surface quality of thermally compressed Douglas fir veneer. Materials and Design, 31 (7): 3574-3577.
https://doi.org/10.1016/j.matdes.2010.02.003.

9. Diouf, P. N.; Stevanovic, T.; Cloutier, A.; Fang, C.-H.; Blanchet, P.; Koubaa, A.; Mariotti, N., 2011: Effects of thermo-hygro-mechanical densification on the surface characteristics of trembling aspen and hybrid poplar wood veneers. Applied Surface Science, 257: 3558-3564.
https://doi.org/10.1016/j.apsusc.2010.11.074.

10. Elbez, G., 1978. Study of wettability of wood. Holzforschung, 32 (3): 82-92.

11. Fang, C.-H.; Mariotti, N.; Cloutier, A.; Koubaa, A.; Blanchet, P., 2012: Densification of wood veneers by compression combined with heat and steam. European Journal of Wood and Wood Products, 70 (1-3): 155-163.
https://doi.org/10.1007/s00107-011-0524-4.

12. Gindl, M.; Reiterer, A.; Sinn, G.; Stanzl-Tschegg, S. E., 2004: Effects of surface ageing on wettability, surface chemistry, and adhesion of wood. Holz als Roh- und Werkstoff, 62 (4): 273-280.
https://doi.org/10.1007/s00107-004-0471-4.

13. Gray, V. R., 1962: The wettability of wood. Forest Products Journal, 12 (9): 452-461.

14. Hse, C. Y., 1972: Wettability of southern pine veneer by phenol formaldehyde wood adhesives. Forest Products Journal, 22 (1): 51-56.

15. Kocaefe, D.; Poncsak, S.; Doré, G.; Younsi, R., 2008: Effect of heat treatment on the wettability of white ash and soft maple by water. Holz als Roh- und Werkstoff, 66 (5): 355-361. https://doi.org/10.1007/s00107-008-0233-9.

16. Kollmann, F.; Kuenzi, E. W.; Stamm, A. J., 1975: Principles of Wood Science and Technology. II Wood Based Materials. Springer Berlin Heidelberg, New York.

17. Kutnar, A.; Kamke, F. A.; Sernek, M., 2008: The mechanical properties of densified VTC wood relevant for structural composites. Holz als Roh- und Werkstoff, 66 (6): 439-446. https://doi.org/10.1007/s00107-008-0259-z.

18. Kutnar, A.; Rautkari, L.; Laine, K.; Hughes, M., 2012: Thermodynamic characteristics of surface densified solid Scots pine wood. European Journal of Wood and Wood Products, 70 (5): 727-734.
https://doi.org/10.1007/s00107-012-0609-8.

19. Liptakova, E.; Kudela, J., 1994: Analysis of the wood-wetting process. Holzforschung, 48 (2): 139-144. https://doi.org/10.1515/hfsg.1994.48.2.139.

20. Liptakova, E.; Kudela, J.; Bastl, Z.; Spirovova, I., 1995: Influence of mechanical surface-treatment of wood on the wetting process. Holzforschung, 49 (4): 369-375. https://doi.org/10.1515/hfsg.1995.49.4.369.

21. Nussbaum, R. M.; Sterley, M., 2002: The effect of wood extractive content on glue adhesion and surface wettability of wood. Wood Fiber Science, 34: 57-71.

22. Piao, C.; Winandy, J. E.; Shupe, T. F., 2010: From hydrophilicity to hydrophobicity: a critical review: Part I. Wettability and surface behavior. Wood Fiber Science, 42: 490-510.

23. Rautkari, L.; Laine, K.; Kutnar, A.; Medved, S.; Hughes, M., 2013: Hardness and density profile of surface densified and thermally modified Scots pine in relation to degree of densification. Journal of Materials Science, 48 (6): 2370-2375.
https://doi.org/10.1007/s10853-012-7019-5.

24. Rowell, R.; Lange, S.; Davis, M., 2000: Steam stabilization of aspen fiberboards. In: *Proceedings of 5th Pacific Rim Bio-based Composites Symposium*, Canberra, Australia, December 10-13, 2000 (ACIAR Proceedings), pp. 425-438.

25. Scheikl, M.; Dunky, M., 1998: Measurement of dynamic and static contact angles on wood for the determination of its surface tension and the penetration of liquids into the wood surface. Holzforschung, 52 (1): 89-94. https://doi.org/10.1515/hfsg.1998.52.1.89.

26. Shupe, T. E.; Hse, C. Y.; Choong, E. T.; Groom, L. H., 1998: Effect of wood grain and veneer side on Loblolly pine veneer wettability. Forest Products Journal, 48: 95-97.

27. Stehr, M.; Gardner, D. J.; Walinder, M. E. P., 2001: Dynamic wettability of different machined wood surfaces. The Journal of Adhesion, 76 (3): 185-200. https://doi.org/10.1080/00218460108029625.

28. Vazques, G.; Gonzalez-Alvarez, J.; Lopez-Suevos, F.; Antorrena, G., 2003: Effect of veneer side wettability on bonding quality of *Eucalyptus globulus* plywoods prepared using a tannin-phenol-formaldehyde adhesive. Bioresource Technology, 87: 349-353.
https://doi.org/10.1016/S0960-8524(02)00230-4.

Corresponding address:

Prof. Ing. PAVLO BEKHTA, DrSc.

Department of Wood-Based Composites, Cellulose and Paper
Ukrainian National Forestry University
Gen. Chuprynky Str. 103
79057 Lviv, UKRAINE
e-mail: bekhta@ukr.net

Obilježavanje 120. obljetnice Šumarskoga fakulteta Sveučilišta u Zagrebu

Kao jedan od najstarijih fakulteta u sastavu Sveučilišta u Zagrebu, Šumarski je fakultet ove godine obilježio 120. godinu održavanja kontinuirane visokoškolske šumarske i 70. godinu visokoškolske drvnotehnološke nastave. Početci visokoškolske šumarske nastave vežu se za 1860. godinu i Gospodarsko-šumarsko učilište u Križevcima, no Šumarska akademija počinje djelovati tek 1898. u sastavu Mudroslovnog fakulteta Sveučilišta u Zagrebu, čime je šumarska nastava dobila sveučilišni status. Gospodarsko-šumarski fakultet Sveučilišta u Zagrebu osnovan je 1919., a sastojao se od dvaju odjela: Gospodarskoga i Šumarskoga. Od 1948. nastava na Šumarskom odjelu razdvojena je u dva smjera: šumsko-uzgojni, nazvan Biološkim smjerom, i šumsko-industrijski, nazvan Tehničkim smjerom. Stoga se 1948. smatra godinom početka kontinuiranog održavanja drvnotehnološke nastave na Šumarskom fakultetu Sveučilišta u Zagrebu. Visoko obrazovanje iz područja šumarstva i drvne tehnologije od 1960. nadalje razvija se na samostalnom fakultetu – Šumarskom fakultetu Sveučilišta u Zagrebu. Navedene su obljetnice proslavljene dvama iznimno posjećenim događanjima: svečanom akademijom održanom 18. listopada 2018. i Međunarodnim znanstvenim savjetovanjem održanim 19. listopada 2018.

Svečana akademija organizirana je pod visokim pokroviteljstvom predsjednice Republike Hrvatske Kolinde Grabar Kitarović, a prisustvovali su joj brojni uzvanici: izaslanik Predsjednice RH i direktor poduzeća Hrvatske šume d.o.o. Krunoslav Jakupčić, dipl. ing.; izaslanik potpredsjednika Vlade i ministra poljoprivrede državni tajnik dr. sc. Željko Kraljičak; izaslanik predsjednika Sabora RH Damir Felak, dipl. ing.; ministrica znanosti i obrazovanja prof. dr. sc. Blaženka Divjak; rektor Sveučilišta u Zagrebu prof. dr. sc. Damir Boras i prorektori prof. dr. sc. Mirjana Hruškar i prof. dr. sc. Miloš Judaš; predsjednik HAZU-a akademik Zvonko Kusić; izaslanica gradonačelnika grada Zagreba gđa Iva Milardović Štimac; rektori, prorektori, dekani i prodekani iz inozemstva te dekani i prodekani brojnih sastavnica Sveučilišta u Zagrebu.

Slika 1. Svečana akademija održana je uz nazočnost više od 300 gostiju u Velikom amfiteatru Šumarskoga fakulteta

Slika 2. Ugledni uzvanici i gosti na svečanoj akademiji

Slika 3. Pozdravni govor dekana Šumarskog fakulteta Sveučilišta u Zagrebu prof. dr. sc. Tibora Penteka na početku svečane akademije

Slika 4. Monografija Šumarskog fakulteta Sveučilišta u Zagrebu

Slika 5. Pojmovnik hrvatskoga drvnotehnološkog nazivlja

Nakon pozdravnih govora dekana Šumarskog fakulteta prof. dr. sc. Tibora Penteka i uzvanika počela je svečana akademija, tijekom koje je predstavljena monografija Šumarskog fakulteta, uz poseban osvrt na aktivnosti i postignuća tijekom posljednja dva desetljeća, tj. u razdoblju nakon izdavanja posljednje monografije. Predstavljen je i Pojmovnik drvnotehnološkog nazivlja objavljen u suradnji Šumarskog fakulteta Sveučilišta u Zagrebu i Instituta za hrvatski jezik i jezikoslovlje u prigodi obilježavanja 70. obljetnice Drvnotehnološkog odsjeka.

Nakon glazbenog predaha dodijeljene su nagrade domaćim i stranim pojedincima i institucijama za izniman doprinos razvoju i promociji Šumarskog fakulte-

Slika 6. Prodekan prof. dr. sc. Josip Margaletić dodjeljuje nagrade najboljim studentima preddiplomskih i diplomskih studija sa Šumarskog odsjeka

Slika 7. Prodekani Šumarskog fakulteta dodjeljuju nagrade institucijama iz Hrvatske za izniman doprinos razvoju i promociji Šumarskog fakulteta

Slika 8. Sudionici međunarodnoga znanstvenog savjetovanja *Položaj i perspektiva šumarstva i drvne tehnologije u 21. stoljeću* – plenarna sesija

Slika 9. Prezentacija akademika Igora Anića tijekom plenarne sesije Međunarodnoga znanstvenog savjetovanja

Slika 10. Prezentacija dekana Šumarskog fakulteta iz Sarajeva prof. dr. sc. Mirze Dautbašića na Šumarskoj tehničkoj sekciji

Slika 11. Predaja darova pročelniku Šumarskog odsjeka Sveučilišta u Padovi prof. dr. sc. Raffaeleu Cavalliju nakon održane prezentacije

ta, jubilarne nagrade zaposlenicima za 30, 35 i 40 godina predanog rada, nagrade upravo umirovljenim kolegama te nagrade i pohvale najboljim studentima preddiplomskih i diplomskih studija.

Međunarodno znanstveno savjetovanje *Position and Perspectives of Forestry and Wood Technology in the 21st Century* održano je pod visokim pokroviteljstvom Ministarstva poljoprivrede i Ministarstva znanosti i obrazovanja te uz potporu međunarodnih organizacija IUFRO i Innovawood. Nakon plenarne sekcije,

tijekom koje su prezentirani važnost poučavanja o šumarstvu za razvoj hrvatskog šumarstva, uloga šuma u globalnom kruženju ugljika te izazovi iskorištavanja drva i utjecaj na bioekonomiju, održane su dvije tehničke sekcije – o šumarstvu i o drvnoj tehnologiji.

Unutar sekcije o šumarstvu prezentirani su brojni zanimljivi radovi, od trendova pridobivanja drva u Europi do značajki šumarske zajednice putem analize radova objavljenih u časopisu CROJFE izdavača Šumarskog fakulteta, ali se mnogo čulo i o utjecajima

Slika 12. Prezentacija prodekana Biotehničkog fakulteta iz Ljubljane prof. dr. sc. Mihe Humara na Drvnotehnološkoj sekciji

Slika 13. Stručne rasprave vodile su se i u pauzama između predavanja

Slika 14. Osobe zadužene za operativnu provedbu organizacije svečane akademije i Međunarodnoga znanstvenog savjetovanja

promjene klime na šumske ekosustave, o očuvanju šumskih genskih izvora, uređenju šuma u promjenjivim socio-okolišnim uvjetima te o prilagodbama strategije uzgoja šuma.

Drvnotehnološka sekcija obuhvatila je teme upotrebe drva za inovativne proizvode, prošlost i budućnost znanosti o drvu, anatomiju drva u 21. stoljeću, budućnost zaštite drva, iskorištavanje drva u kontekstu bioekonomije, poboljšanje svojstava drva različitim

tretmanima, tehnologiju piljenja, razvoj namještaja te ulogu laboratorija u povezivanju znanosti, obrazovanja i prakse.

doc. dr. sc. Josip Miklečić
dr. sc. Miljenko Klarić
dr. sc. Andreja Đuka
dr. sc. Ivica Papa

Tieghemella heckelii Pierre

NAZIVI

Tieghemella heckelii Pierre prihvaćeni je botanički naziv vrste *Dumoria heckelii* A.Chev. iz porodice *Sapotaceae.* Trgovački su nazivi te vrste također: makoré (Belgija, Njemačka, Francuska, Gana, Velika Britanija, Nizozemska, Siera Leone, Šri Lanka); butusu, dumori (Obala Bjelokosti); baku, abacu, makori (Gana); aganokwe, aganope (Nigerija), kondofindo (Kongo).

NALAZIŠTE

Stabla *Tieghemella heckelii* Pierre nalazimo u zapadnoj Africi, od Liberije preko Obale Bjelokosti do Gane i Nigerije. Rastu na vlažnim mjestima tropskih nizinskih kišnih šuma, zajedno s drugim vrstama iz porodice *Sapotaceae*, pojedinačno ili u skupinama.

STABLO

Naraste do 30 – 40 (50) m visoko. Čisto deblo dugo je 20 (30) m, a prsni mu je od promjer od 0,7 do 2,0 m. Debla su valjkastog oblika. Žica drva je pravilna do blago usukana. Kora drva je pukotinasta, a zrelog drva pukotinasta i ljuskasta, sivocrvenkasta. Debljina joj je 1,2...2,0...3,0 cm.

DRVO

Makroskopska obilježja

Drvo je rastresito porozno. Sirova je bjeljika krem do crvenobijele boje, nakon stajanja postane sivoružičasta, a široka je od 4 do 10 cm. Ružičasta do crvenkastosmeđa srž s vremenom potamni, a bojom se neznatno razlikuje od bjeljike. Granica goda je dobro uočljiva. Pore i drvni traci vidljivi su povećalom.

Mikroskopska obilježja

Traheje su pretežito pojedinačno raspoređene, ali mogu biti u paru ili u kratkim radijalnim i dijagonalnim nizovima. Promjer traheja je 70...125...220 mikrometara, a gustoća 5...18...29 na 1 mm² poprečnog presjeka. Volumni udio traheja iznosi oko 14,5...23,0...36,5 %. Traheje su često ispunjene tilama i smeđim sržnim tvarima.

Aksijalni parenhim apotrahealno je vrpčast, gustoće od 4 do 5 vrpci na 1 mm² poprečnog presjeka.

Volumni udio aksijalnog parenhima je 12,5...15,5...19,5 %. Staničje drvnih trakova je heterogeno. Pojedini su drvni traci visoki 100...425...1380 mikrometara, odnosno 4...15...30 stanica, a široki su 15...30...70 mikrometara, odnosno 1...2...3 stanice. Gustoća drvnih trakova je 4...9...15 na 1 mm. Volumni udio drvnih trakova kreće se oko 15,5...24,0...32,0 %. U drvnim tracima i u aksijalnom parenhimu ima kristala. Drvna su vlakanca uglavnom libriformska, a katkad su to i vlaknaste traheide. Dugačka su 475...1220...2000 mikrometara. Debljina staničnih stijenki vlakanaca iznosi 1,7...3,2...6,2 mikrometra, a volumni je udio vlakanaca 26...37,5...45,5 %.

Fizička svojstva

Gustoća apsolutno suhog drva, ρ_o	510...590...680 kg/m³
Gustoća prosušenog drva, ρ_{12-15}	530...640...720 kg/m³
Gustoća sirovog drva, ρ_s	850...900 kg/m³
Poroznost	oko 62 %
Radijalno utezanje, β_r	3,5...4,7...6,5 %
Tangentno utezanje, β_t	4,3...6,3...9,5 %
Volumno utezanje, β_v	7,9...11,2...16,5 %

Mehanička svojstva

Čvrstoća na tlak	40...54...71 MPa
Čvrstoća na vlak, paralelno s vlakancima	30...77...155 MPa
Čvrstoća na vlak, okomito na vlakanca	1,9...2,3 MPa
Čvrstoća na savijanje	41...98...146 MPa
Tvrdoća prema Brinellu, paralelno s vlakancima	40...44...47 MPa
Tvrdoća prema Brinellu, okomito na vlakanca	22...25...31 MPa
Modul elastičnosti	11...12 GPa

TEHNOLOŠKA SVOJSTVA

Obradivost

Drvo se dobro ručno i strojno obrađuje, lijepi, brusi i polira. Pri obradi drva gumaste se sržne tvari mogu zalijepiti za zupce alata i tako otežati rad s drvom.

Sušenje

Drvo se dobro i polako suši. Za vrijeme sušenja mogu nastati pukotine i vitoperenja.

Trajnost i zaštita

Prema normi HRN 350-2, 2005, srž drva vrlo je otporna na gljive uzročnice truleži (razred otpornosti 1) i otporna na termite (razred otpornosti D). Srž je slabo permeabilna (razred 4). Po trajnosti je u razredu 4 i stoga se drvo bez dodatne zaštite može upotrebljavati i u interijeru i u eksterijeru.

Uporaba

Rabi se kao furnirsko drvo, a služi i za izradu kvalitetnoga/luksuznog namještaja, stuba, unutrašnje i vanjske stolarije, podova, mostova, vagona i drvenih ploča, a primjenu nalazi i u brodogradnji, osobito u izradi kobilica, paluba i okvira.

Sirovina

Doprema se u obliku trupaca duljine od 5,0 do 15,0 m, srednjeg promjera 70 do 200 cm.

Napomena

Tieghemella heckelii Pierre nije na popisu ugroženih vrsta međunarodne organizacije CITES, ali je ipak jedna od ugroženih vrsta na popisu međunarodne organizacije IUCN. Zbog svoje boje, teksture i svojstava, drvo te vrste može se upotrebljavati kao zamjena za mahagonijevinu.

Bruševina drva može prouzročiti iritaciju očiju i kože te kihanje, a ozbiljnije su reakcije vrlo rijetke.

Drvo sličnih svojstava imaju i ove vrste: *Autranella congolensis* A.Chev*., Baillonella toxisperma* Pierre*, Tieghemella africana* A.Chev., *Manilkara huberi* Standl.

Literatura

1. Richter, H. G.; Dallwitz, M. J., 2000: Commercial timbers: descriptions, illustrations, identification, and information retrieval. In English, French, German, and Spanish. Version: 25th June 2009. https://www.delta-intkey.com/wood/index.htm, preuzeto 25. studenog 2018.
2. Chudnoff, M., 1984: Tropical Timbers of the World, Forest Products Laboratory USA, Madison, Wis.
3. Wagenführ, R.; Scheiber, C., 1974: HOLZATLAS, Fachbuchverlag Leipzig im Carl Hanser Verlag München, 475-479.
4. The Timber Research and Development Association (TRADA), 1979: Timbers of the world, The Construction Press Ltd., Lancaster, England.
5. https://tropix.cirad.fr/FichiersComplementaires/EN/Africa/MAKORE.pdf, preuzeto 25. studenog 2018.
6. ***HRN EN 350-2, 2005: Trajnost drva i proizvoda na osnovi drva – Prirodna trajnost masivnog drva – 2. dio.

prof. dr. sc. Jelena Trajković
izv. prof. dr. sc. Bogoslav Šefc

Upute autorima

Opće odredbe

Časopis *Drvna industrija* objavljuje znanstvene radove (izvorne znanstvene radove, pregledne radove, prethodna priopćenja), stručne radove, izlaganja sa savjetovanja, stručne obavijesti, bibliografske radove, preglede te ostale priloge s područja biologije, kemije, fizike i tehnologije drva, pulpe i papira te drvnih proizvoda, uključujući i proizvodnu, upravljačku i tržišnu problematiku u drvnoj industriji.

Predaja rukopisa podrazumijeva uvjet da rad nije već predan negdje drugdje radi objavljivanja ili da nije već objavljen (osim sažetka, dijelova objavljenih predavanja ili magistarskih radova odnosno disertacija, što mora biti navedeno u napomeni) te da su objavljivanje odobrili svi suautori (ako rad ima više autora) i ovlaštene osobe ustanove u kojoj je istraživanje provedeno. Cjelokupni sadržaj Drvne industrije dostupan je za skidanje s interneta, tiskanje, daljnju distribuciju, čitanje i ponovno korištenje bez ograničenja sve dok se naznače autor(i) i originalni izvor prema Creative Commons Attribution 4.0 International License (CC BY). Autor(i) zadržavaju izdavačka prava bez ograničenja.

Znanstveni i stručni radovi objavljuju se na hrvatskome, uz sažetak na engleskome, ili se pak rad objavljuje na engleskome, sa sažetkom na hrvatskom jeziku. Naslov, podnaslovi i svi važni rezultati trebaju biti napisani dvojezično. Ostali se članci uglavnom objavljuju na hrvatskome. Uredništvo osigurava inozemnim autorima prijevod na hrvatski. Znanstveni i stručni radovi podliježu temeljitoj recenziji najmanje dvaju recenzenata. Izbor recenzenata i odluku o klasifikaciji i prihvaćanju članka (prema preporukama recenzenata) donosi Urednički odbor.

Svi prilozi podvrgavaju se jezičnoj obradi. Urednici će od autora zahtijevati da tekst prilagode preporukama recenzenata i lektora, te zadržavaju i pravo da predlože skraćivanje ili poboljšanje teksta. Autori su potpuno odgovorni za svoje priloge. Podrazumijeva se da je autor pribavio dozvolu za objavljivanje dijelova teksta što su već negdje objavljeni te da objavljivanje članka ne ugrožava prava pojedinca ili pravne osobe. Radovi moraju izvještavati o istinitim znanstvenim ili tehničkim postignućima. Autori su odgovorni za terminološku i metrološku usklađenost svojih priloga. Radovi se šalju elektroničkom poštom na adresu:

drind@sumfak.hr ili techdi@sumfak.hr

Upute

Predani radovi smiju sadržavati najviše 15 jednostrano pisanih A4 listova s dvostrukim proredom (30 redaka na stranici), uključujući i tablice, slike te popis literature, dodatke i ostale priloge. Dulje je članke preporučljivo podijeliti na dva ili više nastavaka. Tekst treba biti u *doc formatu*, u potpunosti napisan fontom *Times New Roman* (tekst, grafikoni i slike), normalnim stilom, bez dodatnog uređenja teksta.

Prva stranica poslanog rada treba sadržavati puni naslov, ime(na) i prezime(na) autora, podatke o zaposlenju autora (ustanova, grad i država) te sažetak s ključnim riječima (duljina sažetka približno 1/2 stranice A4).

Posljednja stranica treba sadržavati titule, zanimanje, zvanje i adresu (svakog) autora, s naznakom osobe s kojom će Uredništvo biti u vezi.

Znanstveni i stručni radovi moraju biti sažeti i precizni. Osnovna poglavlja trebaju biti označena odgovarajućim podnaslovima. Napomene se ispisuju na dnu pripadajuće stranice, a obrojčavaju se susljedno. One koje se odnose na naslov označuju se zvjezdicom, a ostale uzdignutim arapskim brojkama. Napomene se odnose na tablice pišu se ispod tablica, a označavaju se uzdignutim malim pisanim slovima, abecednim redom.

Latinska imena trebaju biti pisana kosim slovima (italicom), a ako je cijeli tekst pisan kosim slovima, latinska imena trebaju biti podcrtana.

U uvodu treba definirati problem i, koliko je moguće, predočiti granice postojećih spoznaja, tako da se čitateljima koji se ne bave područjem o kojemu je riječ omogući razumijevanje ciljeva rada.

Materijal i metode trebaju biti što preciznije opisane da omoguće drugim znanstvenicima ponavljanje pokusa. Glavni eksperimentalni podaci trebaju biti dvojezično navedeni.

Rezultati trebaju obuhvatiti samo materijal koji se izravno odnosi na predmet. Obvezatna je primjena metričkog sustava. Preporučuje se upotreba SI jedinica. Rjeđe rabljene fizikalne vrijednosti, simboli i jedinice trebaju biti objašnjeni pri njihovu prvom spominjanju u tekstu. Za pisanje formula valja se koristiti Equation Editorom (programom za pisanje formula u MS Wordu). Jedinice se pišu normalnim (uspravnim) slovima, a fizikalni simboli i faktori kosima (italicom).

Formule se susljedno obrojčavaju arapskim brojkama u zagradama, npr. (1) na kraju retka.

Broj slika mora biti ograničen samo na one koje su prijeko potrebne za objašnjenje teksta. Isti podaci ne smiju biti navedeni i u tablici i na slici. Slike i tablice trebaju biti zasebno obrojčane, arapskim brojkama, a u tekstu se na njih upućuje jasnim naznakama ("tablica 1" ili "slika 1"). Naslovi, zaglavlja, legende i sav ostali tekst u slikama i tablicama treba biti napisan hrvatskim i engleskim jezikom.

Slike je potrebno rasporediti na odgovarajuća mjesta u tekstu, trebaju biti izrađene u rezoluciji 600 dpi, crno-bijele (objavljivanje slika u koloru moguće je na zahtjev autora i uz posebno plaćanje), formata jpg ili tiff, potpune i jasno razumljive bez pozivanja na tekst priloga.

Svi grafikoni i tablice izrađuju se kao crno-bijeli prilozi (osim na zahtjev, uz plaćanje). Tablice i grafikoni trebaju biti na svojim mjestima u tekstu te originalnog formata u kojemu su izrađeni radi naknadnog ubacivanja hrvatskog prijevoda. Ako ne postoji mogućnost za to, potrebno je poslati originalne dokumente u formatu u kojemu su napravljeni (*excel* ili *statistica* format).

Naslovi slika i crteža ne pišu se velikim tiskanim slovima. Crteži i grafikoni trebaju odgovarati stilu časopisa (fontovima i izgledu). Slova i brojke moraju biti dovoljno veliki da budu lako čitljivi nakon smanjenja širine slike ili tablice. Fotomikrografije moraju imati naznaku uvećanja, poželjno u mikrometrima. Uvećanje može biti dodatno naznačeno na kraju naslova slike, npr. "uvećanje 7500 : l".

Diskusija i zaključak mogu, ako autori žele, biti spojeni u jedan odjeljak. U tom tekstu treba objasniti rezultate s obzirom na problem postavljen u uvodu i u odnosu prema odgovarajućim zapažanjima autora ili drugih istraživača. Valja izbjegavati ponavljanje podataka već iznesenih u odjeljku *Rezultati*. Mogu se razmotriti naznake za daljnja istraživanja ili primjenu. Ako su rezultati i diskusija spojeni u isti odjeljak, zaključke je nužno napisati izdvojeno. Zahvale se navode na kraju rukopisa. Odgovarajuću literaturu treba citirati u tekstu, i to prema harvardskom sustavu (*ime – godina*), npr. (Bađun, 1965). Nadalje, bibliografija mora biti navedena na kraju teksta, i to abecednim redom prezimena autora, s naslovima i potpunim navodima bibliografskih referenci. Popis literature mora biti selektivan, a svaka referenca na kraju mora imati naveden DOI broj, ako ga posjeduje (http://www.doi.org) (provjeriti na http://www.crossref.org).

Primjeri navođenja literature

Članci u časopisima: Prezime autora, inicijal(i) osobnog imena, godina: Naslov. Naziv časopisa, godište (ev. broj): stranice (od – do). Doi broj.

Primjer

Kärki, T., 2001: Variation of wood density and shrinkage in European aspen (*Populus tremula*). Holz als Roh- und Werkstoff, 59: 79-84. http://dx.doi.org/10.1007/s001070050479.

Knjige: Prezime autora, inicijal(i) osobnog imena, godina: Naslov. (ev. izdavač/editor): izdanje (ev. svezak). Mjesto izdanja, izdavač (ev. stranice od – do).

Primjeri

Krpan, J., 1970: Tehnologija furnira i ploča. Drugo izdanje. Zagreb, Tehnička knjiga.

Wilson, J. W.; Wellwood, R. W., 1965: Intra-increment chemical properties of certain western Canadian coniferous species. U: W. A. Cote, Jr. (Ed.): Cellular Ultrastructure of Woody Plants. Syracuse, N.Y., Syracuse Univ. Press, pp. 551- 559.

Ostale publikacije (brošure, studije itd.)

Müller, D., 1977: Beitrag zür Klassifizierung asiatischer Baumarten. Mitteilung der Bundesforschungsanstalt für Forstund Holzvvirt schaft Hamburg, Nr. 98. Hamburg: M. Wiederbusch.

Web stranice

***1997: "Guide to Punctuation" (online), University of Sussex, www.informatics.sussex.ac.uk/department/docs/punctuation/node 00.html. First published 1997 (pristupljeno 27. siječnja 2010).

Autoru se prije konačnog tiska šalje pdf rada. Rad je potrebno pažljivo pročitati, ispraviti te vratiti Uredništvu s listom ispravaka te s formularom za prijenos autorskih prava na izdavača. Ispravci su ograničeni samo na tiskarske pogreške: dodaci ili znatnije promjene u radu naplaćuju se. Autori znanstvenih i stručnih radova besplatno dobivaju po jedan primjerak časopisa. Autoru svakog priloga također se dostavlja besplatan primjerak časopisa.

Dodatne informacije o načinu pisanja znanstvenih radova mogu se naći na web adresi:

www.ease.org.uk/publications/author-guidelines

Instructions for authors

General terms

The "Drvna industrija" ("Wood Industry") journal publishes scientific papers (original scientific papers, review papers, previous notes), professional papers, conference papers, professional information, bibliographical and survey articles and other contributions related to biology, chemistry, physics and technology of wood, pulp and paper and wood products, including production, management and marketing issues in the wood industry.

Submission of a paper implies that the work has not been submitted for publication elsewhere or published before (except in the form of an abstract or as part of a published lecture, review or thesis, in which case it must be stated in a footnote); that the publication is approved by all co-authors (if any) and by the authorities of the institution where the research has been carried out. The complete content of the journal *Drvna industrija* (Wood Industry) is available on the Internet permitting any users to download, print, further distribute, read and reuse it with no limits provided that the author(s) and the original source are identified in accordance with the Creative Commons Attribution 4.0 International License (CC BY). The authors retain their copyrights.

The scientific and professional papers shall be published either in Croatian, with an extended summary in English, or in English with an extended summary in Croatian. The titles, headings and all the relevant results shall be presented bilingually. Other articles are generally published in Croatian. The Editor's Office shall provide the translation into Croatian for foreign authors. The scientific and professional papers will be subject to a thorough review by at least two selected referees. The Editorial Board shall make the choice of reviewers, as well as the decision about the classification of the paper and its acceptance (based on reviewers' recommendations).

All contributions are subject to proofreading. The editors will require authors to modify the text in the light of the recommendations made by reviewers and language advisers, and they reserve the right to suggest abbreviations and text improvements. Authors are fully responsible for the contents of their contributions. It shall be assumed that the author has obtained the permission for the reproduction of portions of text published elsewhere, and that the publication of the paper in question does not infringe upon any individual or corporate rights. Papers shall report on true scientific or technical achievement. Authors are responsible for the terminological and metrological consistency of their contributions. The contributions are to be submitted by e-mail to the following address: E-mail: drind@sumfak.hr

Details

Papers submitted shall consist of no more than 15 single-sided DIN A-4 sheets of 30 double-spaced lines, including tables, figures and references, appendices and other supplements. Longer papers should be divided into two or more continuing series. The text should be written in doc format, fully written using Times New Roman font (text, graphs and figures), in normal style without additional text editing.

The first page of the paper submitted should contain full title, name(s) of author(s) with professional affiliation (institution, city and state), abstract with keywords (approx. 1/2 sheet DIN A4).

The last page should provide the full titles, posts and address(es) of each author with indication of the contact person for the Editor's Office.

Scientific and professional papers shall be precise and concise. The main chapters should be characterized by appropriate headings. Footnotes shall be placed at the bottom of the same page and consecutively numbered. Those relating to the title should be marked by an asterix, others by superscript Arabic numerals. Footnotes relating to the tables shall be printed under the table and marked by small letters in alphabetical order.

Latin names shall be printed in italics and underlined.

Introduction should define the problem and if possible the framework of existing knowledge, to ensure that readers not working in that particular field are able to understand author's intentions.

Materials and methods should be as precise as possible to enable other scientists to repeat the experiment. The main experimental data should be presented bilingually.

The results should involve only material pertinent to the subject. The metric system shall be used. SI units are recommended. Rarely used physical values, symbols and units should be explained at their first appearance in the text. Formulas should be written by using Equation Editor (program for writing formulas in MS Word). Units shall be written in normal (upright) letters, physical symbols and factors in italics. Formulas shall be consecutively numbered with Arabic numerals in parenthesis (e.g. (1)) at the end of the line.

The number of figures shall be limited to those absolutely necessary for clarification of the text. The same information must not be presented in both a table and a figure. Figures and tables should be numbered separately with Arabic numerals, and should be referred to in the text with clear remarks ("Table 1" or "Figure 1"). Titles, headings, legends and all the other text in figures and tables should be written in both Croatian and English.

Figures should be inserted into the text. They should be of 600 dpi resolution, black and white (color photographs only on request and extra charged), in jpg or tiff format, completely clear and understandable without reference to the text of the contribution.

All graphs and tables shall be black and white (unless requested otherwise with additional payment). Tables and graphs should be inserted into the text in their original format in order to insert them subsequently into the Croatian version. If this is not possible, original document should be sent in the format in which it was made (excel or statistica format).

The captions to figures and drawings shall not be written in block letters. Line drawings and graphs should conform to the style of the journal (font size and appearance). Letters and numbers shall be sufficiently large to be readily legible after reduction of the width of a figure or table. Photomicrographs should have a mark indicating magnification, preferably in micrometers. Magnification can be additionally indicated at the end of the figure title, e.g. "Mag. 7500:1".

Discussion and conclusion may, if desired by authors, be combined into one chapter. This text should interpret the results relating to the problem outlined in the introduction and to related observations by the author(s) or other researchers. Repeating the data already presented in the "Results" chapter should be avoided. Implications for further studies or application may be discussed. A conclusion shall be expressed separately if results and discussion are combined in the same chapter. Acknowledgements are presented at the end of the paper. Relevant literature shall be cited in the text according to the Harvard system ("name – year"), e.g. (Bađun, 1965). In addition, the bibliography shall be listed at the end of the text in alphabetical order of the author's names, together with the title and full quotation of the bibliographical reference. The list of references shall be selective, and each reference shall have its DOI number (http://www. doi.org) (check at http://www.crossref.org).:

Example of references

Journal articles: Author's second name, initial(s) of the first name, year: Title. Journal name, volume (ev. issue): pages (from - to). DOI number.

Example:
Kärki, T., 2001: Variation of wood density and shrinkage in European aspen (*Populus tremula*). Holz als Roh- und Werkstoff, 59: 79-84. http://dx.doi.org/10.1007/s001070050479.

Books:
Author's second name, initial(s) of the first name, year: Title. (ev. Publisher/editor): edition, (ev. volume). Place of publishing, publisher (ev. pages from - to).

Examples:
Krpan, J. 1970: Tehnologija furnira i ploča. Drugo izdanje. Zagreb: Tehnička knjiga.
Wilson, J.W.; Wellwood, R.W. 1965: Intra-increment chemical properties of certain western Canadian coniferous species. U: W. A. Cote, Jr. (Ed.): Cellular Ultrastructure of Woody Plants. Syracuse, N.Y., Syracuse Univ. Press, pp. 551-559.

Other publications (brochures, studies, etc.):
Müller, D. 1977: Beitrag zur Klassifizierung asiatischer Baumarten. Mitteilung der Bundesforschungsanslalt für Forst- und Holzwirtschaft Hamburg, Nr. 98. Hamburg: M. Wiederbusch.

Websites:
***1997: "Guide to Punctuation" (online), University of Sussex, www.informatics.sussex.ac.uk/department/docs/punctuation/node 00.html. First published 1997 (Accessed Jan. 27, 2010).

The paper will be sent to the author in pdf format before printing. The paper should be carefully corrected and sent back to the Editor's Office with the list of corrections made and the form for the transfer of copyrights from the author to the publisher. Corrections should be limited to printing errors; amendments to or changes in the text will be charged. Each contributor will receive 1 copy of the journal.

Further information on the way of writing scientific papers can be found on the following website:

www.ease.org.uk/publications/author-guidelines

PRETPLATNI LIST

Izašao je broj 4 časopisa Drvna industrija, volumen 69, a uskoro tiskamo i prvi broj volumena 70. Pozivamo Vas da obnovite svoju pretplatu ili se pretplatite, ako do sada još niste, na časopis za volumen 70, te na taj način pomognete njegovo izlaženje. Cijena sva četiri broja jednog godišta (volumena) je 300,00 kn bez PDV-a u Hrvatskoj, odnosno 55 EURA u inozemstvu. Ukoliko ste suglasni s uvjetima i cijenom pretplate na cjelokupno godište časopisa molimo Vas da popunite obrazac na poleđini i pošaljete ga na fax broj: +385/1/235 2 528 ili na adresu:

ČASOPIS DRVNA INDUSTRIJA
Šumarski fakultet Zagreb, Svetošimunska cesta 25
HR-10000 Zagreb
Hrvatska

Predsjednik Izdavačkog savjeta   Glavna i odgovorna urednica
časopisa Drvna industrija   časopisa Drvna industrija

prof. dr. sc. Ivica Grbac, v.r.   prof. dr. sc. Ružica Beljo Lučić

ČASOPIS "DRVNA INDUSTRIJA"

Cjenik oglašavanja za 2019. godinu bez PDV-a
ADVERTISING PRICE LIST FOR 2019 VAT excluded

1/1 A4 stranica boja po broju ....3.200,00 kn
A4 stranica boja po broju ....1.600,00 kn

Za oglas tiskan u dva ili više susjednih brojeva odobravamo popust 20%.
Cjenik oglašavanja je podložan promjenama.

1/1 A4 Page on the second, third and fourth cover pages ....910 EUR
1/1 A4 Page on two first inner pages ....860 EUR

Cover and first inner pages are printed in colour. For 2 advertisements published in successive issues a discount of 20 % is granted.
The bill for advertisements is payable in international currency by equivalent change (please contact the Editorial office for details).
Advertising prices can changed.

Glavna i odgovorna urednica   Predsjednik Izdavačkog savjeta
časopisa Drvna industrija   časopisa Drvna industrija

Editor-in-Chief   President of Publishing Council

Prof. Ružica Beljo Lučić, PhD   Prof. Ivica Grbac, PhD

PRETPLATA NA ČASOPIS DRVNA INDUSTRIJA

za volumen 70

Želimo se pretplatiti na časopis Drvna industrija, volumen 70 i želimo primati_____ primjeraka svakog broja. Cijena jednog volumena (godišta) iznosi 300,00 kn bez PDV-a u Hrvatskoj ili 55 EURA u inozemstvu. Obvezujemo se uplatiti iznos od _____ kn (EURA) na IBAN:

HR0923600001101340148
ili
devizna naplata:
SWIFT: ZABA HR 2X
IBAN: HR0923600001101340148
BANK: Zagrebačka banka

s naznakom "Za časopis Drvna industrija, poziv na broj 3 02 03"

Tvrtka:_____

Matični broj tvrtke:_____tel:_____ fax:_____

M.P.

_____
Potpis odgovorne osobe

WOOD INDUSTRY SUBSCRIPTION

We wish to subscribe for the WOOD INDUSTRY journal for Vol. 70 and wish to receive _____ copies of each issue. We shall pay an amount of 55 EUR, VAT excluded by bank draft in EUR funds or international money order by SWIFT to ZAGREBACKA BANKA d. d. - code ZABAHR2X, IBAN: HR0923600001101340148

Name_____

Company/organization_____

Tax number_____ Phone _____ Fax _____

Adress (street, city)_____

Postal code, region, country_____

Signature_____